Human liver glycolate oxidase

Gene identification and protein studies

Emma Louise Williams

A thesis submitted for the degree of

Doctor of Philosophy

University College London

Abstract

Glycolate oxidase (GO) is a peroxisomal flavoenzyme which catalyses the oxidation of short chain α-hydroxy acids, notably glycolate. The reaction product, glyoxylate, is an oxalate precursor and GO is thus of potential interest for its role in the pathogenesis of the primary hyperoxalurias. The project aims were to identify human GO, characterise the kinetics and substrate specificity of the enzyme and establish methods for the analysis of relevant metabolic pathways *in vitro*.

The gene for human GO was cloned from liver and expressed in bacterial cells. The cDNA is 1128 bp in length and has a 1113 bp open reading frame encoding a 372 amino acid protein. The genomic sequence comprises eight exons and spans ~57 kb of chromosome 20p12.

Recombinant human GO protein shares 53% and 89% sequence similarity to GO from spinach and rat respectively, shows α-hydroxy acid oxidase activity *in vitro* and has been purified to homogeneity. Polyclonal anti-GO antibody detects a band of 43 kDa in human liver and, consistent with northern blot analysis, expression is not detected in other tissues including kidney and leucocytes.

Kinetic analysis with a range of α-hydroxy acids indicates GO has highest affinity for glycolate as substrate (K_m = 0.54 mM) and 10 fold less affinity for glyoxylate (K_m = 5.1 mM). Site directed mutagenesis of active site residues demonstrates the importance of chain length for substrate affinity. Thus mutation of a Trp residue, conserved between

spinach and human GO to a less bulky amino acid, permits the catalysis of longer chain length α-hydroxy acids.

HPLC methods were developed for the separation and quantitation of glyoxylate, hydroxypyruvate and pyruvate, enabling analysis of metabolites produced by GO and neighboring enzymes in the metabolic pathway. These assays will be invaluable for future studies in which the pathways of glyoxylate metabolism are constructed *in vitro.*

Abbreviations

Enzymes and EC numbers:

AGT	alanine:glyoxylate aminotransferase (EC 2.6.1.44)
ALDH	aldehyde dehydrogenase (EC 1.2.1.21)
CL	2-oxoglutarate:glyoxylate carboligase (EC 4.1.3.15)
DAO	D-amino acid oxidase (EC 1.4.3.3)
D-GDH	D-glycerate dehydrogenase (EC 1.1.1.29)
DGK	D-glycerate kinase (EC 2.7.1.31)
FCB_2	flavocytochrome b_2 (EC 1.1.2.3)
GDH	glycolate dehydrogenase (EC 1.1.99.14)
GGT	glutamate:glyoxylate aminotransferase (EC 2.6.1.4)
GO	glycolate oxidase (EC 1.1.3.15)
GR	glyoxylate reductase (EC 1.1.1.79)
HAO A	hydroxy acid oxidase type A (EC 1.1.3.15)
HAO B	hydroxy acid oxidase type B (EC 1.1.3.15)
HPD	hydroxypyruvate dehydrogenase (EC 4.1.1.40)
HPR	hydroxypyruvate reductase (EC 1.1.1.79)
LDH	lactate dehydrogenase (EC 1.1.1.27)
LMO	lactate mono-oxygenase (EC 1.13.12.4)
MDH	mandelate dehydrogenase (EC 1.1.2.3)

PGDH	phosphoglycerate dehydrogenase (EC 1.1.1.95)
PGI	phosphoglycerate isomerase (EC 5.4.2.1)
PSA	phosphoserine transaminase (EC 2.6.1.52)
PSP	phosphoserine phosphatase (EC 3.1.3.3)
RUBISCO	ribulose bisphosphate carboxylase/oxygenase (EC 4.1.1.39)
SPT	serine:pyruvate aminotransferase (EC 2.6.1.51)
XAO	xanthine oxidase (EC 1.1.3.22)

General abbreviations:

cDNA	complementary DNA
DNA	deoxyribonucleic acid
dNTP	deoxynucleoside triphosphate
EDTA	ethylenediaminetetra-acetic acid
FMN	flavin mononucleotide
HPLC	high performance liquid chromatography
mRNA	messenger RNA
NAD+	β-Nicotinamide adenine dinucleotide
NADH	β-Nicotinamide adenine dinucleotide, reduced form
NADP+	β-Nicotinamide adenine dinucleotide phosphate
NADPH	β-Nicotinamide adenine dinucleotide phosphate, reduced form
OPD	o-phenylenediamine
PH1	primary hyperoxaluria type 1
PH2	primary hyperoxaluria type 2
PHZ	phenylhydrazine hydrochloride
PTS	peroxisomal targeting signal
PAGE	polyacrylamide gel electrophoresis
RNA	ribonucleic acid
RT-PCR	Reverse transcriptase polymerase chain reaction
SDS	sodium dodecyl sulphate

Table of Contents

Chapter Index

List of Figures

CHAPTER ONE

CHAPTER THREE

CHAPTER FOUR

CHAPTER FIVE

CHAPTER SIX

CHAPTER SEVEN

CHAPTER EIGHT

List of Tables

CHAPTER ONE

CHAPTER TWO

CHAPTER THREE

CHAPTER FOUR

CHAPTER FIVE

CHAPTER SIX

CHAPTER SEVEN

Acknowledgements

Thanks go first and foremost to my project supervisor and mentor Dr. Gill Rumsby for her guidance, enthusiasm and inspiration over the last three years. I would also like to thank my second supervisor, Colin Samuell, for his support and interest in my research.

I would like to thank Tim Weir for his advice and help with technical aspects of this project, in particular the measurement of AGT activity. Thanks also to Professor Chris Danpure for donating the AGXT constructs and Joe Benham for providing the immuno-cytochemistry images of GO.

I also wish to express my gratitude to everyone in the department of Chemical Pathology at UCLH for use of the laboratory and equipment. In particular I would like to thank Dr. John Honour without whom I would never have met Gill and become interested in the primary hyperoxalurias. I would also like to thank the department of Molecular Pathology at UCL.

Finally, I would like to acknowledge the UCL Graduate School for providing me with a PhD scholarship and the Oxalosis and Hyperoxaluria foundation, whose funding enabled this research.

Chapter One

Introduction

1.1 Oxalate

1.1.1 Dietary intake and absorption of oxalate

1.1.2 Renal handling of oxalate

1.2 Endogenous Oxalate Production

1.2.1 Glyoxylate synthesis

1.2.2 Glyoxylate utilisation

1.3 Hyperoxaluria

1.4 Secondary Hyperoxaluria

1.5 Primary Hyperoxaluria

1.5.1 Primary hyperoxaluria type 1

1.5.2 Primary hyperoxaluria type 2

1.5.3 The treatment of primary hyperoxaluria

1.5.4 Atypical hyperoxaluria

1.6 Glycolate Oxidase

1.6.1 GO in plants

1.6.2 GO in animals

Oxalate, a dicarboxylic acid, is an end product of metabolism that is almost entirely excreted through the kidney. The anion is of pathological interest, because of its high affinity for calcium and its role in calcium oxalate stone disease. The metabolic pathways contributing to endogenous oxalate production are unclear. However, the observation of various inherited or acquired disorders leading to raised urinary oxalate has highlighted some of the enzymes involved.

The practical work of this thesis characterises human glycolate oxidase (GO, EC 1.1.3.15), an enzyme with a potentially pivotal role in oxalate synthesis in health and disease. Before focusing upon this enzyme in detail, a wider view of oxalate will be presented.

1.1 Oxalate

Oxalate (Figure 1.1) is found throughout nature, usually as the crystalline form of calcium oxalate, and has been ascribed various functions in both bacteria and plants. For example, it may play structural (Franceschi and Horner, 1980) and defensive (Hodgkinson, 1977) roles in plants and may provide an intracellular calcium pool (Kirkby and Pilbeam, 1984). In some bacteria, such as *Oxalobacter formigenes,* oxalate is an important carbon source (Allison *et al.*, 1995). In contrast, oxalate is an end point of metabolism in mammals where it appears to serve no apparent purpose and is generally regarded as a pathological nuisance. This pathology is due to the insolubility of its calcium salt at physiological pH, as reflected by the observation that calcium oxalate is a constituent of 67% of renal stones in the western world (Samuell and Kasidas, 1995).

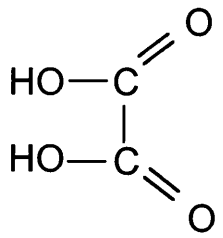

Figure 1.1 Oxalate

In humans oxalate is derived from both exogenous and endogenous sources. There is no apparent mechanism to metabolise oxalate, and it is therefore excreted in the urine. Hence, increased levels of oxalate in the body will lead to increased levels in the urine i.e. hyperoxaluria. Factors determining the level of oxalate in the urine include dietary intake, gut absorption, renal handling and endogenous production (Williams and Wilson, 1990). In normal subjects the majority of urinary oxalate is derived from endogenous sources, with the diet contributing 10–20 % (Wandzilak and Williams, 1990). The metabolic pathways influencing endogenous oxalate production are discussed in detail in section 1.2. The exogenous factors that determine urinary oxalate levels are discussed below.

1.1.1 Dietary intake and absorption of oxalate

A normal diet contains 70–930 mg/day of oxalate, but in countries with a large amount of vegetables in the diet, intake may be up to 2000 mg/day (Williams and Wilson, 1990). Oxalate rich foods include spinach, rhubarb and chocolate (Kasidas and Rose, 1980), although only a small percentage of ingested oxalate is actually absorbed from the gastro-intestinal tract. The bulk of dietary oxalate is excreted in the faeces complexed to calcium or is degraded by gut flora such as *Oxalobacter formigenes* (Allison *et al.*, 1986). The extent to which oxalate is soluble in the gut lumen appears

to determine its absorption, for example sodium oxalate, the more soluble form of oxalate, is more easily absorbed (Williams and Wilson, 1990).

Oxalate absorption appears to occur along the whole of the gastrointestinal tract, including the stomach (Hautman, 1993). Early studies suggested this absorption was by a non energy-dependent passive process (Binder, 1974). However, more recent work has demonstrated that the absorption of oxalate can occur by an active transport process. For example, oxalate absorption in exchange for hydroxyl and chloride anions has been shown in the brush border membrane of the rabbit ileum (Hatch and Vaziri, 1994; Hatch *et al.*, 1994). Oxalate transport in the colon may be influenced by the oxalate concentration gradient across the membrane and both secretory and absorptive processes have been documented. For instance, rats with experimentally induced chronic renal failure were found to secrete oxalate into the colon, suggesting this may be another route for oxalate removal (Hatch *et al.*, 1999). This process may also be aided by oxalate degrading microbes in the gut, scavenging dietary oxalate and creating a transepithelial gradient favouring oxalate secretion by the colon (Hatch and Freel, 1995).

1.1.2 Renal handling of oxalate

Oxalate is freely filtered by the glomerulus, although evidence is conflicting as to whether there is net tubular secretion or absorption. Early studies using ^{14}C oxalate to determine oxalate:creatinine ratios yielded mean values of 1.4 to 1.9 indicating net secretion (Williams *et al.*, 1971; Prenan *et al.*, 1981). More recent studies have shown net absorption in normal subjects, for example Kasidas and colleagues obtained a mean ratio of 0.59 in 24 hour urine collections (Kasidas *et al.*, 1990). The reasons for these

discrepancies are unclear, although individuals' oxalate:creatinine clearance ratios can vary widely on a daily basis (Kasidas *et al.*, 1990).

Oxalate transport across the apical (facing tubule lumen) and basolateral (facing blood supply) membranes of the kidney proximal tubules is mediated by anion-exchange mechanisms. Several transport proteins capable of oxalate transport have been identified in mammalian proximal tubules. These include a sulphate/oxalate exchanger, chloride/oxalate exchanger and hydroxyl/oxalate exchanger on the apical membrane (Karniski and Aronson, 1987; Kuo and Aronson, 1996) and a sulphate/oxalate exchanger on the basolateral membrane (Kuo and Aronson, 1988). Studies using isolated membrane vesicles from rat and rabbit have shown that oxalate may participate in transcellular NaCl reabsorption in the tubules (reviewed in Aronson and Giebisch, 1997). However, whether oxalate exchangers play a role in maintaining salt reabsorption along the nephron *in vivo* remains to be established.

1.2 Endogenous Oxalate Production

Glyoxylate (Figure 1.2) is produced in peroxisomes from glycolate by the action of GO. This anion is the major endogenous precursor of oxalate, and it has been estimated that as much as 50–60 % of urinary oxalate is synthesised in the liver from glyoxylate (Wandzilak and Williams, 1990). Hence, the investigation of glyoxylate metabolism is central to the field of hyperoxaluria, as demonstrated by the huge overproduction of oxalate that ensues in inborn errors affecting glyoxylate metabolism. These inherited diseases, the primary hyperoxalurias, are caused by a functional deficiency of either of two enzymes important for glyoxylate detoxification, namely alanine: glyoxylate aminotransferase (AGT, EC 2.6.1.44) and glyoxylate reductase /hydroxypyruvate reductase (GRHPR, EC 1.1.1.79) (Danpure and Jennings, 1986; Mistry *et al.*, 1988). The chemical structures of the 2 and 3 carbon compounds of glyoxylate metabolism are depicted in Figure 1.2.

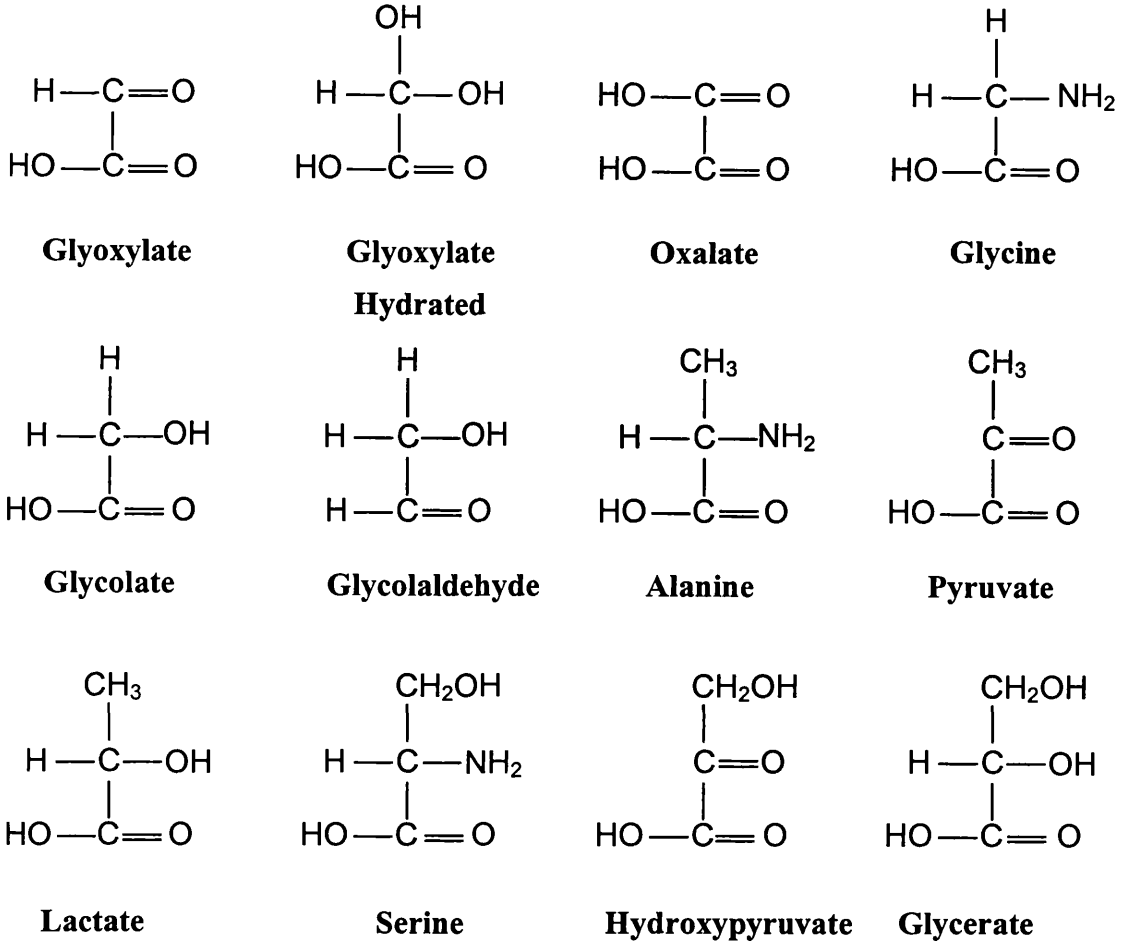

Figure 1.2 Chemical structures of the 2/3 carbon compounds of glyoxylate metabolism.

1.2.1 Glyoxylate synthesis

Glycolate and glycine are the immediate precursors of glyoxylate, their metabolism catalysed by GO (also known as L-α-hydroxy acid oxidase A) and D-amino acid oxidase (DAO or glycine oxidase, EC 1.4.3.3) respectively. Both enzymes are peroxisomal flavin oxidases and yield hydrogen peroxide as a reaction product, which is rapidly removed by peroxisomal catalase. The relative importance of the enzymes is not

clear, but it has been reported for human liver that the activity of DAO is higher than GO (Danpure and Purdue, 1995). However, studies with these enzymes purified from hog kidney found DAO to have a K_m of 60 mM for glycine as substrate (Neims and Hellerman, 1962), and GO a K_m of 0.3 mM for glycolate as substrate (Tokushige and Sizer, 1967). Studies in isolated peroxisomes from guinea pig liver found that glycine oxidation contributed 5% to glyoxylate and oxalate production, relative to the oxidation of glycolate (Poore *et al.*, 1997). Furthermore, in isolated perfused rat liver 60% of absorbed glycolate was converted to oxalate compared to 4% of absorbed glycine (Liao and Richardson, 1972). These findings suggest that DAO activity does not make a significant contribution to the glyoxylate pool and that glycolate is the more important precursor of glyoxylate.

The existence of some minor carbohydrate pathways leading to glyoxylate synthesis has been highlighted by a number of iatrogenic instances involving administration of xylitol, fructose and sorbitol. These sugars have in the past all been used in parenteral nutrition and they have been linked with hyperoxaluria and oxalosis (Thomas *et al.*, 1972; Ludwig *et al.*, 1984; Pfeiffer *et al.*, 1984). While these pathways have not been fully resolved, it is thought that the production of glycolaldehyde, a glycolate precursor, is involved. A xylulose pathway (James *et al.*, 1982) has been proposed in which D-xylulose formed from xylitol is phosphorylated by phosphofructokinase producing xylulose-1-phosphate. The xylulose-1-phosphate is then converted to glycolaldehyde, in a reaction catalysed by fructose-bisphosphate aldolase. The formation of glycolate from glycolaldehyde is catalysed by aldehyde dehydrogenase (EC 1.2.1.5) (Greenfield and Pietruszko, 1977). This reaction becomes significant in cases of ethylene glycol

poisoning, when large quantities of glycolaldehyde are formed by the action of alcohol dehydrogenase (EC 1.1.1.1) (Liao and Richardson, 1972). Inhibition of the latter enzyme with alcohol or fomepizole prevents excess glycolaldehyde synthesis and therefore inhibits oxalate production, following ingestion of ethylene glycol (Brent *et al.*, 1999; Jacobsen, 1999).

Several minor reactions may contribute to glyoxylate production in the liver, an example being hydroxyproline catabolism. This pathway yields 4-hydroxy-2-ketoglutarate, which is cleaved by 4-hydroxy-2-ketoglutarate aldolase (EC 4.1.3.16), a mitochondrial enzyme, to pyruvate and glyoxylate (Maitra and Dekker, 1964). Whether this pathway is of significance in man is unknown. Subjects given a large dose of hydroxyproline did not show a significant increase in oxalate excretion, although urinary glycolate and glyoxylate excretion did show a modest increase (Hockaday *et al.*, 1965). Hyperoxaluria is not observed in patients with conditions associated with increased collagen turnover, a finding that suggests hydroxyproline is not a significant oxalate precursor.

The aromatic amino acids tryptophan, phenylalanine and tyrosine may be metabolised to glyoxylate via glycine, but this contribution is minimal (Gambardella and Richardson, 1977). Hydroxypyruvate, an intermediate of serine metabolism, may be decarboxylated to form glycolaldehyde in a reaction catalysed by hydroxypyruvate decarboxylase (EC 4.1.1.40). The activity of this enzyme has been found localised in the mitochondria and cytosol of rat liver (Rofe *et al.*, 1986). Serine is also a source of the glycolaldehyde precursor ethanolamine. The glycolaldehyde produced as a result of these reactions is converted to glycolate by the action of aldehyde dehydrogenase. The significance of

these minor pathways in human liver is not known as they have only been studied in rats. The pathways of mammalian glyoxylate metabolism are summarised in Figure 1.3.

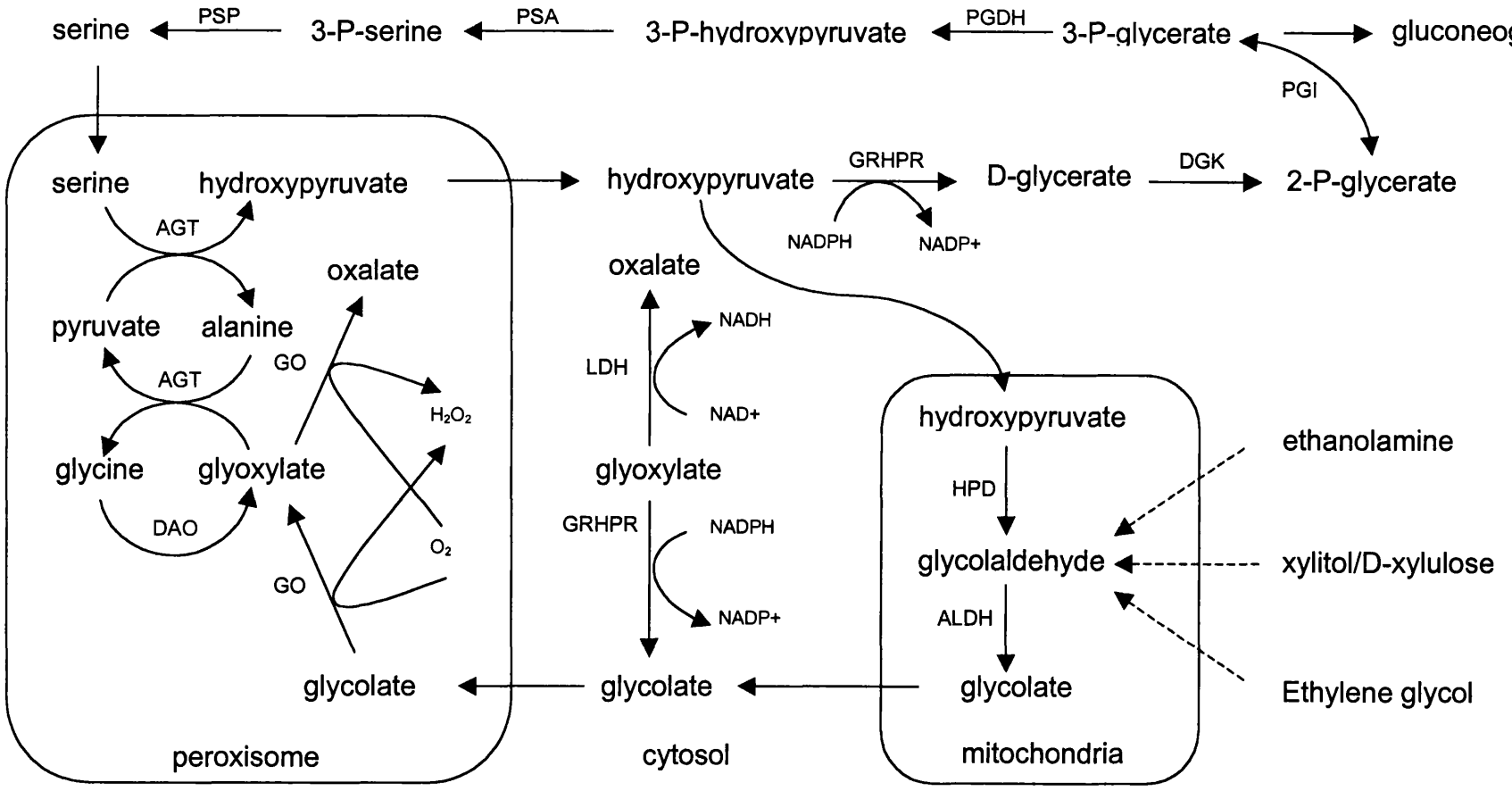

Figure 1.3 The pathways of mammalian glyoxylate metabolism. *(Enzyme abbreviations are listed on pages 4–5).*

In plants, glyoxylate is produced as an intermediate in the glyoxylate cycle as depicted in Figure 1.4.

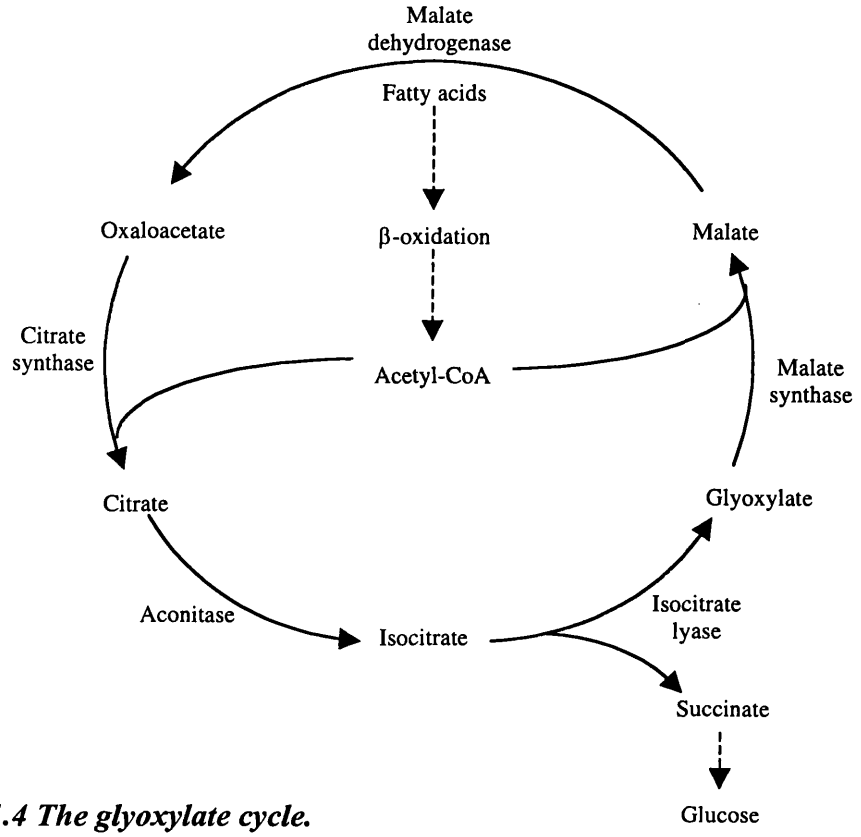

Figure 1.4 The glyoxylate cycle.

This cycle bypasses the decarboxylation steps of the tricarboxylic acid cycle and takes place in specialised peroxisomes known as glyoxysomes. These microbodies develop in lipid rich seeds, and contain enzymes that participate in the conversion of stored lipid to glucose. In glyoxysomes the β-oxidation of fatty acids is tightly coupled to the glyoxylate cycle to ensure a very high preservation of carbon derived from fatty acid breakdown and its conversion to glucose during seed germination. Once the plant acquires an ability to photosynthesise, glyoxysomes are replaced by peroxisomes lacking the glyoxylate cycle enzymes (Masters, 1997). Glyoxylate is formed from isocitrate by isocitrate lyase (EC 4.1.3.1) in a reaction that also produces succinate. The

glyoxylate is converted to malate in a reaction catalysed by malate synthase (EC 4.1.3.2) and the succinate is converted to hexose sugars (Tolbert, 1981).

While the glyoxylate cycle functions in bacteria and fungi as well as plants, it is generally accepted that it does not function in animals (Tolbert, 1981). However, there are several reports in the literature of the existence of isocitrate lyase and malate synthase in animal tissues. These studies include detection of enzyme activities in the brown adipose tissue of the hibernating black bear (Davis *et al.*, 1990) and in the livers of starved rats (Popov *et al.*, 1996) and rats with alloxan induced diabetes (Popov *et al.*, 1998). However, another study could find no evidence of either enzyme in the livers of guinea pig, rat or chick embryo (Holmes, 1993). The activities of both glyoxylate cycle enzymes have been detected in human liver and malate synthase was found to be immunolocalised to the peroxisome (Davis and Goodman, 1992). These findings suggest that some animals may possess the capacity to convert lipid to glucose by the glyoxylate cycle. However, whether this pathway plays a significant role in human glyoxylate metabolism is not known.

1.2.2 Glyoxylate utilisation

Several enzymes capable of the oxidation of glyoxylate to oxalate are present in the mammalian cell. These are peroxisomal GO and xanthine oxidase (XAO, EC 1.1.3.22) and the cytosolic enzyme lactate dehydrogenase (LDH, EC 1.1.1.27). If glyoxylate is allowed to accumulate it may be oxidised to oxalate, a toxic end product of metabolism, by the action of these enzymes. Glyoxylate itself is a very reactive and potentially biochemically toxic molecule, for instance it interferes with ribulose bisphosphate

carboxylase/oxygenase (RUBISCO, EC 4.1.1.39) in plants (Campbell and Ogren, 1990) and has been found to be toxic to animals (Barnes and Lerner, 1943). Therefore, it is essential that pathways exist for glyoxylate removal. Under normal circumstances, two enzymes appear to play a role in minimising oxalate synthesis from glyoxylate by diverting it along other pathways. These enzymes are peroxisomal AGT and cytosolic GRHPR, deficiencies of which cause primary hyperoxaluria types 1 and 2 respectively (Danpure and Jennings, 1986; Mistry *et al.*, 1988). A third enzyme, glutamate: glyoxylate aminotransferase (GGT, EC 2.6.1.4), localised in the cytosol, may also play a role in preventing glyoxylate accumulation and therefore oxalate production (Thompson and Richardson, 1966).

The glyoxylate produced by the GO catalysed oxidation of glycolate is converted to glycine, in a reaction catalysed by the pyridoxine-5'phosphate dependent enzyme AGT (Thompson and Richardson, 1967). This is a transamination reaction in which glyoxylate acts as an amino acceptor from alanine, the latter being deaminated to form pyruvate. AGT also catalyses the transfer of an amino group from serine to pyruvate (SPT activity) forming the gluconeogenic precursor hydroxypyruvate (Noguchi *et al.*, 1978). In humans AGT is liver specific (Kamoda *et al.*, 1980) and is normally located within the peroxisome (Cooper *et al.*, 1988). This intracellular location allows it to remove potentially toxic glyoxylate efficiently by its conversion to glycine. The K_m of pure recombinant human AGT for glyoxylate has been found to be 0.23 mM (Lumb and Danpure, 2000) in comparison to a K_m of 3.54 mM for GO purified from human liver (Fry and Richardson, 1979a). Therefore, it seems unlikely that GO would contribute to oxalate production providing adequate AGT were available to utilise the glyoxylate.

The sub-cellular location of AGT is species dependent and appears to be correlated with dietary habits. In herbivores such as rabbit it is entirely peroxisomal (Danpure *et al.*, 1990), whereas in carnivores, for example dog, it is entirely mitochondrial (Okuno *et al.*, 1979). In some rodents AGT is found in the peroxisome and mitochondria (Noguchi *et al.*, 1979). Mitochondrial AGT is induced by glucagon (Oda *et al.*, 1982) and is thought to play an important role in gluconeogenesis. In comparison, peroxisomal AGT is thought to be important in the detoxification of glyoxylate (Danpure and Jennings, 1986). However, *in vivo* studies in rabbit have shown that peroxisomal AGT activity contributes as much as 90% towards gluconeogenesis from serine (Xue *et al.*, 1999). The peroxisomal enzyme therefore appears to have a dual role, producing gluconeogenic precursors from serine and removing glyoxylate, thereby preventing harmful over production of oxalate (Xue *et al.*, 1999). An herbivorous diet gives an increased glycolate load, as a result of the high levels of glycolate found in plant tissue (Harris and Richardson, 1980). In contrast, a carnivorous diet would produce less glycolate-derived glyoxylate reducing the need for glyoxylate detoxification by peroxisomal AGT.

Another aminotransferase enzyme is GGT, which is localised in the cytosol and catalyses the transfer of an amino group from glutamate to glyoxylate, producing 2-oxoglutarate and glycine (Thompson and Richardson, 1966). However, the activity of AGT is substantially greater than that of GGT in human liver (Thompson and Richardson, 1966). This difference in activity could lead one to conclude that GGT would be unlikely to play a significant role in glyoxylate metabolism. However, given that GGT and AGT reside in different intracellular compartments they will not be competing for substrate, GGT may therefore play a role in maintaining low glyoxylate

concentrations in the cytosol. The transaminase reactions involving glyoxylate are depicted in figure 1.5.

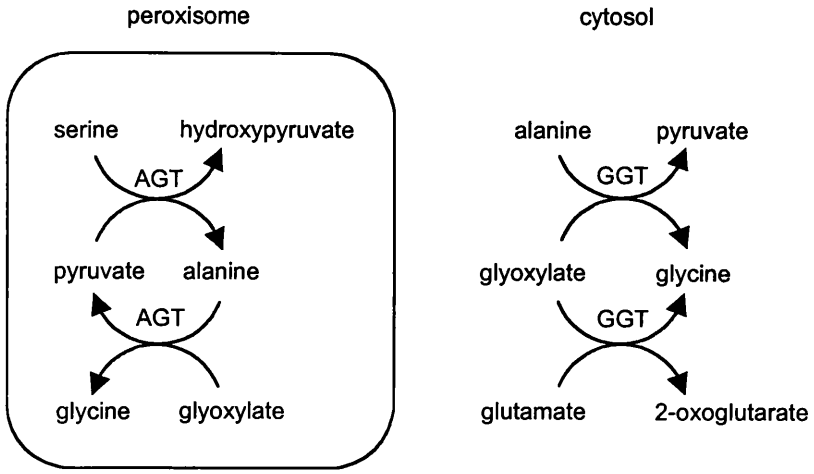

Figure 1.5 The transaminase reactions involving glyoxylate.

In the cytosol glyoxylate is reduced to glycolate by the action of GRHPR, using NADH or NADPH as a cofactor. In addition to glyoxylate reductase (GR) activity, this enzyme also has hydroxypyruvate reductase (HPR) and D-glycerate dehydrogenase (D-GDH) activities, the latter two being reciprocal reduction and dehydrogenation reactions (Dawkins and Dickens, 1965; Willis and Sallach, 1962). The ratio of NADPH (0.3 μmol/g fresh weight) to NADP (0.067 μmol/g fresh weight) in rat liver would favour reduction reactions (Williamson and Brosnan, 1974). Based upon this reducing environment in the cell and the findings of kinetic studies it is now thought that *in vivo* the enzyme functions as an NADPH dependent reductase (Van Schaftingen *et al.*, 1989). Given the lesser importance of the D-GDH reaction, the single protein catalysing the GR, HPR and D-GDH reactions is now referred to as GRHPR. The reactions catalysed by GRHPR are depicted in Figure 1.6.

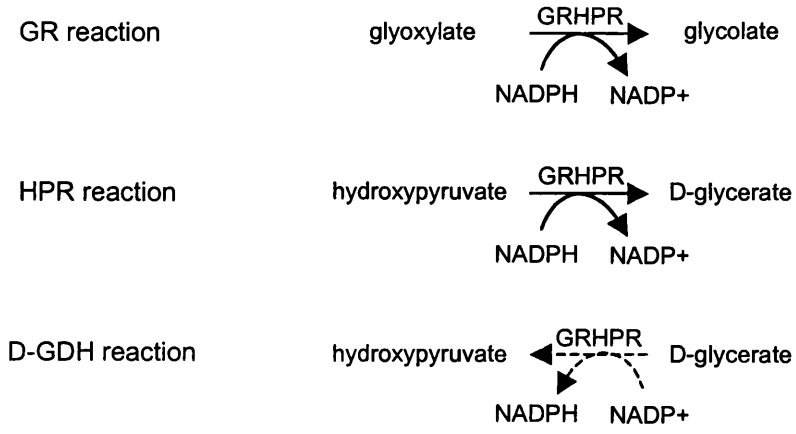

Figure 1.6 The reactions catalysed by GRHPR

That GRHPR functions as a reductase, and not a dehydrogenase, is supported by findings of studies in individuals with D-glyceric aciduria (D-glycerate kinase deficiency) given a serine load. The serine is converted to hydroxypyruvate, but lacking D-glycerate kinase they are unable to convert the D-glycerate formed by HPR action into 2-P-glycerate. Therefore, these patients excrete gram amounts of D-glycerate in the urine (Van Schaftingen, 1989). This observation suggests that the reaction converting D-glycerate to hydroxypyruvate (D-GDH activity) is energetically unfavourable. Otherwise one would expect L-glycerate to be excreted as a consequence of the action of LDH upon the excess hydroxypyruvate produced. These reactions are depicted in Figure 1.7.

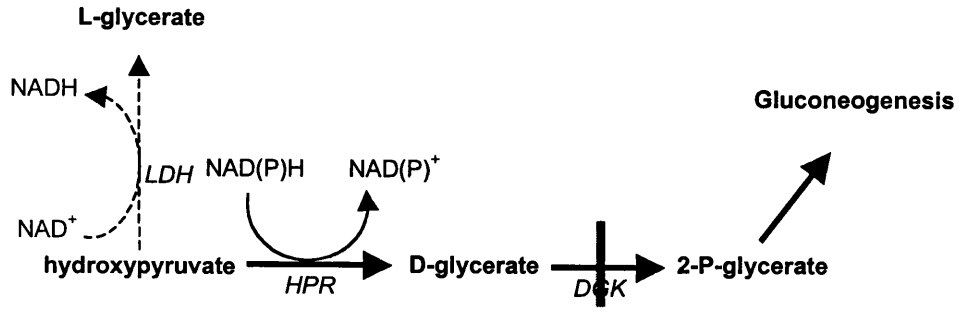

Figure 1.7 D-glycerate kinase (DGK, EC 2.7.1.31) deficiency. *The conversion of D-glycerate to 3-P-glycerate is blocked; D-glycerate accumulates and is excreted in the urine.*

The cytosolic enzyme LDH catalyses glyoxylate oxidation, in a reaction involving the dismutation of two molecules of glyoxylate to one of glycolate and one of oxalate (Warren, 1970; Duncan, 1980). The rate of reaction of LDH with glyoxylate as substrate has been found to be as high as that for lactate for the pig heart and rabbit muscle isoenzymes (Sawaki *et al.*, 1967). However, the cytosolic lactate concentration is known to be orders of magnitude higher than that of glyoxylate (Yanagawa *et al.*, 1990; Funai and Ichiyama, 1986). GR has a lower K_m for glyoxylate than LDH with NADH as cofactor, suggesting it is the more significant reaction *in vivo* (Warren, 1970). This finding is consistent with the observation that patients deficient in various LDH isoenzymes do not have reduced urinary oxalate (Yanagawa *et al.*, 1990).

XAO is potentially capable of oxidising glyoxylate to oxalate, but it is not clear whether it makes a significant contribution to oxalate production *in vivo*. Xanthinuric patients have normal oxalate excretion, and the XAO inhibitor allopurinol had no effect upon oxalate excretion in subjects with gout (Gibbs and Watts, 1966). Studies of human liver supernatant found that allopurinol and pteridylaldehyde, another XAO inhibitor, had a

limited effect upon oxalate production (Gibbs and Watts, 1967). Based upon these findings it has been concluded that XAO does not contribute significantly to oxalate synthesis.

Being largely hydrated in aqueous solution, glyoxylate is a suitable substrate for GO in a reaction producing oxalate. Several studies have concluded that GO plays a significant role in oxalate production (Liao and Richardson, 1973 and 1978). These studies were however in rats, where several important differences in glyoxylate metabolism exist. For instance AGT in the rat is mitochondrial with little, if any, in the peroxisome (Danpure and Purdue, 1995) and the level of GO activity has been found to be ten fold higher in rat than in human (Vamecq and Draye, 1989). Furthermore, the rate of glyoxylate oxidation relative to glycolate for human GO has been found to be only 16% (Fry and Richardson, 1979a), compared to 40% in the rat (Ushijima, 1973). The roles of both GO and LDH in glyoxylate utilisation in the human liver are not fully resolved and further investigation is needed to assess their relative contributions to oxalate production.

1.3 Hyperoxaluria

Hyperoxaluria may be due to secondary (environmental) or primary (genetic) causes as listed in Table 1.1. The latter are disorders of glyoxylate metabolism and are discussed in detail in section 1.5. The secondary causes of hyperoxaluria are the subject of the following section.

Secondary hyperoxaluria
Increased oxalate intake
Decreased calcium intake
Enteric hyperoxaluria
Excessive ingestion of oxalate precursors
Ethylene glycol
Xylitol
Glycine irrigation
Methoxyfluorane anaesthesia
Pyridoxine deficiency
Primary hyperoxaluria
Primary hyperoxaluria type 1
Primary hyperoxaluria type 2
Atypical primary hyperoxaluria

Table 1.1 The causes of hyperoxaluria.

1.4 Secondary Hyperoxaluria

Secondary causes of hyperoxaluria are more common and as such should be excluded before primary causes are investigated. Increased ingestion of oxalate rich foods is a documented cause of hyperoxaluria (Finch *et al.*, 1981). However, the amount available for gastro-intestinal (GI) absorption will depend upon the form of oxalate and its solubility (Brinkley *et al.*, 1981). Since calcium complexes with oxalate in the gut lumen preventing its uptake, oxalate absorption is inversely related to the intraluminal calcium concentration. Therefore, calcium deficiency may lead to hyperoxaluria. Conversely it has been shown that an increased calcium intake while eating oxalate rich foods can prevent hyperoxaluria (Hess *et al.*, 1998). A high intake of dietary protein has been shown to increase oxalate, calcium and uric acid excretion (Robertson *et al.*, 1979) and epidemiological studies have found a positive correlation between protein intake and kidney stone formation (Robertson, 1990 and 1993).

Enteric hyperoxaluria is due to hyperabsorption of oxalate as a secondary effect of GI disturbances or surgery. It is associated with inflammatory bowel conditions, such as ulcerative colitis and Crohn's disease. In these diseases, excess oxalate is absorbed through the damaged cells of the bowel wall. In patients with steatorrhea (fat malabsorption) gut luminal calcium forms soaps with fatty acids leaving less ionised calcium to complex with oxalate and increased free oxalate available for intestinal absorption (Binder, 1974). A similar effect is seen in patients with small bowel resection or jejunoileal bypass who have excess bile acids reaching the colon (Hylander *et al.*, 1978). The bile acids are thought to increase oxalate absorption by increasing colonic permeability with respect to oxalate (Dobbins and Binder, 1976). Enhanced

oxalate secretion in the kidney (Verkoelen and Romijn, 1996), reduced secretory oxalate flux in the gut (Hatch *et al.*, 1994) and absence of intestinal oxalate degrading bacteria are also potential causes of enteric hyperoxaluria. The latter is thought to be a contributory factor to stone formation in cystic fibrosis patients, where enteric hyperoxaluria is observed secondary to pancreatic insufficiency (Hoppe *et al.*, 1998) and is aggravated by the loss of colonic *Oxalobacter formigenes* due to prolonged use of antibiotic therapy (Sidhu *et al.*, 1998).

Ethylene glycol and xylitol are potential causes of hyperoxaluria and calcium oxalate deposition when taken in excess. The metabolic routes by which these precursors lead to endogenous oxalate production have been discussed in section 1.2.1. Glycine solution is used as an irrigant in the transurethral resection of prostate (TURP). Post-operative hyperoxaluria, accompanied by hyponatraemia and raised urinary glycolate in some cases of TURP has been documented (Fitzpatrick *et al.*, 1981). However, in another study an IV infusion of glycine in ten normal volunteers failed to cause hyperoxaluria (Hahn and Sikk, 1994). The mechanism by which glycine irrigation leads to hyperoxaluria is not clear, given that glycine is thought not to be a major precursor of glyoxylate and oxalate *in vivo* (section 1.2.1). Post-operative hyperoxaluria and calcium oxalate deposition in the renal tubules has been associated with the 2-carbon anaesthetic agent methoxyfluorane. Two pathways of oxalate synthesis have been postulated, one via dichloroacetate and the other via difluorohydroxy-acetic acid (Mazze *et al.*, 1971).

Deficiency of pyridoxine, the cofactor of AGT and other transaminases is a potential cause of hyperoxaluria, although documented cases are rare (Williams and Wandzilak,

1989). The hyperoxaluria is due to impaired transamination activity, which will increase the amount of glyoxylate available for oxalate synthesis.

1.5 Primary Hyperoxaluria

The primary hyperoxalurias (PH) are rare, autosomal recessive disorders of glyoxylate metabolism leading to oxalate overproduction (Danpure, 2001). Since oxalate is an end product of metabolism, normally excreted via the kidney into the urine, its increased production in PH is accompanied by hyperoxaluria. The tendency of oxalate to complex with calcium forming a low solubility salt is responsible for the pathologic features of the disease. These features are urolithiasis (stone formation) and nephrocalcinosis (deposition in the kidney) thereby reducing renal function and leading ultimately to end stage renal failure. The consequent retention of oxalate leads to systemic oxalosis in virtually all areas of the body, but particularly in calcium rich tissues such as bone. Two forms of PH have been documented, PH1 (MIM 259900) and PH2 (MIM 260000); the former is caused by AGT deficiency (Danpure and Jennings, 1986) and the latter by GRHPR deficiency (Mistry *et al.*, 1988). It is possible that other forms of less clearly defined hyperoxaluria may eventually be considered as other variants of PH.

1.5.1 Primary hyperoxaluria type 1

PH1 displays a wide clinical heterogeneity in terms of age at onset of symptoms and rate of disease progression. Furthermore, there are marked variations in the relative contribution made by each of the disease sequelae and in the degree of hyperoxaluria and hyperglycolic aciduria (Danpure, 1991). At one extreme of the clinical spectrum is the neonatal form of the disease, which typically presents in the first few months of life

with renal failure due to nephrocalcinosis, but without urolithiasis (Leumann, 1985). Death frequently follows within one year due to the complications of oxalosis. At the other extreme, there are some patients with the more common progressive form of the disease who may remain asymptomatic until middle age.

The exact incidence rate of PH1 is not known, however several estimates have been reported in the literature. In France the average prevalence rate was calculated to be 1.05 per 10^6 individuals and the average incidence rate 0.12 per 10^6 per year (Cochat *et al.*, 1995). Another study estimated the incidence of renal failure due to PH1 to be 1 in 5 x 10^6 to 15 x 10^6 between 0 and 15 years of age (Latta and Brodehl, 1990). It is likely that these values underestimate the true incidence of the disease, given its wide clinical spectrum and the lack of investigation of metabolic abnormalities in adult patients presenting with recurrent renal stones.

PH1 is characterised biochemically by hyperoxaluria and usually, but not always, hyperglycolic aciduria (Danpure, 2001). These are due to the metabolic consequences of the AGT deficiency. In the absence of AGT, glyoxylate may be oxidised to oxalate within the peroxisomes by GO. Alternatively, the glyoxylate may diffuse into the cytosol, where it is oxidised to oxalate by LDH and reduced to glycolate by GRHPR (Danpure and Jennings, 1986; Danpure, 1989). Hence, the concentrations of oxalate and glycolate in body fluids will increase resulting in hyperoxaluria and hyperglycolic aciduria. A model of hepatic glyoxylate metabolism in PH1 is depicted in Figure 1.8.

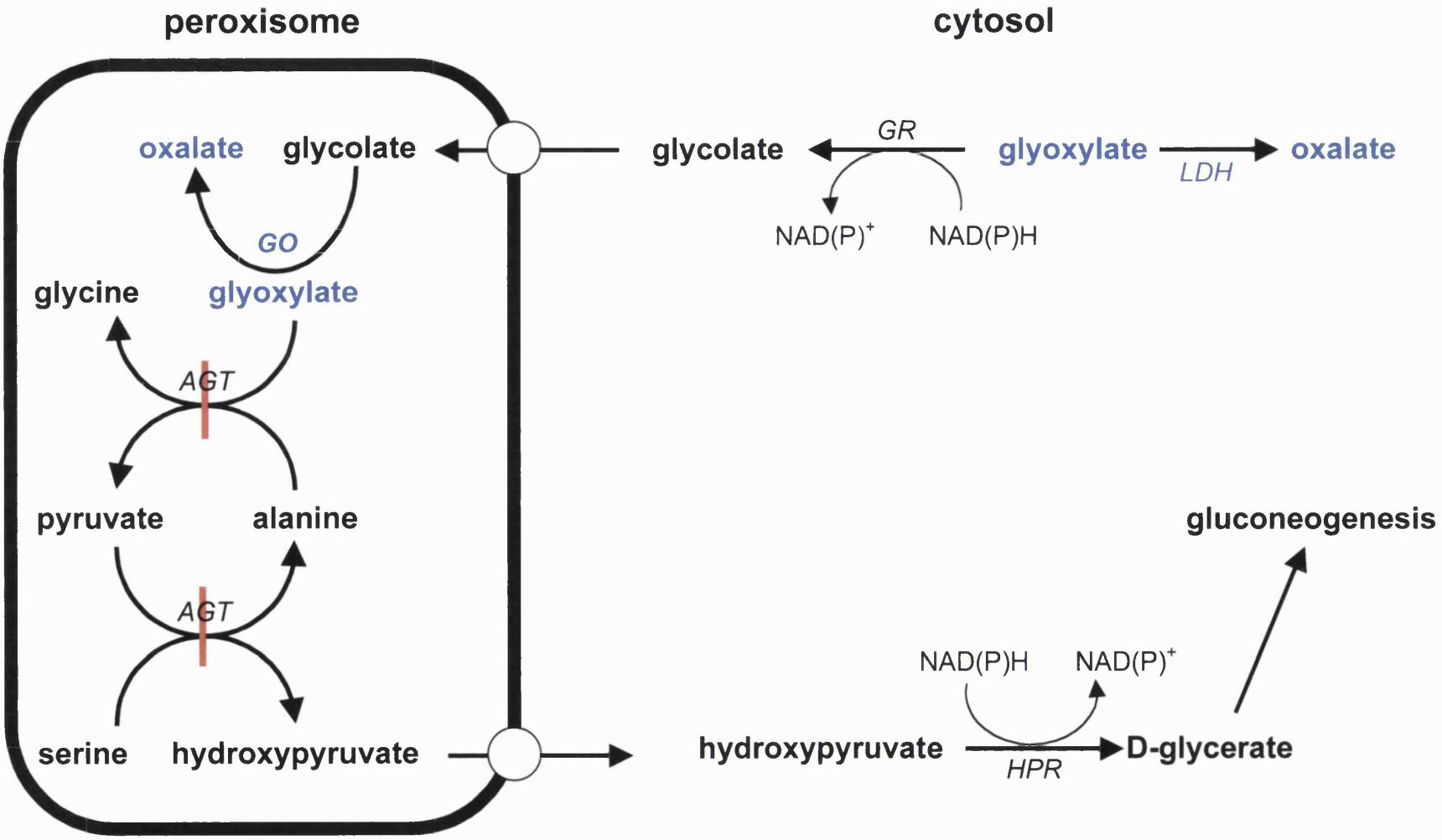

Figure 1.8 Hepatic glyoxylate metabolism in PH1. *AGT deficiency leads to the accumulation of glyoxylate, which is converted to oxalate by the pathways shown in blue.*

The first case report of a patient with PH1 was published in 1925, although the disease was not described in detail until twenty-five years later (reviewed in Danpure and Purdue, 1995). Given the excessive oxalate production in PH1, attempts to establish the metabolic basis of the disease were focused upon the metabolism of glyoxylate, the major precursor of oxalate. The presence of both raised oxalate and glycolate were not consistent with deficiencies in enzymes carrying out glyoxylate oxidation and reduction respectively. Therefore, attention was directed towards enzymes catalysing the transamination of glyoxylate. Several *in vivo* studies showed an inverse relationship between oxalate synthesis and glyoxylate transamination (reviewed in Danpure, 1989). However, *in vitro* studies initially failed to show reduced transamination of glyoxylate in PH1 patients' liver homogenates (Wyngaarden and Elder, 1966; Crawhall and Watts, 1962a and 1962b).

In 1962 another metabolic route for glyoxylate was discovered involving the decarboxylation of glyoxylate and 2-oxoglutarate, in a reaction catalysed by carboligase (CL, EC 4.1.3.15) (Crawhall and Watts, 1962a). However, levels of activity of this enzyme were found to be unaltered in mitochondria prepared from patients with PH1 compared to normal controls (Crawhall and Watts, 1962b). Subsequently, a cytosolic form of CL was found to be deficient in liver, kidney and spleen homogenates prepared from PH1 patients (Koch and Stockstad, 1966). However, several studies failed to demonstrate reduced cytosolic CL activity in PH1 patients (Bourke *et al.*, 1972; Danpure *et al.*, 1986) and investigation into glyoxylate aminotransferases continued.

With the purification and characterisation of human liver AGT and GGT a possible role for either of the enzymes in the aetiology of PH1 was postulated, (Thompson and Richardson, 1966 and 1967). Subsequently, it was shown that several enzymes involved in glyoxylate metabolism were concentrated in the peroxisomes (De Duve and Baudhuin, 1966). As a result of these findings, a role for peroxisomes in the pathogenesis of PH1 was proposed (Vandor and Tolbert, 1970; Tolbert, 1981). Subsequently AGT, the most important enzyme for glyoxylate transamination, was found to be localised to the peroxisomes (Noguchi and Takada, 1978 and 1979).

Definitive evidence for AGT deficiency as the cause of PH1 was obtained in 1986 when peroxisomal AGT deficiency was demonstrated in the livers of two PH1 patients (Danpure and Jennings, 1986). This deficiency was also found in the livers from a further twenty patients (Danpure and Jennings, 1988) and has now been documented in over 150 PH1 patients (Danpure *et al.*, 1994a; Danpure and Rumsby, 1995). The loss of AGT activity is accompanied by a deficiency in SPT activity, since the same protein catalyses both reactions (Noguchi *et al.*, 1978). Many PH1 patients have also been shown to be deficient in immunoreactive AGT protein (Wise *et al.*, 1987; Danpure, 1991).

It is possible to categorise PH1 into four types based upon the immunoreactivity (CRM) and catalytic activity (ENZ) of AGT (Danpure *et al.*, 1994a). 40% have no immunologically detectable AGT and no catalytic activity (CRM^-/ENZ^-). Absence of catalytic activity, but with immunologically detectable AGT is seen in 16% (CRM^+/ENZ^-). 41% have both immunological and enzymic activity (CRM^+/ENZ^+), in

most cases of which the AGT is mistargeted to the mitochondria. ~3% have a mistargeting variation in which the AGT is equally distributed between the mitochondria and peroxisome, but in the peroxisomes it is aggregated into unusual core-like structures (Danpure *et al.*, 1993).

The AGT gene (designated AGXT) has been cloned from normal liver, comprises 11 exons covering 10 kb and maps to chromosome 2q36-q37 (Takada *et al.*, 1990). The cDNA isolated from a HepG2 library contains an open reading frame of 1179 nucleotides and encodes a 392 residue polypeptide with predicted molecular mass of 43 kDa (Takada *et al.*, 1990). To date more than forty mutations have been described for the gene (reviewed in Danpure, 2001).

AGT exists in two main polymorphic variants, one encoded by the major AGXT allele and the other by the minor AGXT allele (Danpure *et al.*, 1994a). A common C154T polymorphism together with an A1142G change (leading to an Ile340Met substitution) and a 74 bp duplication in intron 1 constitute the minor AGXT allele, which has a frequency of 15–20 % in Caucasian populations (Danpure *et al.*, 1994a). There is also a polymorphic variable number tandem repeat (VNTR) in intron 4, with four possible variations in the number of copies of a 29/32 bp repeating unit (Danpure *et al.*, 1994b). The minor allele is always found on the background of the type 1 variation, which has 38 copies of the repeating unit (Tarn *et al.*, 1997). The frequencies of the minor AGXT allele and the type 1 VNTR are much higher in PH1 patients than the normal population. This finding may have functional significance although in part reflects the high frequency of the G630A mutation that segregates with these polymorphisms (Danpure, 2001).

One of the mutations in the AGT gene leads to a PH1 phenotype where the protein is mistargeted to the mitochondria. Cloning of the gene from the liver of a PH1 patient with this mistargeting defect identified two base changes (Purdue *et al.*, 1990). The first was the common T154 polymorphism, which causes a Pro11Leu substitution and creates a weak mitochondrial targeting signal. When the polymorphism is combined with a Gly170Arg substitution caused by a G630A point mutation, which slows down dimerisation of the protein, AGT is mistargeted to the mitochondria (Leiper *et al.*, 1996). The T154 polymorphism encodes a protein with approximately 50% activity of the more common C154 allele, decreases the rate of dimerisation under some conditions and sensitises the protein to the effects of several other mutations besides the G630A mutation (Lumb and Danpure, 2000).

The crystal structure of AGT has recently been resolved at 0.28 nm resolution (Zhang *et al.*, 2001). This has provided information on the three-dimensional structure of the enzyme and will lead to increased understanding of how the mutations exert their effects upon the AGT protein.

1.5.2 Primary hyperoxaluria type 2

The presenting features of PH2 are similar to PH1 and are the consequences of hyperoxaluria, including hematuria, renal colic and nephrolithiasis (Williams and Smith, 1968a; Chalmers *et al.*, 1984; Seargeant *et al.*, 1991; Johnson *et al.*, 2002). There are many more documented cases of PH1 than PH2 and the latter is thought to be more rare. However, it is probable that many patients with PH2 have in the past been incorrectly assumed to have PH1. This was mainly due to the lack of available assays for urine

glycolate and L-glycerate. For example, a re-evaluation of PH1 patients by Milliner and colleagues showed that 5 of 30 in fact had PH2 (Chlebeck *et al.*, 1994). Several reports in the literature have suggested that PH2 may be more common than previously thought (Chlebeck *et al.*, 1994; Marangella *et al.*, 1995; Milliner *et al.*, 1998 and 2001). PH2 has been shown to follow a more benign clinical course than PH1 (Milliner *et al.*, 2001; Johnson *et al.*, 2002). However, the potential for more serious sequelae is highlighted by the documentation of PH2 patients with nephrocalcinosis (Mansell, 1995; Kemper and Muller Wiefel, 1996) and end stage renal failure (Marangella *et al.*, 1995; Kemper *et al.*, 1997).

PH2 was first recognised as a separate entity from PH1 in 1968, when several patients were shown to have a deficiency of D-GDH in peripheral blood leucocytes (Williams and Smith, 1968a). D-GDH was known to function as a reductase with either hydroxypyruvate or glyoxylate as substrate (Dawkins and Dickens, 1965; Willis and Sallach, 1962) and it was subsequently shown that PH2 patients were deficient in both hepatic D-GDH and GR activities (Mistry *et al.*, 1988; Seargeant *et al.*, 1991). As discussed previously in section 1.2.2, studies of the mammalian enzyme found the HPR reaction to be more kinetically favourable than the reverse D-GDH reaction and it was concluded that the enzyme functions *in vivo* as a reductase (Van Schaftingen *et al.*, 1989). The HPR reaction is thought to be involved in the production of the gluconeogenic precursor D-glycerate from hydroxypyruvate and the GR reaction is important for the detoxification of glyoxylate by its reduction to glycolate (Mistry *et al.*, 1988).

Studies of GRHPR activity in crude tissue homogenates have revealed significant HPR activity in liver, kidney, leucocytes and fibroblasts, however GR activity was found predominantly in liver (Giafi and Rumsby, 1998a and 1998b). This finding is consistent with the importance of the GR reaction for glyoxylate removal in the liver to prevent its oxidation to oxalate. Chromatofocusing has been used to fractionate human liver HPR into two forms, one with GR activity and one without (Cregeen and Rumsby, 1999). This result indicates that at least two enzymes exist in liver with HPR activity that use NADPH as a substrate, but only one of these uses glyoxylate. The HPR activity of the peak without GR activity was most likely due to LDH, which has been found to use hydroxypyruvate with NADPH as cofactor, but not glyoxylate (Van Schaftingen *et al.*, 1989). This observation would account for the aforementioned differences in the tissue distribution of HPR and GR activity.

Biochemically PH2 is characterised by hyperoxaluria, usually accompanied by L-glyceric aciduria (Williams and Smith, 1968a; Chalmers *et al.*, 1984; Vilarinho *et al.*, 1993), although exceptions are starting to be recognised (Rumsby *et al.*, 2001). L-glycerate is an abnormal metabolite of hydroxypyruvate not usually found in urine, produced in PH2 as a result of hydroxypyruvate reduction catalysed by LDH (Williams and Smith, 1968a). Hepatic glyoxylate metabolism in PH2 is depicted in Figure 1.9.

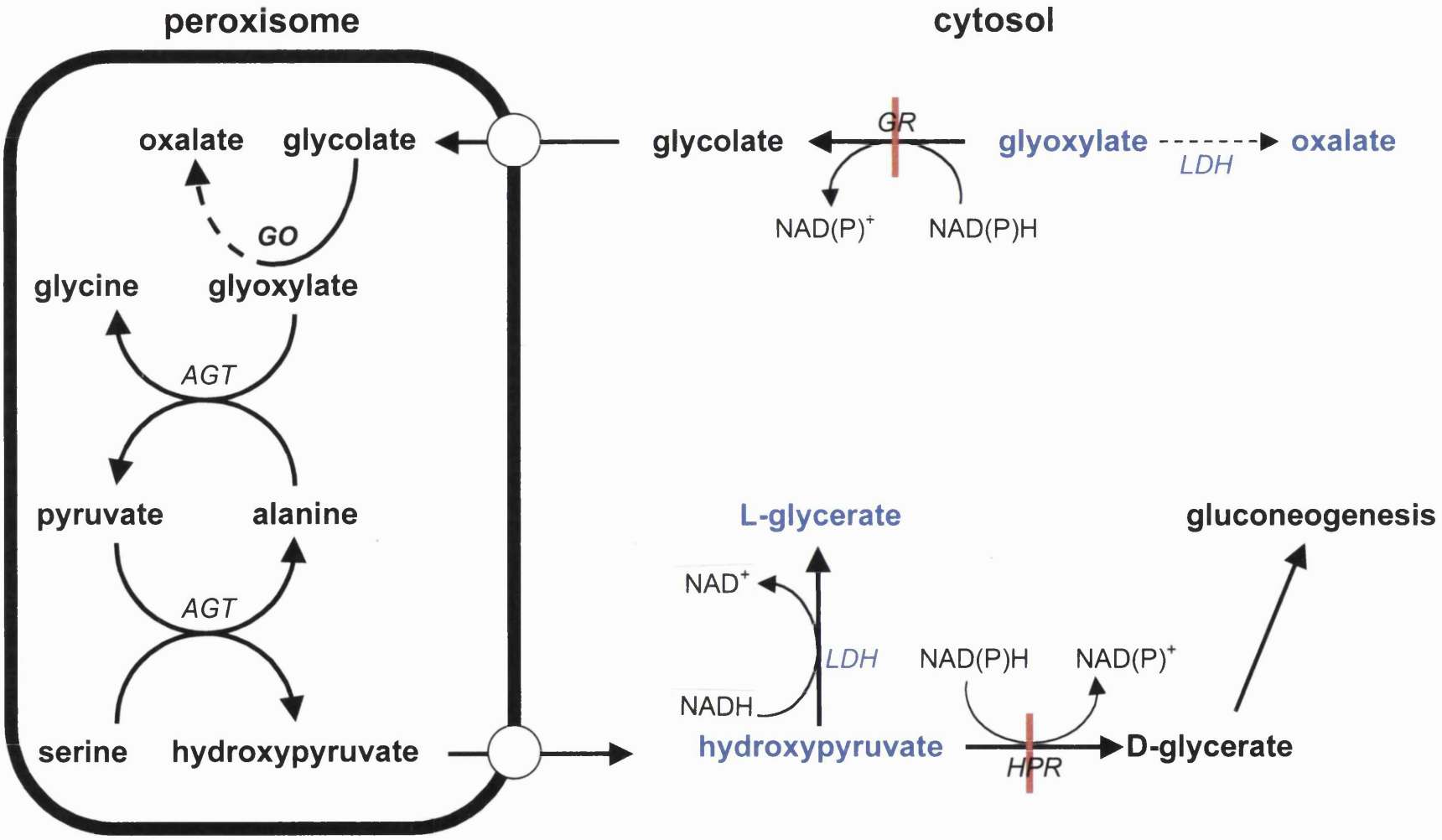

Figure 1.9 Hepatic glyoxylate metabolism in PH2. *GRHPR deficiency leads to accumulation of glyoxylate and hydroxypyruvate, which are converted to oxalate and l-glycerate respectively by LDH (reactions shown in blue).*

It is most likely that the hyperoxaluria of PH2 is due to failure of the GR catalysed reduction of glyoxylate and the subsequent oxidation of this organic acid to oxalate catalysed by LDH (Williams and Smith, 1968a; Gibbs and Watts, 1973; Mistry *et al.*, 1988). However, several other hypotheses have been advanced. These include the conversion of hydroxypyruvate to oxalate via glycolaldehyde and glycolate (Liao and Richardson, 1978). This reaction would seem unlikely given that hyperglycolic aciduria is not a feature of PH2 (Williams and Smith, 1968b) and most of the hydroxypyruvate produced would appear to be converted to L-glycerate. Another hypothesis suggests that a build up of hydroxypyruvate directly influences LDH, increasing its oxidative role and decreasing its reductive role due to a shift in the NADH/NAD ratio (Williams and Smith, 1971). This hypothesis is supported by *in vitro* studies of chicken liver LDH, which have shown that hydroxypyruvate promotes the oxidation of glyoxylate, thereby increasing oxalate production (Lluis and Bozal, 1977). Finally, it has been proposed that hydroxypyruvate can be auto-oxidised non-enzymatically to form oxalate (Raghavan and Richardson, 1983; Raghavan *et al.*, 1997).

The gene for GRHPR has been cloned and sequenced (Cramer *et al.*, 1998; Rumsby and Cregeen, 1999). The cDNA is 1235 bp in length with a predicted open reading frame of 987 bp and encodes a 328 amino acid protein of 40 kDa. Cells transfected with the cDNA showed HPR and GR (Rumsby and Cregeen, 1999) and D-GDH (Cramer *et al.*, 1999) activities. The gene comprises nine exons and eight introns and spans ~9 kb pericentromeric on chromosome 9 (Cramer *et al.*, 1999). To date six mutations in the GRHPR gene leading to PH2 have been described in the literature. Screening of eleven patients by polymerase chain reaction single stranded conformation polymorphism

(PCR-SSCP) analysis and sequence analysis identified 6 novel mutations including missense, nonsense and deletion mutations (Cramer *et al.*, 1999; Webster *et al.*, 2000). The missense mutations were found to result in a dysfunctional GRHPR when expressed *in vitro* (Webster *et al.*, 2000).

Traditionally the two forms of PH have been distinguished on the basis of the presence of organic acids in urine. Hyperglycolic aciduria is indicative of PH1 and L-glyceric aciduria indicative of PH2. However, not all PH1 patients have raised urinary glycolate and a case of a PH2 patient without raised urinary L-glycerate has recently been reported (Rumsby *et al.*, 2001). Therefore, for the definitive diagnosis of PH it is necessary to measure hepatocyte enzyme activities of AGT and GRHPR. Methods are now available which allow both enzyme activities to be measured in a single liver needle biopsy (Rumsby *et al.*, 1997; Giafi and Rumsby, 1998a). The accurate diagnosis of PH is important for the therapeutic management of patients with the disease and there follows a discussion of the treatment of PH.

1.5.3 The treatment of primary hyperoxaluria

The treatment of PH in the early stages of disease progression is preventative conservative management, aimed at decreasing oxalate production and increasing urinary calcium oxalate solubility. Urinary oxalate concentration exceeding 0.4 mM increases the risk of stone formation, especially if urinary calcium exceeds 4 mM (Cochat and Basmaison, 2000). Therefore, treatment is aimed at keeping oxalate and calcium levels below these limits. This treatment includes maintaining a generous fluid intake to increase urine volume to produce an output of 3 litres per 24 hours (Watts,

1994a) and the use of calcium oxalate crystallisation inhibitors primarily citrate, magnesium or orthophosphate. Citrate binds calcium thereby inhibiting calcium oxalate crystal nucleation and growth (Leumann *et al.*, 1995) and has been shown to be effective in adult and paediatric patients (Leumann *et al.*, 1993). Magnesium reduces oxalate solubility in the renal tract by forming magnesium oxalate, which is 50 times more soluble than calcium oxalate (Hodgkinson, 1977). Orthophosphate is widely used to treat patients with other forms of hyperoxaluria (Watts, 1994b) and has been associated with preservation of renal function in PH1 patients (Milliner *et al.*, 1994).

Administration of pyridoxine, the cofactor of AGT, has been shown to be an effective treatment for some PH1 patients (Gibbs and Watts, 1970). This has been found to significantly reduce urinary oxalate excretion in 20% of patients (Kopp and Leumann, 1995), those most likely to respond having residual activity (Marangella, 1999). Usually pharmacological doses have to be administered of 450–1000 mg/24 hours in equally divided doses (Watts, 1994b). Responsiveness is defined as a greater than 30% reduction in urinary oxalate excretion from baseline after stepwise increase of daily dosage of pyridoxine (5–10 to15–20 mg/kg after several weeks) (Leumann and Hoppe, 1999). It is recommended that responsiveness be assessed before committing to long-term pyridoxine therapy as high doses of pyridoxine carry a risk of neuropathy (Watts, 1998). It is impossible to predict which patients will respond to pyridoxine and not all those with residual activity (which correlates with the mistargeting defect) are responsive (Danpure, 2001). The molecular mechanism of pyridoxine action is not fully understood, but it may act by boosting AGT activity or via the activation of other transaminases in the cell.

Although dietary restriction of foods containing oxalate is advocated in the treatment of other forms of hyperoxaluria, it is thought to have minimal effect in PH treatment. This is because dietary oxalate contributes little to the hyperoxaluria, given the extremely high levels of endogenous oxalate production. Therefore, it is usually sufficient to avoid foods with a very high oxalate content such as beetroot, spinach, rhubarb and strawberries (Kasidas and Rose, 1980). Calcium restriction is not recommended, since this would make less calcium available to bind oxalate in the gut to prevent its absorption (Leumann and Hoppe, 2001).

When the disease has progressed to end stage renal failure (ESRF) dialysis becomes necessary to treat the uraemia. However, neither peritoneal or haemodialysis can clear oxalate from the body at a pace to match its rate of synthesis resulting in calcium oxalate deposition throughout the body (Watts, 1998; Cochat and Basmaison, 2000). Therefore, dialysis is generally regarded as a temporary treatment while the patient is awaiting transplant. For PH1, three transplantation strategies have been adopted, these being renal only (Allen *et al.*, 1996), renal and hepatic (Watts *et al.*, 1987; Jamieson, 1998; Cochat *et al.*, 1999; Ellis *et al.*, 2001) and hepatic only (Gruessner, 1998). Renal transplants have been most successful in patients without significant oxalosis and who are pyridoxine responsive (Allen *et al.*, 1996; Marangella, 1999). Combined liver and kidney transplant replaces both the enzyme deficient liver and the damaged kidneys and is the preferred choice for patients with ESRF in Europe (reviewed in Jamieson, 1998). Whatever the transplant strategy, the outcome is improved when patients are transplanted early to limit systemic oxalosis (Cochat *et al.*, 1999).

1.5.4 Atypical hyperoxaluria

Several children have been described in the literature with moderate to marked hyperoxaluria, with or without nephrocalcinosis or urolithiasis, in the absence of any known secondary or primary cause. Van Acker and colleagues described two unrelated patients with hyperoxaluria and hyperglycolic aciduria in whom AGT activity and cellular localisation were normal (Van Acker *et al.*, 1996). The hyperoxaluria was in the range seen in PH1, was unresponsive to pyridoxine and both nephrocalcinosis and urolithiasis were absent. Presence of hyperoxaluria in other family members seemed to indicate an autosomal dominant inheritance. Another report documented six children with moderate hyperoxaluria and with urolithiasis present in four (Monico and Milliner, 1999). Urine glycerate and glycolate were normal as were hepatic AGT and GRHPR activities. Secondary causes of hyperoxaluria including excess dietary oxalate, pyridoxine deficiency and malabsorption had been excluded. Recently two further children have been identified with persistent hyperoxaluria and early onset bilateral calcium oxalate stone formation (Neuhaus *et al.*, 2000). Their urine glycolate and glycerate levels were normal and PH1 and PH2 had been excluded by liver biopsy analysis. Pyridoxine had no effect upon urinary oxalate excretion in these patients.

The novel hyperoxaluria described above has been termed 'atypical hyperoxaluria' (Monico and Milliner, 1999) and the degree of hyperoxaluria observed is suggestive of metabolic oxalate overproduction. It is therefore possible that these patients have an as yet undefined metabolic defect leading to excess oxalate synthesis. GO is a candidate enzyme for a third form of inherited hyperoxaluria. Firstly it is possible that a mutation in the GO gene could increase its affinity for glyoxylate, thereby increasing oxalate

production. Alternatively a deficiency of GO would be expected to lead to glycolate accumulation, which could result in excess oxalate production by as yet undefined pathways. GO deficiency could also lead to hyperglycolic aciduria without hyperoxaluria and patients with these symptoms have also been described in the literature (Craigen, 1996; Kist-van Holthe *et al.*, 2000).

1.6 Glycolate Oxidase

GO is a peroxisomal flavin mononucleotide (FMN) dependent enzyme that catalyses the oxidation of short chain α-hydroxy acids. Studies of the spinach enzyme indicate that the enzymatic reaction can be divided into 2 steps (Macheroux *et al.*, 1991). Firstly, the α-hydroxy acid is dehydrogenated to its corresponding α-keto acid by a two-electron transfer to the FMN. In order to retain catalytic function the reduced FMN must be reoxidised at the expense of an electron acceptor. Molecular oxygen is used as an electron acceptor in a second reaction step yielding hydrogen peroxide.

GO is a member of a family of α-hydroxy acid oxidases/dehydrogenases all of which specifically oxidise the L-isomer of α-hydroxy acids to their corresponding α-keto acids. These enzymes (summarised in Table 1.2) share a common active site arrangement and sequence motif (Le and Lederer, 1991; Lindqvist *et al.*, 1991) typically having between 30–50 % sequence identity. On the basis of these similarities the reductive half of the reaction is thought to proceed through the same mechanism for all members of the family (Stenberg *et al.*, 1995). However, the enzymes differ in the second stage of the reaction in terms of the ultimate oxidant used. GO and other oxidases utilise oxygen, whereas the dehydrogenases do not. In the case of yeast flavocytochrome b_2 (FCB_2) intramolecular haem receives the electrons from the FMN and these are ultimately passed on to cytochrome c (Appleby and Morton, 1954). Membrane associated bacterial dehydrogenases, such as mandelate dehydrogenase (MDH), transfer electrons from the flavin to a component of the electron transfer chain within the membrane (Xu and Mitra, 1999). While mechanistically similar in many

ways, the members of the α-hydroxy acid oxidase/dehydrogenase family have varying substrate specificities and intracellular localisation.

Flavoenzyme	Species	Localisation	Substrate	Reference
Flavocytochrome b_2	*Saccharomyces cerevisiae*	Mitochondrial intermembrane space	Lactate	(Ghrir and Becam, 1984)
Glycolate oxidase	*Spinacea*	Peroxisome	Short chain L-α–hydroxy acids	(Volokita and Somerville, 1987)
Hydroxy acid oxidase B	*Rattus*	Peroxisome	Long chain L-α–hydroxy acids	(Le and Lederer, 1991)
Lactate monooxygenase	*Mycobacterium smegmatis*	Cytoplasm	Lactate	(Giegal *et al.*, 1990)
Mandelate dehydrogenase	*Pseudomonas putida*	Bacterial membrane	L-mandelate	(Tsou *et al.*, 1990)

Table 1.2. The family of L-α-hydroxy acid oxidising flavoenzymes.

GO displays a number of features that are characteristic of the flavoenzymes. These features and the unique spectroscopic properties of the flavin have been utilised for enzymological studies of the α-hydroxy acid oxidases/dehydrogenases (reviewed in Massey and Hemerich, 1980 and Fraaije and Mattevi, 2000). Biochemical and enzyme mechanism studies have focused primarily on FCB_2 (Urban and Lederer, 1985; Reid *et al.*, 1988; Daff *et al.*, 1994; Rouviere *et al.*, 1997; Mowat *et al.*, 2000; Gondry *et al.*, 2001) and lactate mono-oxygenase (LMO) (Massey *et al.*, 1980; Ghisla and Massey, 1980; Muh *et al.*, 1994a, 1994b and 1994c). Spinach GO and yeast FCB_2 have been crystallised and are structurally the best characterised (Lindqvist, 1989; Xia and Mathews, 1990). More recent additions to the family are long chain hydroxy acid

oxidase B (HAO B) from rat kidney (Cromartie and Walsh, 1975; Le and Lederer, 1991) and MDHs from *Pseudomonas putida* (Tsou *et al.*, 1990) and *Rhodotorula graminis* (Illais *et al.*, 1998).

Two α-hydroxy acid oxidases have been described differing in their substrate specificities. GO, also referred to as hydroxy acid oxidase A (HAO A), shows a preference for short chain aliphatic α-hydroxy acids. It is found in plant peroxisomes (Tolbert, 1981) and has been isolated from several plant species, including spinach (Zelitch and Ochoa, 1953), tobacco (Kenten and Mann, 1952), pumpkin (Nishimura *et al.*, 1983) and pea (Kerr and Groves, 1975). GO has also been isolated from several animal species including rat (Kopp and Leumann, 1995), pig (Schuman and Massey, 1971a) and chicken (Dupuis *et al.*, 1990). The enzyme was first purified from human liver tissue in 1979 and found to have maximal activity with glycolate (Fry and Richardson, 1979a). HAO B is also peroxisomal, has specificity for long chain, aliphatic and aromatic α-hydroxy acids and has been isolated from rat kidney (Cromartie and Walsh, 1975; Duley and Holmes, 1976; Le and Lederer, 1991).

As with other peroxisomal proteins, GO is nuclear encoded and post translationally imported into the peroxisome. These proteins are directed to the organelle by a peroxisomal targeting signal (PTS), of which there are two types. Most peroxisomal proteins have PTS-1, which is a carboxy terminal tri-peptide based on a loose consensus Ser-Lys-Leu sequence (Gould *et al.*, 1989). PTS-2 is found at or near the amino terminus in the thiolases (Swinkels *et al.*, 1991; Preisig-Muller and Kindl, 1993) and malate dehydrogenase (Gietl, 1990). Of the HAO enzymes that have been sequenced all

have a PTS-1 type carboxy terminus, with some variation from the consensus. Spinach GO terminates in the sequence Ala-Arg-Leu (Volokita and Somerville, 1987), mouse liver GO in Ser-Lys-Ile (Kohler *et al.*, 1999) and HAO B of rat kidney terminates in Ser-Arg-Leu (Le and Lederer, 1991).

1.6.1 GO in plants

GO was first purified from tobacco leaves in 1952 (Kenten and Mann, 1952) and spinach leaves in 1953 (Zelitch and Ochoa, 1953). It was found to be a flavoprotein that catalysed the conversion of glycolate to glyoxylate. Results on the oxidation of glyoxylate were conflicting and it was not clear whether this activity was carried out by GO or another enzyme. However, spinach GO was subsequently shown to catalyse the production of oxalate from glyoxylate (Richardson and Tolbert, 1961). The same study also found that oxalate acts as a competitive inhibitor of GO, in particular of glyoxylate oxidation. It is now generally accepted that glycolate and glyoxylate are precursors of oxalate in plants with GO catalysing the oxidation of both.

GO is found in leaf peroxisomes, where it is involved in photorespiration as part of the so-called glycolate pathway (Tolbert, 1981). Photorespiration is the uptake of O_2 and the formation of CO_2 in light, resulting from glycolate synthesis in the chloroplast with subsequent peroxisomal and mitochondrial glycolate metabolism. GO catalyses the oxidation of glycolate to glyoxylate, which is rapidly converted to glycine by aminotransferase action. In the absence of an amino donor for the transamination reaction, glyoxylate can also be metabolised by spinach GO, to form oxalate (Morris

and Garcia-Rivera, 1955). Hence, by extrapolation, GO has been implicated as a possible factor in endogenous oxalate production in humans.

1.6.2 GO in animals

In most animals studied to date, GO is localised to the liver, with the exception of pig and hog (Tokushige and Sizer, 1967) where the enzyme is also found in kidney. Peroxisomes from pig kidney were found to contain both forms of hydroxy acid oxidase, whereas only GO was present in liver. Both enzymes oxidised L-α-hydroxyisocaproate, but only GO used glycolate, and lactate as substrates (McGroarty *et al.*, 1974). Similarly, rat liver GO was found to utilise glycolate, L-α-hydroxyisocaproate, lactate and glyoxylate (Ushijima, 1973). In addition to catalysing the oxidation of long chain α-hydroxy acids, rat kidney HAO B also catalyses the oxidative deamination of L-amino acids at comparable rates (Nakano *et al.*, 1967). This latter activity has not been observed with other hydroxy acid oxidases.

Many studies have been conducted to determine the role played by GO in oxalate production in rodents. The synthesis of oxalate from glyoxylate was completely inhibited by DL-phenyllactate, a competitive inhibitor of GO, in isolated perfused rat liver (Liao and Richardson, 1973). Furthermore, urinary oxalate excretion in rats is positively correlated with GO activity, but not LDH or XAO (Richardson, 1964; Sharma and Schwille, 1997; Yoshihara *et al.*, 1999). These findings are in contrast to *in vitro* studies, which have mainly concluded that LDH is the major contributor to oxalate production (Yanagawa *et al.*, 1990; Poore *et al.*, 1997). It has been suggested that GO

and LDH co-operate in the production of oxalate, the former being important for glycolate utilisation and the latter for glyoxylate metabolism (Asker and Davies, 1983).

The inhibition of GO and LDH in isolated rat hepatocytes reduced oxalate production from glycolate and glyoxylate, but did not abolish it completely (Ludt and Kindl, 1990). This finding supports the existence of other enzymes in the liver capable of oxalate production. A candidate enzyme is glycolate dehydrogenase (GDH, EC 1.1.99.14), which has been isolated from human liver and shown to convert glycolate to oxalate directly (Fry and Richardson, 1979b). However, an *in vitro* study of oxalate formation from glycolate failed to detect GDH activity in rat and human liver supernatants (Yanagawa *et al.*, 1990). This finding led the authors to suggest that the reaction measured in the original study represented the combined actions of GO and XAO. Furthermore, the reaction catalysed by GDH (direct conversion of an alcohol to a ketone) is thought to be energetically unfavourable (Holmes, 1998).

Clearly there is a need for further investigation of the possible role played by GO in the pathogenesis of primary hyperoxaluria. Unlike LDH, whose principal reaction is the oxidation of lactate, GO has a pivotal role in glyoxylate metabolism. It catalyses the production of glyoxylate from glycolate in the normal liver and may play a role in oxalate production in diseases such as PH1 where excess glyoxylate is present. The primary aim of this thesis is to identify the gene for human liver GO and characterise the protein encoded by that gene. The investigation of the role of GO in human glyoxylate metabolism, and in the production of oxalate in PH, will then be possible.

Chapter Two

General Methods

2.1 Introduction

2.2 Materials

2.2.1 Chemicals

2.2.2 Buffers

2.2.3 Bacterial media and antibiotics

2.3 Methods

2.3.1 Isolation of human liver RNA

2.3.2 Reverse transcription-polymerase chain reaction (RT-PCR)

2.3.3 TA cloning of PCR products

2.3.4 Sequencing

2.3.5 Northern blot analysis

2.3.6 Transfection into BL21 competent cells

2.3.7 Expression of recombinant protein in BL21 cells

2.3.8 Protein SDS-PAGE

2.3.9 Protein staining with Coomassie brilliant blue

2.3.10 Western blots of protein gels

2.3.11 Measurement of GO activity

2.3.12 Preparation of human tissue sonicates

2.3.13 Determination of protein concentration

2.3.14 DNA and protein analysis software

2.1 Introduction

All experimental methods were carried out according to standard laboratory procedures for control, spillage and disposal and in accordance with the relevant departmental safety policies (Immunology and Molecular Pathology, University College London; Chemical Pathology, UCL hospitals). Human tissue samples were obtained from UCL Hospitals Primary Hyperoxaluria diagnostic service. Ethical approval for these studies was obtained from the Joint UCL/UCLH committees on the ethics of human research.

The procedures described in this chapter are those commonly used within this thesis. Methods that were adapted and/or are specific to individual chapters are included within the relevant sections.

2.2 Materials

2.2.1 Chemicals

All reagents and chemicals were Analar grade, purchased from BDH Chemicals (Poole, UK) or Sigma Chemical Company (Poole, UK) unless otherwise stated.

2.2.2 Buffers

All buffers were prepared with deionised water and stored at 4 °C prior to use, unless indicated otherwise.

General buffers

Potassium phosphate

0.2 M stocks of K_2HPO_4 (34.836 g anhydrous K_2HPO_4 dissolved in 1 litre H_2O) and KH_2PO_4 (27.218 g anhydrous KH_2PO_4 dissolved in 1 litre H_2O) were mixed together to obtain the required pH, and the resulting solution was diluted to obtain the required concentration of phosphate.

Sodium phosphate

0.2 M stocks of Na_2HPO_4 (28.4 g anhydrous Na_2HPO_4 dissolved in 1 litre H_2O) and NaH_2PO_4 (24 g anhydrous NaH_2PO_4 dissolved in 1 litre H_2O) were mixed together to obtain the required pH, and the resulting solution was diluted to obtain the required concentration of phosphate.

Electrophoresis buffers and solutions

5x TBE

TBE stock was prepared by dissolving 60.6 g Trizma base, 25.7 g orthoboric acid and 10 ml 0.5 M EDTA in 1 litre of H_2O. This buffer was stored at room temperature. A 1x working solution was prepared for use in agarose gels and DNA electrophoresis tanks.

10x bromophenol blue/xylene cyanol loading buffer

0.125 g bromophenol blue and 0.125 g xylene cyanol were mixed with 30 ml H_2O, 12.5 g Ficoll 400 (Amersham Pharmacia Biotech, St Albans, UK) was added and stirred until dissolved. Volume was adjusted to 50 ml with H_2O and 1 ml aliquots stored at –20 °C.

5x SDS-PAGE denaturing buffer

Stock sample buffer was prepared by dissolving 3 g of trizma base in 40 ml H_2O, the pH was adjusted to 7.5 with acetic acid and the volume made up to 50 ml with H_2O. Denaturing buffer was prepared with 1 ml stock sample buffer, 0.5 g sodium dodecyl sulphate, 77 mg dithiothreitol and 5 mg bromophenol blue and the volume was made up to 10 ml with H_2O. 1 ml aliquots were stored at –20 °C.

Blotting buffers and solutions

These buffers were made using deionised water and stored at room temperature.

20x SSPE

174 g NaCl and 31.2 g of NaH_2PO_4 were dissolved in 40 ml of 0.5 M EDTA. The pH was adjusted to 7.4 with NaOH, and the volume made up to 1 litre with H_2O.

Western blotting buffer

72 g glycine and 15 g trizma base were dissolved in 4 litres of H_2O. Following this, 1 litre of methanol was added.

Phosphate buffered saline (PBS)

8 g NaCl, 0.2 g KCl, 1.174 g Na_2HPO_4 and 0.2 g K_2HPO_4 were dissolved in 1 litre H_2O

10x Tris buffered saline (TBS)

24.2 g Trizma base and 292.2 g NaCl were dissolved in 1 litre of H_2O. The pH was adjusted to 7.5 with HCl and a 1x working solution was prepared for use in western blotting.

TBS and tween (TTBS)

This buffer was prepared by adding 450 µl of tween 20 to 900 ml of 1x TBS.

2.2.3 Bacterial media and antibiotics

All media was prepared with deionised water, sterilised by autoclaving and stored at 4 °C prior to use.

Luria-Bertani medium (LB)

5 g sodium chloride, 5 g tryptone (Difco, Detroit, Michigan, USA) and 2.5 g yeast extract were dissolved in 400 ml of H_2O. The pH was adjusted to 7.5 with 10 M NaOH and the volume made up to 500 ml.

LB-agar

6 g bactoagar (Difco) was added to 500 ml LB. Following autoclaving, the agar was cooled to 50 °C in a water bath and ~20 ml was poured into 90 mM petri dishes. The plates were allowed to set at room temperature and stored at 4 °C until used.

SOB medium

10 g tryptone, 2.5 g yeast extract and 0.25 g sodium chloride were dissolved in ~ 400 ml H_2O. 5 ml of 250 mM potassium chloride was added and the pH adjusted to 7.0 with 10 M NaOH. After autoclaving, 2.5 ml filter sterilised 2 M magnesium chloride was added.

SOC medium

This was prepared from SOB by the addition of 20 ml filter sterilised 1 M glucose.

Ampicillin

500 mg ampicillin was dissolved in 5 ml H_2O and 1ml aliquots were stored at –20 °C until use. When used in media, ampicillin was at a final concentration of 50 μg/ml.

5-bromo-4-chloro-3-indolyl b-D-galactoside (X-gal)

100 mg x-gal was dissolved in 5 ml dimethylformamide and 1 ml aliquots were stored at –20 °C. This solution was used in media at a final concentration of 40 μg/ml.

2.3 Methods

2.3.1 Isolation of human liver RNA

Total RNA was extracted from human liver tissue using RNA isolator reagent (Sigma Genosys, Poole, UK), which uses an acid guanidinium thiocyanate-phenol-chloroform extraction method (Chomczynski, 1993). All plastics were baked at 80 °C for three hours to remove nucleases, which if not removed, would degrade the RNA.

Tissue was homogenised in RNA isolator (100 mg tissue/ml) with a glass homogeniser and RNA was isolated as follows: 0.2 ml chloroform was added per ml of isolator reagent and the tubes shaken for 15 seconds. Following incubation at room temperature for 2–15 minutes the tubes were centrifuged at 15,000 g for 15 minutes at 4 °C. The upper aqueous phases containing the RNA were transferred to fresh eppendorf tubes and 0.5 ml isopropanol was added. Following incubation at room temperature for 5 minutes the tubes were centrifuged at 15,000 g for 15 minutes at 4 °C. The supernatants were decanted and the RNA pellets were washed with 1 ml 75% ethanol. Following centrifugation at 7,500 g for 5 minutes at 4 °C all the ethanol was removed and the RNA pellets allowed to air dry for a few minutes. RNA pellets were dissolved in 0.1% diethyl pyrocarbonate (DEPC) treated water and frozen at –80 °C.

2.3.2 Reverse transcriptase-polymerase chain reaction (RT-PCR)

cDNA was synthesised by reverse transcriptase-polymerase chain reaction (RT-PCR) using the following conditions: 2 μg RNA was added to a solution containing 5 mM potassium chloride, 20 mM Tris-HCl pH 8.4, 5 mM magnesium chloride, 1 mM dNTP,

1x hexanucleotide mix (Boehringer Mannheim, Lewes, UK), 20 units Rnasin® RNase inhibitor (Promega, Southampton, UK) and 50 units M-MLV reverse transcriptase (Life Technologies, Paisley, UK) in a final volume of 20 µl. After incubation at room temperature for 10 minutes the RT reaction was carried out at 42 °C for 15 minutes. Following this the RT was inactivated by incubation at 99 °C for 5 minutes.

5 µl of the RT product was added to a PCR mix containing final concentrations of 50 mM potassium chloride, 10 mM Tris HCl, pH 9.0, 0.1% Triton® X-100, 2 mM magnesium chloride, 200 µM dNTP, 0.6 µM each primer and 0.25 units Taq polymerase (Promega) in a total volume of 25 µl. Oligonucleotide primer sequences and PCR reaction conditions are listed in Appendix 1. RT-PCR products were mixed with loading buffer and electrophoresed in a 0.8% agarose (Life Technologies) gel containing 0.5 mg/ml ethidium bromide at 100 mA, 200 V and visualised by UV illumination. DNA was quantified by comparison of band intensity in agarose gels to similar sized bands of known concentration in lambda DNA/*Hin*dIII, or PhiX174 DNA/*Hae*III markers (Promega).

2.3.3 TA cloning of PCR products

PCR products were purified from agarose using the Geneclean® spin kit (Anachem, Luton, UK) according to the manufacturer's instructions. The DNA was eluted from the column in a volume of 10 µl and 6 µl of this was ligated into the pCR® TA cloning vector (Invitrogen, The Netherlands) in an overnight incubation at 4 °C. One Shot® cells (Invitrogen) were transformed with 2 µl of the ligation reaction. Both the ligation and

transformation steps were carried out according to the kit protocol. 50 µl and 200 µl of the transformation product were plated onto LB-agar plates containing ampicillin and x-gal, which had been prepared as outlined in section 2.2.3. After incubation overnight white colonies were picked, plasmid DNA was isolated and analysed for the presence of correct sized insert as follows:

5 ml aliquots of SOB medium plus ampicillin (50 µg/ml) were inoculated with individual colonies and cultured overnight at 37 °C with shaking. Plasmid DNA was extracted from 3 ml of overnight cultures using the QIAprep spin miniprep kit (Qiagen, Crawley, UK). The plasmid DNA was eluted into 50 µl 10 mM Tris-HCl, pH 8.5 and restriction digested overnight by standard procedures (Sambrook *et al.*, 1989). The digest was electrophoresed in a 0.8% agarose gel containing 0.5 µg/ml ethidium bromide and visualised by UV illumination to confirm the presence of correct sized digestion products.

2.3.4 Sequencing

Automated Sanger dideoxy sequencing with fluorescence labelled nucleotides using an ABI-3100 sequencer was carried out by a commercial provider. Plasmid DNA, containing the appropriate insert, was sequenced in both directions by means of M13-universal and M13-reverse primers.

2.3.5 Northern blot analysis

cDNA inserts were excised from plasmids with appropriate enzymes and purified using the Geneclean® spin kit. 25 ng of purified DNA was used as a template for the synthesis of a [^{32}P] dCTP-labelled cDNA probe, using the Rediprime™II labelling system (Amersham) following the manufacturer's instructions. Northern blots containing mRNA from a variety of tissues (Clontech MTN™, Clontech, Palo Alto, Ca) were hybridised with the [^{32}P] dCTP-labelled cDNA probe according to the MTN™ kit protocol. The blots were prehybridised in 2x SSPE at 68 °C for 30 minutes. The probe, denatured by heating at 95 °C for 5 minutes, was added to the blots and hybridised for 1 hour at 68 °C. After this time the probe was removed and the membranes were washed three times in 2x SSPE, 0.05% SDS at room temperature and twice in 0.1x SSPE, 0.1% SDS at 50 °C for twenty minutes each.

2.3.6 Transfection into BL21 competent cells

Epicurean coli BL21 (DE3) competent cells (Stratagene Ltd, Cambridge, UK) were transfected with plasmid constructs as follows: 100 µl aliquots of BL21 cells were transfected with 3 µl of plasmid. 200 µl aliquots of each transformant sample were plated onto LB agar plates with ampicillin and incubated overnight at 37 °C. Individual colonies were picked and analysed for the presence of correct sized insert as described previously in section 2.3.3.

2.3.7 Expression of recombinant protein in BL21 cells

Recombinant protein was expressed using the Xpress® system (Invitrogen) in accordance with the manufacturer's instructions. The protocol used for isopropylthio-β-D-galactoside (IPTG) induction of protein expression is given below:

Individual colonies of BL21 cells transfected with plasmid constructs were cultured overnight in 2 ml SOB medium with ampicillin. 0.2 ml of overnight cultures were inoculated into 50 ml aliquots of SOB containing ampicillin (50μg/ml). The cells were grown with aeration until an absorbance of 0.6 at 600 nm was reached, at which time 0.5 ml of 100 mM IPTG (238 mg dissolved in 10 ml H_2O) was added and the culture incubated for a further 5 hours. The cells were harvested by centrifugation at 2,000 g for 10 minutes and the pellets frozen at –80 °C.

2.3.8 Protein SDS-PAGE

Protein samples were electrophoresed in rehydrated 10% polyacrylamide gels (Clean gel 36S, Amersham) according to the manufacturer's instructions. Protein samples and Rainbow™ coloured protein molecular weight markers (Amersham) were denatured by heating at 95 °C in 1x SDS-PAGE sample buffer for 3 minutes and 2 minutes respectively, and immediately transferred to ice. Electrophoresis was carried out using a MultiphorII (Amersham) unit cooled to 10 °C at 200 V, 70 mA and 40 W for 10 minutes followed by 600 W, 100 mA and 40 W until the dye front had migrated across the width of the gel. Proteins were visualised with Coomassie blue staining or transferred to nitrocellulose membrane for immunoblotting.

2.3.9 Protein staining with Coomassie brilliant blue

Solutions:

Fixing solution	250 ml isopropanol, 100 ml glacial acetic acid in 1 litre H_2O
Destain solution 1	400 ml methanol, 70 ml glacial acetic acid in 1 litre H_2O
Destain solution 2	50 ml methanol, 70 ml glacial acetic acid in 1 litre H_2O
Staining solution	0.5 g Coomassie brilliant blue, 800 ml methanol and 140 ml glacial acetic acid in 2 litres H_2O

All solutions were stored at room temperature. After SDS-PAGE, proteins were visualised using the following procedure: the gel was placed in fixing solution for twenty minutes, transferred to destain solution 1 for three minutes, followed by staining with staining solution for one hour at 60 °C. The gel was destained in solution 1 for thirty minutes, followed by solution 2 overnight.

2.3.10 Western blots of protein gels

For western blots, nitrocellulose membrane (Hybond-C extra, Amersham) was cut to the size of the gel to be blotted and soaked in water followed by western blotting buffer. Four pieces of 3MM (Whatman, Maidstone, UK) were cut to the same size as the membrane and wetted with blotting buffer. The gel was soaked in western blotting buffer for three minutes, stripped from the plastic backing and overlaid with the nitrocellulose. The nitrocellulose was laid gel side up on two pieces of wetted 3MM in the dry blot apparatus (Transblot-SD, Biorad, Hemel Hempstead, UK). The gel was overlaid with the remaining pieces of 3MM and air bubbles rolled out using a plastic tube. The lid was placed on the apparatus and transfer conducted at 15 volts for 1 h.

The nitrocellulose was removed from the blotting apparatus and non-specific binding sites were blocked by immersion in PBS containing 3% (w/v) milk proteins for 10 minutes. Following this the blot was incubated overnight with primary antibody in 3% milk proteins at appropriate dilution. Excess antiserum was removed by washing twice for 10 minutes in PBSA and the blot was incubated with alkaline phosphatase conjugated secondary antibody for 3 hours. After two 10 minute washes in PBSA, the blot was immersed in alkaline phosphatase colour development reagent (BioRad) for ten minutes, or until bands could be clearly visualised. The developed blot was rinsed in deionised water and the nitrocellulose blotted dry and wrapped in cling film.

2.3.11 Measurement of GO activity

Solutions:

25 mM glycolate 19 mg of glycolic acid was dissolved in 10 ml H_2O

0.5 mM DCIP 1.45 mg of 2,6 dichlorophenol indophenol dissolved in 10 ml H_2O

GO activity measurement was based upon an assay described previously (Zelitch and Ochoa, 1953) in which DCIP is used in place of oxygen as the electron acceptor, with glycolate as substrate. The reduction of DCIP was monitored by the measurement of its absorbance at 600 nm using an Uvicon 922 spectrophotometer (Bio-Tek Kontron, Watford, UK). In a cuvette, 500µl of 50 mM potassium phosphate buffer pH 8.3 was mixed with 200 µl of 25 mM glycolate, 50 µl of deionised water and 200 µl of 0.5 mM DCIP. The reaction was started by the addition of 50 µl of the sample to be assayed and the absorbance at 600 nm was recorded for 10 minutes. The absorbance change per min was calculated and using an extinction coefficient of 22,000 for DCIP (Armstrong,

1964) activity was expressed as nmol DCIP reduced/min.

2.3.12 Preparation of human tissue sonicates

The tissue was suspended in 0.1 M potassium phosphate buffer, pH 8.0, 0.24 M sucrose at a concentration of 2% w/v. The suspension was sonicated on ice using cycles of 10 second bursts, with 30 second intervals between bursts, using a Microson XL-sonicator (Misonix, New York, USA) until the mass was uniformly dispersed. Particulate material was pelleted by centrifugation at 15,000 g for 10 minutes at 4 °C. Protein concentration was determined as described in section 2.3.13 and samples were stored at –80 °C prior to use.

2.3.13 Determination of protein concentration

Protein concentration of tissue sonicates was determined by the method of Lowry *et al.*, 1951.

Lowry reagent A: 2 g anhydrous sodium carbonate dissolved in 100 ml of 0.1 M sodium hydroxide

Lowry reagent B: 50 mg copper II sulphate pentahydrate dissolved in 10 ml of trisodium citrate

Lowry reagent C: 50 ml reagent A mixed with 1 ml reagent B (this reagent is stable for 8 hours)

Lowry reagent D: Folin-Ciocalteu reagent (Fisons, Loughborough, UK) diluted 1:1 with deionised H_2O.

Bovine serum albumin (BSA) (Pierce Chemical Company, Rockford, Illinois, USA) solution was used to prepare standards as indicated in table 2.1 below:

	Protein concentration (mg/ml)						
	0	0.025	0.05	0.125	0.25	0.375	0.5
Deionised H_2O	200	195	190	175	150	125	100
1 mg/ml BSA (µl)	0	5	10	25	50	75	100

Table 2.1 Preparation of standard curve for Lowry protein assay.

Samples were diluted 1 in 30 with deionised H_2O, i.e. 20 µl sample plus 580 µl water with both samples and standards run in duplicate. 1 ml of reagent C was added to each tube. The tubes were vortexed and allowed to stand for 10 minutes at room temperature. 100 µl of reagent D was added to each tube, which were then vortexed rapidly. Tubes were left to stand for 30 minutes at room temperature and their absorbance was read at 660 nm. A standard curve of absorbance versus protein concentration (mg/ml) was plotted and used to determine unknowns. The values obtained from the standard curve were multiplied by 30 (the dilution factor) in order to determine protein concentration in mg/ml. An example calibration curve is shown in Appendix 2a.

2.3.14 DNA and protein analysis software

ENTREZ	http://www.ncbi.nlm.nih.gov/Entrez/
BLAST	http://www.ncbi.nlm.nih.gov/Blast/
WebCutter	http://www.firstmarket.com/cutter/cut2.html
Chromas	http://www.technelysium.com.au/chromas.html
Translate	http://www.expasy.ch/tools/dna.html
CLUSTALW	http://clustalw.genome.ad.jp/

Chapter Three

Identification and Expression of Human GO

3.1 Introduction

3.2 Methods

3.2.1 Sub cloning into pTrcHisB expression vector

3.2.2 Determination of the kinetics of IPTG induction

3.2.3 3' rapid amplification of cDNA ends (3'RACE)

3.2.4 5' rapid amplification of cDNA ends (5'RACE)

3.3 Results

3.3.1 Cloning and sequencing of a cDNA for HAO1

3.3.2 Expression of recombinant GO protein

3.3.3 Enzyme activity of crude extracts

3.3.4 Investigation of the tissue distribution of HAO1 expression

3.3.5 Rapid amplification of cDNA ends

3.4 Discussion

3.1 Introduction

Glycolate oxidase has been isolated from several species including spinach leaves (Zelitch and Ochoa, 1953) and the livers of pig (Schuman and Massey, 1971a), chicken (Dupuis *et al.*, 1990) and rat (Ushijima, 1973). The enzyme from human liver was first identified in 1979 (Schwam *et al.*, 1979; Fry and Richardson, 1979a), although the protein sequence was not determined and the gene encoding human GO had yet to be identified. The traditional approach for gene identification is to purify the protein of interest from a source tissue and determine its amino acid sequence. However, this technique is often very time consuming involving multiple purification steps and doesn't always purify the relevant protein to homogeneity. With the advent of the human genome project large numbers of partially sequenced cDNA "survey sequences" or expressed sequence tags (ESTs), have been produced (Adams *et al.*, 1991). This type of incomplete, but readily available, sequence data may be used to "phylum-hop" to enable the discovery of new genes, when the equivalent gene has been cloned in another organism (Boguski, 1995).

GO activity was first noted in plants including spinach (Zelitch and Ochoa, 1953) and tobacco (Kenten and Mann, 1952) and more recently the gene encoding spinach GO has been cloned (Volokita and Somerville, 1987). Using *in silico* techniques I identified a human cDNA with protein sequence homology to the GO enzymes from spinach and *Arabidopsis*. The sequence information obtained allowed a full-length cDNA to be amplified from human liver RNA by RT-PCR. The identification and cloning of the human GO gene and expression of the resulting protein is described in this chapter.

3.2 Methods

3.2.1 Sub cloning into pTrcHisB expression vector

The primers used for RT-PCR were designed such that following excision from the TA vector by overnight digestion at 37 °C with *Pst*1 and *Hin*dIII restriction enzymes (New England Biolabs, Hitchin, UK) the cDNA could be ligated into the pTrcHisB expression vector in frame with the plasmid initiation codon.

After excision from the TA vector with *Pst*1 and *Hin*dIII the cDNA was inserted into the multiple cloning site of the pTrcHisB expression vector, in frame with the plasmid initiation codon. The expression vector had also been cut with the same enzymes and phosphorylase treated before ligation with insert. To determine the amount of calf intestinal alkaline phosphatase (CIAP) (Promega) needed to dephosphorylate 1 μg of vector, the amount of pmoles of DNA were calculated using the following formula:

(μg DNA/kb size of DNA) x 3.04 = pmol ends

Cut vector was incubated with 0.01 units of CIAP (Promega) per pmol of ends in 1x CIAP buffer for 15 minutes at 37 °C, followed by 15 minutes at 56 °C. A further 0.01 units of CIAP (Promega) per pmol of ends were added and the sample incubated for 30 minutes at 37 °C. 2 μl of 0.5 M EDTA was added to stop the reaction and the sample was incubated for 20 minutes at 65 °C. The dephosphorylated DNA was purified using the Wizard™ DNA Clean-up System (Promega) according to the manufacturer's instructions, with elution in 50 μl of 10 mM Tris-HCl, pH 7.6, 1 mM EDTA.

The cDNA insert was ligated into the cut and dephosphorylated pTrcHisB expression vector, using 1:1 and 1:3 molar ratios of vector:insert. Reaction mixtures for the two molar ratios and three control ligations (vector and ligase with no insert, vector only, vector and insert with no ligase) are summarised in the table below (all volumes are in µl). Following overnight incubation at 4 °C, 3 µl of each ligation sample was electrophoresed in a 0.8% agarose gel to confirm whether the cDNA had ligated successfully.

	1:1	1:3	Control 1	Control 2	Control 3
Vector DNA (50ng/µl)	2	1	2	2	1
Insert DNA (20ng/µl)	5	4	0	0	4
T4 DNA ligase (1U/µl)	1	1	1	0	0
T4 DNA ligase buffer (10x)	1	1	1	1	1
Nuclease free water	1	3	6	7	4
Total volume (µl)	10	10	10	10	10

Table 3.1 Reaction mixtures for ligation of inserts into pTrcHisB expression vector.

3.2.2 Determination of the kinetics of IPTG induction

Expression of the recombinant protein was induced by the method outlined in section 2.3.7. A 1 ml aliquot of cells was taken from the bacterial culture prior to induction with IPTG. Following induction, 1 ml samples were taken from the culture at hourly intervals for a 5 hour incubation period. The samples were pelleted by centrifugation for one minute at 15,000 g and the supernatants transferred to separate tubes. The pellets were resuspended in 100 µl of 20 mM potassium phosphate buffer pH 7 and subjected

to freeze thawing and sonication as described in the Xpress™ system kit protocol. Both pellet and supernatant samples were electrophoresed by SDS-PAGE, protein stained and western blotted as described in sections 2.3.8 to 2.3.10.

3.2.3 3' rapid amplification of cDNA ends (3'RACE)

The 3' untranslated region (UTR) was determined by 3'RACE using a kit produced by Gibco (Life Technologies). Refer to Appendix 1 for oligonucleotide primer sequences and PCR conditions. A cDNA was synthesised by RT-PCR as follows:

500 nM adaptor primer (5' GGCCACGCGTCGACTAGTACTTTTTTTTTTTTTTT) was added to 2 μg of total liver RNA prepared by the method outlined in section 2.3.1. Primer annealing was accomplished by incubation at 70 °C for 10 minutes, followed by 1 minute on ice. RT reagents were added to the tube to give final concentrations of 50 mM potassium chloride, 20 mM Tris-HCl pH 8.4, 2.5 mM magnesium chloride, 500 μM dNTP, 10 mM DTT and 200 units of Superscript II RT. The RT reaction was carried out at 42 °C for 50 minutes, followed by 15 minutes at 70 °C. Following this RNA was degraded by incubation with 2 units of RNase H for 20 minutes at 37 °C.

2 μl of the RT product was added to a PCR mix containing 50 mM potassium chloride, 20 mM Tris-HCl pH 8.4, 1.5 mM magnesium chloride, 200 μM dNTP, 200 nM each of a gene specific forward primer (GSP1A) and a reverse primer complementary to the adapter primer (AUAP) and 0.1 unit Taq polymerase (Promega) in a final volume of 50 μl. The PCR product was diluted 1/1000 and 2 μl was subjected to nested PCR with a downstream gene specific forward primer (GSP2A) and AUAP as the reverse primer.

The product was inserted into the pCR 2.1 TA vector as described in section 2.3.3 and sequenced in full.

3.2.4 5' rapid amplification of cDNA ends (5'RACE)

5'RACE was carried out using a kit produced by Gibco (Life Technologies, Paisley, UK). Reaction conditions for first strand synthesis by RT were as described for 3'RACE, except 100 nM of a gene specific primer (5' ATCTGTTTCAGCAACAT) was used. Following this the cDNA product was purified by Glassmax isolation as follows: 120 µl of 6 M sodium iodide was added to the first strand reaction tube and this was transferred to a Glassmax spin cartridge and centrifuged at 13,000 g for 20 seconds. The cartridge was washed 4 times with 400 µl 1x wash solution followed by 2 washes of 400 µl 70% ethanol. The cDNA was eluted in 50 µl of sterile water and was dCTP tailed as follows: 10 µl of cDNA was added to a reaction mix containing10 mM Tris-HCl, 25 mM potassium chloride, 1.5 mM magnesium chloride, 200 uM dCTP and 1 unit terminal deoxynucleotidyl transferase (TdT) in a total volume of 25 µl. The tube was incubated at 37 °C for 10 minutes, following which the TdT was inactivated by incubation at 65 °C for 10 minutes.

PCR of 2 µl dCTP tailed cDNA was conducted using the same reaction conditions as those used for 3'RACE, with 400 nM each of a nested gene specific reverse primer (GSP2B) and a polyG containing forward primer included in the kit (AAP). Nested PCR was conducted with a forward primer included in the kit (AUAP) and an upstream gene specific reverse primer (GSP3B). The PCR product was inserted into the pCR 2.1 TA vector and sequenced in full.

3.3 Results

3.3.1 Cloning and sequencing of a cDNA for HAO1

The Entrez database (http://www.ncbi.nlm.nih.gov/htbin-post/Entrez/) was screened using the term 'glycolate oxidase' and a 1176 bp human cDNA identified with peptide sequence homology to GO from *Arabidopsis thaliana* (Figure 3.1). The DNA sequence of this cDNA (Accession number T64673, Appendix 3a) was used to screen the EST database for longer length clones, which identified a 1195 bp EST (Accession number T74667, Appendix 3b). The clones were obtained from the integrated molecular analysis of genomes and their expression (I.M.A.G.E) consortium (http://bbrp.llnl.gov/bbrp/image) (Lennon *et al.*, 1996) and the longest one sequenced in full (Appendix 3c). However, the absence of a termination codon indicated that this clone was missing the 3' end. The translated peptide sequence of this cDNA shares 54% identity with spinach GO (Appendix 3d).

A subsequent BLAST search identified an almost identical cDNA (Accession number AB024079, Appendix 3e), which included additional 3' sequence. PCR primers (Genosys Biotechnologies Ltd, Pampisford, UK) were designed based upon the 5' end of the IMAGE clone and the genomic sequence available through Genbank (Accession number AL021879, Appendix 3f), incorporating restriction sites for *Pst*I and *Hin*dIII at the 5' and 3' ends respectively. This primer pair was used for cDNA synthesis by RT-PCR from human liver RNA as described in section 2.3.2. Oligonucleotide primer sequences and conditions are listed in Appendix 1. The PCR product was inserted into the pCR2.1 TA cloning vector (Invitrogen) according to the method outlined in section

2.3.3. Sequencing of plasmid DNA containing the cDNA insert identified an 1128 bp sequence with an 1113 bp open reading frame, which upon translation was found to encode a 370 amino acid protein (Figure 3.1). The full-length cDNA sequence was submitted to Genbank (AF244134) and assigned the symbol HAO1 by the Nomenclature Committee of the Human Genome Project.

Analysis of the peptide sequence with the Prosite program (Bairoch *et al.*, 1997) revealed signatures for a FMN-dependent, α-hydroxy acid dehydrogenase active site (residues 258–264) and a C-terminal peroxisomal targeting signal (residues 368–370). These residues are underlined in Figure 3.1. The amino acid sequence is predicted to encode a 40.9 kDa protein with a pI of 9 (http://www.expasy.ch/tools/pi-tool.html).

Alignment of the peptide sequence with those of mouse liver, spinach and *Arabidopsis* glycolate oxidases revealed 89% sequence similarity to GO from mouse liver and 53% similarity to the spinach and *Arabidopsis* enzymes. This alignment is depicted in Figure 3.2.

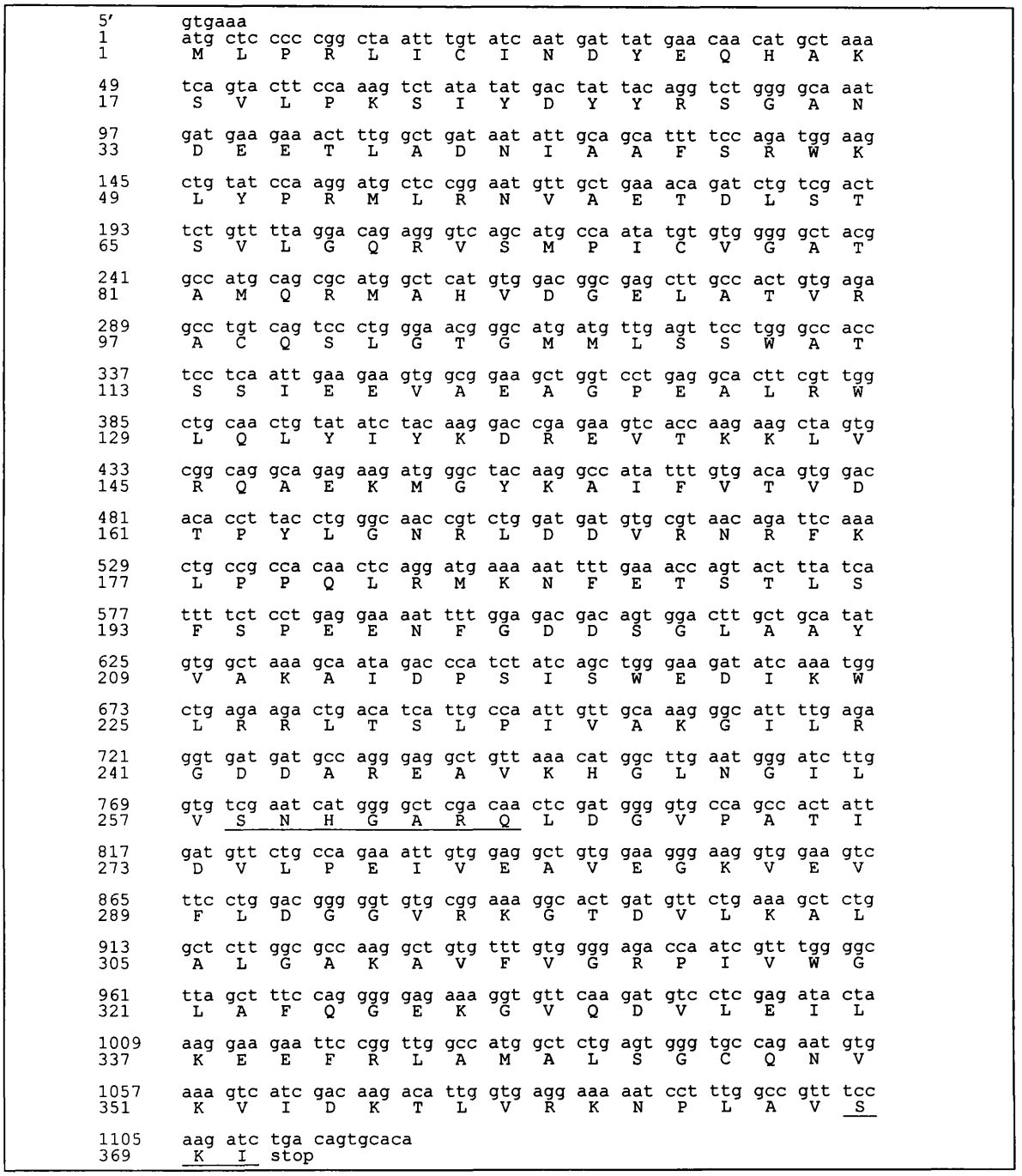

Figure 3.1 cDNA and predicted protein sequence of human HAO1 (Genbank AF244134). *The FMN-dependent α-hydroxy acid dehydrogenase active site (residues 258–264) and peroxisomal targeting signal (residues 368–370) are underlined.*

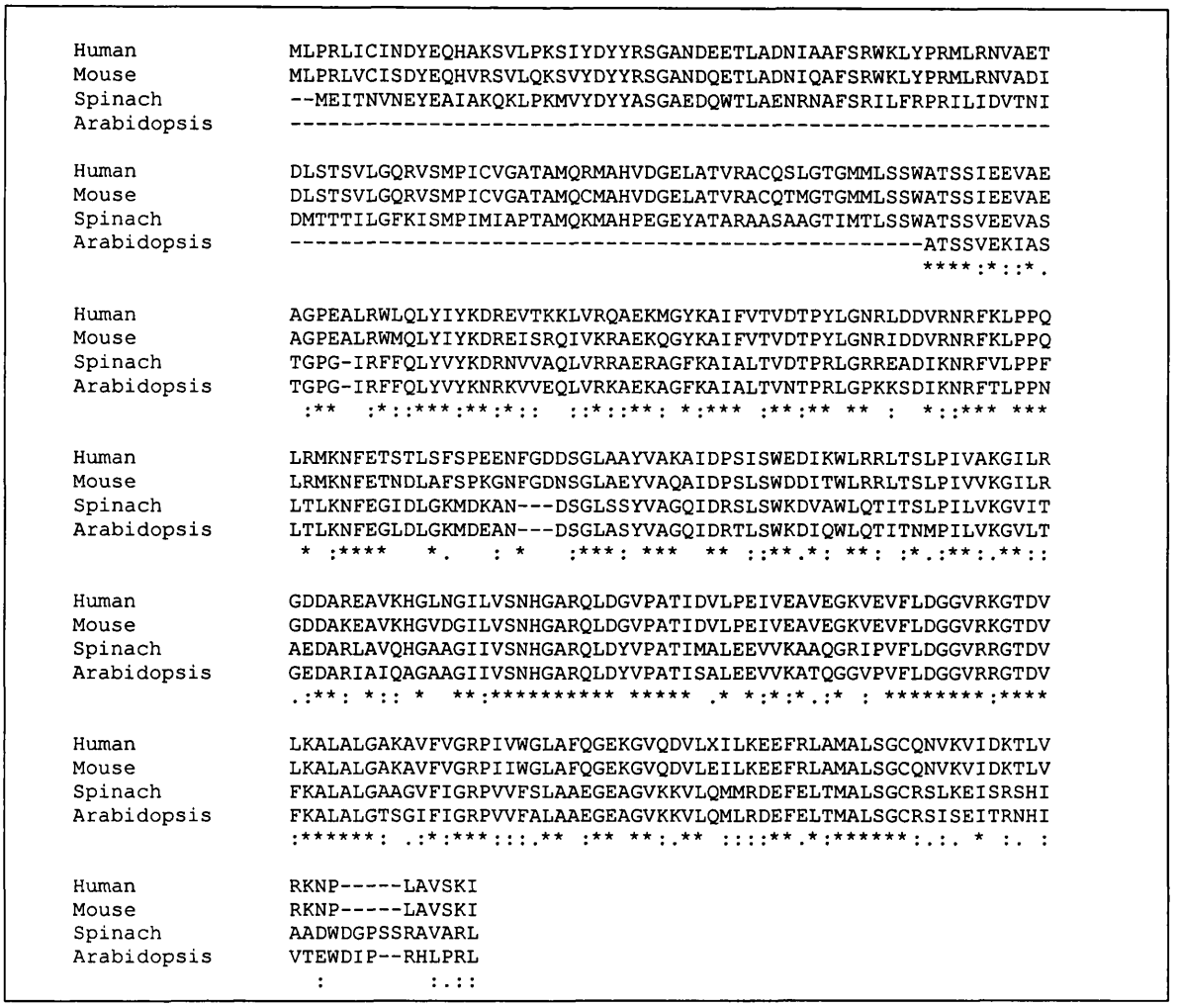

Figure 3.2 Peptide sequence similarity of glycolate oxidases. *The human GO sequence (Genbank AF244134) is aligned with the enzymes from mouse (Genbank AAD25332) spinach (Genbank AAA34030) and Arabidopsis (Genbank AAB80700).*

Comparison of the full length HAO1 cDNA with the genomic sequence deposited in Genbank (accession number AL021879, Appendix 3f) revealed 8 exons ranging in size from 70 to 256 bp, which mapped to chromosome 20p12 (http://www.ncbi.nlm.nih.gov/UniGene). The genomic organisation of the human HAO1 gene is depicted in Figure 3.3.

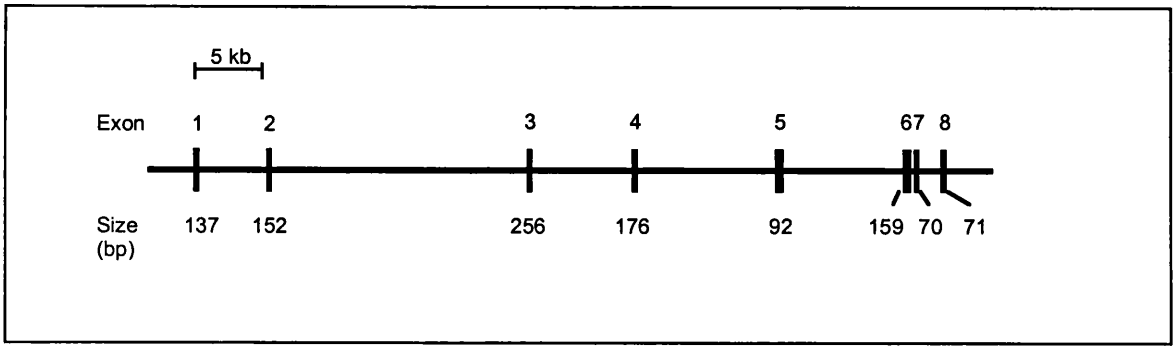

Figure 3.3 Genomic organisation of the human HAO1 gene. *Boxes represent exons, lines introns.*

3.3.2 Expression of recombinant GO protein

The pTrcHisB expression vector (Invitrogen) was used to express the desired protein by means of IPTG induction. The recombinant protein produced is fused to a N-terminal His tag of six tandem histidine residues, which enables purification using nickel affinity chromatography. Since the His tag is small and uncharged at physiological pH it would not be expected to interfere with protein structure and function. The recombinant protein also contains an Anti-Xpress ™ epitope to enable protein detection by western blotting.

Following excision from the TA vector by overnight digestion at 37 °C with *Pst*I and *Hin*dIII restriction enzymes the HAO1 cDNA was ligated into the pTrcHisB expression vector by the method outlined in section 3.2.1. BL21 cells transfected with pTrcHisB-HAO1 constructs were induced to express recombinant GO protein and the kinetics of the IPTG induction investigated by the method outlined in section 3.2.2. The results, as can be seen from figure 3.4, showed maximal GO protein expression at three hours with decreasing amounts of protein thereafter. From the western blot, which detects the Anti-

Xpress™ epitope, it can be concluded that the intense band at 46 kDa represents recombinant GO protein. If the additional 3 kDa added in the fusion protein is accounted for, this indicates a 43 kDa protein, which approximates the predicted size of 40.9 kDa. Expression of this protein peaked at 3 hours post induction, after which time increasing amounts were found in the pellet (Figure 3.4 a). The pellet represents inclusion bodies, which are a common occurrence during recombinant protein expression. Since ample protein was present in the soluble fraction, inclusion bodies were not studied further. Future experiments used supernatants from cells induced for three hours only.

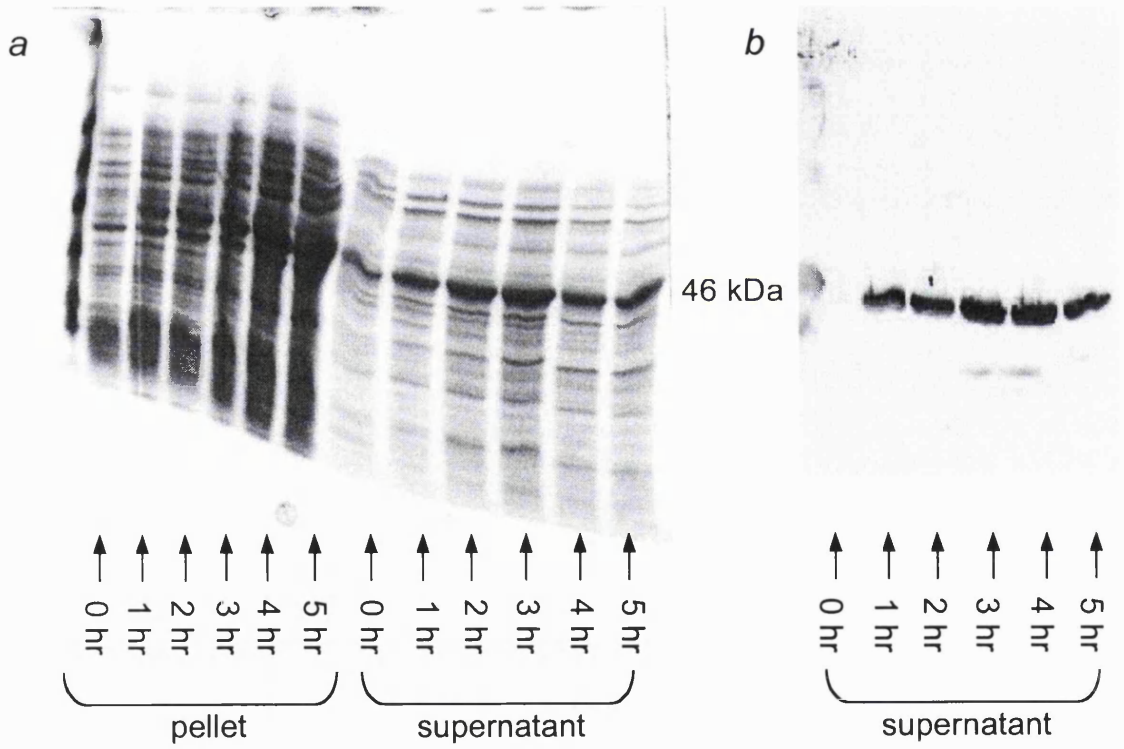

Figure 3.4 Kinetics of IPTG induction of recombinant GO protein expression by BL21 cells. *(a) Coomassie blue stained SDS-PAGE gel (b) western blot with anti-Xpress™ antibody. The 46 kDa band represents recombinant GO protein.*

3.3.3 Enzyme activity of crude extracts

GO activity was measured in crude extracts from BL21 cells with and without the HAO1 insert, by means of DCIP reduction as described in section 2.3.2. Crude extracts from cells containing the pTrcHisB-HAO1 construct had activity of 474 ± 20 nmol DCIP reduced/min/mg protein (mean ± 2 SD, n=3) compared to 5 ± 3 in those cells transfected with vector alone. Crude extracts of bacteria transfected with pTrcHisB-HAO1 were tested for oxidising activity with a range of α–hydroxy acids. The results were expressed relative to GO activity and are depicted in Figure 3.5.

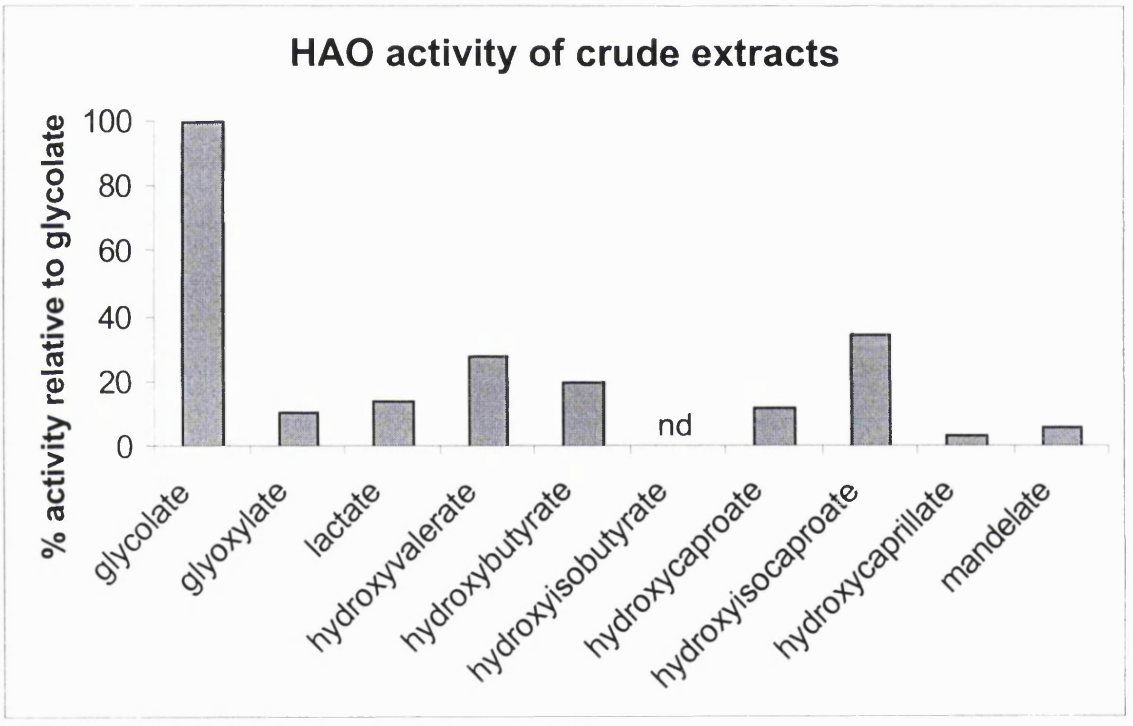

Figure 3.5 Hydroxy acid oxidase activity in BL21 cells transfected with pTrcHisB-HAO1. *Crude extracts of BL21 cells were assayed for activity with a range of hydroxy acids by monitoring DCIP reduction, results are expressed relative to GO activity. nd = not detected.*

3.3.4. Investigation of the tissue distribution of HAO1 expression

Northern blots containing mRNA from a variety of tissues were hybridised with the [^{32}P] dCTP-labelled full-length cDNA probe as described in section 2.3.5. This showed a single species of approximately 1.8 kb, with expression restricted to the liver (Figure 3.6). The calibration curve used to estimate the size of this transcript is shown in Appendix 2b.

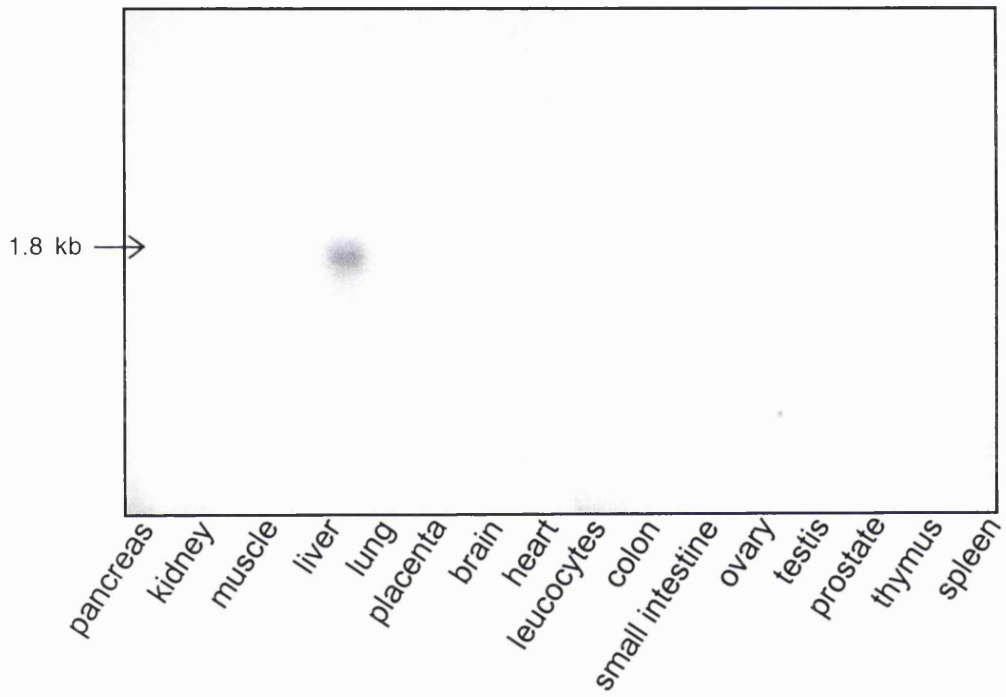

Figure 3.6 Tissue distribution of HAO1 expression. *Multiple tissue northern blots were hybridised with a full-length, radiolabelled HAO1 cDNA probe.*

3.3.5 Rapid amplification of cDNA ends

5' and 3' RACE yielded a 35 bp 5' and a 608 bp 3' UTR respectively. These sequences are shown in Figure 3.7. Together with the 1113 bp reading frame of the HAO1 cDNA, they constitute a 1756 bp sequence excluding the polyA tail, and this closely approximates the 1.8 kb product observed in the northern blot of liver RNA.

5'UTR

5′ ACGAACTCCATCTGGGATAGCAATAACCTGTGAAA**ATG**

3'UTR

TGACAGTGCACAATATTTTCCCATCTGTATTATCTTTTTTCAGCATGTATTACTTGAC
AAAGAGACACTGTGCAGAGGGTGACCACAGTCTGTAATTCCCCACTTCAATACAAAGG
GTGTCGTTCTTTTCCAACAAAATAGCAATCCCTTTTATTTCATTGCTTTTGACTTTTC
AATGGGTGTCCTAGGAACCTTTTAGAAAGAAATGGACTTTCATCCTGGAAATATATTA
ACTGTTAAAAAGAAAACATTGAAAATGTGTTTAGACAACGTCATCCCCTGGCAGGCTA
AAGTGCTGTATCCTTTAGTAAAATTGGAGGTAGCAGACACTAAGGTGAAAAGATAATG
ATCTCATTGTTTATTAACCTGTATTCTGTTTACATGTCTTTAAAACAGTGGTTCTTAA
ATTGTAAGCTCAGGTTCAAAGTGTTGGTAATGCCTGATTCACAACTTTGAGAAGGTAG
CACTGGAGAGAATTGGAATGGGTGGCGGTAATTGGTGATACTTCTTTGAATGTAGATT
TCCAATCACATCTTTAGTGTCTGAATATATCCAAATGTTTTAGGATGTATGTTACTTC
TTAGAGAGAAATAAAGCATTTTTGGGAAGAAAAAAAAAAAAAAAAAAAAAAAAAAA
AA 3′

Figure 3.7 Nucleotide sequences of the 5' and 3' UTR of HAO1. *The start and stop codons are shown in bold and the consensus polyadenylation signal is underlined.*

3.4 Discussion

Prior to this research project, the only vertebrate homologue of GO to have been cloned was that of the mouse (Kohler *et al.*, 1999). This clone contained an open reading frame (ORF) of 1110 nucleotides and coded for a 370 amino acid protein. *In vitro* transcription and translation produced a 42 kDa protein with GO enzyme activity. The human GO identified in this thesis shares 89% amino acid sequence similarity with the mouse enzyme (Figure 3.2). Both proteins terminate in the near consensus type 1 peroxisomal targeting signal (PTS1) C-terminal tri-peptide Ser-Lys-Ile. In contrast, spinach GO has Ala-Arg-Leu (Volokita and Somerville, 1987) and HAO B from rat kidney has Ser-Arg-Leu (Le and Lederer, 1991). The Ser-Lys-Ile tripeptide has been demonstrated to target a construct of mouse GO and green fluorescence protein to peroxisomes in green monkey Cos cells and mouse fibroblasts *in vitro* when present at the C-terminus (Recalcati *et al.*, 2000). This targeting was found to be as effective as the PTS1 consensus tripeptide Ser-Lys-Leu appended to the same constructs.

Human GO protein contains the amino acid sequence S N H G A R Q, which represents a FMN-dependent α-hydroxy acid dehydrogenase active site (Figure 3.1) and is fully conserved between spinach and human GO (Figure 3.2). The structure of spinach GO has been solved by crystallographic studies (Lindqvist, 1989), which enabled active site amino acids critical for catalysis to be identified (Lindqvist and Branden, 1989; Lindqvist *et al.*, 1991). Alignment of the two protein sequences enables identification of the equivalent active site residues in human GO. A model of the active site of human GO adapted from that of the spinach enzyme is shown in Figure 3.8.

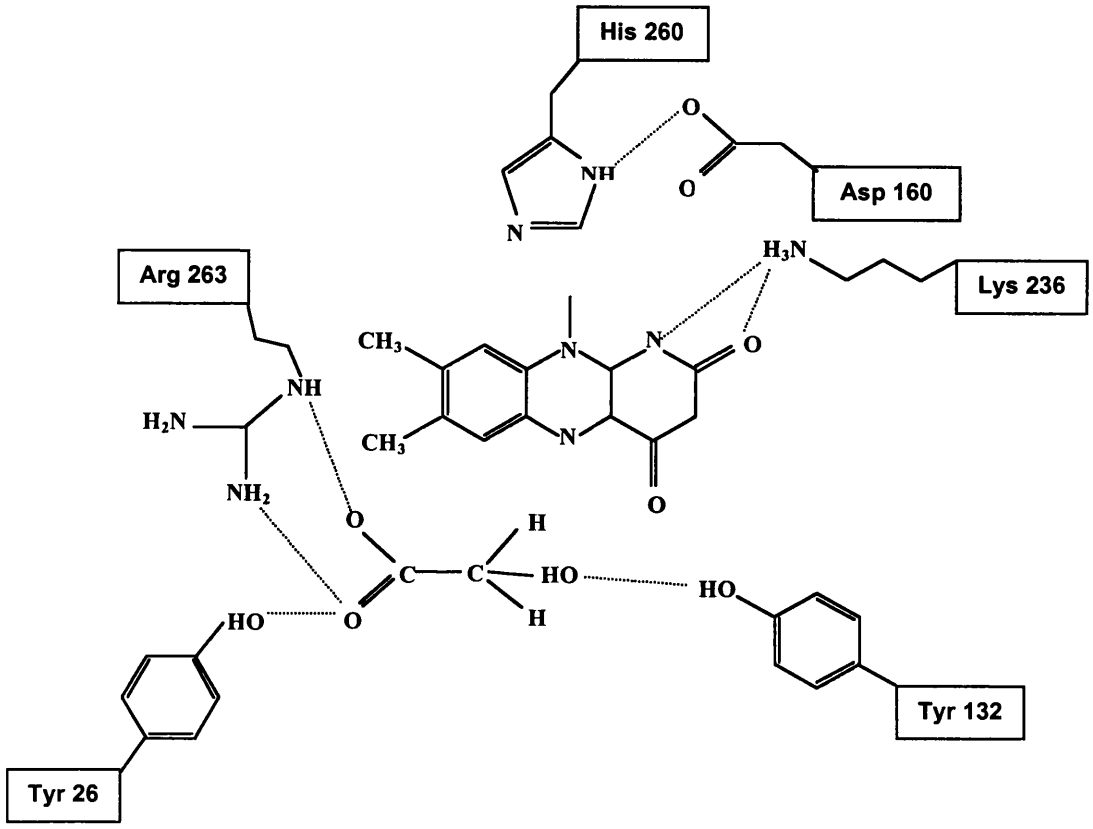

Figure 3.8 A schematic diagram of the active site of human GO. *Amino acid residues fully conserved between the spinach and human enzymes are depicted. Tyr 26, Tyr 132 and Arg 263 are involved in substrate binding; His 260 is the active site base that abstracts the α-proton of the substrate; Lys 236 stabilises the negative charge of the flavin and Asp160 stabilises the protonated His 260 during catalysis (Adapted from Lindqvist and Branden, 1989).*

The active site amino acids shown in Figure 3.8 are conserved between all of the FMN-dependent HAO enzymes so far sequenced, including spinach GO (Volokita and Somerville, 1987), HAO B from rat (Le and Lederer, 1991), LMO from *Mycobacterium smegmatis* (Giegal *et al.*, 1990), FCB_2 from *Saccharomyces cerevisae* (Ghrir and Becam, 1984) and MDH from *Pseudomonas putida* (Tsou *et al.*, 1990). These are all flavoenzymes, which perform dehydrogenation reactions coupled to the transfer of two electrons to the flavin (Fraaije and Mattevi, 2000). The only exception to this homology is in rat HAO B, where Tyr 26 is replaced by a Phe residue (Le and Lederer, 1991). These 5 enzymes in addition to the human GO described in this thesis all share 54 totally conserved residues (Figure 3.9). From enzyme studies in solution of the various flavoenzymes, and more recently by manipulation of the active site amino acids in recombinant proteins, the roles of the amino acids depicted in Figure 3.8 have been elucidated as discussed below.

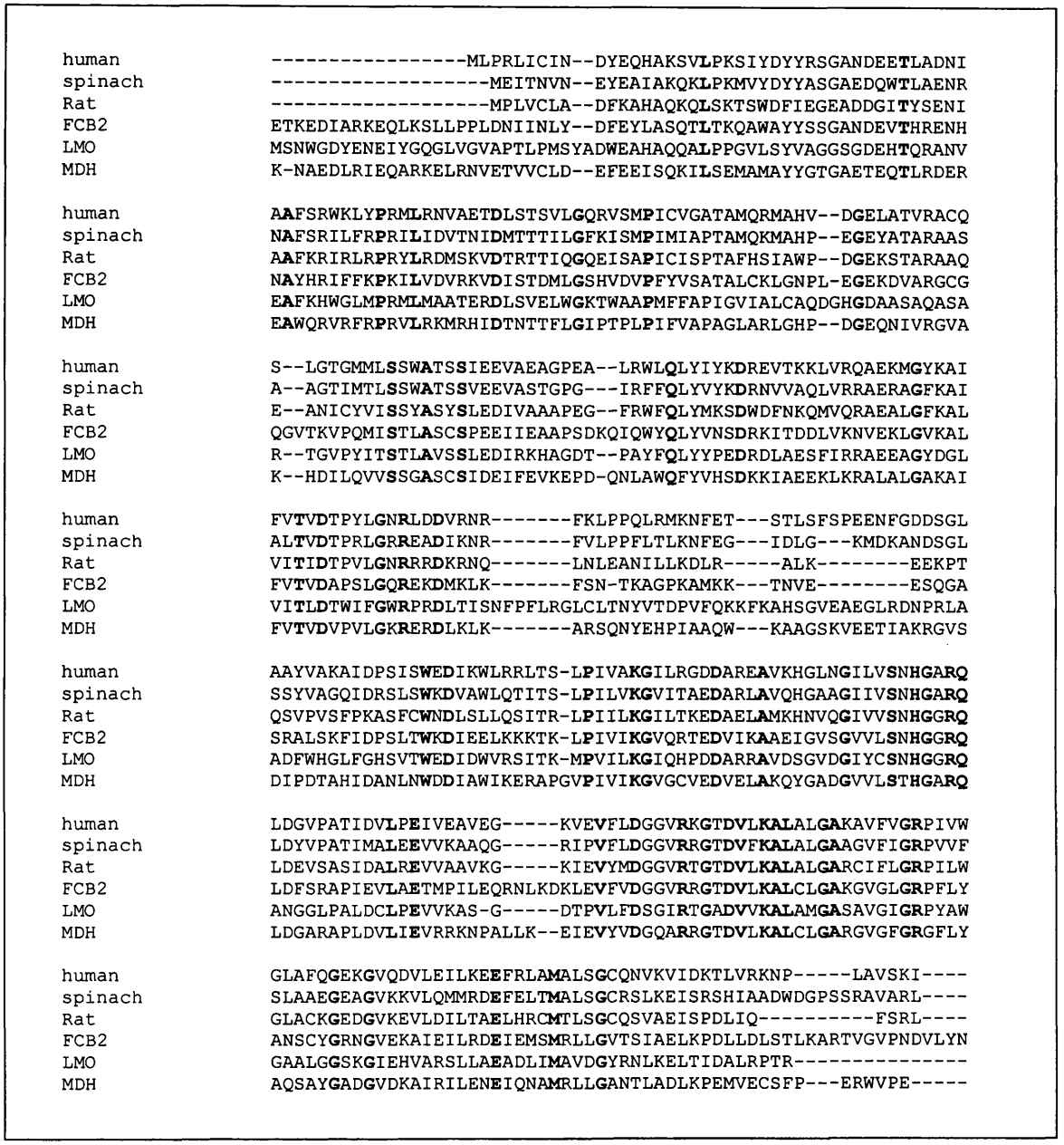

Figure 3.9 Peptide sequence similarity of hydroxy acid oxidising flavoenzymes.

Human GO (Genbank AF244134) is aligned with spinach GO (Genbank J03492) rat HAO B (Genbank NM_032082) yeast FCB2 (Genbank X03215) M. Smegmatis LMO (Genbank J05402) and R Graminis MDH (Genbank AJ001431). Fully conserved amino acids are shown in bold typeface.

Tyr 26 is thought to be involved in substrate binding by way of hydrogen bond formation between the hydroxyl group and the substrate carboxylate group. Replacement of Tyr 24, the equivalent residue in the spinach enzyme, with Phe caused a 10 fold increase in K_m although enzyme turnover and substrate specificity was unchanged (Stenberg *et al.*, 1995). Tyr 129 in spinach GO is proposed to form a hydrogen bond to the α-hydroxy group of glycolate, participating in the reductive step of the enzyme reaction and stabilising a highly negatively charged transition state intermediate during catalysis. Replacement of this residue with Phe resulted in a decrease in enzyme turnover and only a small increase in K_m (Macheroux *et al.*, 1993).

Lys 236 in human GO is the equivalent of Lys 230 in the spinach enzyme. This residue is hydrogen bonded to the N1–C2=02 FMN locus (Stenberg *et al.*, 1995) where the positive charge of the lysine stabilises the negative charge. This amino acid facilitates electron transfer to the flavin during catalysis and is therefore important for flavin reduction (Fraaije and Mattevi, 2000). The oxidative half of the reaction is thought to be initiated by abstraction of a proton from the substrate α-carbon. His 260 in human GO is thought to be the active site base responsible for this step. Arg 263 interacts with the substrate carboxyl group and its positive charge is also thought to stabilise the negatively charged intermediate in a similar fashion to Tyr 129 (Lindqvist and Branden, 1989).

An amino acid conserved between human and spinach GO, but not among the other known FMN-dependent HAO enzymes is Trp 110 (Trp 108 in spinach GO) (Volokita and Somerville, 1987). The size of the amino acid in this position influences the size of

the substrate molecule that can be fitted into the active site. In FCB_2 and LMO (which both utilise lactate) Leu is found (Lindqvist and Branden, 1989), whereas in MDH from *Rhodotorula graminis* a Gly residue occupies this position (Illais *et al.*, 1998). Long chain HAOs from rat and human have Tyr and Phe respectively (Jones *et al.*, 2000). Evidence that the residue in this position confers the enzyme's substrate specificity comes from site directed mutagenesis studies in which the residues have been replaced by alternative amino acids. For example, in spinach GO replacement of Trp 108 with serine resulted in a 100 fold increase in the K_m for glycolate (Stenberg *et al.*, 1995). Furthermore, when Leu 230 in FCB_2 was replaced with alanine, the mutant enzyme displayed activity with mandelate (K_m 0.16 mM) and the K_m for lactate showed a 12 fold increase (Sinclair *et al.*, 1998).

In animals, the existence of two forms of hydroxy acid oxidising enzymes has been reported (Duley and Holmes, 1976). One has short chain HAO activity and is expressed in liver (Fry and Richardson, 1979a) and the other acts as a long chain HAO and is found in kidney (Duley and Holmes, 1976). The cDNA isolated in this project represents the human homologue of the gene encoding short chain HAO. Evidence for this is firstly that the enzyme shows maximal activity with short chain α-hydroxy acids and secondly northern blot analysis revealed expression of human HAO1 was confined to liver. In a similar study of the mouse gene, a 2.2 kb transcript was detected in liver, but not in spleen, skeletal muscle, kidney, embryos or fibroblasts (Kohler *et al.*, 1999).

During the course of this work, Jones and colleagues reported the identification of three human HAO genes (Jones *et al.*, 2000). One of these cDNAs was identical to the HAO1

identified by this project. However, in addition to a major band in liver, northern blot analysis by Jones *et al* indicated the presence of HAO1 transcripts at lower levels in kidney and pancreas. The band in kidney was the same size as that in liver (1.8 kb) and the band in pancreas was about 500 bases smaller and may represent an alternatively spliced transcript. It is unclear as to why these minor bands were not observed in my northern blot, since the blots were from the same commercial source and the same probes and comparable stringency conditions were used. Searching of the EST database using the full length HAO1 cDNA sequence identifies numerous human ESTs from liver and one from pancreatic islet cells (Genbank BG656034.1). The latter clone is only 535 bp, but is identical to the 3' end of the full-length cDNA identified here and may therefore represent a splice variant of HAO1. However, this does not necessarily indicate that GO protein is expressed in the pancreas and absence of a band in this tissue on my northern blot would suggest that if RNA is present it is at very low levels. Jones *et al* did not speculate as to the possible role of GO in the pancreas and the significance of this finding is unknown.

The mouse HAO1 gene was found to contain an iron response element (IRE)-like sequence in the 5'UTR. These elements are hairpin sequences, which are bound by iron regulatory proteins (IRPs) to control the synthesis of proteins important in iron metabolism (Barton *et al.*, 1990). IREs form stem loop structures with a conserved CAGUGN loop where N is any nucleotide except G and are composed of an upper stem of five perfectly paired bases and a lower stem, usually separated by a single cytosine on the 5' side. The IRE-like sequence in the mouse HAO1 exhibited strong binding to IRPs *in vitro*. However, its nucleotide sequence differed from functional IREs by a

mismatch in the middle of the upper stem and didn't confer iron-dependent regulation in cells (Kohler *et al.*, 1999).

The findings of an IRE-like sequence in the HAO1 cDNA from mouse prompted my investigation of the UTRs of human HAO1. Using RACE techniques the sequences of both the 5' and 3' UTRs were determined, although no part of either sequence resembled an IRE. The human HAO1 3' UTR extends 208 bp beyond the stop codon and contains the consensus polyadenylation site AATAAA 12 bp upstream of the poly A tail. The 5' UTR is only 35 bp in length and is just downstream of a run of 16 A nucleotides. This size may be artefactual as the run of identical nucleotides may have interfered with cDNA synthesis during RACE. This possibility remains unlikely however, since the total 1756 bp length of cDNA including both UTRs and the ORF corresponds very closely in size to the 1.8 kb transcript observed in the northern blot.

To summarise, screening of the Entrez database identified a human EST with peptide sequence homology to GO from *Arabidopsis thaliana*. Although this clone did not encompass the entire coding region of the gene, a BLAST search using its sequence identified a longer EST enabling primers to be designed for the synthesis of a full length cDNA from human liver RNA by RT-PCR. The gene identified showed a liver specific expression and encoded a protein with short chain HAO activity *in vitro*. The enzyme showed highest activity with glycolate as substrate. The identification and expression of human liver GO permits the characterisation of the enzyme and enables investigation of its role in glyoxylate metabolism, as will be described in subsequent chapters.

Chapter Four

Purification and Characterisation of Human GO

4.1 Introduction

4.2 Methods

4.2.1 Purification of recombinant GO protein

4.2.2 Western blot analysis of recombinant GO

4.2.3 Chemical crosslinking

4.2.4 Enzyme kinetics

4.3 Results

4.3.1 Purification of recombinant GO protein

4.3.2 Absorption spectrum of recombinant GO

4.3.3 Investigation of GO sub-unit structure

4.3.4 Kinetic characterisation of pure recombinant GO

4.3.5 Absorption spectrum of reduced pure recombinant GO

4.4 Discussion

4.1 Introduction

The GO enzyme from spinach has been well characterised and the 3D structure has been determined by X-ray crystallography (Lindqvist, 1989). This focus on the spinach enzyme is presumably in part due to the ready availability of spinach leaves from which to purify the enzyme. Investigation of mammalian GO has been more limited, although human GO has been purified from liver (Schwam *et al.*, 1979; Fry and Richardson, 1979a) and partially characterised. This enzyme preferred glycolate as substrate when tested with a variety of α-hydroxy acids, an observation consistent with the spinach enzyme. GO has also been purified from pig (Schuman and Massey, 1971a), chicken (Dupuis *et al.*, 1990) and rat (Ushijima, 1973) livers as well as hog kidney renal cortex (Tokushige and Sizer, 1967). In none of these animal species was the protein sequence of GO determined and the kinetics with substrates other than glycolate were rarely investigated.

The cloning of a gene enables the production of large amounts of recombinant protein by utilising bacterial expression vectors. These vectors have been designed to include N-terminal and C-terminal additions to the expressed protein. For example, the addition of an antibody epitope allows immunodetection and the addition of a His tag makes possible purification by nickel affinity chromatography. These techniques enable the rapid production of large amounts of pure recombinant protein for subsequent analysis. This chapter describes the purification of human recombinant GO protein and the determination of its physical and kinetic characteristics.

4.2 Methods

4.2.1 Purification of recombinant GO protein

Pellets of BL21 cells frozen after induction of protein expression (described in section 2.3.7) were removed from the freezer, placed on ice and resuspended in 10 ml of 20 mM sodium phosphate buffer pH 7.8, containing 500 mM sodium chloride. The cells were treated with lysozyme at a concentration of 100 μg/ml on ice for fifteen minutes. The cell suspensions were subjected to sonication by three, ten second bursts from a Microson XL sonicator (Misonix), followed by flash freezing in liquid nitrogen and thawing at 37 °C. This cycle was repeated three more times, following which the cell lysates were treated with RNase (Qiagen) at a final concentration of 5 μg/ml. The cell debris was pelleted by centrifugation at 15,000 g for ten minutes at 4 °C, and the supernatants cleared by passage through a 0.8 μM syringe filter.

Recombinant protein was purified at 4 °C by means of the N-terminal His tag using nickel affinity chromatography, with the Xpress™ purification System (Invitrogen). 5 ml of supernatant was loaded onto a ProBond column and the resin resuspended by repeated inversion of the column. The column was rotated on a test tube rotator for ten minutes, to keep the resin resuspended and allow the poly His containing protein to fully bind. The resin was allowed to settle and the supernatant separated by gravity flow chromatography. This was repeated for each 5 ml aliquot of cell lysate supernatant until a total volume of 40 ml had been batch bound.

The column was washed by resuspending the resin in 4 ml of 20 mM sodium phosphate buffer pH 7.8 containing 500 mM sodium chloride, rotating for two minutes and

separating the resin from the supernatant using a pump at a flow rate of 1ml/min. This wash step was repeated three times in total to remove the less strongly bound bacterial contaminant proteins. Remaining contaminant proteins were washed from the column by resuspending the resin in 4 ml of 20 mM sodium phosphate buffer pH 6, containing 500 mM sodium chloride, rotating for two minutes and separating the resin from the supernatant using a pump at a flow rate of 1ml/min. This wash step was repeated twenty-two times in total, by which time the absorbance of eluates was less than 0.01. The recombinant protein was eluted from the column by washing with either:

1. one 5 ml wash of 20 mM sodium phosphate buffer pH 5.5, followed by two washes of 20 mM sodium phosphate buffer pH 4.0.

or 2. one 5 ml wash of each of 50 mM, 200 mM and 350 mM imidazole, followed by four 500 mM washes and one 1 M imidazole wash.

or 3. two 4 ml washes of each of 50 mM, 200 mM, 350 mM and 1 M glycine solutions in 50 mM tris buffer pH 8.3. Prior to this the column was brought to pH 8.3 using 250 mM tris buffer at the same pH.

The suitability of each of these elution methods was assessed in terms of ability to purify the protein to homogeneity and retention of GO enzyme activity. GO activity was measured in crude and pure fractions by DCIP reduction, as described in section 2.3.11. Protein was estimated by measuring the absorbance at 280 nm and specific activity was expressed as nmol DCIP reduced/min/mg protein. Purification factors were determined as follows:

$$\text{Purification factor} = \frac{\text{specific activity of pure fraction}}{\text{specific activity of crude extract}}$$

4.2.2 Western blot analysis of recombinant GO

Western blotting and detection of recombinant GO was carried out according to the procedure outlined in section 2.3.10. Anti-Xpress™ antibody (Invitrogen) was used at a 1/5000 dilution for the primary antibody. Alkaline phosphatase conjugated goat anti-mouse IgG (Sigma) was used at a 1/1000 dilution as the secondary antibody. These were the dilutions recommended by the manufacturers.

4.2.3 Chemical crosslinking

Stock solutions of 0, 12.5, 25, 62.5 and 125 mM Bis(sulfosuccinimidyl) suberate (BS3; Pierce Chemical Company) in 5 mM sodium citrate buffer pH 5 (3.5 ml 5 mM citric acid and 6.5 ml 5 mM trisodium citrate) were prepared. 2 µl of each stock solution was added to 23 µl of purified GO in 20 mM sodium phosphate buffer, 0.15 M NaCl, pH 7.5. This produced final concentrations of 0, 1, 2, 5 and 10 mM BS3 in the crosslinking reactions. The tubes were incubated at room temperature for thirty minutes. 1 µl of 1M Tris was added to each tube to stop the reaction, and the tubes were left to stand at room temperature for a further thirty minutes. After this time, 8 µl of each sample was added to 2 µl of SDS-PAGE 5x sample buffer and electrophoresis with protein staining and western blotting were carried out by the procedures described in sections 2.3.8 to 2.3.10.

4.2.4 Enzyme Kinetics

The method of two-substrate kinetics was used in which the concentrations of both substrates are simultaneously varied (Cornish-Bowden, 1995; Fell, 1997). This is explained fully in the referenced texts and is outlined briefly below.

Five different concentrations across a chosen range were selected for each of the two substrates. Enzyme activity was measured for each possible pair of substrate concentrations and the initial velocity (v) determined for each reaction condition in triplicate. Average initial velocity was calculated for each set of triplicates resulting in 25 different values of v, as shown in table 4.1.

Concentration of substrate B	Concentration of substrate A				
	A1	A2	A3	A4	A5
B1	$v_{A1,B1}$	$v_{A2,B1}$	$v_{A3,B1}$	$v_{A4,B1}$	$v_{A5,B1}$
B2	$v_{A1,B2}$	$v_{A2,B2}$	$v_{A3,B2}$	$v_{A4,B2}$	$v_{A5,B2}$
B3	$v_{A1,B3}$	$v_{A2,B3}$	$v_{A3,B3}$	$v_{A4,B3}$	$v_{A5,B3}$
B4	$v_{A1,B4}$	$v_{A2,B4}$	$v_{A3,B4}$	$v_{A4,B4}$	$v_{A5,B4}$
B5	$v_{A1,B5}$	$v_{A2,B5}$	$v_{A3,B5}$	$v_{A4,B5}$	$v_{A5,B5}$

Table 4.1 A schematic of the set of results obtained for two-substrate kinetics. *Adapted from (Fell, 1997).*

The concentration of substrate A which was used for the determination of each value of v was divided by that value of v, and a primary plot of A against A/v was plotted for each concentration of substrate B as shown in Figure 4.1(a). The slope and intercept of each line were determined and used for the secondary plots shown in Figure 4.1(b).

(a)

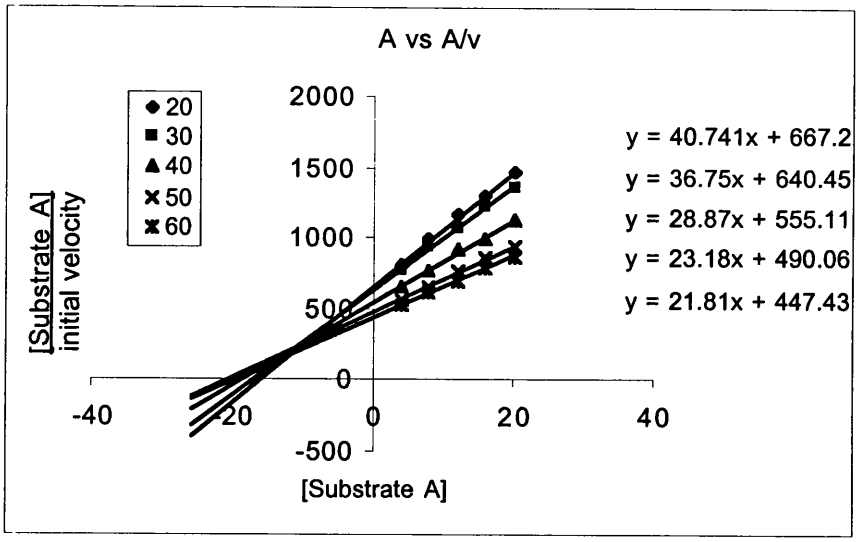

(b)

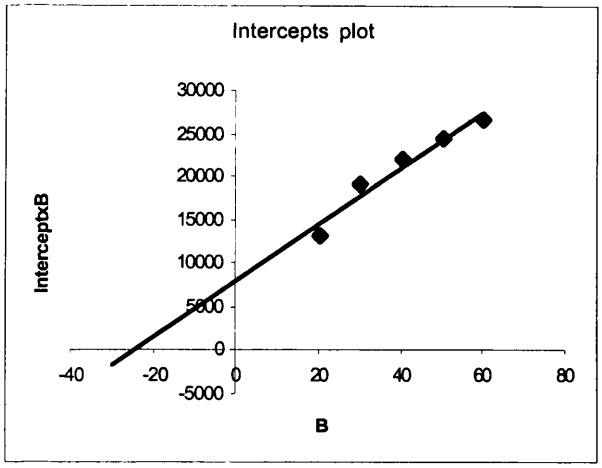

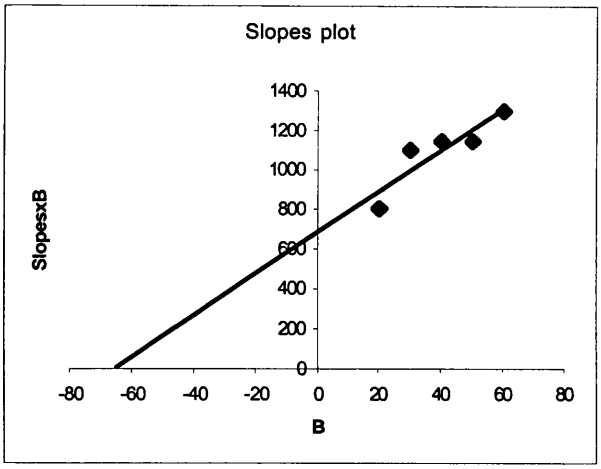

Figure 4.1 Primary and secondary plots of two-substrate kinetic data. *(a) Primary plot of [substrate A] vs [substrate A]/Initial velocity (v) (b) Secondary plots of [substrate B] vs [substrate B] x slopes from (a) and [substrate B] vs [substrate B] x intercepts from (a)*

Straight-line equations were determined by linear regression on the secondary plot data and values of V_{max} and K_m for each substrate were calculated as follows:

From the slopes plot: intercept with y axis = K_B/V hence, K_B = intercept x V

slope = $1/V_{max}$, hence V_{max} = 1/slope

From the intercepts plot: slope = K_A/V_{max}, hence K_A = slope x V_{max}

Estimates of uncertainty in V_{max} and K_m were determined using lines of worst fit to the secondary plots.

K_m values obtained were concentration of substrate in either μM (DCIP) or mM (hydroxy acids) and V_{max} values were in absorbance units/min. The flavin content of the protein sample was determined by dividing the absorbance at 450 nm by the extinction co-efficient of FMN (22,000) (Whitby, 1953). This enabled the amount of flavin present in the enzyme assay to be determined. The V_{max} values were therefore expressed as moles of DCIP reduced per min per mole of FMN as follows:

$$\text{Initial velocity } \frac{\text{(OD units/min)}}{E_{DCIP}} = \text{mmole DCIP reduced . min}^{-1}\text{ . ml}^{-1}$$

where, E_{DCIP} is 22, 000 (Armstrong, 1964) and since 1 mole of DCIP is reduced per mole of hydroxy acid utilised:

$$\text{mmole DCIP reduced . min}^{-1}\text{ . ml}^{-1} = \text{mmole hydroxy acid oxidised . min}^{-1}\text{ . ml}^{-1}$$

$$V_{max}\text{ (mole hydroxy acid oxidised. min}^{-1}\text{ . mole flavin}^{-1}\text{)} = \frac{\text{mmole DCIP reduced . min}^{-1}\text{ . ml}^{-1}}{\text{mmoles flavin in assay}}$$

4.3 Results

4.3.1 Purification of recombinant GO protein

Three different methods of elution from the nickel column were tested for efficacy. These methods were decreasing pH, increasing imidazole concentration and increasing glycine concentration. GO activity was measured in crude and pure fractions and specific activities and purification factors were calculated as described in Section 4.2.1. Purity of protein post nickel column was assessed by densitometric scanning of SDS-PAGE gels and western blotting with detection using the anti-Xpress™ antibody. The results are presented in Table 4.2 and Figure 4.2.

Purification method	Specific activity of crude extract	Specific activity of pure fraction	Purification factor
pH	544	0	Not applicable
Imidazole	674	832	1.2
Glycine	259	1360	5.3

Table 4.2 Effect of elution method upon specific activity of recombinant GO post purification on nickel affinity column.

Decreasing the pH did not elute the protein from the nickel column, as revealed by the absence of enzyme activity and presence of many peaks in the densitometric scan. 500 mM imidazole was more effective at purifying GO, as indicated by the presence of two peaks in the densitometric scan (Figure 4.2). These peaks are presumed to represent monomers and dimers of GO, since both bands showed immunoreactivity with the anti-Xpress™ antibody. 500 mM glycine was also effective at purifying the GO as indicated by the densitometric scan. Elution with glycine not only gave low background

contamination, but also yielded enzyme with specific activity greater than 4 fold higher than the imidazole purification. These results suggest that there is loss of enzyme activity during purification by imidazole and therefore, glycine elution was the most effective purification method.

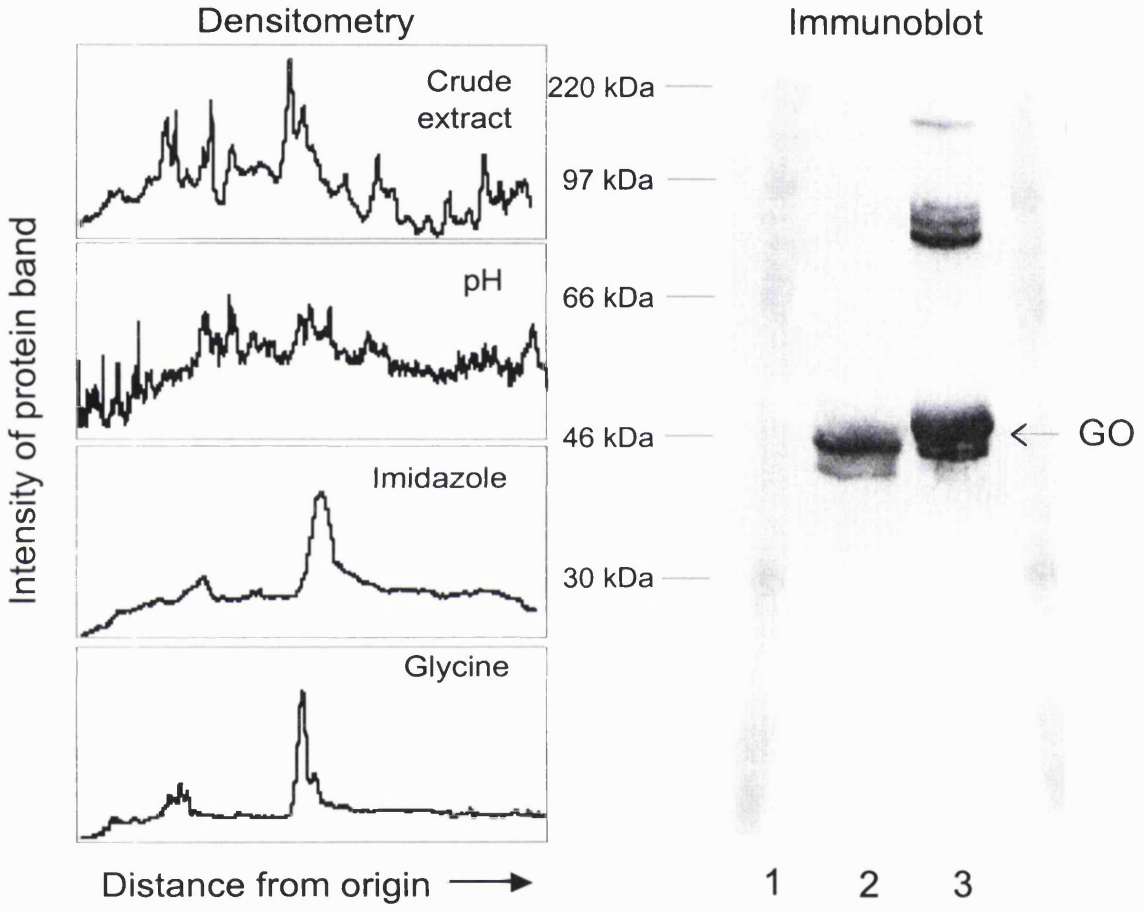

Figure 4.2 Purification of recombinant GO by nickel affinity chromatography.

Densitometric scans of Coomassie stained SDS-PAGE gels of crude bacterial extracts prior to purification and elution with pH 4, imidazole and glycine elution buffers. Immunoblot of recombinant GO detected with anti-Xpress™ antibody. Lane 1 – molecular weight markers , lane 2 – crude extract, lane 3 – glycine eluate.

4.3.2 Absorption spectrum of recombinant GO

Pure recombinant GO appears yellow in colour due to the presence of the FMN prosthetic group. This flavin has a characteristic absorption spectrum, which is detectable in the wavelength spectrum of pure flavoproteins. The wavelength spectrum of recombinant GO is depicted in Figure 4.3 and shows the characteristic flavin peaks.

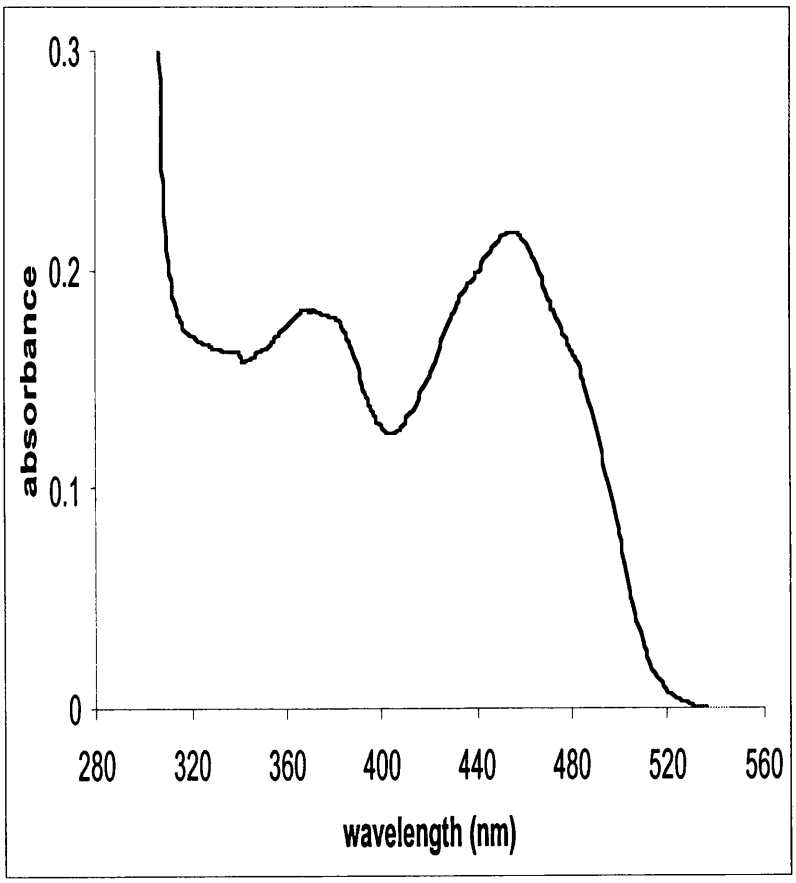

Figure 4.3 The wavelength spectrum of pure recombinant human GO. *The peaks at 370 nm and 450 nm, with 2 marked shoulders at 430 nm and 480 nm are characteristic of the FMN prosthetic group.*

4.3.3 Investigation of GO sub-unit structure

The sub-unit structure of GO was investigated by means of chemical crosslinking with BS3. This holds the sub units together by reacting with primary amines in the protein, resulting in the formation of covalent amide bonds. The results of the chemical crosslinking are shown in Figure 4.4.

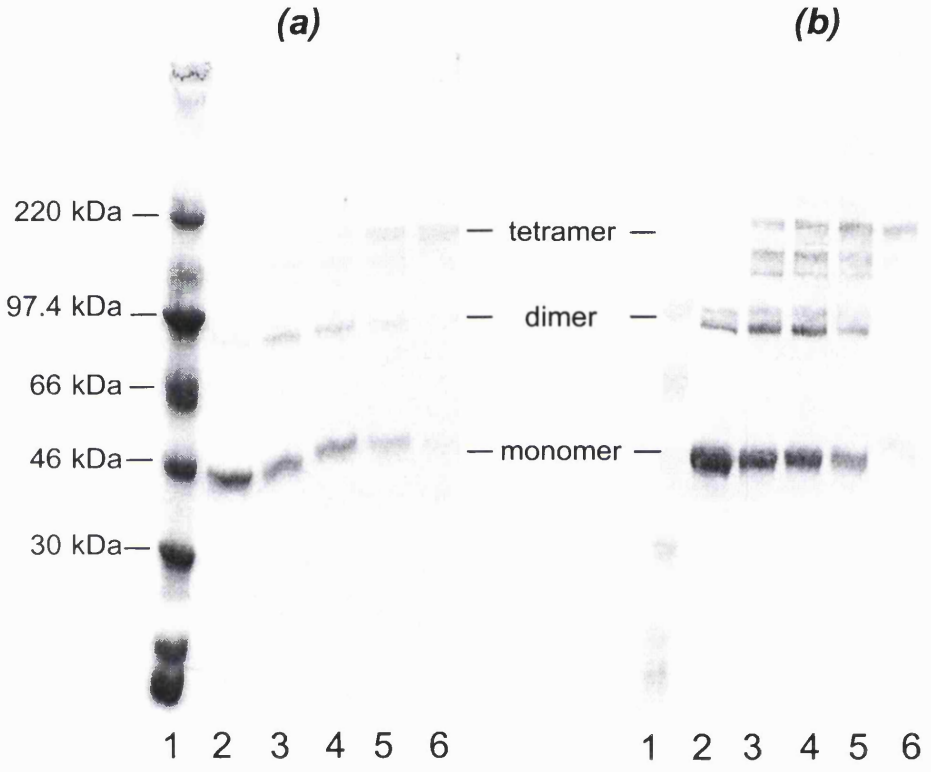

Figure 4.4 SDS page gels of crosslinked recombinant GO. *(a) Coomassie blue stained SDS-PAGE gel (b) western blot incubated with detection of GO by anti-Xpress™ antibody. Lane 1 – molecular weight markers, Lane 2 – pure GO without crosslinker, Lanes 3 – 6 represent pure GO incubated with increasing amounts of BS3.*

Upon electrophoresis of crosslinked GO by SDS-PAGE, different sized bands were observed. These were 46 kDa, ~90 kDa and ~180 kDa and represent monomers, dimers and tetramers of GO respectively. With increasing crosslinker concentration the band at ~180 kDa was most apparent, which suggests that native GO exists as a homotetramer.

4.3.4 Kinetic characterisation of pure recombinant GO

A variety of α-hydroxy acids of varying chain length were investigated by two-substrate kinetics, using DCIP as the second substrate. The α-hydroxy acids chosen were those which showed highest catalytic activity when assayed in crude bacterial extracts (Figure 3.5). The reactions investigated are summarised in Table 4.3.

α-hydroxy acid	**chain length (number of carbons)**
Glycolate	2
Glyoxylate	2
L-lactate	3
DL-α-hydroxybutyrate	4
L-α-hydroxyvalerate	5
L-α-hydroxyisocaproate	6

Table 4.3 Hydroxy acid substrates of GO, analysed by two substrate kinetics

The substrate concentrations tested were chosen so that they encompassed as wide a range as possible. However, in all cases this range was limited at the lower end by detection limits and at the upper end by increased substrate inhibition. The determination of K_m and V_{max} for each hydroxy acid and DCIP substrate pair is shown in Figures 4.5– 4.10, where the A vs v plots show the mean ± S.D. of triplicate values.

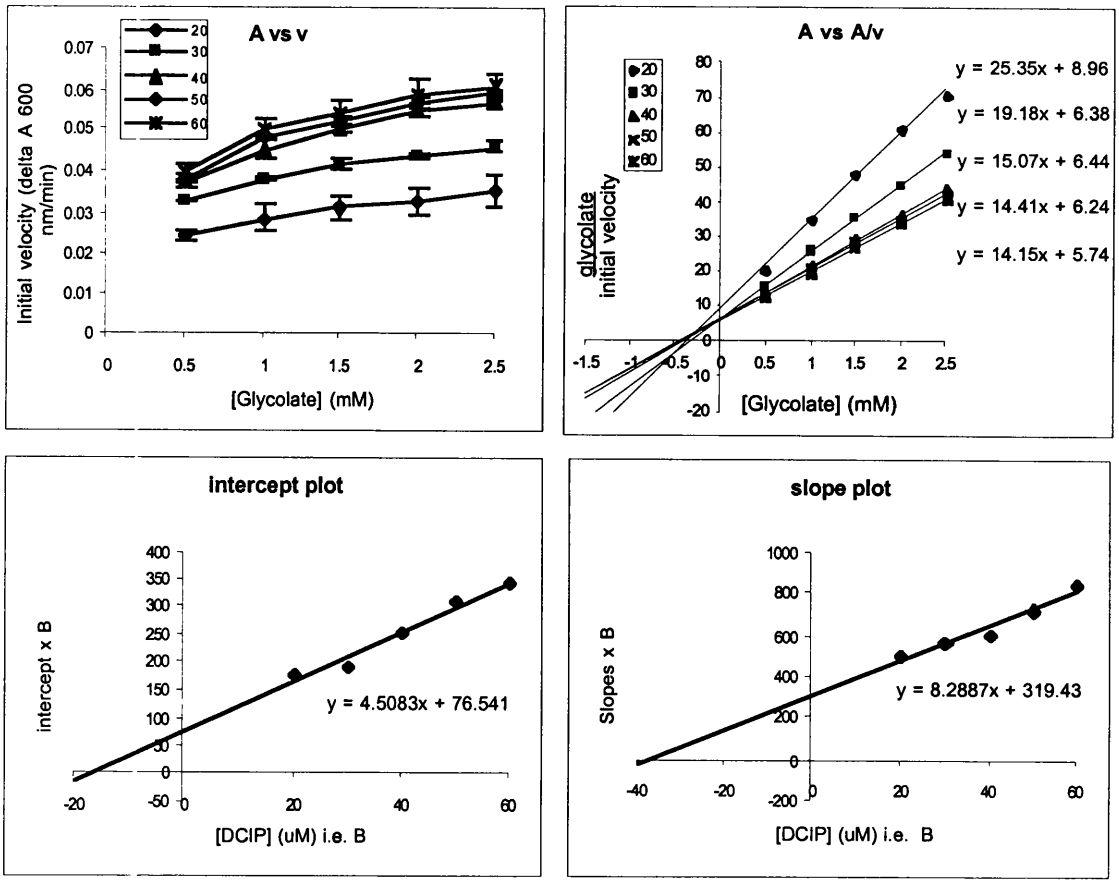

From the slopes plot:

slope = $1/V_{max}$, hence V_{max} = 1/8.2887

= 0.121 absorbance units/min

intercept on y axis = K_m DCIP/V_{max} , hence K_m DCIP = 319.43 x 0.121

= 38.5 μM

From the intercepts plot: slope = K_m glycolate/V_{max} , hence

K_m glycolate = 4.5083 x 0.121

= 0.54 mM

Figure 4.5 Two-substrate kinetics plots with glycolate and DCIP as substrates. *K_m and V_{max} were calculated from the slopes and intercepts as described in the text.*

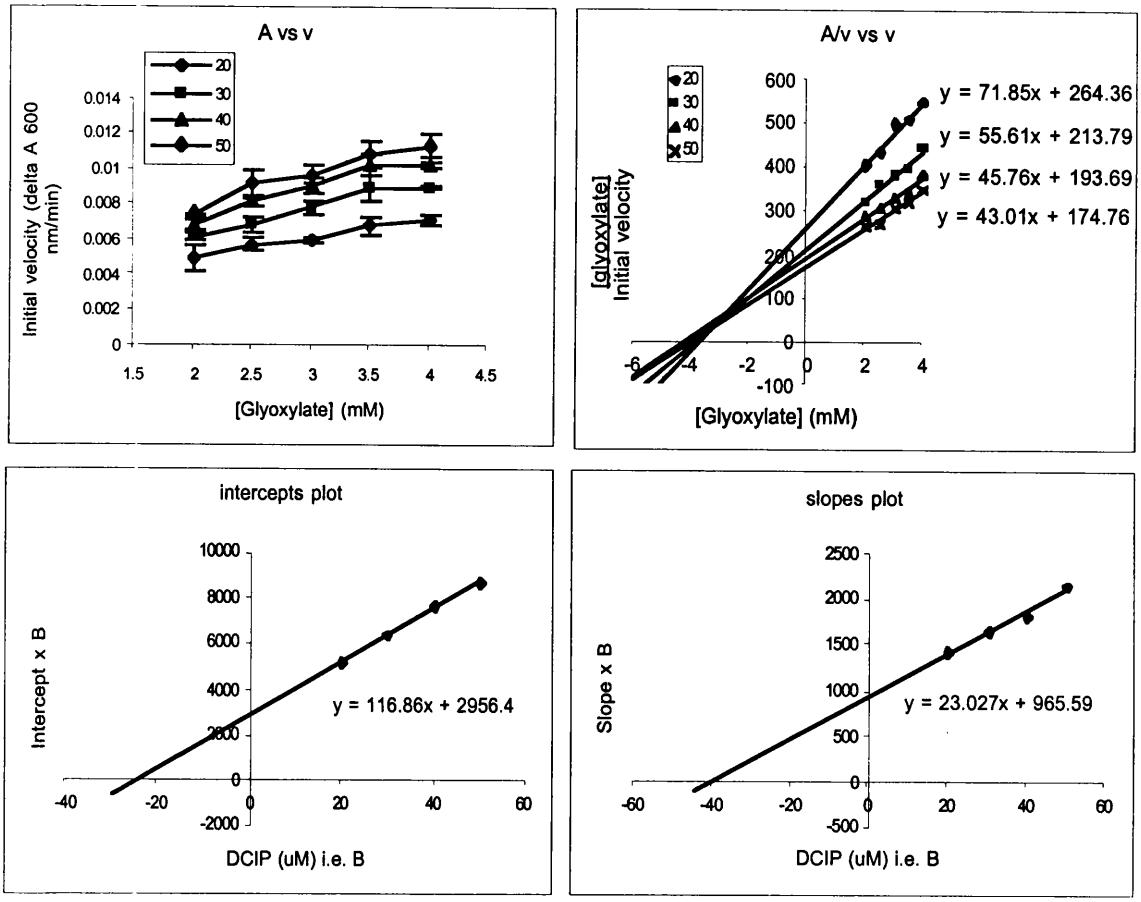

From the slopes plot:

slope = $1/V_{max}$, hence V_{max} = 1/23.027

= 0.043 absorbance units/min

intercept on y axis = K_m DCIP/V_{max} , hence K_m DCIP = 965.59 x 0.043

= 41.9 μM

From the intercepts plot: slope = Km glyoxylate/V_{max} , hence

K_m glyoxylate = 116.86 x 0.043

= 5.08 mM

Figure 4.6 Two-substrate kinetics plots with glyoxylate and DCIP as substrates. *K_m and V_{max} were calculated from the slopes and intercepts as described in the text.*

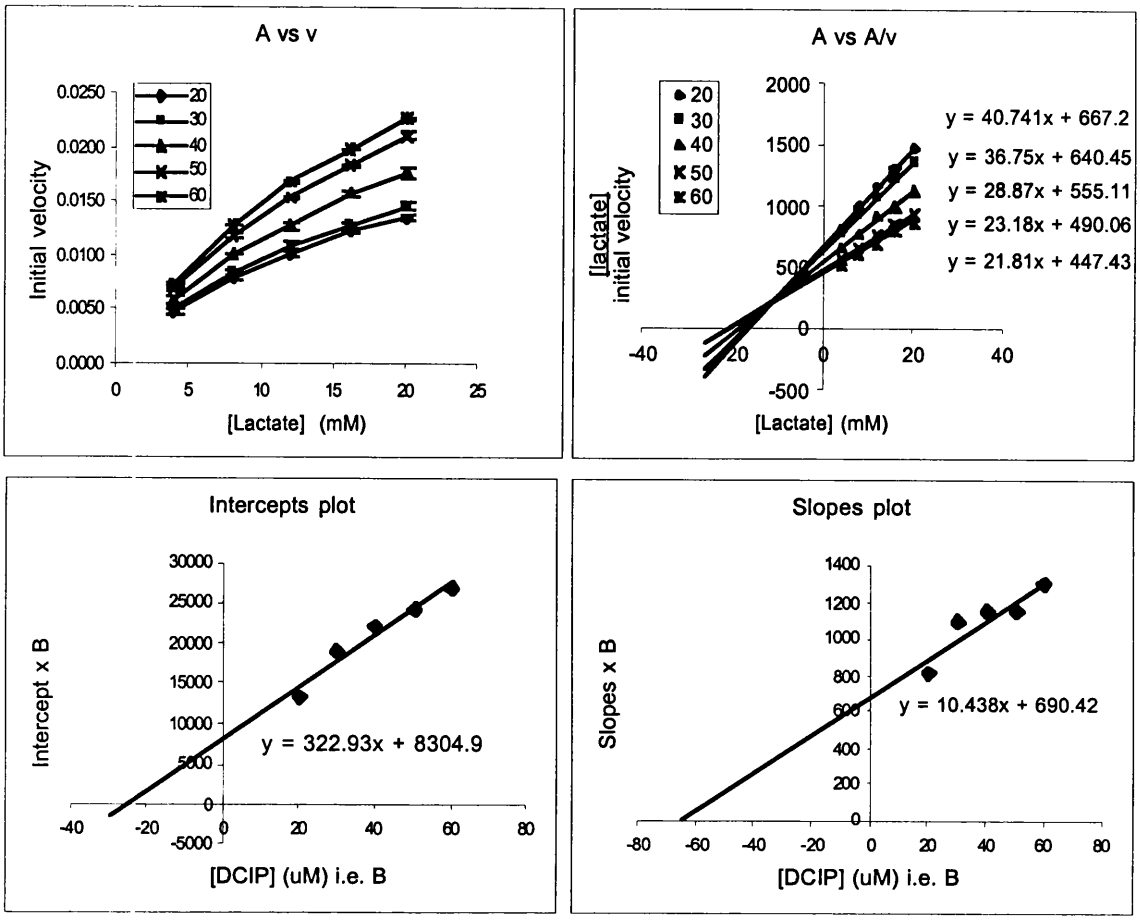

From the slopes plot:

slope = $1/V_{max}$, hence V_{max} = 1/10.438

= 0.096 absorbance units/min

intercept on y axis = K_m DCIP/V_{max}, hence K_m DCIP = 690.42 x 0.096

= 66.2 μM

From the intercepts plot: slope = K_m lactate/V_{max}, hence

K_m lactate = 322.93 x 0.096

= 30.9 mM

Figure 4.7 Two-substrate kinetics plots with lactate and DCIP as substrates. *K_m and V_{max} were calculated from the slopes and intercepts as described in the text.*

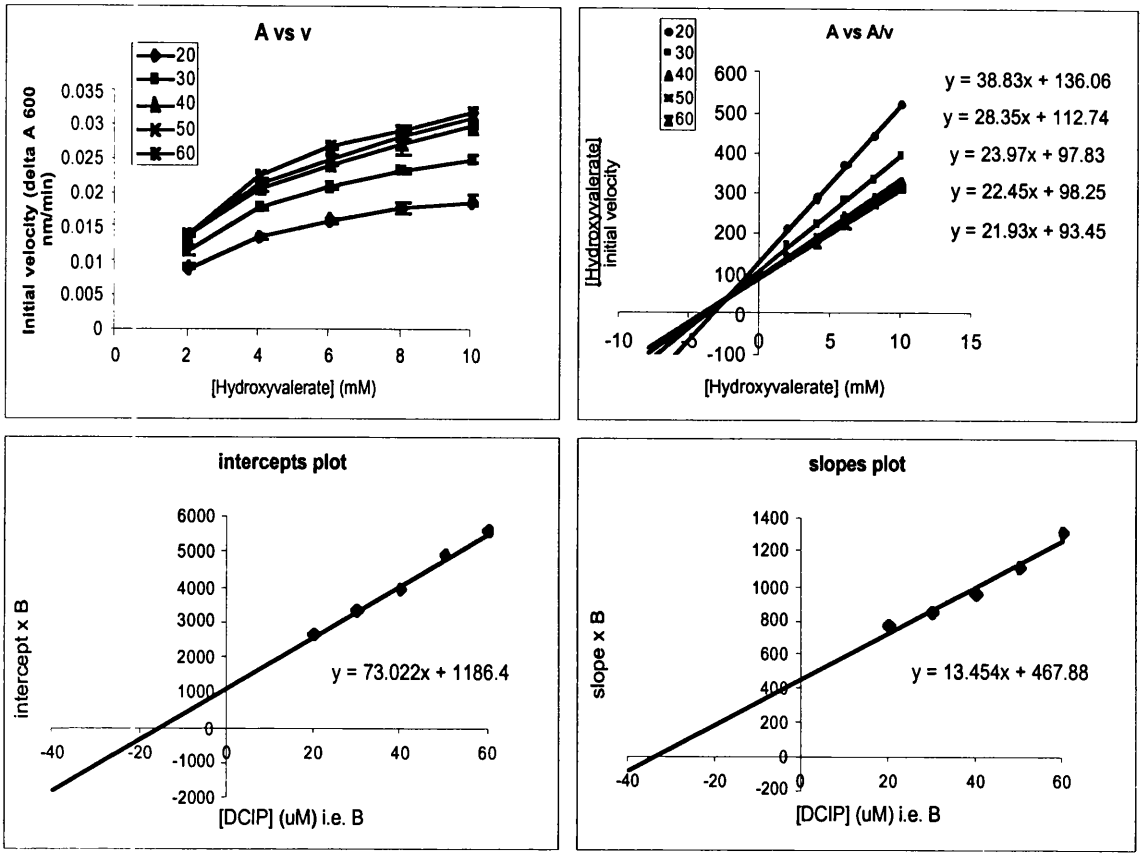

From the slopes plot:

slope = $1/V_{max}$, hence V_{max} = 1/13.454

= 0.074 absorbance units/min

intercept on y axis = $K_m DCIP/V_{max}$, hence $K_m DCIP$ = 467.88 x 0.074

= 34.8 μM

From the intercepts plot: slope = $K_m$hydroxyvalerate/V_{max}, hence

K_m hydroxyvalerate = 73.022 x 0.074

= 5.43 mM

Figure 4.8 Two-substrate kinetics plots with hydroxyvalerate and DCIP as substrates.

K_m and V_{max} were calculated from the slopes and intercepts as described in the text.

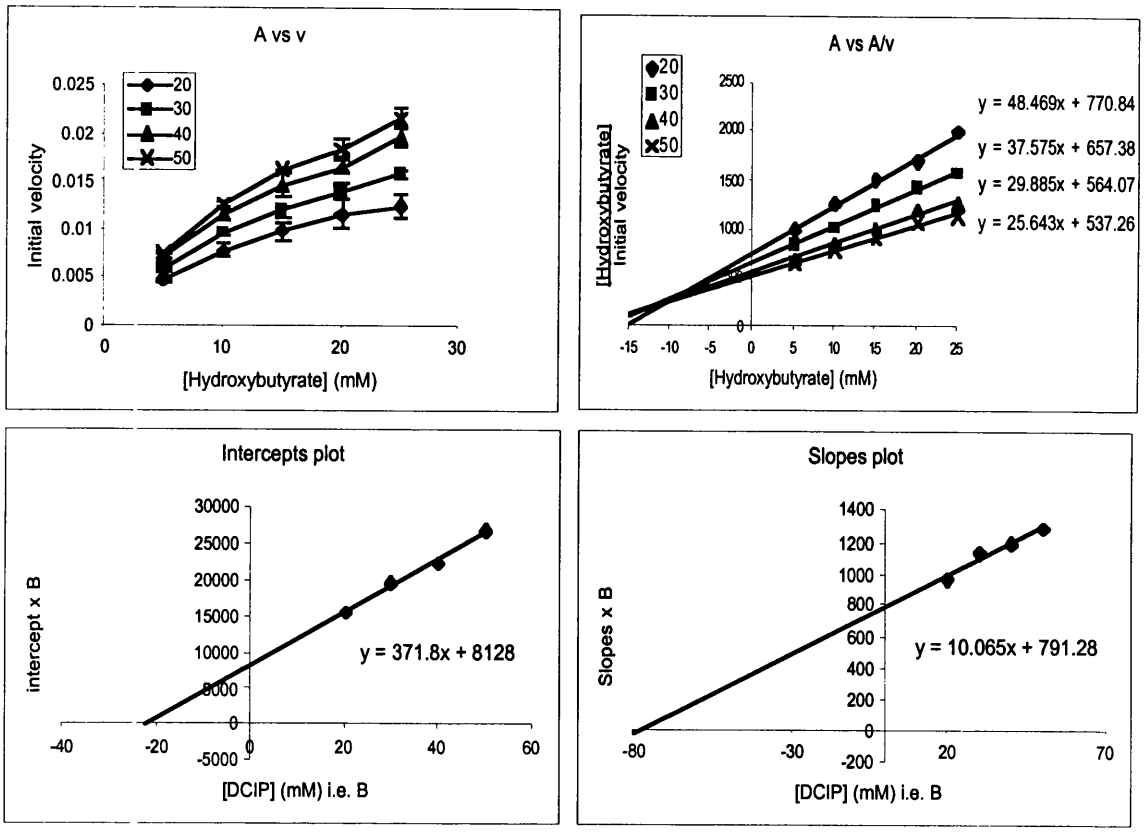

From the slopes plot:

slope = $1/V_{max}$, hence V_{max} = 1/10.065

= 0.099 absorbance units/min

intercept on y axis = K_mDCIP/V_{max}, hence K_mDCIP = 791.28 x 0.099

= 79.6 μM

From the intercepts plot: slope = K_m hydroxybutyrate/V_{max}, hence

K_m hydroxybutyrate = 371.8 x 0.099

= 36.9 mM

Figure 4.9 Two-substrate kinetics plots with hydroxybutyrate and DCIP as substrates.

K_m and V_{max} were calculated from the slopes and intercepts as described in the text.

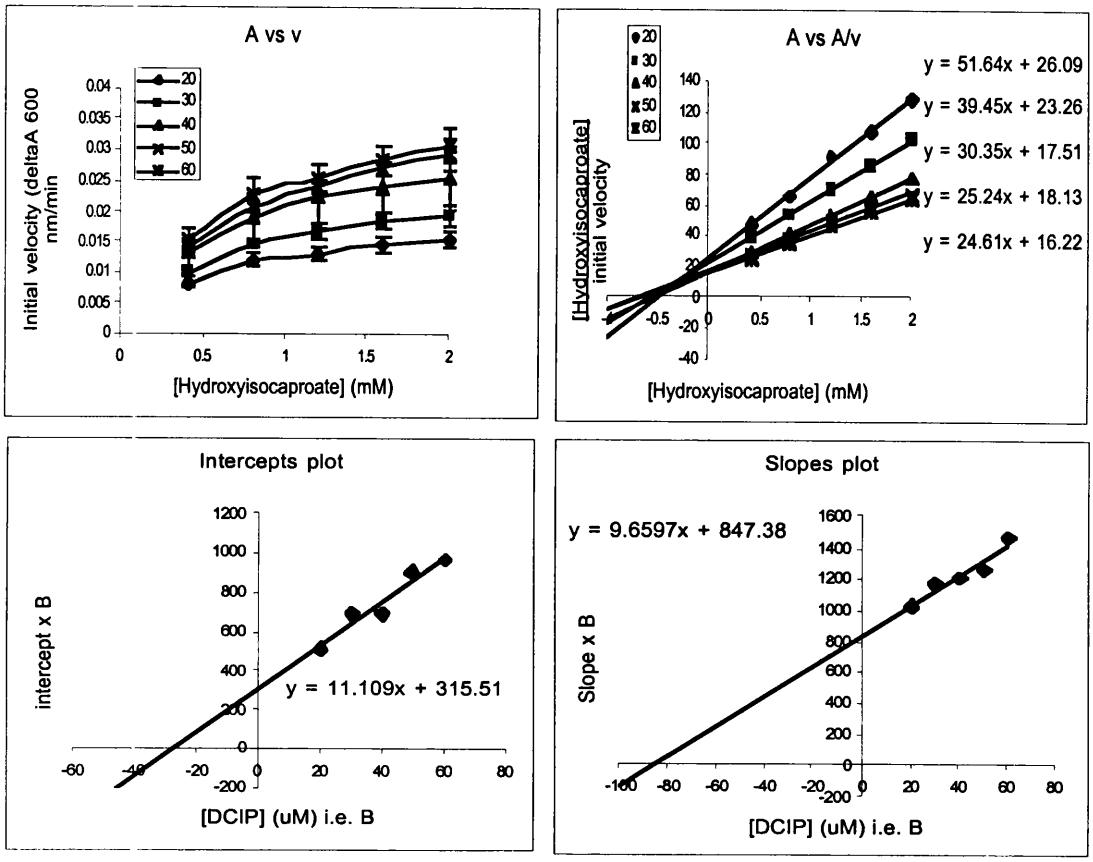

From the slopes plot:

slope = $1/V_{max}$, hence V_{max} = 1/9.6597

= 0.103 absorbance units/min

intercept on y axis = K_mDCIP/V_{max}, hence K_mDCIP = 847.38 x 0.103

= 87.4 μM

From the intercepts plot: slope = Km hydroxyisocaproate/V_{max}, hence

K_m glycolate = 11.109 x 0.103

= 1.15 mM

Figure 4.10 Two-substrate kinetics plots with hydroxyisocaproate and DCIP as substrates. *K_m and V_{max} were calculated from the slopes and intercepts as described in the text.*

The results of two-substrate kinetics are summarised in Table 4.4, where V_{max} values have been expressed relative to FMN as described in section 4.2.4.

	K_m hydroxy acid (mM)	K_m DCIP (μM)	V_{max}
Hydroxy acid			
Glycolate	0.54 ± 0.1	39 ± 8	126 ± 18
Glyoxylate	5.1 ± 0.5	42 ± 5	72 ± 7
Lactate	31 ± 9	66 ± 20	10 ± 3
Hydroxyvalerate	5.4 ± 0.6	35 ± 6	39 ± 4
Hydroxybutyrate	37 ± 8	80 ± 20	34 ± 6
Hydroxyisocaproate	1.2 ± 0.3	87 ± 18	56 ± 10

Table 4.4 Summary of results for two-substrate kinetics with a range of hydroxy acids with DCIP. *Kinetic constants were determined from straight-line equations of the slope and intercept plots ± error estimates determined from lines of worst fit. Units of V_{max} are mole hydroxy acid oxidised . min^{-1} . mole flavin^{-1}.*

The kinetics of pure GO with glycolate and oxygen as substrates was also investigated using an oxygen electrode as a more physiological means of assessing enzyme activity. Glycolate concentration was varied over the range 0.5 – 2.5 mM and the rate of oxygen decrease was monitored in the presence of 107, 141 and 217 μM oxygen. The kinetics plots are shown in Figure 4.11.

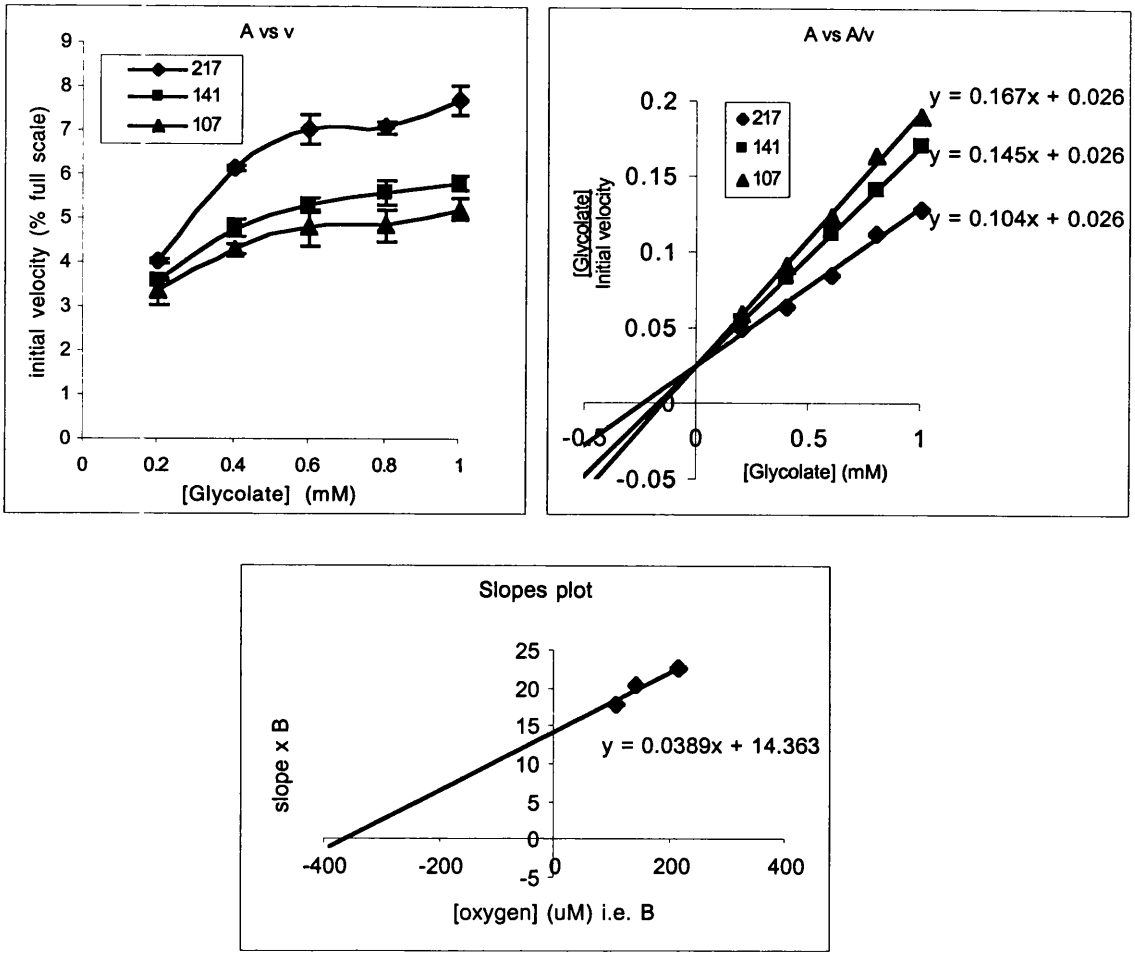

From the slopes plot:

slope = $1/V_{max}$, hence V_{max} = 1/0.0369

= 25.707

relative to flavin, V_{max} = 648 ± 175 mole hydoxy acid oxidised. min^{-1} . mole $flavin^{-1}$

intercept on y axis = $K_m$oxygen/V_{max}, hence $K_m$oxygen = 14.363 x 25.707

= 369 ± 110 μM

Figure 4.11 Two-substrate kinetics plots with glycolate and oxygen as substrates. *K_m and V_{max} were calculated from the slopes and intercepts as described in the text.*

4.3.5 Absorption spectrum of reduced pure recombinant GO

The wavelength spectrum of a sample of pure recombinant GO in the oxidised state was measured after which the sample was degassed under a stream of nitrogen and covered in parafilm. The enzyme was reduced by addition of glycolate and the wavelength was scanned again to obtain the reduced spectrum. The results are shown in Figure 4.12.

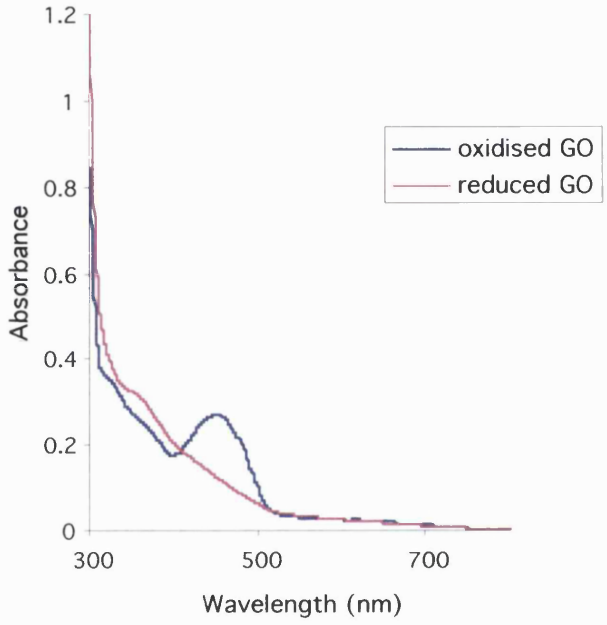

Figure 4.12 The oxidised and reduced wavelength spectrum of purified GO*. The wavelength spectrum was measured before and after saturation with glycolate in the absence of oxygen.*

As can be seen from Figure 4.12, it was possible to identify the reduced intermediate of GO when glycolate is bound to the enzyme and the hydrogen atoms have been transferred to the flavin. In the absence of oxygen the reduced flavin was unable to be reoxidised, resulting in the reduced spectrum shown in the figure. Upon reoxygenation of the buffer the spectrum returned to the oxidised state, due to reoxidation of the FMN.

4.4 Discussion

Recombinant GO expressed in BL21 *E. coli* cells has been purified to homogeneity by means of nickel affinity chromatography. Glycine elution was most efficient in terms of retention of enzyme activity and purity of the protein. The glycine purification protocol also included a neutralisation step to raise the pH to 8.3 after washing with pH 6 buffer. This may have contributed to the preservation of enzyme activity observed, since it limited the exposure of GO to low pH. Using this method, recombinant GO was purified over 5 fold from crude bacterial extracts yielding pure protein with a specific activity of 1360 nmol DCIP reduced/min/mg protein.

Purified GO protein was yellow in colour indicating the presence of oxidised flavin and displayed the characteristic flavoenzyme wavelength spectrum, with absorbance peaks at 370 nm and 450 nm. The ratio of absorbances at 280 nm to 450 nm is used to assess the purity of flavoproteins and the pure recombinant GO isolated here displayed a ratio of 6.4. This compares favourably to the value of 6.1 reported for GO purified from human liver (Schwam *et al.*, 1979) and 7.3 for the enzyme from pig (Schuman and Massey, 1971a). In contrast, the ratio reported by Jones and colleagues for human recombinant GO purified by nickel affinity chromatography using imidazole elution was 32.3 (Jones *et al.*, 2000). They suggested that approximately 80% of their GO protein would have been catalytically inactive due to flavin loss.

The anti-Xpress antibody detected a major band at 46 kDa in western blots of SDS-PAGE gels, however some higher molecular weight bands of immunoreactivity were also present. This result suggested that GO in its native form consists of several monomers bound together and hence the sub-unit structure was investigated by chemical

crosslinking with BS3. This chemical holds the sub-units together by forming covalent amide bonds between lysine residues, which resist the reducing conditions of the SDS buffer. This treatment revealed monomers, dimers and tetramers of GO. As can be seen from Figure 4.3, tetramers of GO were most apparent with the highest concentration of crosslinker, indicating that the native protein is composed of 4 identical monomers. The GO enzyme purified from human liver also showed similar results on crosslinking. BS3 treatment at pH 9.5 revealed a single band at ~160 kDa, in contrast to a single band at ~ 40 kDa revealed by SDS-PAGE in 5M guanidine HCl (Schwam *et al.*, 1979).

Pure recombinant GO prefers glycolate as substrate, in common with GO purified from the livers of various species and from spinach. The K_m for pure recombinant GO was 0.54 mM, compared to 0.34 mM for the enzyme purified from human liver (Fry and Richardson, 1979a), 0.42 mM for the pig enzyme (Schuman and Massey, 1971b) and 0.3 mM for GO from hog kidney (Tokushige and Sizer, 1967). The enzyme displayed a 10 fold reduced affinity for glyoxylate as substrate than for glycolate, as represented by the K_m value of 5.4 mM for glyoxylate.

Two-substrate kinetics for a range of α-hydroxy acids with DCIP as the second substrate all showed lines converging in the upper left quadrant of the A vs A/v plot (Figures 4.5 – 4.10). This is indicative of a catalytic mechanism involving the formation of a ternary complex (Cornish-Bowden, 1995). That is to say that during catalysis more than one substrate or product are bound simultaneously. However, this is in contrast to the findings reported previously for spinach GO. Using steady state and rapid reaction studies with oxygen as substrate, the spinach enzyme was found to react in a ping-pong mechanism i.e. only involving binary complexes (Macheroux *et al.*, 1991). In this

mechanism, the α-hydroxy acid substrate is oxidised to the corresponding α-keto acid at the expense of flavin reduction. The product is released from the active site and the reduced flavin is re-oxidised by the second substrate (oxygen or DCIP). The reduced second substrate is then released from the active site as the second product of the reaction and the enzyme is ready to start the catalytic cycle again.

A binary complex mechanism has also been reported for GO from pig liver with oxygen as substrate (Dickenson and Massey, 1963). This is in contrast to the findings of DCIP kinetics with the same enzyme, which indicated a ternary complex mechanism (Schuman and Massey, 1971b). The kinetics carried out with the oxygen electrode in this thesis, though not as extensive as the work with DCIP, displayed lines converging on the y axis in the A vs A/v plot consistent with a binary complex mechanism. Therefore, it would seem possible that GO forms a ternary complex when DCIP is the second substrate and a binary complex when oxygen is the second substrate. However, this may not be the case as it has been shown that in the absence of oxygen, kinetics with DCIP display a binary complex mechanism (Fry and Richardson, 1979a). Hence, the differences observed seem to be due to the presence of oxygen in the DCIP studies.

To investigate the catalytic mechanism of GO further the reductive half of the reaction was studied by probing the FMN spectrum. It was possible to identify enzyme containing reduced flavin, when the enzyme was saturated with glycolate in the absence of oxygen. This observation supports a ping-pong mechanism, involving only binary complexes. Therefore, it appears most likely that GO operates a ping-pong mechanism involving binary complexes, at least with its physiological substrate of oxygen.

The kinetic studies of pure recombinant GO have shown that the enzyme is capable of utilising glyoxylate as a substrate. This confirms that it is a candidate enzyme for the production of oxalate in primary hyperoxaluria, although the extent to which this reaction actually operates *in vivo* in PH is unknown. It would seem unlikely that GO would catalyse the conversion of glyoxylate to oxalate in normal metabolism as glyoxylate would be quickly removed by AGT. The peroxisomal location of GO would suggest that it is more likely to play a role in oxalate production in PH1, when the glyoxylate would build up in the peroxisome. In contrast it would seem less likely that GO contributes to oxalate production in PH2, when the glyoxylate would build up in the cytosol. In this instance, cytosolic LDH would be the more likely candidate for oxalate production.

The extent to which GO would produce oxalate from glyoxylate in PH1 would depend upon several factors. Firstly, the level of glyoxylate would need to increase to such levels that it could compete effectively with glycolate. Based upon the K_m values of the two substrates, glyoxylate would need to be present at a concentration 10 fold higher than glycolate for GO to bind it to the same extent. However, given the V_{max} with glyoxylate as substrate is approximately half that for glycolate oxidation the turnover with the former substrate will also be halved. These differences mean that glycolate is the most specific substrate and therefore the most favourable reaction. Liver glyoxylate concentration has been found to be 5 nmol/g and 10 nmol/g wet weight of homogenised tissue in rat (Funai and Ichiyama, 1986) and guinea pig (Holmes *et al.*, 1995) respectively. These values don't reveal the actual concentration inside the cell, although calculations made on similar measurements for glycolate estimated its concentration in

the cytosol to be 0.2 mM (Holmes *et al.*, 1995). As the amount of glyoxylate per gram of liver is less than that of glycolate (Holmes *et al.*, 1995), the cellular concentration of glyoxylate in normal human liver will be lower than 0.2 mM. However, if the glyoxylate in a cell is assumed to be predominantly peroxisomal (the site of glyoxylate synthesis catalysed by GO), a higher local concentration can be expected (Yanagawa *et al.*, 1990).

Another factor that will influence glyoxylate oxidation by GO is the rate of its diffusion out of the peroxisome, which would need to be slower than the rate of its oxidation by GO for glyoxylate oxidation to be favourable. Little is known about intracellular membrane transport and it isn't clear whether such movement would occur by passive diffusion across organelle membranes or by an active transport process. A family of proton-linked monocarboxylate transporters exists in mammals, residing in the plasma membrane and the mitochondrial membrane (reviewed in Halestrap and Price, 1999). An anion-selective porin-like channel protein has been found in the membrane of spinach leaf peroxisomes (Reumann *et al.*, 1995). The channel was found to have a minimum diameter of 0.6 nm (Reumann *et al.*, 1998) and allowed the passage of glycolate and glycerate (Reumann *et al.*, 1995). This porin was distinctly different to the transporters of mitochondrial and plasma membranes and it is not known whether it occurs in mammalian peroxisomes.

In favour of GO is the fact that the enzyme is responsible for glyoxylate production from glycolate. Glyoxylate is therefore both a product and a substrate for GO in comparison to LDH, which is reported to be unable to catalyse glycolate oxidation (Yanagawa *et al.*, 1990). In isolated rat hepatocytes, GO inhibition produced a more marked decrease in oxalate production from glycolate than from glyoxylate. In contrast,

LDH inhibition caused a greater decrease in oxalate production from glyoxylate than from glycolate (Bais *et al.*, 1989). This observation highlights the importance of GO for glycolate conversion to glyoxylate.

Given the liver specific expression of AGT, it follows that it is in the liver that glyoxylate accumulates in PH1. The hepatic and peroxisomal location of GO, coupled with its kinetically favourable role in glyoxylate production highlights the importance of AGT for glyoxylate detoxification. Furthermore, it seems likely that the liver will be the main organ producing oxalate in PH since this is where the glyoxylate will accumulate. GO and LDH are the candidate enzymes for catalysing oxalate production. However, comparison of the two enzymes is difficult given the lack of investigation of the kinetics of LDH with glyoxylate as substrate. Clearly both GO and LDH are capable of contributing to oxalate production from glyoxylate. However, the extent to which each enzyme contributes to the pathogenesis of PH remains to be established.

To summarise, human recombinant GO has been purified to homogeneity by means of nickel affinity chromatography. Elution by glycine was the most efficient method in terms of purity obtained and preservation of catalytic activity. Kinetic analysis indicated the most specific substrate for the enzyme to be glycolate. Glyoxylate oxidation, although kinetically possible, appears less favourable and would seem unlikely to occur *in vivo* in normal metabolism. A convenient and rapid method for the production of purified recombinant GO protein has been established, and can be utilised to purify mutant recombinant proteins created by site directed mutagenesis. Thus the roles of active site amino acid residues may be investigated by kinetic analysis, which is the subject of the following chapter.

Chapter Five

Investigation of the Active Site of Human GO

5.1 Introduction

5.2 Methods

5.2.1 Generation of mutant constructs

5.2.2 Characterisation of recombinant mutant proteins

5.3 Results

5.3.1 Generation and expression of mutant GO proteins

5.3.2 Kinetic characterisation of mutant GO proteins

5.4 Discussion

5.1 Introduction

The three-dimensional structure of GO from spinach has been elucidated by X-ray crystallography (Lindqvist and Branden, 1989) and has been refined to 0.2 nm resolution (Lindqvist, 1989). Prior to these structural studies, a general hypothesis for the catalytic mechanism of FMN oxidases had been postulated, based upon the findings of spectroscopic and kinetic analysis of lactate oxidase (Ghisla and Massey, 1991). However, the crystallographic studies of spinach GO identified the active site and allowed the specific amino acid residues likely to be involved in the various steps of the enzyme mechanism to be identified (described in chapter 3). The equivalent residues in human GO include Arg 263, thought to bind the substrate carboxyl group, and His 260 proposed to be important for abstracting the substrate αC hydrogen as a proton during catalysis by the spinach enzyme (Lindqvist and Branden, 1989). Alignment of the protein sequence of spinach GO with the sequences of other flavoproteins identified a unique amino acid, Trp 108, which upon mutation was shown to influence substrate specificity (Stenberg *et al.*, 1995). The equivalent amino acid in human GO is Trp110.

The cloning of the human HAO1 gene described in this thesis (Chapter 3) has enabled amino acids potentially critical for catalysis in human GO to be identified, by comparison to the protein sequence of spinach GO (Figure 3.2). This chapter describes the generation and kinetic analysis of five mutant forms of human recombinant GO, in which residues Arg 263, His 260 and Trp 110 have been replaced by amino acids which cannot functionally substitute for the original amino acid, by means of site directed mutagenesis of the isolated gene.

5.2 Methods

5.2.1 Generation of mutant constructs

Oligonucleotide primers containing the desired mutation were designed to anneal to the same DNA segment on opposite strands of the plasmid template. These primers were synthesised to order by Sigma Genosys Biotechnologies (Pampisford, UK). The mutations and primer sequences are listed in Table 5.1. Mutant constructs were generated by means of a Quickchange® site directed mutagenesis kit (StratageneLtd, Cambridge, UK) as follows:

25 ng of plasmid template and 125 ng of each primer were added to a PCR mix containing final concentrations of 10 mM potassium chloride, 10 mM Tris HCl, pH 8.8, 10 mM diammonium sulphate, 2 mM magnesium sulphate, 0.1% Triton® X-100, 1 mM dNTPs and 2.5 units *Pfu turbo* DNA polymerase in a total volume of 50 µl. SDM reactions were carried out in an OmniGene thermal cycler (Hybaid, Ashford, UK) according to the following programme:

30 seconds denaturation at 95 °C

16 cycles of:

30 seconds denaturation at 95 °C

1 minute annealing at 55 °C

8 minutes extension at 68 °C

2 minutes at 4 °C

Following this 10 units of *Dpn*I were added to each reaction tube below the mineral oil overlay and the non-mutated plasmid template was digested by incubation for 1 hour at 37 °C. XL1-Blue supercompetent cells (Stratagene) were transfected with 1 μl of the *Dpn*I treated samples according to the kit protocol. 250 μl of transformation products were plated onto LB-agar plates containing ampicillin. Following overnight incubation at 37 °C colonies were picked and analysed for presence of plasmid by the method outlined in section 2.3.3. All mutant constructs were sequenced along the entire length of the coding region, to confirm the presence of the desired mutation and ensure that no spurious mutations had occurred during the mutagenesis reactions.

Primer name	Primer sequence	Nucleotide change	Amino acid change
W110FA	5' GCATGATGTTGAGTTCCTTTGCCACCTC	G352T; G353T	Trp110Phe
W110FB	5' GAGGTGGCAAAGGAACTCAACATCATGC		
W110GA	5' GCATGATGTTGAGTTCCGGGGCCACCTC	T351G	Trp110Gly
W110GB	5' GAGGTGGCCCCGGAACTCAACATCATGC		
W110LA	5' GCATGATGTTGAGTTCCTTGGCCACCTC	G352T	Trp110Leu
W110LB	5' GAGGTGGCCAAGGAACTCAACATCATGC		
H260GA	5' GGATCTTGGTGTCGAATGGTGGGGCTCG	C801G; A802G	His260Gly
H260GB	5' CGAGCCCCACCATTCGACACCAAGATCC		
R263GA	5' CGAATCATGGGGCTGGACAACTCGATGG	C810G	Arg263Gly
R263GB	5' CCATCGAGTTGTCCAGCCCCATGATTCG		

Table 5.1 Summary of mutations and primer sequences for SDM studies.

5.2.2 Characterisation of recombinant mutant proteins

Mutant plasmid constructs were transfected into *Epicurean coli* BL21 cells and recombinant protein was expressed according to the methods outlined in sections 2.3.6 and 2.3.7 respectively. Crude bacterial extracts were analysed for GO activity by the DCIP assay as described in section 2.3.11. Active mutant proteins were purified by nickel affinity chromatography with elution by glycine as described in section 4.2.1.

The pure proteins were investigated by steady-state kinetic analysis using DCIP as the electron acceptor. Hydroxy acid concentrations were varied while DCIP was the fixed substrate and velocity values of OD units/min were determined from the raw data. These velocity values were converted to moles of hydroxy acid utilised . min^{-1}. mole of $flavin^{-1}$ as described in section 4.2.4.

Means of triplicate measurements were calculated, Hanes plots of A vs A/v were plotted and straight-line equations were determined by linear regression. From these equations kinetic constants were determined as follows:

Slope = $1/V_{max}$, hence V_{max} = 1/slope

Intercept = K_m/V_{max} , hence K_m = Intercept x V_{max}

Estimates of uncertainty in K_m and V_{max} were determined using lines of worst fit to the Hanes plots.

5.3 Results

5.3.1 Generation and expression of mutant GO proteins

Sequencing of mutant plasmid constructs confirmed the presence of desired nucleotide changes and the absence of spurious mutations elsewhere in the coding sequence. Sequencing traces of the mutated and wild-type plasmid are shown in Figure 5.1.

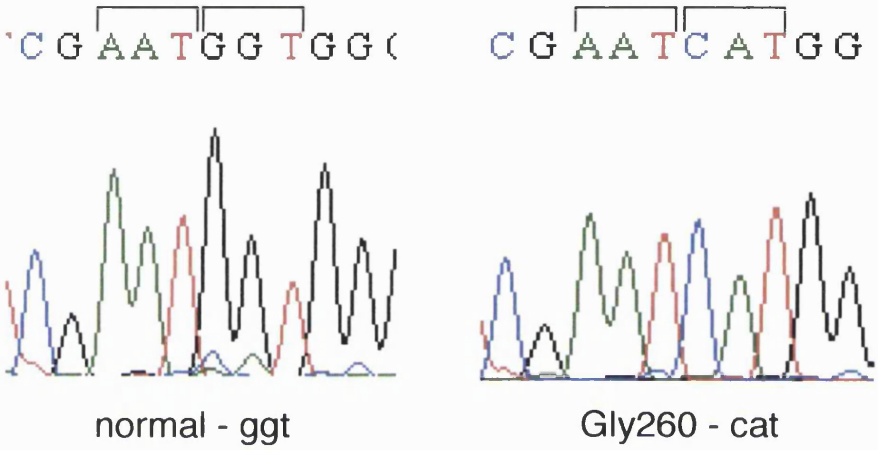

Figure 5.1 (a) Sequencing profile of the Gly 260 mutant.

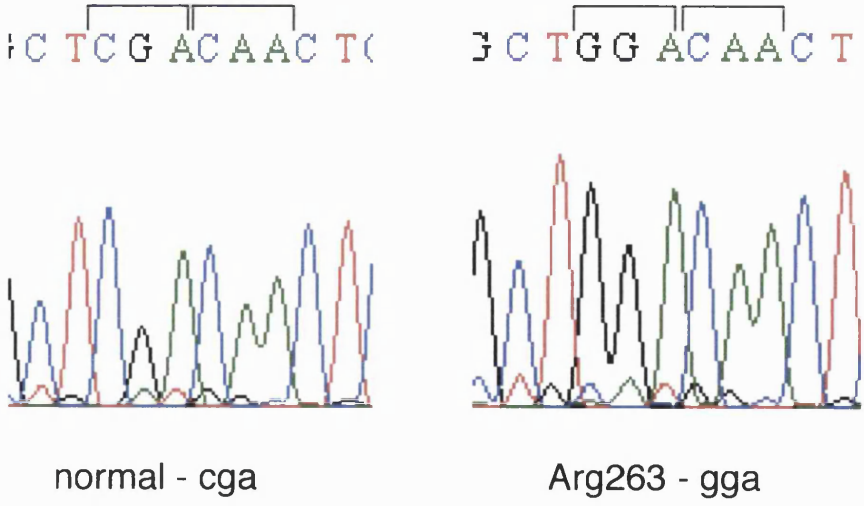

Figure 5.1 (b) Sequencing profile of the Arg 263 mutant.

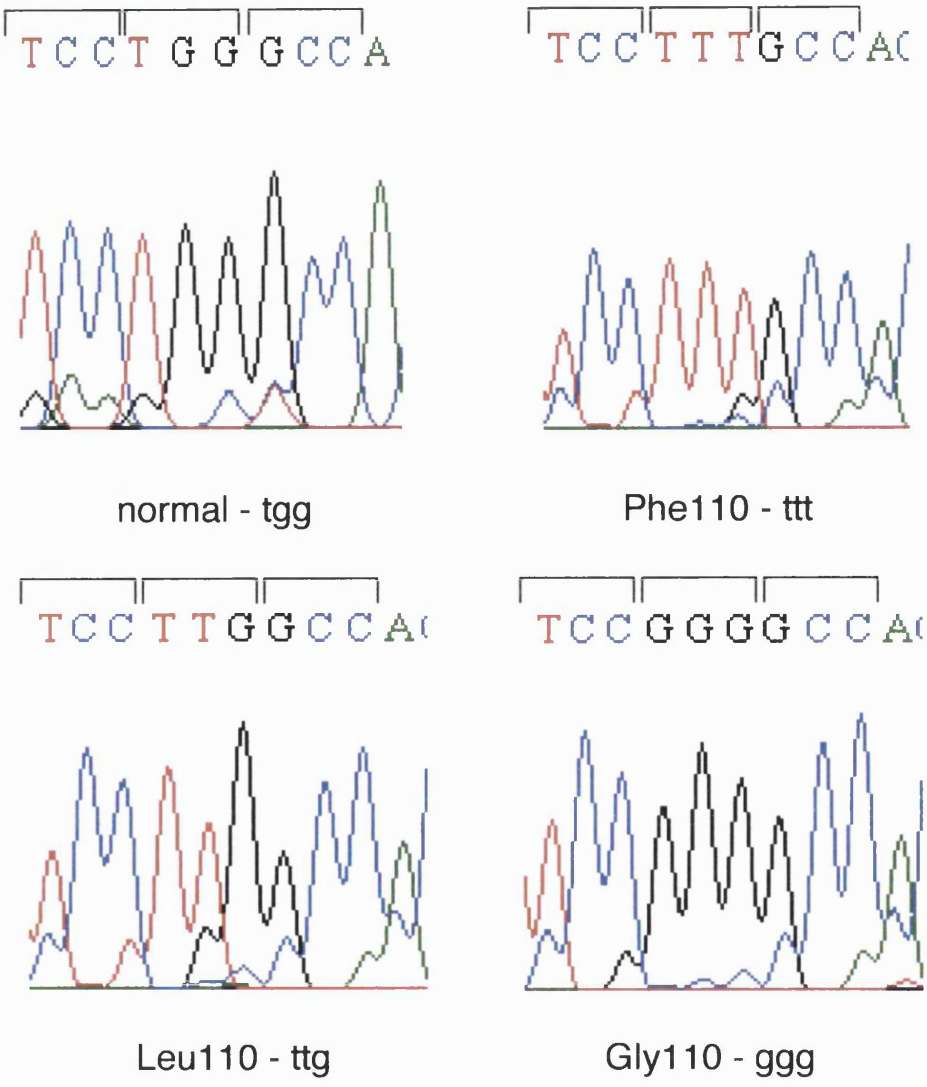

Figure 5.1 (c) Sequencing profiles of the Phe 110, Leu 110 and Gly 110 mutants.

As can be seen from Figure 5.1, active site mutants of human recombinant GO have been successfully constructed by means of the Quickchange® site directed mutagenesis kit. Analysis of crude bacterial extracts, by means of the DCIP assay, found that the mutants exhibited decreased oxidation rates with glycolate as substrate in comparison to the wild-type recombinant GO extract (Table 5.2).

Protein	Activity of crude extract	Activity of pure protein	Purification factor
Wild-type	3622	6349	1.8
Phe 110	213	1410	6.6
Gly 110	1.85	22.0	12
Leu 110	201	1532	7.6
Gly 260	nd	38.2	na
Gly 263	4.56	7.77	1.7

Table 5.2 Purification of mutant recombinant GO proteins. *Units of activity are nmol of glycolate oxidised . $^{-1}$. min $^{-1}$. mg protein $^{-1}$.*

In order to estimate the levels of protein expression, 6 μg of total protein from each crude extract was analysed by SDS-PAGE with Coomassie blue staining and western blots were analysed by incubation with Anti-Xpress antibody. These results revealed reduced protein expression for all mutants in comparison to wild-type GO (Figure 5.2). This was particularly the case for the Gly 263 mutant, which was barely detectable in Coomassie blue stained SDS-PAGE gels and western blots, although catalytic activity was detectable. This finding is in contrast to the Gly 260 mutant, where crude extracts showed no detectable catalytic activity (Table 5.2) even though Coomassie blue stained SDS-PAGE gels and western blots indicated relatively high levels of protein expression. The mutant proteins were all purified to homogeneity, by means of nickel affinity chromatography, as indicated by SDS-PAGE and western blot analysis (Figure 5.3).

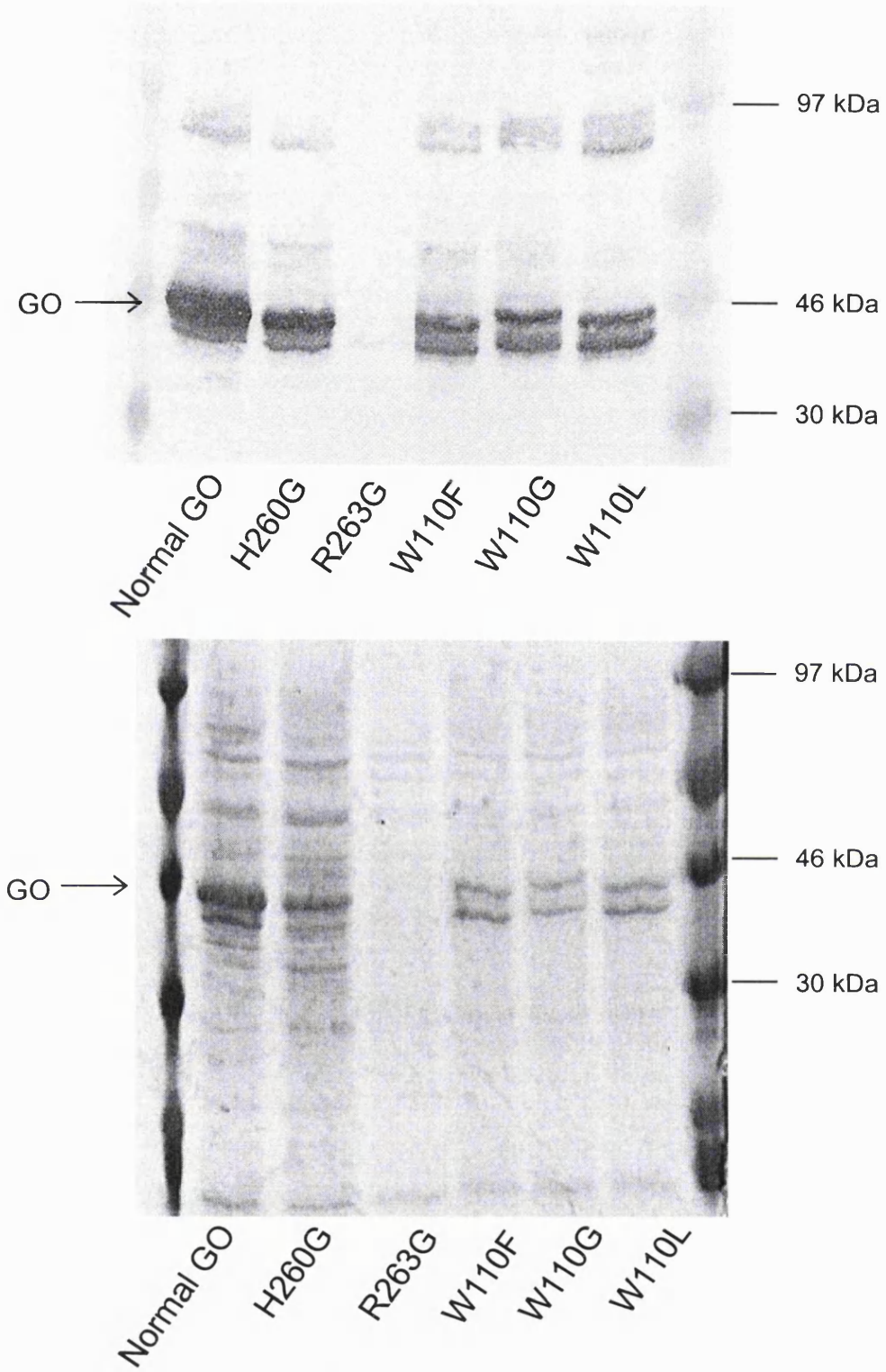

Figure 5.2 (a) Western blot and (b) Coomassie blue stained SDS-PAGE gel of crude extracts of mutant GO proteins.

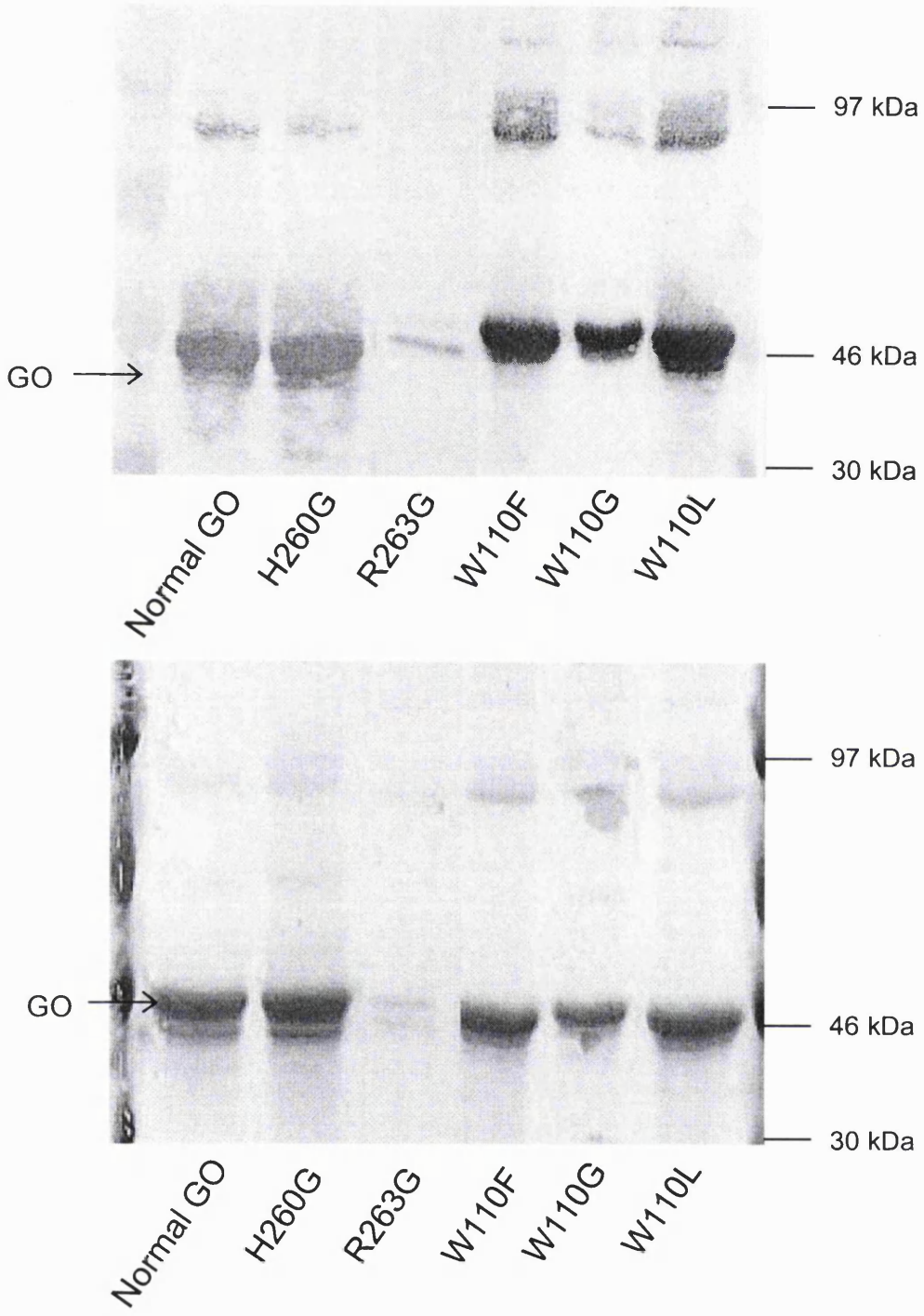

Figure 5.3 (a) Western blot and (b) Coomassie blue stained SDS-PAGE gel of purified mutant GO proteins. *Molecular weight markers are shown at the edges of the figure.*

5.3.2 Kinetic characterisation of mutant GO proteins

In order to assess the effects of each mutation, pure recombinant proteins were subjected to kinetic analysis to determine the apparent K_m and V_{max} values. Despite the very low level of protein expression of the Gly 263 mutant, and the absence of GO activity in crude bacterial extracts of the Gly 260 mutant, kinetic analysis of glycolate oxidation by the pure proteins was possible. Hanes plots for the Gly 260, Gly 263 mutants and normal GO are shown in Figure 5.4.

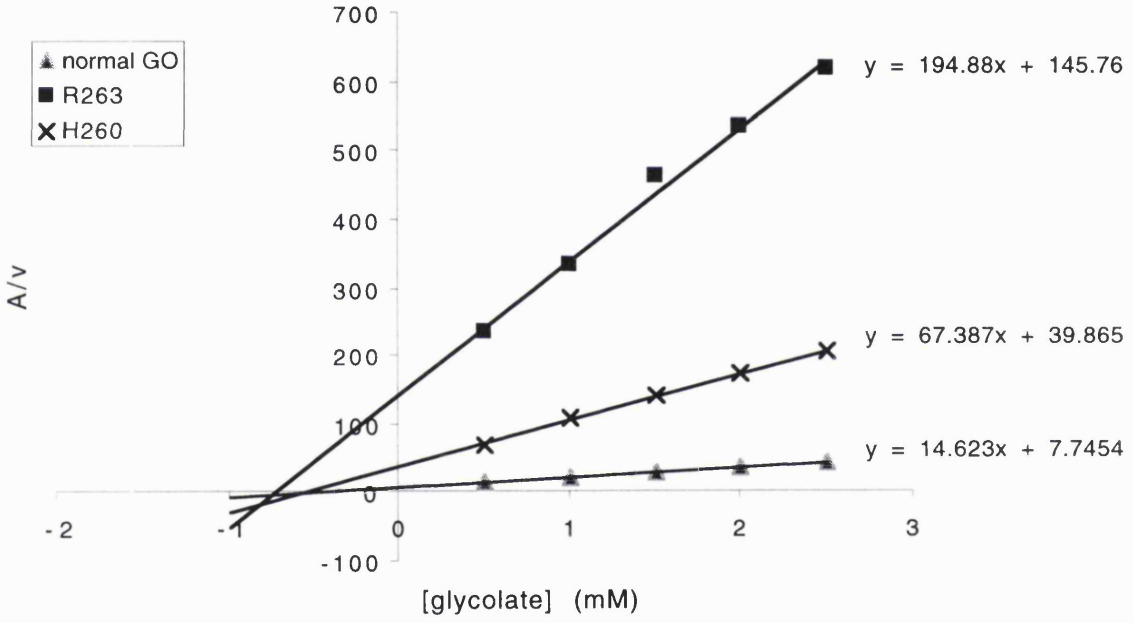

Figure 5.4 Hanes plot of the kinetic analysis of the Gly 260 and Gly 263 mutant GO proteins. *DCIP was fixed at 50 μM while glycolate was varied from 0.5 to 2.5 mM, results shown are the mean of three separate analyses.*

Kinetic constants (apparent K_m and V_{max}) were calculated from the straight-line equations shown in Figure 5.4. The results are summarised in Table 5.3, where V_{max} values are expressed as moles of hydroxy acid utilised. min^{-1}. mole of $flavin^{-1}$.

Enzyme	K_m (mM)	V_{max}
Wild-type	0.53 ± 0.04	372 ± 9
Gly 260	0.59 ± 0.04	1.15 ± 0.03
Gly 263	0.75 ± 0.1	0.31 ± 0.02

Table 5.3 Kinetic properties of wild-type and mutant GO protein. *Kinetic constants were determined from straight-line equations of the Hanes plot s ± error estimates from lines of worst fit. Units of V_{max} are mole of hydroxy acid utilised. min^{-1}. mole of $flavin^{-1}$.*

Kinetic analysis of wild-type GO and of the Trp 110 mutants was carried out with a range of hydroxy acid substrates of varying chain length, and K_m and V_{max} values were determined. The results of these experiments are shown in Figures 5.5 – 5.8 and the kinetic constants obtained are summarised in Table 5.4.

In order to compare the substrate specificities of wild-type GO and each mutant enzyme, specificity constants were calculated by dividing the V_{max} values by their corresponding K_m values for all enzymes with each hydroxy acid tested. These specificity constants are shown in Table 5.5 and for ease of comparison are also depicted in graphical form in Figure 5.9.

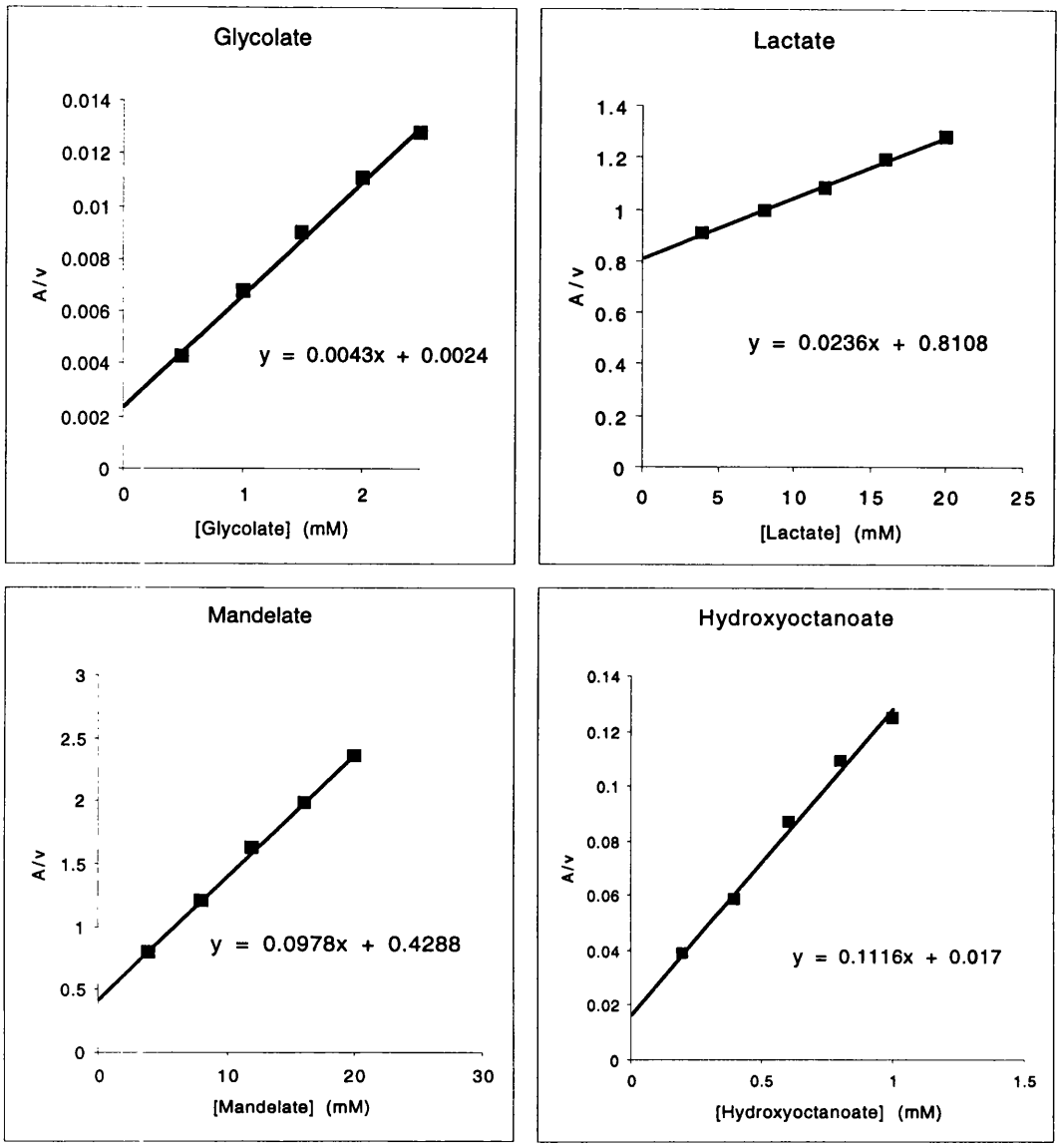

Figure 5.5 Kinetic analysis of wild-type GO with glycolate, lactate, mandelate and hydroxyoctanoate as substrates. *Hanes plots are shown of the data obtained when DCIP was fixed at 50 μM while hydroxy acid concentrations were varied. Results shown are the mean of three separate analyses.*

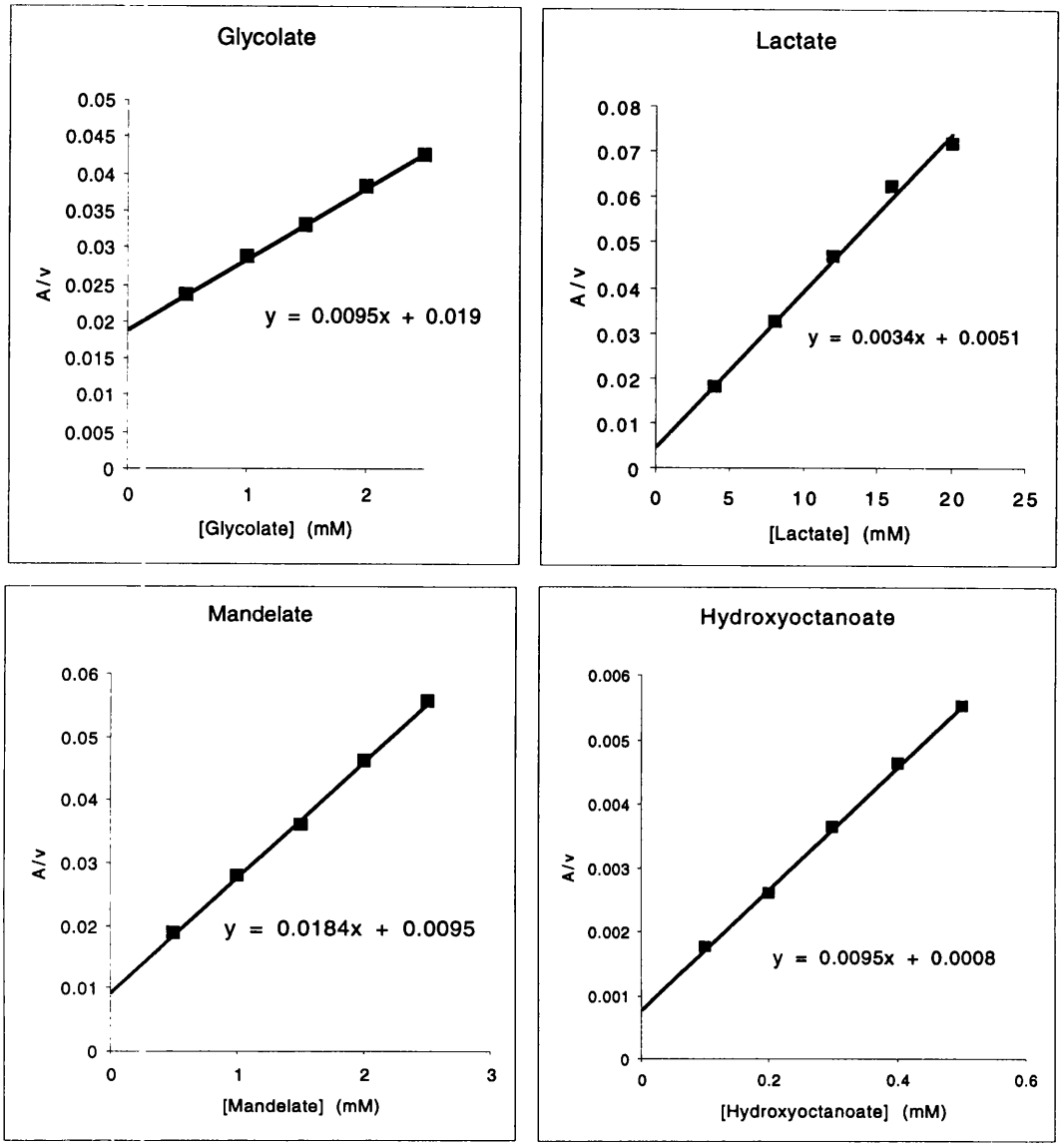

Figure 5.6 Kinetic analysis of Phe 110 mutant GO with glycolate, lactate, mandelate and hydroxyoctanoate as substrates. *Hanes plots are shown of the data obtained when DCIP was fixed at 50 μM while hydroxy acid concentrations were varied. Results shown are the mean of three separate analyses.*

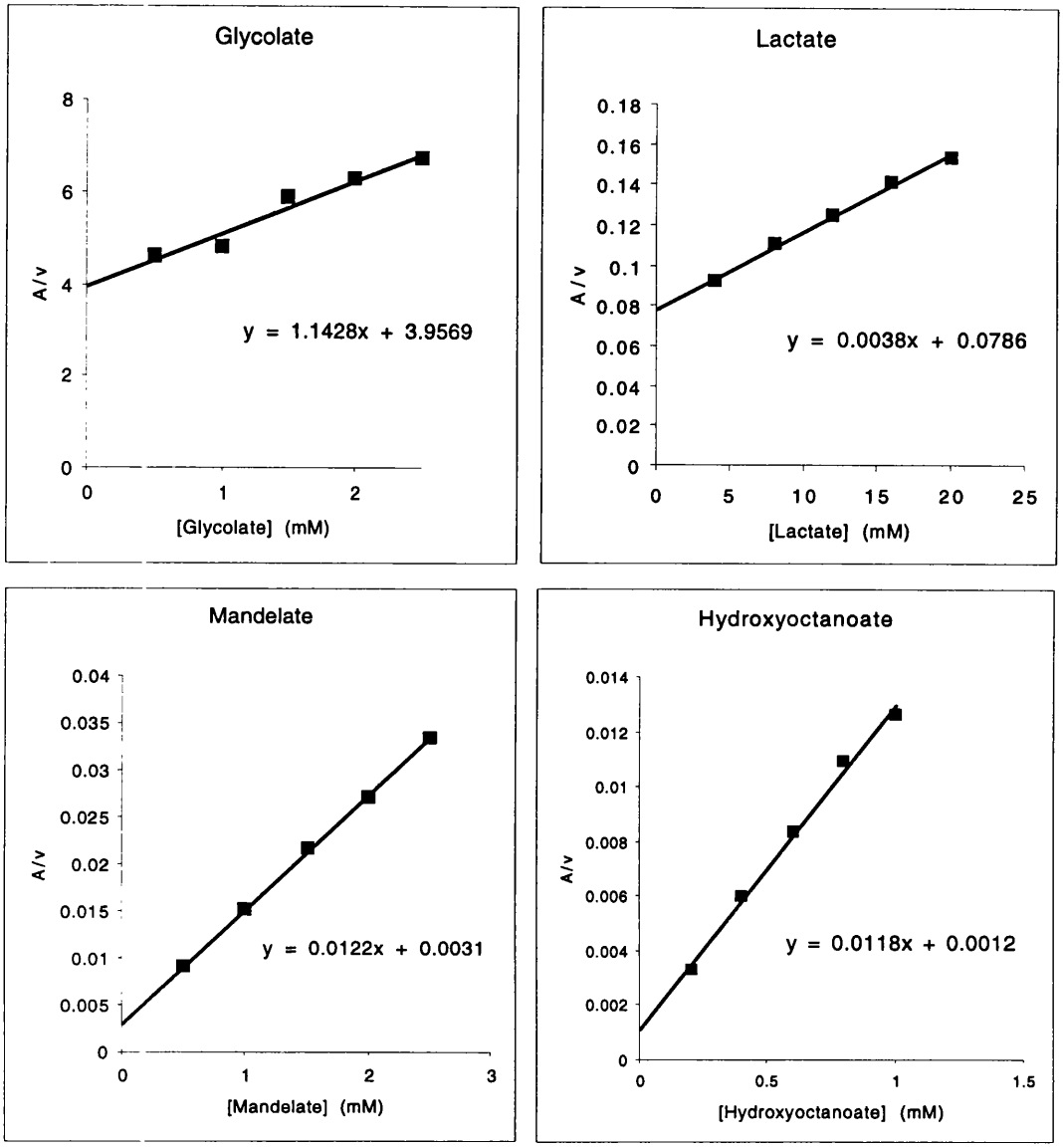

Figure 5.7 Kinetic analysis of Gly 110 mutant GO with glycolate, lactate, mandelate and hydroxyoctanoate as substrates. *Hanes plots are shown of the data obtained when DCIP was fixed at 50 μM while hydroxy acid concentrations were varied Results shown are the mean of three separate analyses.*

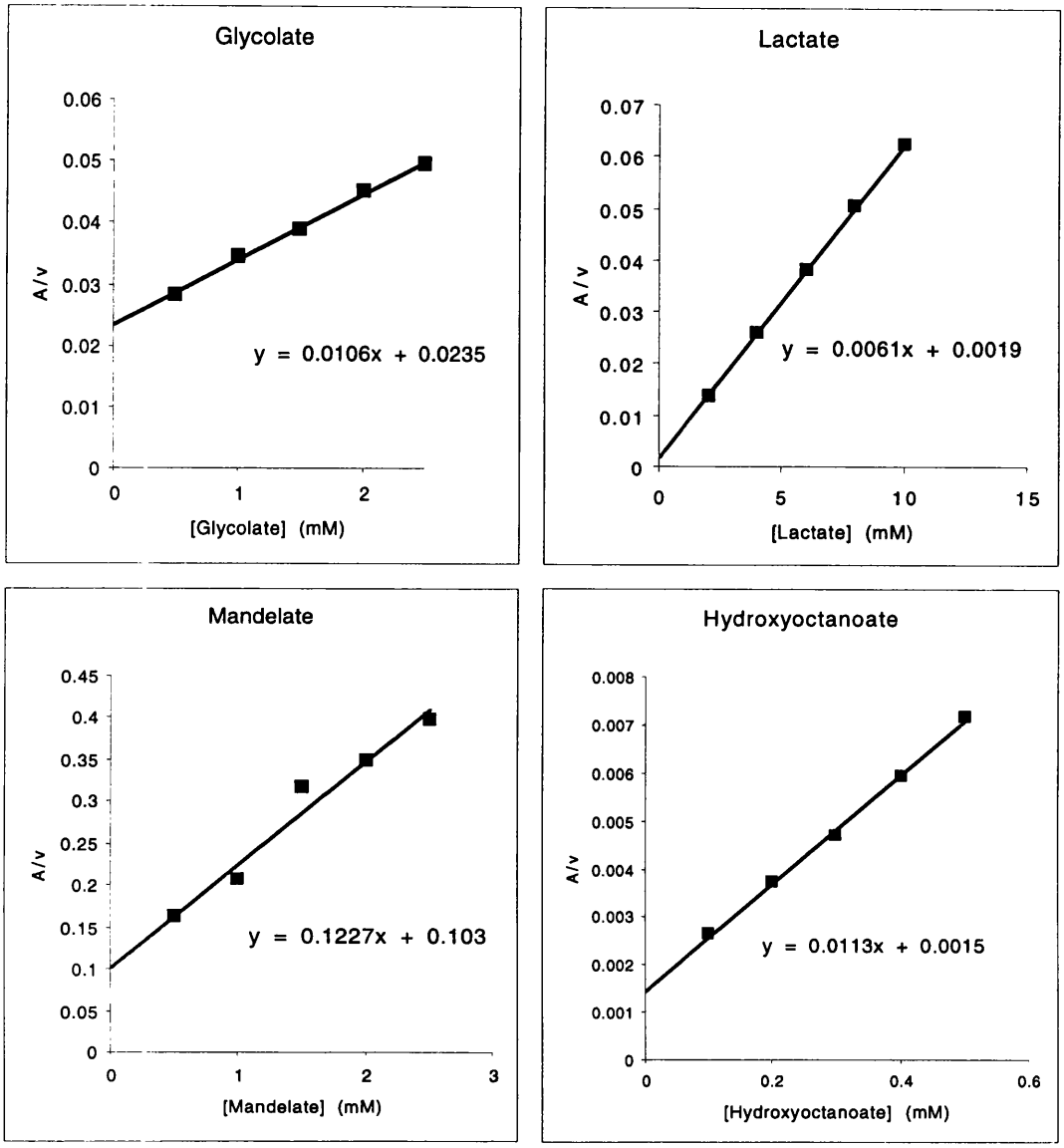

Figure 5.8 Kinetic analysis of Leu 110 mutant GO with glycolate, lactate, mandelate and hydroxyoctanoate as substrates. *Hanes plots are shown of the data obtained when DCIP was fixed at 50 μM while hydroxy acid concentrations were varied Results shown are the mean of three separate analyses.*

	Wild-type GO		Phe 110		Gly 110		Leu 110	
Substrate	V_{max}	K_m	V_{max}	K_m	V_{max}	K_m	V_{max}	K_m
glycolate	230 ± 9	0.56 ± 0.7	105 ± 2	2.0 ± 0.05	0.88 ± 0.1	3.5 ± 0.5	94 ± 4	2.2 ± 0.1
lactate	42 ± 1	34 ± 1	290 ± 13	1.5 ± 0.5	260 ± 9	21 ± 0.8	160 ± 1	0.31 ± 0.02
mandelate	8.4 ± 0.2	2.8 ± 0.2	54 ± 1	0.52 ± 0.04	82.0 ± 1	0.25 ± 0.02	8.7 ± 1	0.91 ± 0.2
hydroxyoctanoate	9.0 ± 0.5	0.15 ± 0.4	105 ± 2	0.08 ± 0.007	85 ± 3	0.10 ± 0.03	89 ± 3	0.13 ± 0.01

Table 5.4 Kinetic properties for wild-type and Trp 110 mutant proteins with substrates of different chain length. *Kinetic constants were determined from straight-line equations of Hanes plot s ± error estimates from lines of worst fit. Units of K_m are mM and V_{max} is expressed as moles of hydroxy acid utilised. min^{-1}. mole of $flavin^{-1}$.*

	Wild -type GO	Phe 110	Gly 110	Leu 110
glycolate	417	52.6	0.25	42.6
lactate	1.23	196.1	12.7	526
mandelate	2.94	105	323	9.55
hydroxyoctanoate	58.8	1250	833	667

Table 5.5 Specificity constants for wild-type and mutant GO. V_{max}/K_m ($mM^{-1}.min^{-1}$).

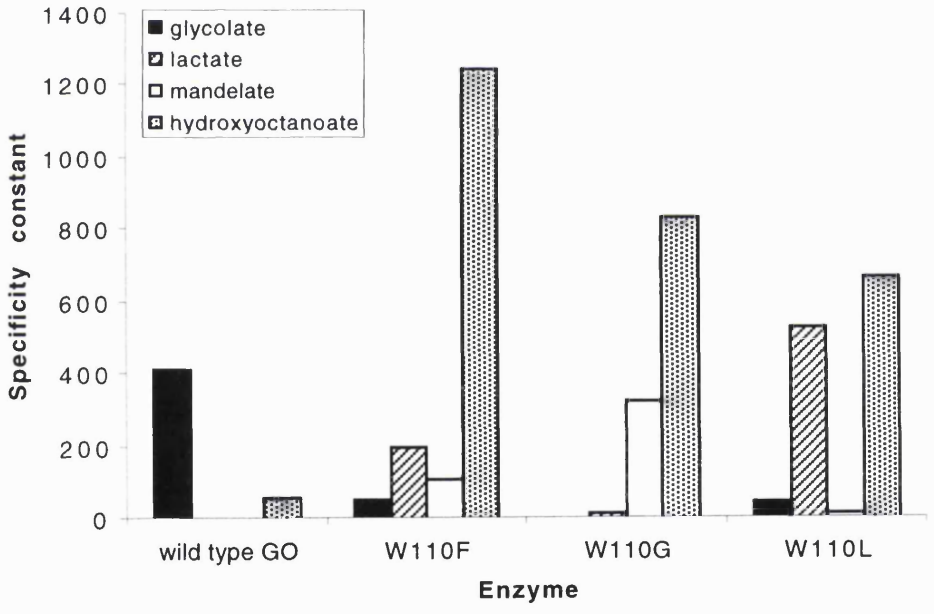

Figure 5.9 Substrate-specificity profiles of wild-type and Phe 110 mutant GO proteins. Units of specificity constants are $mM^{-1}.min^{-1}$.

5.4 Discussion

Active site residues were identified where the equivalent amino acids have been shown to be catalytically important in other flavoenzymes. Mutagenesis techniques were utilised to mutate these residues in recombinant human GO to alternative synonymous amino acids. The mutant proteins were expressed and purified to homogeneity by means of nickel affinity chromatography using the method developed in chapter 4. His 260 and Arg 263 were mutated to glycine to produce Gly 260 and Gly 263 mutants and Trp 110 was mutated to Gly, Phe and Leu to produce Gly 110, Phe 110 and 110 mutants respectively. All five mutant proteins retained sufficient catalytic activity to permit their kinetic characterisation. The findings of this kinetic analysis were compared to those with wild-type GO to assess the effects of the mutations.

Kinetic constants for the Gly 263 and Gly 260 mutants were determined from Hanes plots of the rates of enzyme turnover measured at a range of glycolate concentrations (Figure 5.4). The K_m values showed a slight increase, giving values of 0.53 mM for wild-type GO, 0.59 mM for Gly 260 and 0.75 mM for Gly 263. In comparison the V_{max} values for Gly 260 and Gly 263 showed in excess of a 300 fold and a 1000 fold reduction respectively in comparison to wild-type GO. These findings indicate that both mutations had a much greater influence on enzyme turnover, as reflected by the greatly reduced V_{max} values, than on substrate binding, as reflected by the small change in K_m values. This observation is consistent with the hypothesis that these residues play an important role in enzyme catalysis as opposed to substrate binding.

According to the mechanistic model of flavoenzyme catalysis the first step in the reaction is the abstraction of a proton from the α-C of the substrate by a base in the active site of the enzyme. Analysis of the crystal structure of FCB_2 revealed that His 273 was suitably positioned to fulfil the role of catalytic base (Lindqvist *et al.*, 1991) and His 260 is the homologous amino acid in human GO. Since this residue is of essential importance to enzyme catalysis, its mutation should have a profound effect upon the rate of reaction of the enzyme. In contrast, replacement of this residue would not be expected to change the K_m for glycolate because it is not thought to take part in substrate binding. The Gly 260 mutant displayed a very similar K_m to wild-type GO, whereas the V_{max} showed a 300 fold reduction. This decrease is far less than expected and does not correlate with the results of similar mutations in other flavoenzymes. Mutation of this His residue to a Glu in LMO (Muh *et al.*, 1994b) and FCB_2 yielded mutants with V_{max} values decreased by factors of 10^7 and 5×10^5, compared to wild-type enzymes. The reasons for this difference are not clear and require further investigation.

Arg 263 in human GO is equivalent to Arg 273 in yeast flavocytochrome b_2 (FCB_2), which was observed to be bound to a molecule of pyruvate, the product of lactate oxidation, in one of the sub-units of the crystal structure (Xia and Mathews, 1990). Comparison of the refined crystallographic structures of spinach GO and FCB_2 revealed that Arg 257 in the spinach flavoenzyme was in an equivalent position to bind to the carboxyl group of glycolate (Lindqvist *et al.*, 1991). Mutation of this residue has not been investigated in spinach GO, however the conservative Arg 273 Lys substitution in FCB_2 (Reid *et al.*, 1988) produced inactive protein. In the human GO mutant described

here the positively charged Arg has been replaced by a neutral residue i.e. Gly. Replacement of Arg with the neutral amino acid Gly in MDH from *Pseudomonas putida* produced a mutant with a 400 fold decrease in V_{max} and a 5 fold increase in K_m (Lehoux and Mitra, 2000). These findings are similar to those reported here for human GO and suggest that the positively charged Arg residue is critical for catalysis. This positive charge is thought to be important for the stabilisation of a highly negatively charged intermediate during catalysis, consistent with the so-called carbanion mechanism that has been postulated for flavoenzyme catalysis (Ghisla and Massey, 1991).

Of all the mutants Arg 263 showed the lowest yield of protein, as can be seen in Figure 5.3. Activity was only detectable using three fold more pure protein than was used for the other mutants and wild-type GO. Furthermore, this mutant showed a large loss of activity upon freezing and during storage at – 80 °C. Replacement of the Arg 263 residue appears to have reduced the stability of the protein. This has been reported for other flavoenzymes where the equivalent residue was mutated by site directed mutagenesis (Reid *et al.*, 1988; Lehoux and Mitra, 2000).

The equivalent residue to Trp 110 in human GO in the spinach enzyme is Trp108, and when this latter residue was mutated to a Ser the results indicated that the Trp residue was of major importance for catalysis and in determining the substrate specificity of the enzyme (Stenberg *et al.*, 1995). This Trp residue is not conserved among other α-hydroxy acid oxidising enzymes. FCB_2 has a Leu in this position (Ghrir and Becam, 1984) whereas MDH from *Rhodotorula graminis* has a Gly (Illais *et al.*, 1998) and human long chain HAO has a Phe (Jones *et al.*, 2000). The size of the amino acid in this

position appears to be inversely correlated to the size of the substrate molecule that can be fitted into the active site (discussed previously in chapter 3). Therefore, Trp 110 in human GO was mutated to Gly, Phe and Leu to produce Gly 110, Phe 11 and Leu 110 mutants respectively and the effects upon substrate specificity were investigated.

As can be seen from Figure 5.9 all of the Trp110 mutants showed greatly reduced specificity for glycolate as substrate in comparison to the wild-type enzyme. However, they all now show highest specificity for the 8-carbon long chain hydroxyoctanoic acid. It appears therefore, that the Trp110 residue serves two functions due to its size. Firstly, it will occupy a large space in the active site optimising it for occupation by the small hydroxy acid glycolate. Secondly, its bulk appears to restrict entry of longer chain length hydroxy acids to the active site. Replacement of this residue with a slightly smaller Phe or with the tiny Gly or Leu residue optimises the active site for long chain hydroxy acids. Of the three mutants Phe 110 showed highest specificity for hydroxyoctanoic acid consistent with Phe being the residue found in human long chain HAO (Jones *et al.*, 2000). Even though the Gly 110 and Leu 110 mutants displayed highest preference for hydroxyoctanoate, of all enzymes, Gly 110 was the most effective at utilising mandelate and Leu 110 was the most effective at utilising lactate. These findings are consistent with Gly occurring in this position in MDH (Illais *et al.*, 1998) and Leu occurring in this position in FCB_2 (Ghrir and Becam, 1984). However, the results also indicate that other residues elsewhere in the protein sequences of MDH and FCB_2 must also be responsible for the substrate specificity of these enzymes.

The results of kinetic analysis of the Trp 110 mutant GO proteins have several implications for human glyoxylate metabolism. Firstly, the Trp residue appears essential for conferring substrate specificity for glycolate. Therefore, the other hydroxy acid isoenzymes recently identified, namely medium and long chain HAO (Jones *et al.*, 2000), which do not have this residue would not be expected to catalyse glycolate oxidation to produce glyoxylate. Since human GO shows a liver specific expression this indicates that hydroxy acid oxidase catalysed glyoxylate production will be confined to liver. This observation reinforces the importance of the liver in glyoxylate metabolism. The identification of GO activity in crude homogenates of human renal cortex has been reported (Applewhite *et al.*, 2000). This activity was attributed to GO protein, but the findings of this thesis indicate that GO is not expressed in kidney. Furthermore, long chain HAO found in kidney (Jones *et al.*, 2000) would be unlikely to catalyse glycolate oxidation, due to the presence of a Phe in place of Trp 110 in human GO.

It is well established that human AGT shows a liver specific expression. This observation, coupled with the liver specific expression of GO, would suggest that at least the peroxisomal branch of glyoxylate metabolism is confined to liver. The remainder of the thesis will focus upon the investigation of glyoxylate metabolism in the liver, with particular reference to GO, using two alternative strategies. In chapter 6 the catalytic activity and immunoreactivity of human GO is investigated in liver sonicates of PH patients and of those without AGT and GRHPR deficiency. In chapter 7 HPLC methods to separate and quantitate glyoxylate are developed and applied to the study of peroxisomal glyoxylate metabolism catalysed by purified AGT and GO *in vitro*.

Chapter Six

Investigation of Human GO in Liver Sonicates

6.1 Introduction

6.2 Methods

6.2.1 Production of an anti-GO antibody

6.2.2 Western blot analysis of human liver GO protein

6.2.3 Measurement of GO enzyme activity in tissue samples

6.3 Results

6.3.1 Characterisation of an anti-GO antibody

6.3.2 The tissue distribution of GO protein

6.3.3 Western blots of human liver sonicates

6.3.4 Optimisation of an assay for GO activity

6.4 Discussion

6.1 Introduction

Primary hyperoxaluria is widely regarded as a disease of the liver since AGT is a liver specific enzyme (Kamoda *et al.*, 1980) and GRHPR shows a predominantly hepatic expression (Cregeen, 2001). My observation that GO shows a liver specific expression (Chapter 3) further reinforces the importance of the liver in glyoxylate metabolism, in terms of glyoxylate production (catalysed by GO) and glyoxylate removal (catalysed by AGT in the peroxisome and GRHPR in the cytosol) to prevent its conversion to oxalate. PH1 and PH2 show wide phenotypic heterogeneity and a factor that may contribute to this observation is variation of the activity of other enzymes in the pathway, such as GO. This variation may be due to functional polymorphisms in the genes encoding these enzymes or by differences in gene expression. In either case variable enzyme activity may influence the flux of metabolites through the pathways of glyoxylate metabolism and hence the severity of disease in PH.

The development of an assay to measure GO activity in human tissue sonicates will enable data regarding the inter-individual variation of this enzyme to be collected. The availability of large amounts of pure GO protein enables polyclonal antibodies to be produced, which can be used for the specific detection of immunoreactive GO in human liver sonicates and also for immunocytochemistry. This chapter describes the production of an anti-GO antibody and its use for the detection of immunoreactive GO in western blots of total liver proteins. The development and evaluation of an assay for measuring catalytic GO activity in liver sonicates is also described.

6.2 Methods

6.2.1 Production of an anti-GO antibody

3 mg of purified recombinant GO protein in 5 ml of 25 mM potassium phosphate buffer pH 8.0 was freeze dried and used for immunisation of 2 rabbits to produce a polyclonal anti-GO antibody (Genpak Limited, Brighton, UK) according to the protocol illustrated in table 6.1.

Day 0	Pre-Bleed + first immunisation
Day 14	Booster antigen Injection
Day 35	Booster antigen Injection
Day 56	Booster antigen Injection
Day 77	Booster antigen Injection
Day 87	Bleed + separate serum

Table 6.1 Immunisation protocol for the production of an anti-GO antibody.

50 ml of immune serum was obtained from each rabbit and precipitated with ammonium sulphate to produce an enriched IgG fraction. 1 ml aliquots were stored frozen at – 80 °C and on thawing, sodium azide was added to a final concentration of 0.1% and samples stored at 4 °C prior to use.

6.2.2 Western blot analysis of human liver GO protein

Human liver sonicates containing 6 μg of total protein were electrophoresed by SDS-PAGE and western blots produced according to the methods outlined in sections 2.3.8 and 2.3.10 respectively. Following this, the nitrocellulose blot was placed briefly in TBS and quickly transferred to 5% (w/v) milk proteins in TBS. Blocking of non-specific binding sites was accomplished by incubation for one hour. Following two ten minute washes in TTBS, the blot was incubated overnight with primary anti-GO antibody in TTBS at appropriate dilution. Excess antiserum was removed by washing twice for ten minutes in TTBS and the blot was incubated with biotinylated goat anti-rabbit antibody in TTBS at a 1/3000 dilution for 2 hours. Following two ten minute washes in TTBS, the blot was incubated with a streptavidin-biotinylated alkaline phosphatase complex in TTBS at a 1/3000 dilution for two hours. After four ten minute washes in TTBS, the blot was developed using alkaline phosphatase colour development reagent as outlined in section 2.3.10. All incubations were carried out at room temperature.

6.2.3 Measurement of GO Enzyme Activity in tissue samples

GO activity was assayed by a method adapted from that of Kasidas and Rose (Kasidas and Rose, 1979), based upon the Trinder reaction (Barham and Trinder, 1972). The hydrogen peroxide formed by glycolate oxidation catalysed by GO was used to oxidatively couple sulphonated 2,4 dichlorophenol and 4-aminophenazone, in a reaction catalysed by horseradish peroxidase. The soluble purple quinoneimine dye formed was measured by the absorbance increase at 515 nm.

Solutions:

Trinder reagent	A stock solution was prepared by dissolving 50 mg di-ammonium hydrogen phosphate, 174 mg di-potassium hydrogen phosphate, 100 mg 4-aminophenazone and 50 mg orthoboric acid in 100 ml of deionised water. A working solution was prepared by adding 10 mg of horseradish peroxidase (~2,000 units) and 400 µl of sulphonated 2,4 dichlorophenol to 10 ml of stock reagent. This was prepared fresh and used within 1 hour.
100 mM glycolate	16 mg of glycolic acid was dissolved in 10 ml deionised water and the pH adjusted to pH 7 with a few drops of 8 M NaOH.
Tris buffer pH 8.8	50 ml of 0.1 M tris and 8.5 ml of 0.1 M HCl were combined and made up to 100 ml with deionised water.

In a cuvette, 500 µl of buffer was mixed with 200 µl of 100 mM glycolate, 50 µl of deionised water and 200 µl of Trinder reagent. The reaction was started by the addition of 50 µl of the sample to be assayed and the absorbance at 515 nm was recorded for 10 minutes in a Kontron 922 double beam spectrophotomoter (Watford, UK).

To enable results to be expressed as nmol of glycolate oxidised/min, the assay was calibrated with hydrogen peroxide, which had been titrated with potassium permanganate.

6.3 Results

6.3.1 Characterisation of an anti-GO antibody

Using pure recombinant GO as antigen, a polyclonal anti-GO antibody was raised in rabbits according to the method outlined in section 6.2.1. This antibody was tested for immunoreactivity against pure recombinant GO, using rabbit pre-immune serum as a control. The antibody detected a 46 kDa protein band when used to probe a western blot containing pure recombinant GO (Figure 6.1 a, lane 2). No such band was observed when the antibody was replaced with pre-immune serum (Figure 6.1 b, lane 2).

The anti-GO antibody failed to detect the presence of immunoreactive GO protein in western blots loaded with up to 12 μg of total liver protein (Figure 6.1 a, lanes 3 – 4). When more concentrated solutions of antibody were used a faint band of immunoreactivity was observed. However, this was not sufficient to detect GO in all liver biopsies tested. The sensitivity of the assay was therefore increased by the use of an amplified antibody detection kit. This kit incorporates an amplification step in which a biotinylated secondary antibody binds to the primary antibody. The secondary antibody is then bound to a tertiary antibody via a streptavidin-biotin complex. This produces a ten fold greater sensitivity than that of the standard protocol giving a lower limit of detection of 10 ng protein. The kit was used to detect immunoreactive GO in tissue sonicates by the method outlined in section 6.2.2.

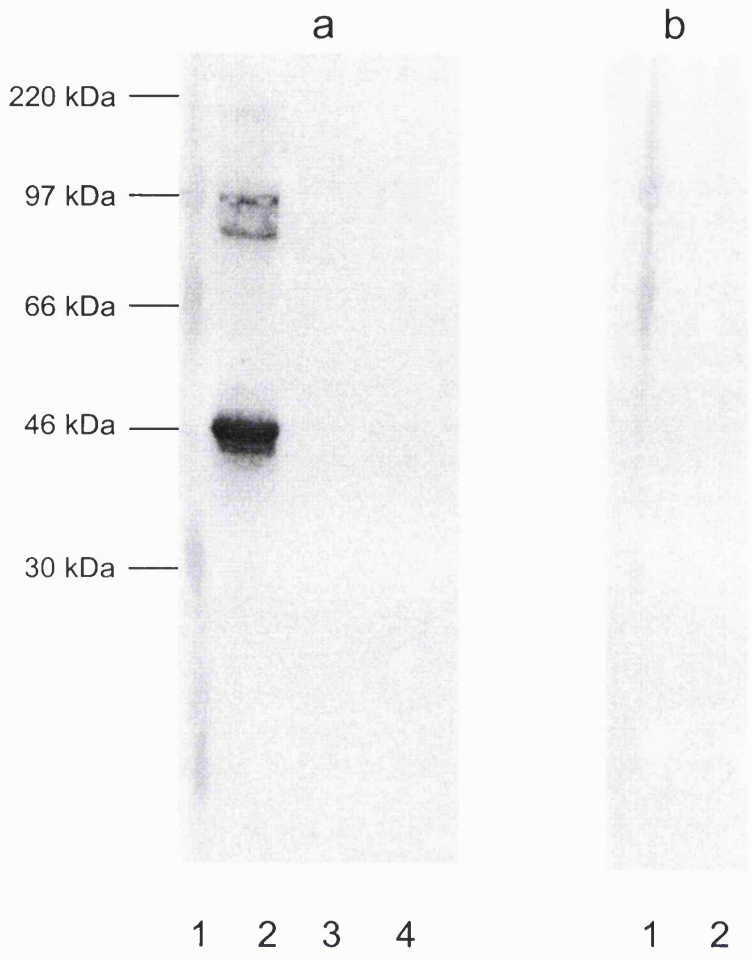

Figure 6.1 Immunoreactivity of the anti-GO antibody. *A band of 46 kDa representing GO was detected by the antibody (a), but not by pre-immune serum (b). Lane 1, molecular weight markers; Lane 2, pure recombinant GO; Lane 3, 6 μg total liver protein and Lane 4, 12 μg total liver protein.*

By means of the amplified detection kit, the anti-GO antibody detected a protein of approximately 43 kDa in human liver. The difference in size seen with the recombinant protein reflects the additional N-terminal His tag and anti-Xpress™ epitope in the fusion protein. The signal in 12 μg of liver proteins is at a similar intensity to 40 ng of purified

recombinant GO (Figure 6.2), and thus the concentration of GO in human liver was estimated to be 0.3% of soluble liver proteins. This result is subject to some error, due to the different methods used to measure protein concentration, namely the Lowry method for liver proteins and absorbance at 280 nm for pure recombinant GO. However, it allows crude comparison of abundance with other liver enzymes in the glyoxylate metabolic pathway such as AGT and GRHPR.

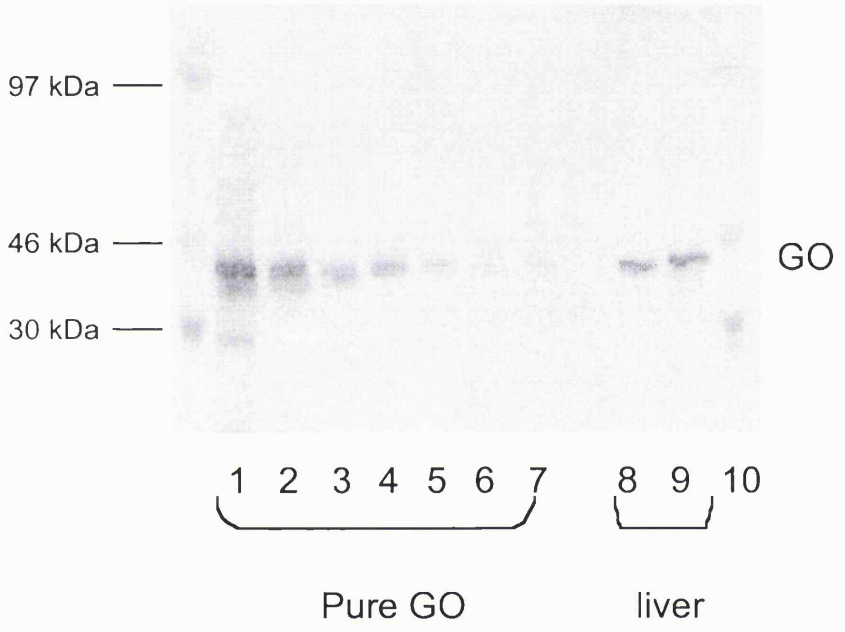

Figure 6.2 Estimation of the concentration of GO protein in human liver. *Western blots of 6 μg and 12 μg total liver proteins were compared to known amounts of pure GO to estimate the level of GO protein present. Lanes 1 – 7 contain 100, 40, 20, 10, 7.5, 5, and 4 ng pure GO; Lane 8, 6 μg total liver protein; lane 9, 12μg total liver protein and lane 10, molecular weight marker proteins.*

In order to determine optimum antibody dilution western blots containing varying, known amounts of GO protein were probed with a range of dilutions of anti-GO antibody. The results of these titre experiments are shown in Figure 6.3.

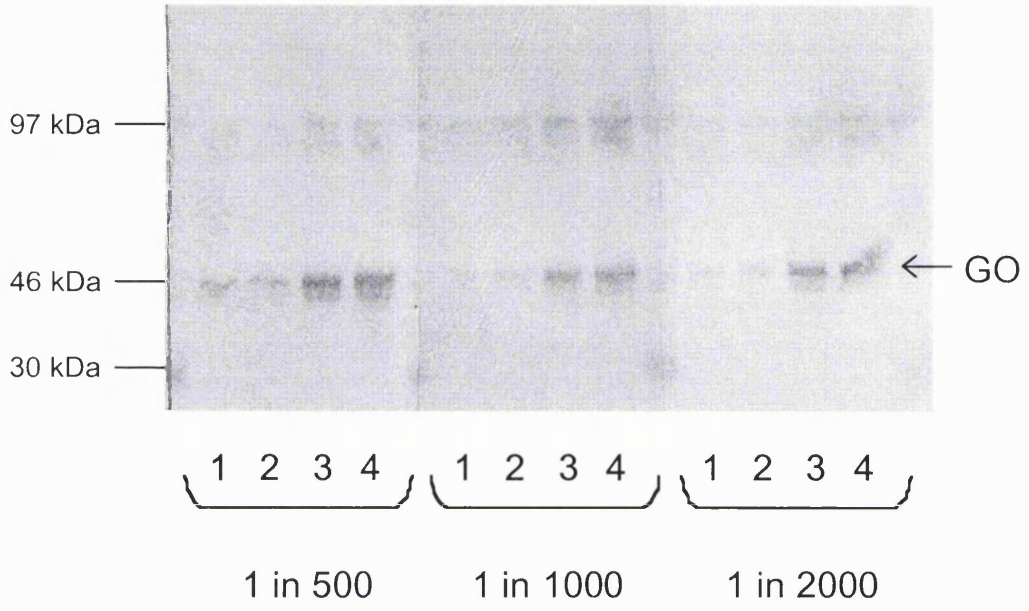

Figure 6.3 Western blot to determine optimum dilution of anti-GO antibody. *Western blots of a series of dilutions of pure recombinant GO were incubated with 1/500, 1/1000 or 1/2000 dilutions of anti-GO antibody and developed using the amplified detection kit. Lane 1, 10 ng; lane 2, 25 ng; lane 3, 50 ng and lane 4, 100 ng pure recombinant GO.*

As can be seen from Figure 6.3 the 1/500 dilution of anti-GO antibody showed the strongest signal with 10 ng of pure GO protein. Since the 1/500 dilution offers increased sensitivity in comparison to the 1/1000 and 1/2000 dilutions this dilution was used in all subsequent blots.

6.3.2 The tissue distribution of GO protein

The anti-GO antibody was used to look for immunoreactive GO protein in tissue sonicates from a range of tissues. A band of 43 kDa representing GO was detected in liver, but was absent from the other tissues tested. Although fewer tissues were available for testing, these findings support the results of the northern blot (Figure 3.6), which also indicated that expression of human GO was confined to liver.

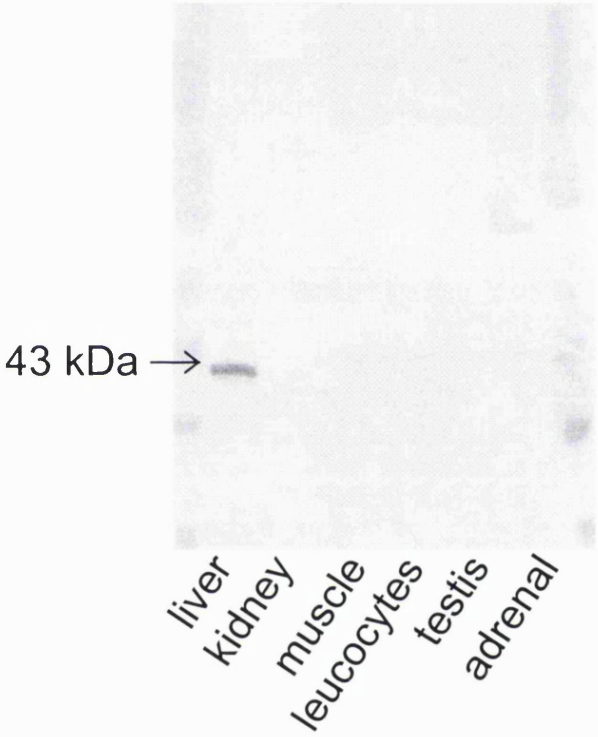

Figure 6.4 The tissue distribution of human GO protein. *A western blot of 12 μg total protein from a variety of tissues was probed with the anti-GO antibody. Immunoreactive protein was detected in liver only. Molecular weight marker proteins are shown at either end of the blot and the band at 43 kDa is GO.*

6.3.3 Western blots of human liver sonicates

Inter-individual variation in GO expression was tested by analysing western blots prepared from liver tissue sonicates of a range of liver biopsies. The samples included PH1 (n=6) and PH2 (n=2) patients and hyperoxaluric patients in whom PH1 and PH2 had been excluded (n=4). A band of 43 kDa representing GO was detected in 12 μg of total liver proteins in all the samples tested. As can be seen in figure 6.5, there was little difference in signal intensity between samples. This finding suggests that GO protein is present at a similar concentration in all livers tested, although the detection is limited by the sensitivity of the assay.

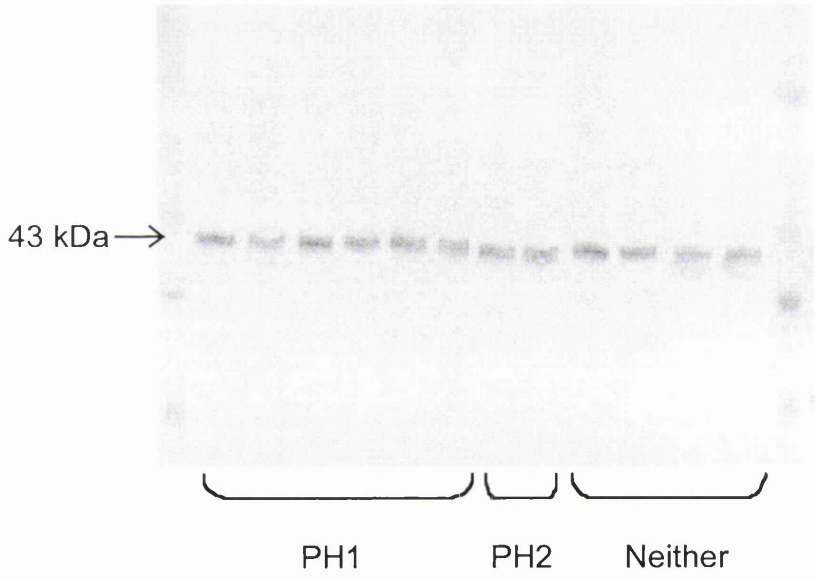

Figure 6.5 Western blots of GO protein in human liver sonicates. *A western blot of 12 μg total liver proteins from PH1, PH2 and hyperoxalurics in whom PH1 and PH2 had been excluded, was incubated with the anti-GO antibody. Molecular weight markers are shown at each end of the blot and the band at 43 kDa is GO.*

6.3.4 Optimisation of an assay for GO activity

The optimal pH for the assay was determined by varying the pH from 7 to 8 in a final concentration of 25 mM potassium phosphate buffer and from 7.8 to 8.8 in a final concentration of 25 mM tris buffer. The results are shown in Figure 6.6.

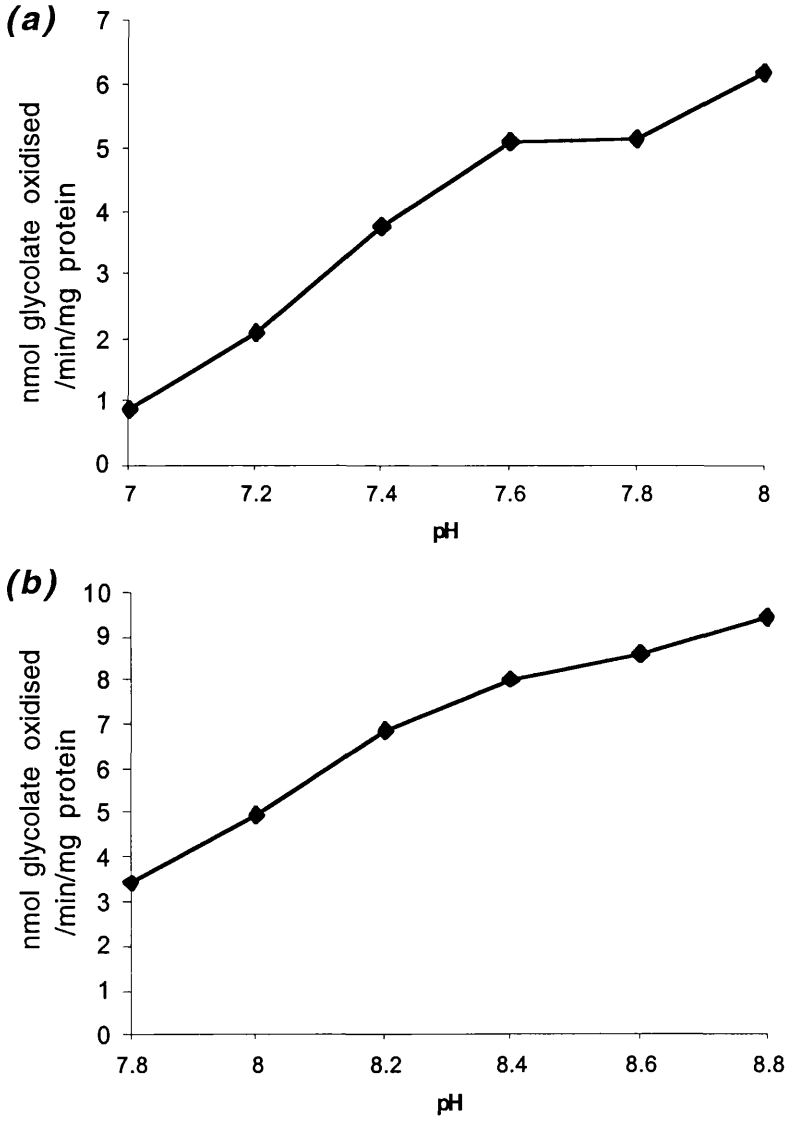

Figure 6.6 pH profiles of GO activity in a 12,000 g supernatant of human liver sonicate. *(a) pH varied from 7 to 8 in 25 mM potassium phosphate and (b) pH varied from 7.8 to 8.8 in 25 mM tris buffer.*

Highest activity was observed in 25 mM tris pH 8.8 and this was used in all future measurements. Optimum glycolate concentration for the assay was determined by varying the glycolate concentration from 0.5 mM to 20 mM. A Hanes plot of [substrate]/Initial velocity vs [substrate] was plotted, where the x axis intercept is $-K_m$ and the y axis intercept is K_m/V_{max}. From the Hanes plot (Figure 6.7) the K_m for glycolate was determined to be 0.35 mM. Since no substrate inhibition was detected over the range tested, a final concentration of 20 mM glycolate was therefore adopted for routine use of the assay.

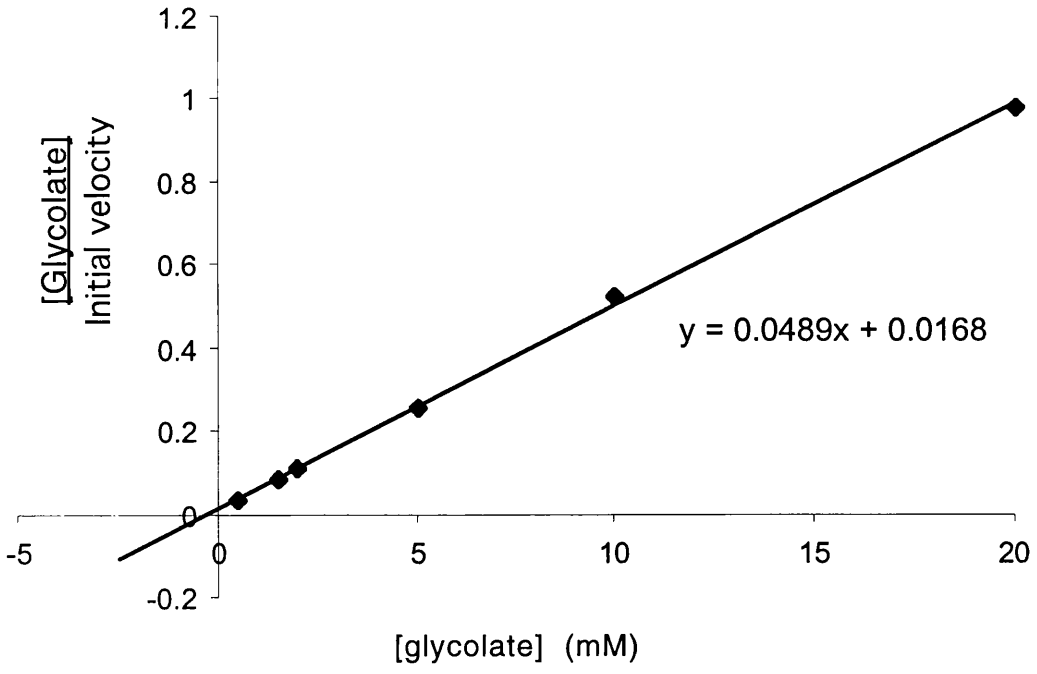

Figure 6.7 Hanes plot to show kinetics of glycolate oxidation by a 12,000g supernatant of human liver sonicate. *Glycolate was varied from 0.5 mM to 20 mM and the K_m determined from the straight-line equation as described in the text.*

In order to determine the optimum time range of the assay over which to determine the OD/minute, several supernatants were assayed using the optimum pH and substrate concentration and the OD/minute was determined from the raw data over the first 10 minutes. Raw data and the calculated OD change per minute are displayed in Figure 6.8.

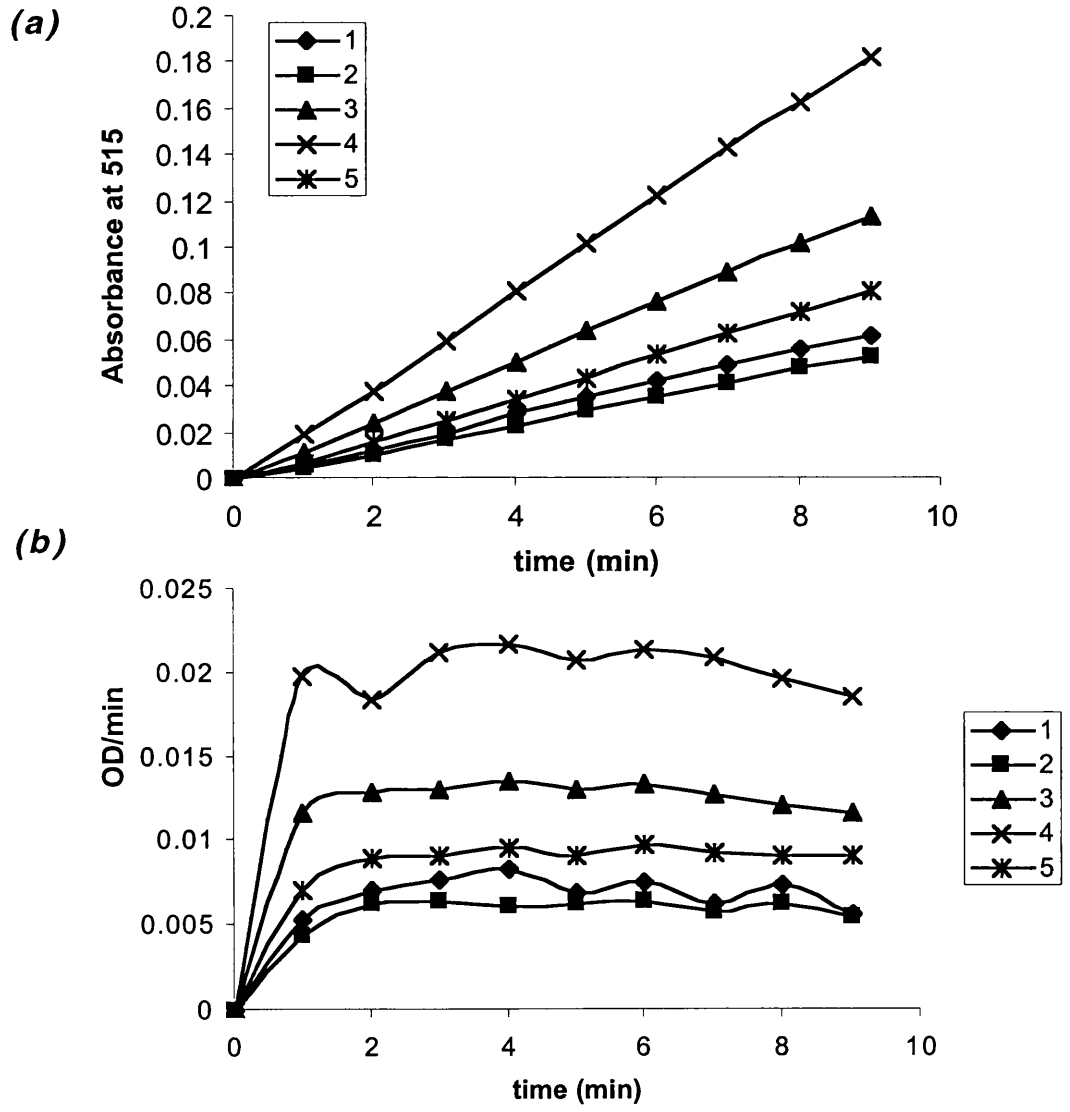

Figure 6.8 Measurement of catalytic GO activity in liver supernatants. *(a) The absorbance increase at 515 nm was monitored for ten minutes and (b) OD/min calculated across the time period to assess the linearity of the absorbance increase.*

As can be seen from Figure 6.8, the absorbance increase at 515 nm showed a lag during the first 2 minutes of the assay, which is most apparent in the OD/min data. The change in absorbance was linear from 2 to 6 minutes and hence the OD/min was calculated over this range for subsequent assays. Using the optimised reaction conditions, the linearity of the method response was assessed by measuring serial dilutions of a 12,000 g supernatant. The results are shown in Figure 6.9.

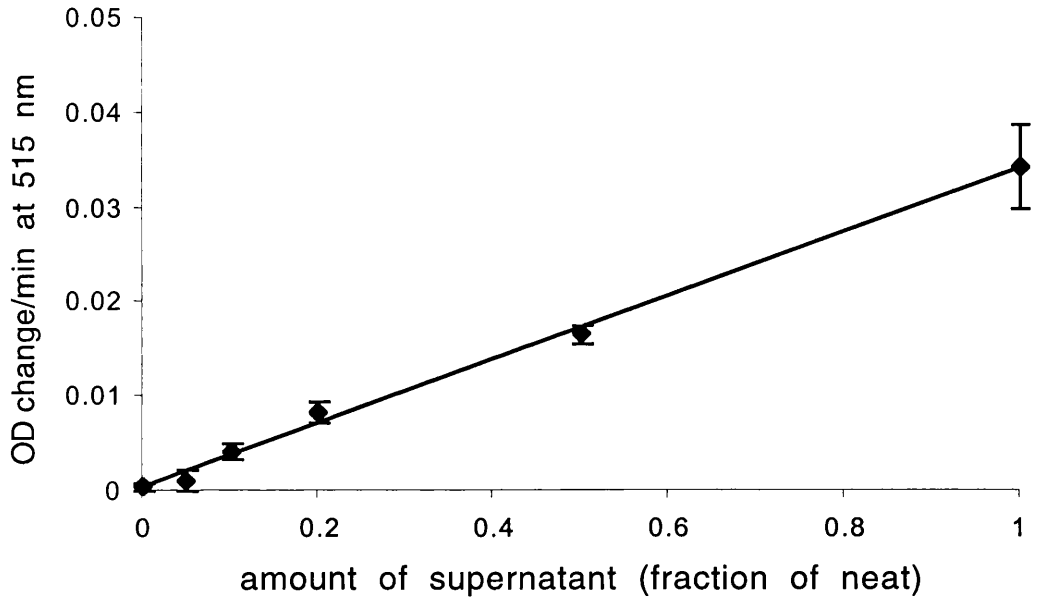

Figure 6.9 Linearity of the GO assay. *A 12,000 g supernatant was diluted in deionised water over a suitable range and GO activity was measured by means of the Trinder assay. Data shown represents the mean ± S.D. of triplicate measurements.*

The minimum detectable activity, defined as the mean plus 3 standard deviations of a suitable blank, was determined from triplicate substrate blank measurements i.e. no glycolate. The minumum detectable activity was found to be an absorbance change of 0.0004 OD units per minute.

The intra-assay coefficient of variation defined as mean/standard deviation x 100 (%) was determined from 9 replicate measurements of GO activity in a 12,000 g supernatant. The CV was 1.6% at an activity of 0.016 OD units per minute.

15 liver supernatants were assayed for GO activity, including non-PH1/PH2 (n=4), PH1 (n=9) and PH2 (n=2) patients. Protein concentration of the liver supernatants was determined by the Lowry assay (Lowry *et al.*, 1951) as described in section 2.3.13. Specific activity (nmol of glycolate utilised. min^{-1}. mg^{-1}) was calculated as follows:

velocity (OD / min) × 75/20 × (protein [ ] of supernatant in mg/ml)

where the utilisation of 75 μM H_2O_2 is equivalent to an absorbance change of 1 unit and 50 μl of supernatant is assayed in a total volume of 1 ml. The results (Figure 6.10) show that GO has a wide inter-individual variation.

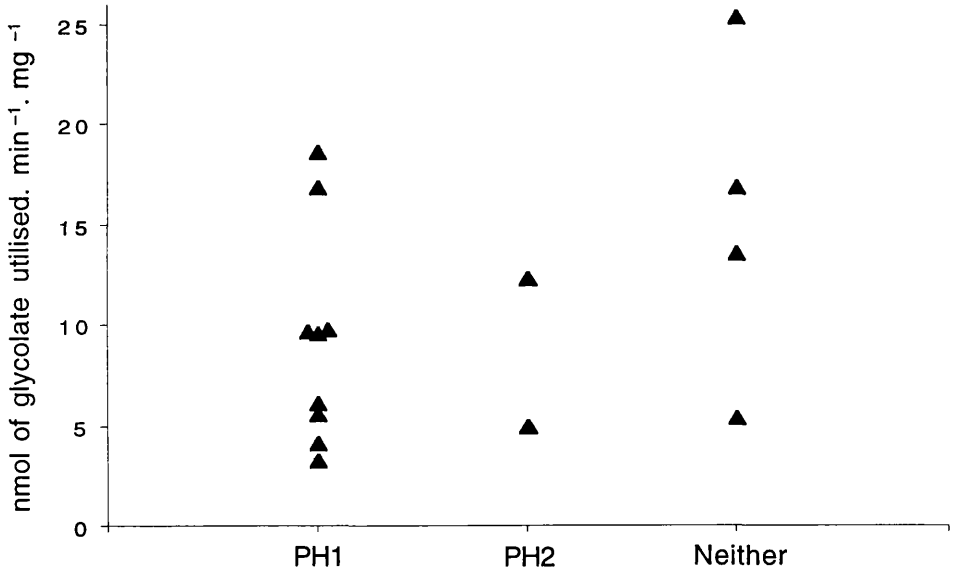

Figure 6.10 GO activity of 12,000 g supernatants of human liver sonicates. *15 liver biopsies were analysed including PH1(n=9), PH2 (n=2) and hyperoxaluric patients in whom PH1 and PH2 had been excluded (n=4).*

6.4 Discussion

A polyclonal antibody was raised in rabbits to purified human recombinant GO protein. This anti-GO antibody detected a 43 kDa protein in human liver sonicates, approximately 3 kDa smaller than the recombinant fusion protein. This result is to be expected since the anti-Xpress epitope and His tag contribute approximately 3 kDa to the recombinant protein. Probing of a multiple tissue western blot with the anti-GO antibody detected a single band in liver, but not in kidney, muscle, leucocytes, testis and adrenal tissues. These findings are consistent with those of the northern blot reported in chapter 3 and confirm the liver specificity of this enzyme. GO catalytic activity has previously been measured in crude human tissue homogenates using an oxygen electrode to measure oxygen consumption during glycolate incubation (Fry and Richardson, 1979a). In that study GO activity was detected in liver, but not in kidney, heart, brain, adrenal, testis, thyroid, pancreas, spleen, lung, muscle or lymph node (Fry and Richardson, 1979a).

For detection of immunoreactive GO in liver sonicates it was necessary to use an amplified detection kit with 10 fold higher sensitivity than the standard alkaline phosphatase conjugated antibody. Using this kit the level of GO expression was estimated to be approximately 0.3% of total liver proteins. This level is in comparison to estimates of 0.2% for GRHPR expression (Cregeen, 2001) and 3% for AGT expression (Chapter 7). The higher expression of AGT suggests that it would be influential in removing peroxisomal glyoxylate by catalysing its conversion to glycine, and therefore effective in glyoxylate detoxification. All livers tested showed similar

levels of immunoreactive GO, however this could be due to the insensitivity of the detection.

An assay to measure catalytic GO activity in 12,000 g liver supernatants has been developed. The assay is based upon the Trinder reaction, which is linked to hydrogen peroxide production (Barham and Trinder, 1972). Since the assay is measuring the product of the first enzyme reaction, i.e. H_2O_2, with a second enzyme reaction (catalysed by peroxidase) a lag phase is observed for the first two minutes of the assay, while the H_2O_2 channels into the second enzyme. This effect is a common observation in two-enzyme assay systems (Cornish-Bowden, 1995).

Following the lag at the start of the reaction the absorbance increase is linear for four minutes before slowly tailing off. This decrease after six minutes is not due to substrate depletion and was not eliminated by increasing the peroxidase. However, the decrease is not observed with purified recombinant protein suggesting that it could be due to assay interference from substances present in liver. Since the liver sonicates have been dialysed the interference is most likely due to another enzyme. Given the assay is reproducibly linear for four minutes following the lag phase, this time period was used to calculate OD change per minute.

No activity is detected in the absence of glycolate, which indicates the assay is specific for measuring GO activity. The optimised assay shows low coefficient of variation of 1.6%) and high sensitivity with a minimum detectable activity of 0.0004 OD units per min. The smallest absorbance change observed in all livers tested was 0.003 OD units

per min, which indicates the assay is suitable for routine measurement of catalytic GO activity.

The Trinder assay has several advantages over other methods that could have been applied to the measurement of GO activity. Firstly smaller sample volumes (50 µl) may be used in contrast to the oxygen electrode, which has a larger sample chamber requiring 150 µl of liver sonicate and is a less sensitive method. Secondly, the DCIP assay is limited by the high molar absorbance of DCIP and substrate inhibition at a glycolate concentration greater than 2.5 mM. Thus it would be impossible to saturate the system with either substrate. Furthermore, when the DCIP assay was tested with liver sonicates it showed a high non-linear blank rate in the absence of glycolate. This effect has been reported by other authors (Schuman and Massey, 1971a; Fry and Richardson, 1979a; Meyers and Schuman Jorns, 1981) and is likely to be due to DCIP reduction caused by reducing substances in the liver.

Prior to this study very little was known about the amount of GO in human liver. However, there is a report in the literature where human liver GO was measured by a hydrogen peroxidase linked assay and found to be 1.09 ± 0.21 nmol/min per mg of protein (Wanders *et al.*, 1991). The values reported in this thesis are higher, where the lowest activity observed was 3.3. These differences are most likely due to the use of optimised reaction conditions in the method I have developed. For instance the pH and substrate concentration were both chosen to give maximal activity, Whereas Wanders *et al* conducted measurements in pH 7.6 buffer with10 mM glycolate as substrate. GO activity has also been measured in cultured cells of the hepatoblastoma cell line

HepG2. The specific activity in these cells was 0.1 ± 0.02 and 0.07 ± 0.02 nmol/min per mg of protein (Wanders *et al.*, 1991; Holmes *et al.*, 1999) indicating that GO activity is at least 10 fold higher in the liver than in HepG2 cells. These differences must be considered before extrapolating findings from experiments with HepG2 cells to human liver glyoxylate metabolism.

GO expression appears to have a wide inter-individual variation as reflected by the range of catalytic GO in the liver sonicates tested. Values obtained varied from 3.3 to 25.4 nmol glycolate utilised . min^{-1} . mg^{-1}. Such a variation in GO activity could influence disease severity in PH patients by affecting glyoxylate production and thereby oxalate production. In addition, it may also influence the amount of glycolate utilised, which could in turn have an effect upon the levels of urinary glycolate. It is well documented that approximately 25% of PH1 patients do not have hyperglycolic aciduria (Danpure, 1991). Thus, increased GO activity may be linked with absence of hyperglycolic aciduria in some PH1 patients and conversely reduced GO may lead to accumulation of glycolate.

The inter-individual differences in GO activity observed may be caused by functional polymorphisms in the gene or differences in gene expression. A recent analysis of the GO gene in patients with atypical hyperoxaluria has been conducted within the laboratory (Monico *et al.*, 2002). PCR-SSCP analysis and gene sequencing failed to show any functional variants of GO. However, this study only characterised the gene of a small patient cohort (n=9). In order to determine the existence of any functional polymorphisms in the gene for GO a more detailed analysis would need to be carried out

in a larger number of samples. Another factor that may influence GO activity is the status of vitamin B_2 or riboflavin, the precursor of FMN. A recent investigation found erythrocyte FMN levels responded significantly to riboflavin supplementation showing an 87% increase (Hustad *et al.*, 2002). It is therefore likely that differences in FMN status would influence the level of enzyme activity of flavoenzymes, including GO.

The GO assay is to be transferred to the Cobas Bio centrifugal analyser (Roche Diagnostic Systems, Welwyn Garden City, UK) to enable the method to be semi-automated. This will allow GO activity to be measured in liver sonicates, in addition to AGT and GRHPR, as part of the UCLH Primary Hyperoxaluria Diagnostic Service. Hence the levels of GO can be compared to PH phenotype and possible effects of this enzyme upon disease severity can be investigated.

Chapter Seven

In vitro Investigation of Glyoxylate Metabolism

7.1 Introduction

7.2 Methods

7.2.1 HPLC Reagents

7.2.2 Phenylhydrazine derivatisation

7.2.3 0-phenylenediamine derivatisation

7.2.4 HPLC

7.2.5 Purification of recombinant AGT

7.2.6 Western blot analysis of recombinant AGT

7.2.7 Measurement of AGT enzyme activity

7.2.8 *In vitro* investigation of glyoxylate metabolism by GO and AGT

7.2.9 Assay for the measurement of glycolate

7.2.10 Assay for the measurement of oxalate

7.3 Results

7.3.1 Evaluation of phenylhydrazine derivatisation

7.3.2 Evaluation of o-phenylenediamine derivatisation

7.3.3 Optimisation of an HPLC method to measure α-keto acids

7.3.4 Purification of AGT

7.3.5 *In vitro* investigation of glyoxylate metabolism by GO and AGT

7.4 Discussion

7.1 Introduction

Although the genetic causes of PH1 and PH2 are now well established, the primary route to oxalate production in either disease is still poorly understood. It has been postulated that in PH1 the excess glyoxylate is oxidised to oxalate by GO within the peroxisomes, or that the glyoxylate diffuses into the cytosol to be oxidised to oxalate, in a reaction catalysed by LDH (Williams and Smith, 1983; Danpure and Jennings, 1986; Danpure, 1989). The relative contributions of GO and LDH to oxalate production in PH1 are unknown. Previous studies have usually focused upon the enzymes from species other than human and extrapolation of the results is complicated by the fact that the enzymes may be in different intracellular compartments. Furthermore, nothing is known about the levels of glyoxylate in human liver of either PH patients or normal individuals.

The investigation of glyoxylate metabolism has also been hampered by the lack of a sensitive and reliable method for glyoxylate quantitation. Petrarulo and colleagues have used phenylhydrazine derivatisation for the measurement of glyoxylate in urine (Petrarulo *et al.*, 1988) and for the measurement of glycolate (Petrarulo *et al.*, 1991) and L-glycerate (Petrarulo *et al.*, 1992) following their enzymatic conversion to keto acids and subsequent HPLC analysis of derivatised keto acids. A method for the assay of pyruvate in plasma has recently been described which utilises o-phenylenediamine derivatisation and HPLC analysis (Wulkan *et al.*, 2001). This chapter describes the assessment of both derivatisation reactions (Figure 7.1) and the development of an HPLC assay for the simultaneous measurement of glyoxylate and other α-keto acids

important in glyoxylate metabolism, namely pyruvate and hydroxypyruvate. This HPLC method, when used in conjunction with spectrophotometric methods to measure glycolate and oxalate already in use in the laboratory, will permit the quantitation of all the relevant metabolites of glyoxylate metabolism. The application of these methods for the *in vitro* investigation of peroxisomal glyoxylate metabolism catalysed by GO and AGT is described in this chapter.

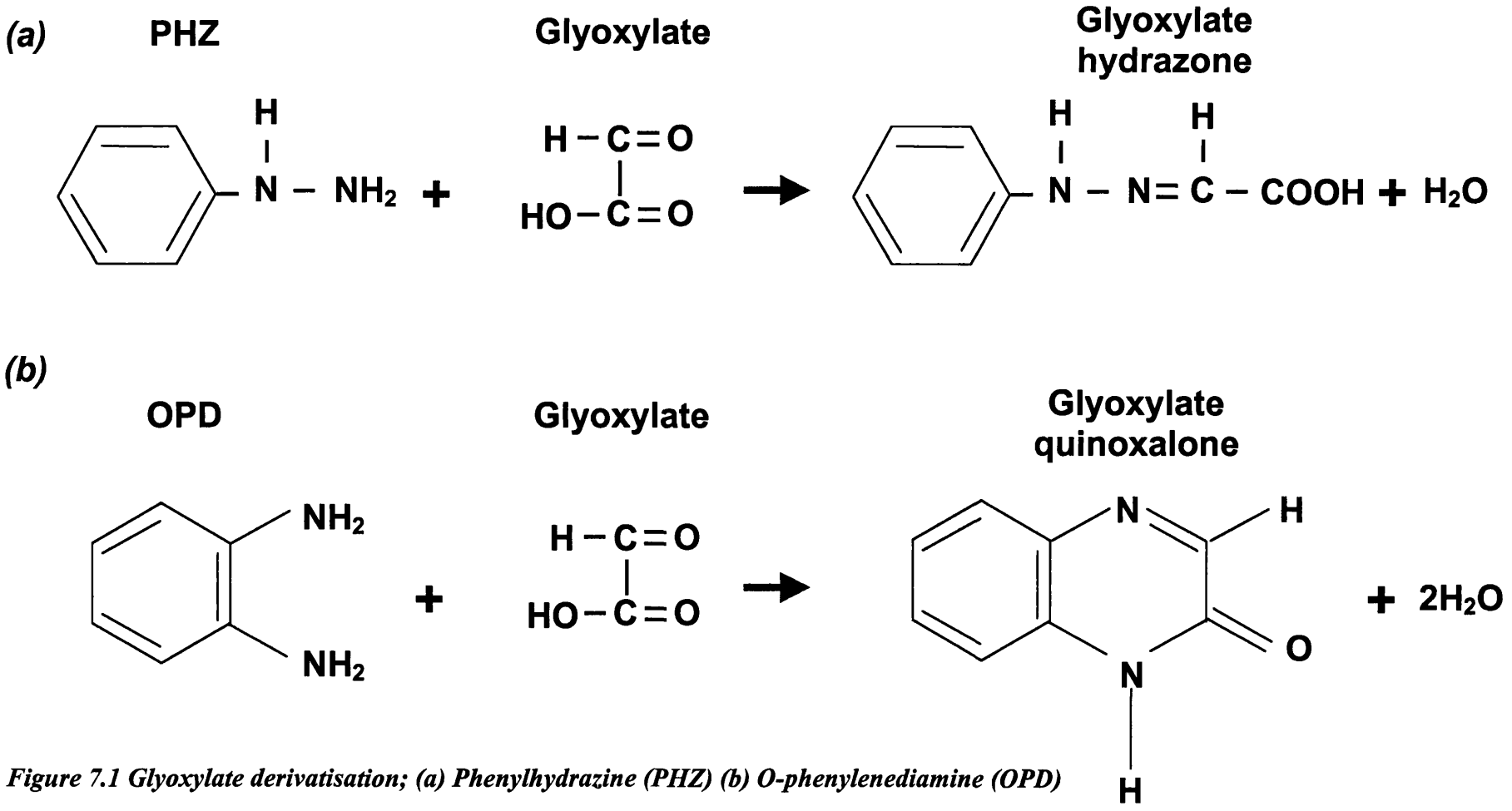

Figure 7.1 Glyoxylate derivatisation; (a) Phenylhydrazine (PHZ) (b) O-phenylenediamine (OPD)

7.2 Methods

7.2.1 HPLC Reagents

HPLC grade solvents purchased from BDH were used for mobile phases, which were freshly prepared weekly and filtered through a 0.2 μM filter before use. Keto acid standards were of Analar grade and were purchased from Sigma or Aldrich unless indicated otherwise.

7.2.2 Phenylhydrazine derivatisation

Keto acids were derivatised by phenylhydrazine hydrochloride (PHZ) to form hydrazones based upon the method of Petrarulo and colleagues (Petrarulo *et al.*, 1988).

Solutions:

PHZ reagent	A 100 mM stock solution was prepared by dissolving 144.6 mg of PHZ in 10 ml of deionised water.
Potassium phosphate pH 8	A 0.1 M solution was prepared by combining 47.35 ml of 0.2 M K_2HPO_4 and 2.65 ml 0.2 M KH_2PO_4 and the total volume was made up to 100 ml with deionised water.

Derivatives were prepared as follows:

A 200 μl aliquot of the sample to be assayed was added to 600 μl of 0.1 M potassium phosphate buffer and 200 μl PHZ reagent. The tubes were vortexed and incubated at room temperature for 20 minutes prior to injection in the HPLC.

7.2.3 0-phenylenediamine derivatisation

Keto acids were derivatised by o-phenylenediamine (OPD) to form quinoxalones based upon the method of Wulkan and colleagues (Wulkan *et al.*, 2001).

Solutions:

3 M HCl	A 1 in 3 dilution of concentrated HCl was prepared and stored in an amber glass bottle at room temperature.
OPD reagent	A 12 mM solution was prepared by dissolving 12.97 mg in 10 ml of 3 M HCl.

Derivatives were prepared as follows:

A 250 µl aliquot of the sample to be measured was added to 1 ml of OPD reagent. The tubes were vortexed and incubated in a heating block at 60 °C for 1.5 h.

7.2.4 HPLC

The HPLC system (Cecil Instruments Ltd, Cambridge) consisted of two model CE1100 solvent pumps, a model CE1200 UV detector and a column oven, which housed a Lichrosorb guard column (Merck, Poole) coupled to a 'µbondapack' analytical column (0.39 × 15 cm, 10 µM particle size, Waters Ltd, Elstree). Gradient programming, peak integration and quantitation were controlled by a Datacontrol software package (Cecil). Solvent was degassed by means of an inline degasser.

20 µl samples were injected into the HPLC column and separated at 37 °C at a flow rate of 1 ml per minute. For HPLC of hydrazones, the mobile phase consisted of 5% ethanol in 25 mM potassium phosphate buffer pH 6. For HPLC of OPD quinoxalone

derivatives, the mobile phase consisted of varying amounts of acetonitrile (%) in 10 mM potassium phosphate buffer pH 2.5. All derivatives were detected at 324 nm with the detector set at 0.02 absorbance units full-scale deflection. The optimisation of separation conditions is described in the results section.

7.2.5 Purification of recombinant AGT

Plasmid constructs of the pTrcHisA expression vector containing AGXT inserts corresponding to the major and minor allele as defined in section 1.5.1 were obtained from Professor Danpure (Department of Biology, University College London). *Epicurean coli* BL21 cells were transfected with these constructs according to the procedure outlined in section 2.3.6.

Expression of recombinant AGT protein from the minor allele (Pro11 AGT) and the major allele (Leu11 AGT) was induced by means of IPTG induction as described in section 2.3.7 and bacterial pellets were stored at – 80 °C. Crude bacterial extracts were prepared from pellets using 'bug buster' reagent (Novogen, Nottingham) as follows:

Pellets were resuspended in 5 ml of bug buster reagent and cell suspensions were treated with 100 μg/ml of lysozyme, 5 mg/ml RNase and 1 unit of DNase on ice for 15 minutes. The tubes were then rotated on a test tube rotator for 20 minutes at room temperature. Following this the tubes were centrifuged at 15,000 g for 15 minutes to pellet cellular debris. Supernatants containing soluble cellular proteins were dialysed overnight in T3 dialysis membrane (Pierce and Warriner) against 300 volumes of 20 mM sodium phosphate buffer pH 7.8, containing 500 mM sodium chloride. AGT protein was purified from dialysed extracts by means of nickel affinity chromatography with elution

by imidazole as described in section 4.2.1. Pure protein was quantified by measurement of its absorbance at 280 nm.

7.2.6 Western blot analysis of recombinant AGT

Western blotting and detection of recombinant AGT was carried out according to the procedures outlined in section 2.3.10. A polyclonal anti-AGT antibody obtained from Professor Danpure was used at a 1/300 dilution as primary antibody and alkaline phosphatase conjugated goat anti-rabbit IgG (Sigma) was used at a 1/1000 dilution as the secondary antibody.

7.2.7 Measurement of AGT enzyme activity

The catalytic activity of purified AGT was determined as previously described (Rumsby *et al.*, 1997) in which the sample to be measured is incubated with alanine and glyoxylate. Pyruvate produced as a result of glyoxylate transamination is measured indirectly by monitoring the utilisation of NADH at 340 nm, in a reaction catalysed by LDH. The reactions are as follows:

$$\text{alanine} + \text{glyoxylate} \xrightarrow{\text{AGT}} \text{glycine} + \text{pyruvate}$$

$$\text{pyruvate} + \text{NADH} + \text{H}^+ \xrightarrow{\text{LDH}} \text{lactate} + \text{NAD}^+$$

7.2.8 In vitro investigation of glyoxylate metabolism by GO and AGT

Solutions:

600 mM alanine	534.54 mg of alanine was dissolved in 10 ml deionised water and used in experiments at a final concentration of 5 mM.

20 mM serine	21.02 mg of serine was dissolved in 10 ml deionised water and used in experiments at a final concentration of 2 mM.
10 mM glycolate	1.6 mg of glycolic acid was dissolved in 10 ml deionised water, the pH was adjusted to pH 7 with a few drops of 8 M NaOH and it was used in experiments at a final concentration of 200 μM.
2 mM glyoxylate	9.2 mg glyoxylic acid was dissolved in 50 ml deionised water, the pH was adjusted to pH 7 with a few drops of 8 M NaOH and it was used in experiments at a final concentration of 200 μM.

Incubations were carried out in volumes of 1 ml in a final concentration of 50 mM potassium phosphate buffer at 37 °C. GO was present at 1 unit per ml, Pro 11 AGT at 10 units per ml, Leu 11 AGT at 6 units per ml and catalase at 70 units per ml, where 1 unit is the utilisation of 1 μmole of substrate per minute. Reactions were stopped at 0, 5, 10, 15 and 25 minutes by the addition of 20 μl 50% trichloroacetic acid (TCA). The tubes were kept on ice for 5 minutes, following which they were centrifuged at 10,000 g for 5 minutes to remove acid-precipitated material. 250 μl aliquots of the supernatants were derivatised according to the method outlined in section 7.2.3 and glyoxylate, pyruvate and hydroxypyruvate measured by HPLC. 200 μl aliquots were taken and the pH adjusted to pH 7 with 4 μl 8 M NaOH. These aliquots were incubated with 10 units of AGT and a final concentration of 50 mM alanine at room temperature for 10 minutes to remove residual glyoxylate, which would otherwise interfere in the glycolate assay (section 7.2.9). Following this the samples were assayed for glycolate and oxalate by the methods outlined in sections 7.2.9 and 7.2.10 respectively.

7.2.9 Assay for the measurement of glycolate

Glycolate was measured on the Cobas Bio centrifugal analyser (Roche Diagnostic System, Welwyn Garden City, UK) using the method of Kasidas and Rose (Kasidas and Rose, 1979).

Solutions:

Trinder reagent	A stock solution was prepared by dissolving 10 mg of horseradish peroxidase (~ 2,000 units), 100 mg 4-aminophenazone, 50 mg di-ammonium hydrogen phosphate, 174 mg di-potassium hydrogen phosphate and 50 mg orthoboric acid in 100 ml of deionised water.

A working solution was prepared by adding 400 µl of sulphonated 2,4 dichlorophenol to 10 ml of stock reagent. This was prepared fresh and used within 1 hour.

20 mM glycolate stock	196 mg sodium glycolate was dissolved in 100 ml of deionised water.

Glycolate working standards were prepared from the 20 mM stock solution as follows:

100 µM glycolate	0.5 ml stock was made up to 100 ml with deionised H_2O.
200 µM glycolate	1.0 ml stock was made up to 100 ml with deionised H_2O.
400 µM glycolate	2.0 ml stock was made up to 100 ml with deionised H_2O.

100 µl of the samples to be measured were aliquoted into sample tubes placed in a Cobas Bio sample rotor. Sufficient volumes of Trinder reagent (100 µl per reaction) and glycolate oxidase (40 µl per reaction) and 500 µl of each glycolate standard solution

were dispensed into the appropriate wells of the Cobas reagent tray. Glycolate concentrations of samples were determined by monitoring the production of a purple quinoneimine dye at 515 nm based upon the following reactions:

$$\text{glycolate} + O_2 \xrightarrow{GO} \text{glyoxylate} + H_2O_2$$

$$H_2O_2 + \text{2,4 DCP} + \text{4-aminophenazone} \xrightarrow{\text{peroxidase}} \text{quinoneimine dye} + H_2O$$

7.2.10 Assay for the measurement of oxalate

Oxalate was measured on the Cobas Bio centrifugal analyser (Roche Diagnostic Systems, Welwyn Garden City, UK) using a commercial oxalate kit (Sigma).

Solutions:

Oxalate reagent A	0.2 mM 3-methyl-2-benzothiazolinone hydrazone 3.2 mM 3-dimethylamino-benzoic acid.
Oxalate reagent B	Barley oxalate oxidase 3,000 units/litre Horseradish peroxidase 100,000 units/litre.
5 mM oxalate stock	126 mg oxalic acid dihydrate was dissolved in 200 ml 0.01 M HCl.

Oxalate working standards were prepared from the 5 mM stock solution as follows:

5 μM oxalate	0.2 ml stock was made up to 200 ml with 0.01 M HCl.
10 μM oxalate	0.4 ml stock was made up to 200 ml with 0.01 M HCl.
20 μM oxalate	0.8 ml stock was made up to 200 ml with 0.01 M HCl.

250 μl of the samples to be measured were aliquoted into sample tubes placed in a

Cobas Bio sample rotor. Sufficient volumes of reagent A (220 µl per reaction) and reagent B (20 µl per reaction) and 500 µl of each oxalate standard solution were dispensed into the appropriate wells of the Cobas reagent tray. Oxalate concentrations of samples were determined by following the production of a purple indamine dye at 580 nm based upon the following reactions:

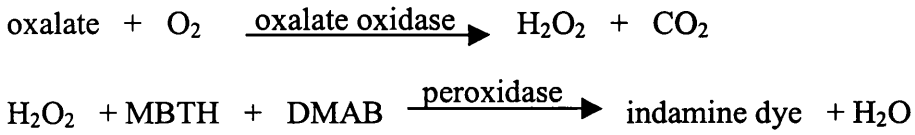

7.3 Results

7.3.1 Evaluation of phenylhydrazine derivatisation

Given the poor absorbance of glyoxylate and other small organic acids it was necessary to form derivatives prior to injection in the HPLC system to aid their UV-visible detection. Two derivatisation reagents (PHZ and OPD) were assessed in terms of production of adequate signal with all keto acids tested and the stability of the derivatives formed. Both these reagents have the advantage that they are specific for keto acids and will therefore potentially increase the specificity of the assay.

When derivatisation by PHZ was evaluated, several disadvantages of the method were revealed. Firstly, a final concentration of 20 mM PHZ was required to ensure adequate formation of derivatives. As can be seen in Figure 7.2 the absorbance was lower and derivative formation proceeded more slowly if concentrations of PHZ below 20 mM were used. Since the reaction is reversible it was not possible to remove the excess PHZ reagent prior to injection and hence the resulting chromatograms were compounded by the presence of a large PHZ peak, which obscured the hydroxypyruvate and pyruvate derivatives (Figure 7.3). Varying the solvent concentration, type of solvent, temperature and pH of the mobile phase did not prove effective at either changing the order of elution of the peaks of interest or moving them sufficiently away from the PHZ peak. Furthermore, analysis of derivative stability over 24 hours revealed that peak height was stable for only two hours. After this time the peak height decreased due to the breakdown of the hydrazone derivatives (Figure 7.4). The PHZ method of derivatisation was therefore rejected and the OPD method was evaluated.

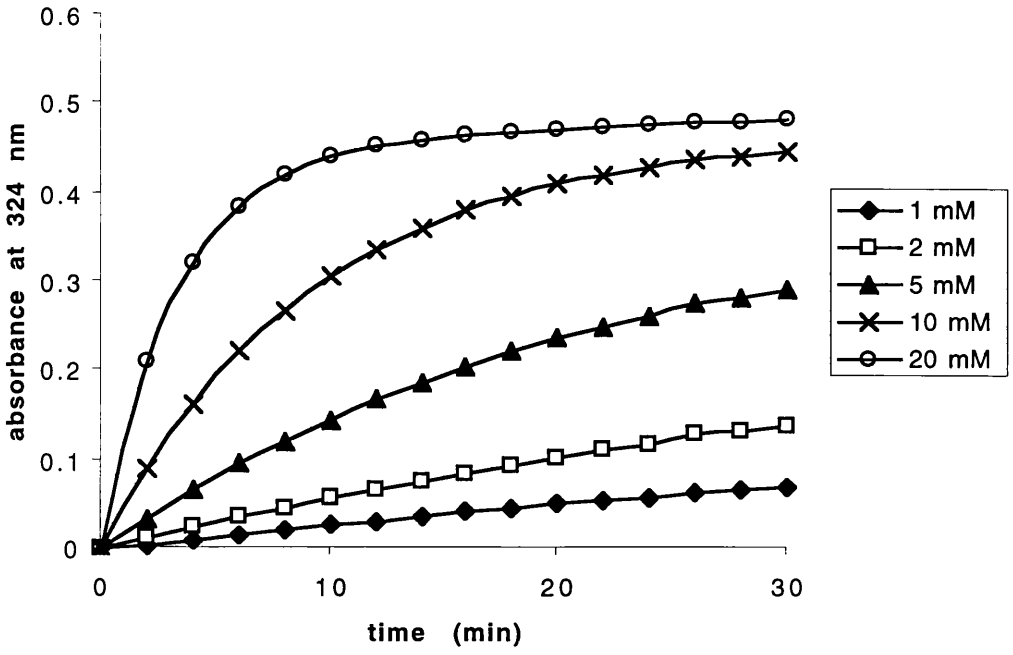

Figure 7.2 Formation of hydrazone derivatives in the presence of PHZ.

Hydroxypyruvate was incubated in the presence of increasing PHZ concentrations and the absorbance was monitored at 324 nm.

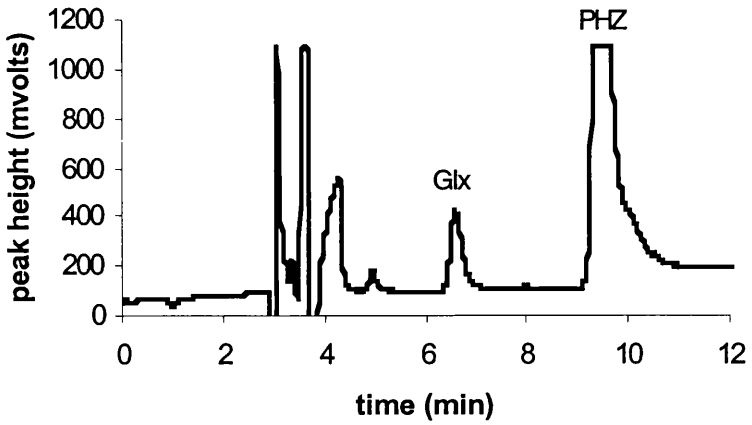

Figure 7.3 HPLC chromatograph of α-keto acid hydrazone derivatives. Glx = glyoxylate. *The hydroxypyruvate and pyruvate are obscured by the PHZ peak.*

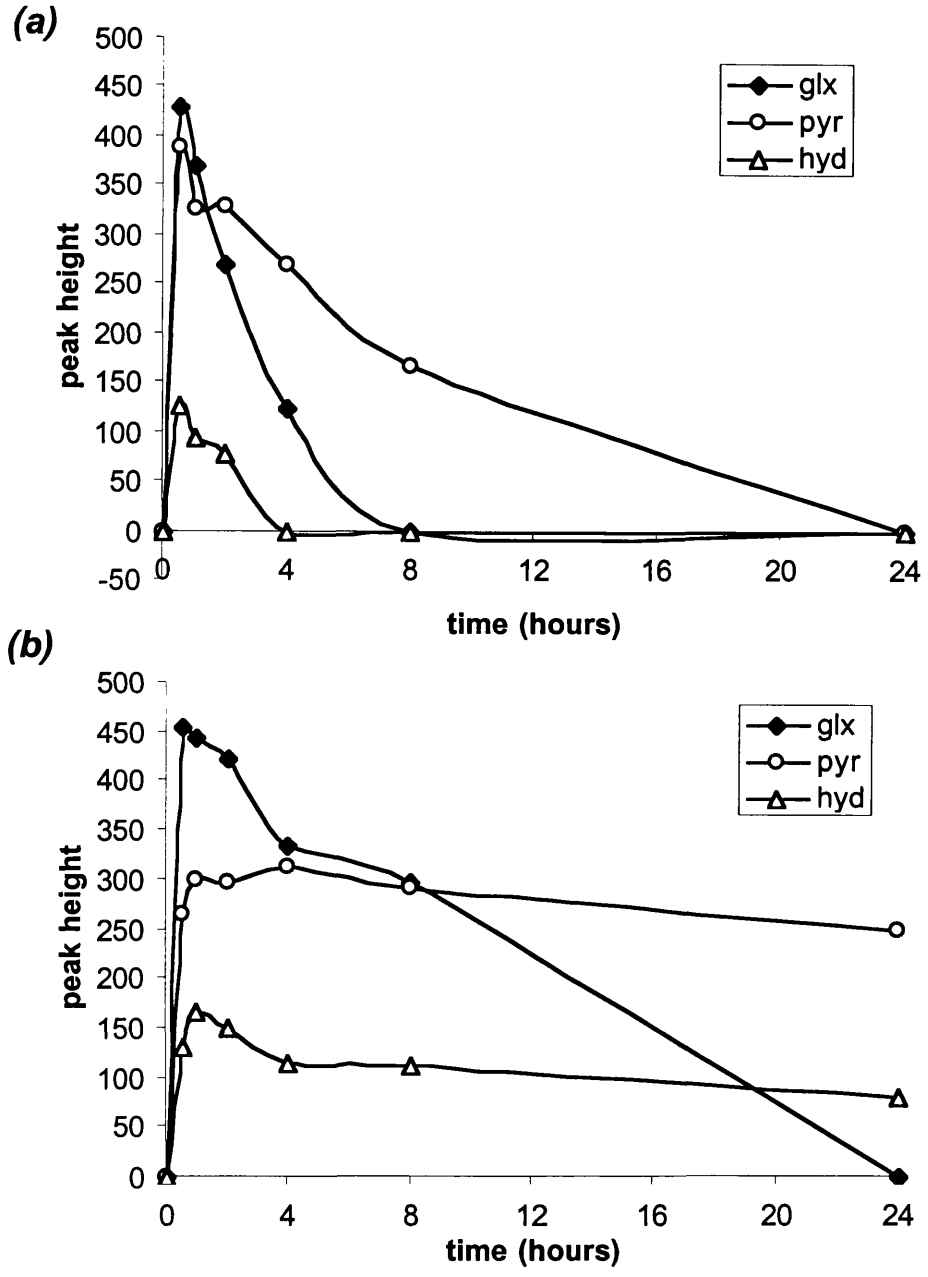

Figure 7.4 24 hour stability profiles of α-keto acid hydrazone derivatives. *500 mM standard solutions were derivatised with 20 mM PHZ at (a) pH 6 and (b) pH 8 and injected into the HPLC over a period of 24 hours. Glx – glyoxylate; pyr – pyruvate; hyd – hydroxypyruvate. Units of peak height are mvolts.*

7.3.2 Evaluation of o-phenylenediamine derivatisation

The formation of quinoxalones by OPD is an irreversible reaction and derivatisation was complete within 1.5 hours when incubated at 60 °C. No decrease in peak height was observed when the stability of derivatives was assessed over 24 hours (Figure 7.5).

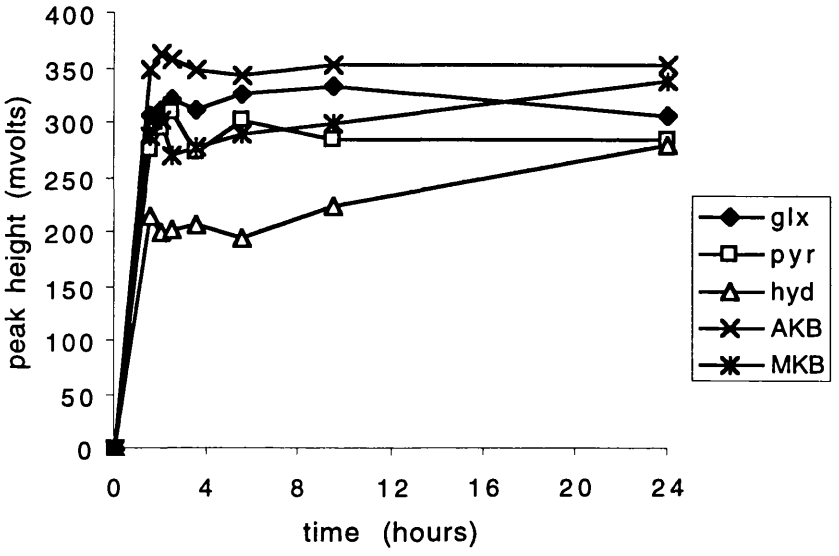

Figure 7.5 24 hour stability profiles of α-keto acid quinoxalone derivatives. *500 μM standard solutions were derivatised at 60 ° C for 1.5 hours and injected into the HPLC over a period of 24 hours. Glx – glyoxylate; pyr – pyruvate; hyd – hydroxypyruvate; AKB – alpha-ketobutyrate; MKB – methyl-ketobutyrate.*

The presence of excess OPD did not interfere in the chromatogram, because it showed minimal column retention and eluted before the peaks of interest (Figure 7.6). Therefore this derivatisation method was selected for optimisation of chromatographic separation.

7.3.3 Optimisation of an HPLC method to measure α-keto acids

In order to determine whether isocratic elution was possible, a scouting gradient was carried out over the range 0–60 % acetonitrile in 10 mM potassium phosphate buffer pH 2.5 over 60 minutes. To ensure accurate peak identification, standards of each metabolite were injected separately and retention times determined. The results are summarised in Table 7.1.

Derivative	Elution time (min)
glyoxylate	16
pyruvate	19
alpha-ketobutyrate	27
hydroxypyruvate	35
keto-methylbutyrate	37

Table 7.1 Retention times of quinoxalone derivatives eluted by a scouting gradient of 0 – 60 % acetonitrile in 10 mM potassium phosphate buffer pH 2.5 over 60 minutes.

For the scouting gradient $\Delta t_R/t_G = 0.31$, where Δt_R is the difference between retention times of the first and last peaks and t_G is total gradient run time. This finding indicates that isocratic elution should be possible (Snyder *et al.*, 1997). However, the range of retention values that would be expected under isocratic conditions would be $0.5 < k < 20$, where

$$k = \frac{\text{peak retention time } (t_R) - \text{column dead time } (t_0)}{\text{column dead time } (t_0)}$$

To avoid the late eluting peaks being unacceptably broad it is more desirable to have $1 < k < 10$. To satisfy this narrower retention range, the last peak in the scouting gradient would need to be eluted within 30 minutes. Therefore gradient elution was examined further. Based upon the elution times of the peaks in the scouting gradient, a gradient of 10–30 % was carried out. An HPLC chromatogram of a mixture of α-keto acid derivatives is shown in Figure 7.6 (a). As can be seen in the figure, the pyruvate peak was now eluting at a very similar time to a background contaminant peak (*). Therefore, isocratic elution for 5 minutes was added to the start of the run and the resulting chromatogram is shown in Figure 7.6 (b) in which it can be seen that pyruvate is completely resolved away from the contaminant.

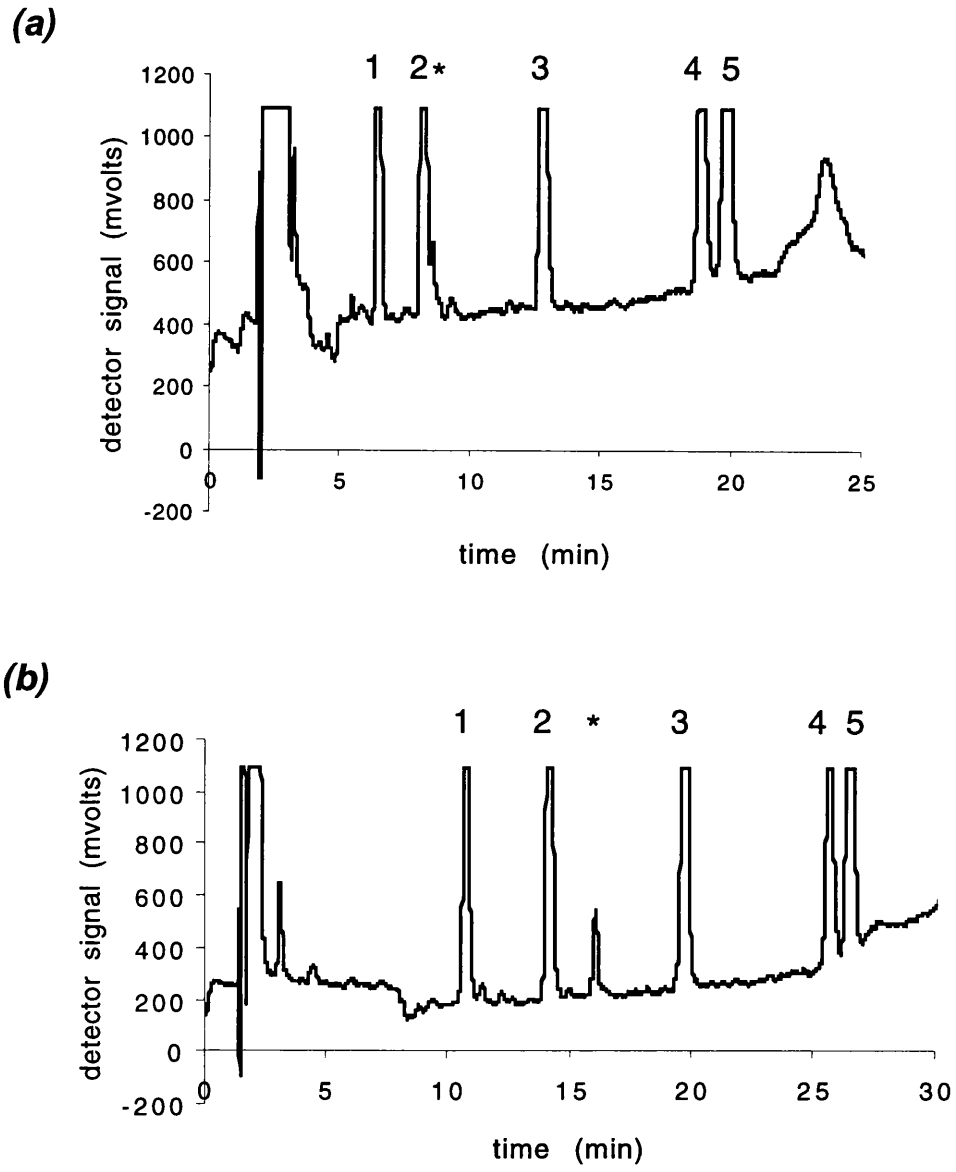

Figure 7.6 Gradient elutions of α-keto acid quinoxalone derivatives. *(a) 10 – 30 % acetonitrile gradient over 20 min and (b) 10% for 10 min and 10 – 30 % gradient over 20 min. Peak 1 – glyoxylate, peak 2 – pyruvate, peak 3 – alpha-ketobutyrate, peak 4 – hydroxypyruvate and peak 5 – methyl-ketobutyrate. (* represents a contaminant peak.)*

The optimised gradient elution parameters are summarised in Table 7.2. Using these optimised parameters, α-keto acid standards were derivatised as described in section 7.2.3 and injected into the HPLC column. Calibration curves were constructed from the resulting chromatograms to enable the measurement of glyoxylate, pyruvate and hydroxypyruvate with alpha-ketobutyrate and methyl-ketobutyrate as internal standards. These calibration curves are shown in Figure 7.7.

Time (min, sec)	% Buffer A	% Buffer B	Flow (ml/min)
0.00	100	0	0
0.01	100	0	1
4.59	100	0	1
24.59	0	100	1
29.59	100	0	1
34.59	100	0	1
35.00	100	0	0

Table 7.2 Optimised parameters for gradient elution of OPD derivatives of α-keto acids from HPLC column. *Buffer A is 10% acetonitrile in 10 mM potassium phosphate buffer pH 2.5 and buffer B is 30% acetonitrile in 10 mM potassium phosphate buffer pH 2.5.*

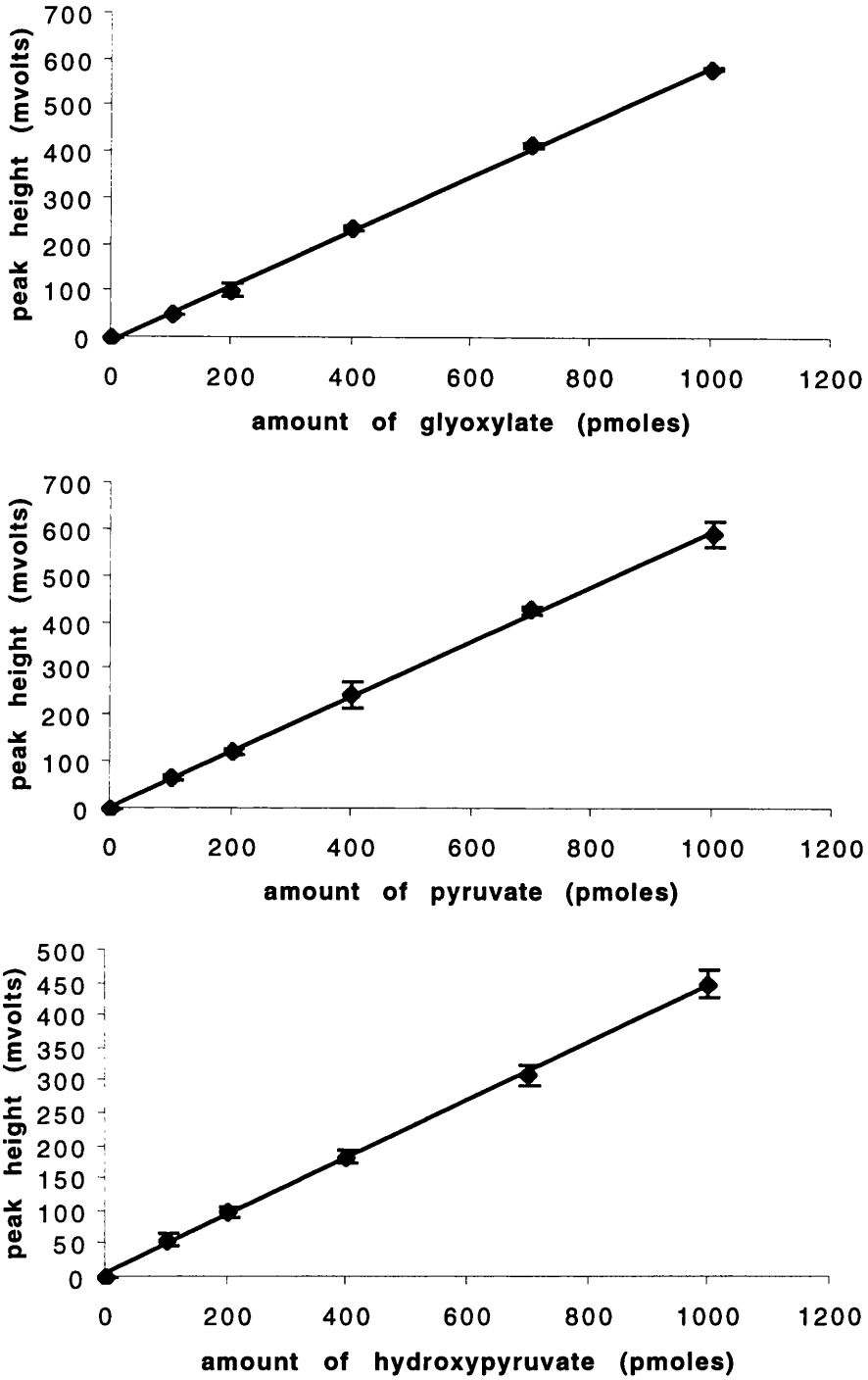

Figure 7.7 Calibration curves for measurement of α-keto acids. *(a) glyoxylate (b) pyruvate (c) hydroxypyruvate (d) alpha-ketobutyrate (e) methyl-ketobutyrate. Results shown are the mean ± S.D. of three separate injections.*

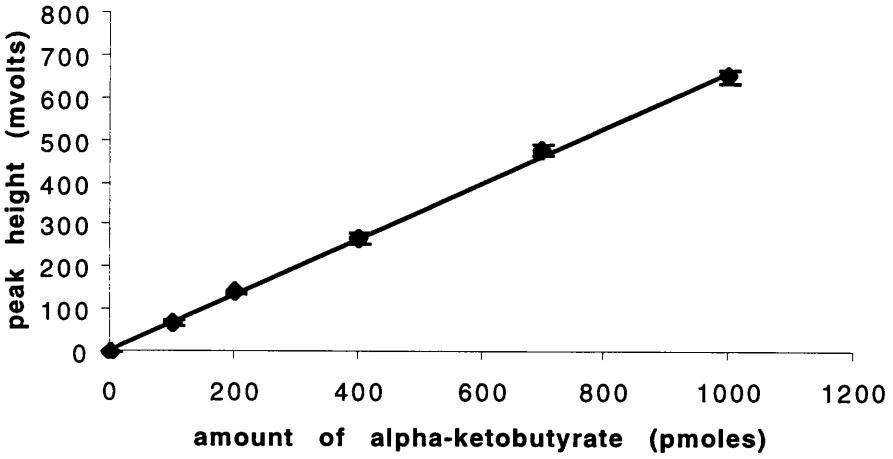

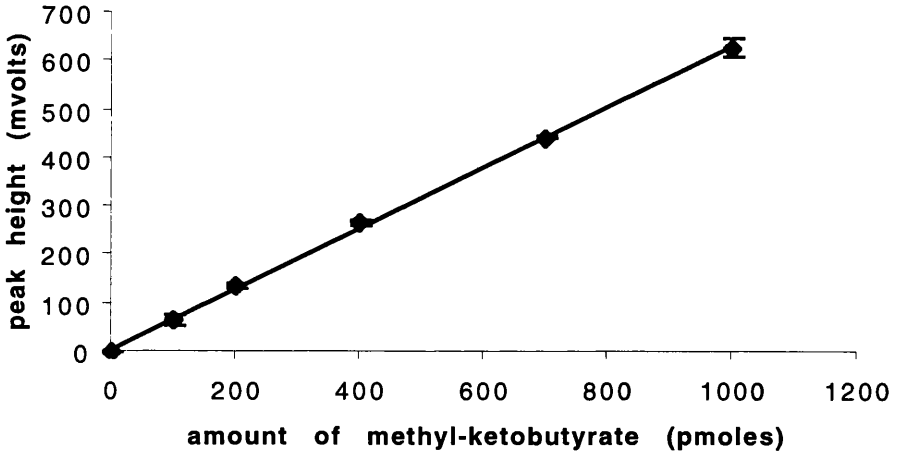

Figure 7.7 Contd.

7.3.4 Purification of AGT

To enable the investigation of peroxisomal glyoxylate metabolism, plasmid constructs of the major and minor AGXT alleles were obtained from Professor Danpure and recombinant AGT protein was expressed and purified according to the procedure outlined in section 7.2.5. Crude bacterial extracts and post nickel column extracts were analysed by SDS-PAGE with Coomassie blue staining and by western blotting with anti-AGT antibody as described in section 7.2.6. The results are shown in Figure 7.8.

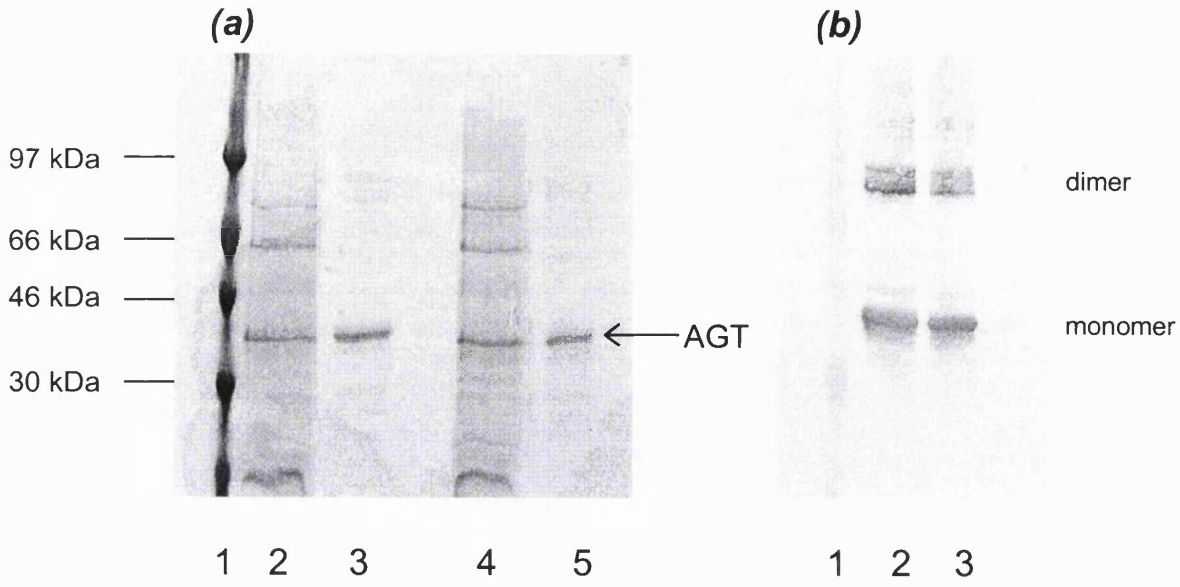

Figure 7.8 Purification of AGT by nickel affinity chromatography. *(a) SDS-PAGE; lane 1, molecular weight marker; lanes 2 – 3, crude extracts and purified protein from major allele transfectants; lanes 4 – 5, crude extracts and purified protein from minor allele transfectants (b) Western blot probed with anti-AGT antibody; lane 1, molecular weight marker; lane 2, purified protein from major allele transfectants; lane 3, purified protein from minor allele transfectants.*

In order to estimate the concentration of AGT in human liver, known amounts of total liver proteins and known amounts of recombinant Pro11AGT were electrophoresed and western blots were incubated with anti-AGT antibody. The signal obtained with 12 μg of liver proteins was of a similar intensity to 375 ng of purified recombinant AGT (Figure 7.9), thus the concentration of AGT in human liver was estimated to be approximately 3% of soluble liver proteins. This result indicates that AGT is present in human liver at approximately 10 times the concentration of GO (Chapter 6).

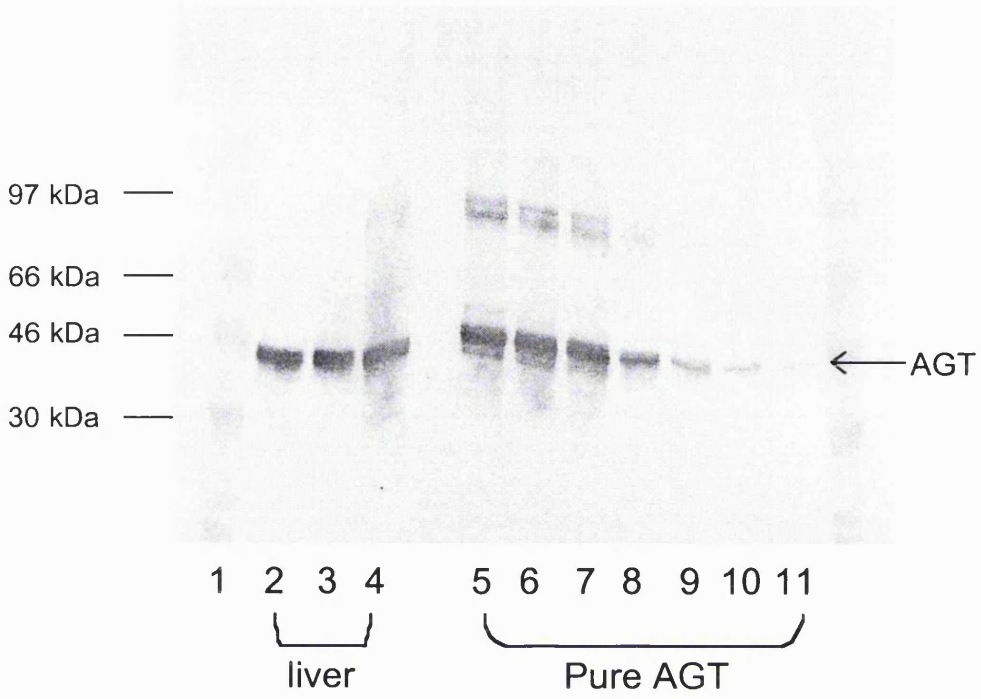

Figure 7.9 Estimation of the concentration of AGT protein in human liver. *Western blots of 3, 6 and 12 μg of total liver proteins were compared to known amounts of pure AGT to estimate the level of AGT present. Lane 1, molecular weight marker proteins; lane2, 3μg total liver protein; lane 3, 6 μg total liver protein; lane 4, 12 μg total liver protein; lanes 5 – 11 contain 1500, 750, 375, 150, 75, 50 and 20 ng of pure AGT protein respectively.*

Purified AGT was assayed by the method outlined in section 7.2.7. The Pro 11 AGT and Leu 11 AGT alleles yielded purified AGT protein with specific activities of 2513 μmol and 1596 μmol pyruvate transformed/hour/mg protein respectively.

7.3.5 In vitro investigation of glyoxylate metabolism by GO and AGT

To investigate the role of GO in peroxisomal glyoxylate metabolism *in vitro,* GO and AGT were incubated with glycolate and glyoxylate and a profile of the change in concentration of glycolate, glyoxylate and oxalate were determined as described in section 7.2.8. The experiments conducted are summarised in Table 7.3.

Enzymes	Metabolites
No enzymes	200 μM glycolate, 5 mM alanine, 2 mM serine
GO	200 μM glycolate, 5 mM alanine, 2 mM serine
GO and major allele AGT	200 μM glycolate, 5 mM alanine, 2 mM serine
GO and minor allele AGT	200 μM glycolate, 5 mM alanine, 2 mM serine
No enzymes	As above plus 200 μM glyoxylate
GO	As above plus 200 μM glyoxylate
GO and major allele AGT	As above plus 200 μM glyoxylate
GO and minor allele AGT	As above plus 200 μM glyoxylate
GO	200 μM glyoxylate, 5 mM alanine, 2 mM serine

Table 7.3 Summary of experimental conditions for the investigation of peroxisomal glyoxylate metabolism.

The results of HPLC analysis for incubations continuing glycolate, alanine and serine are shown in Figure 7.10.

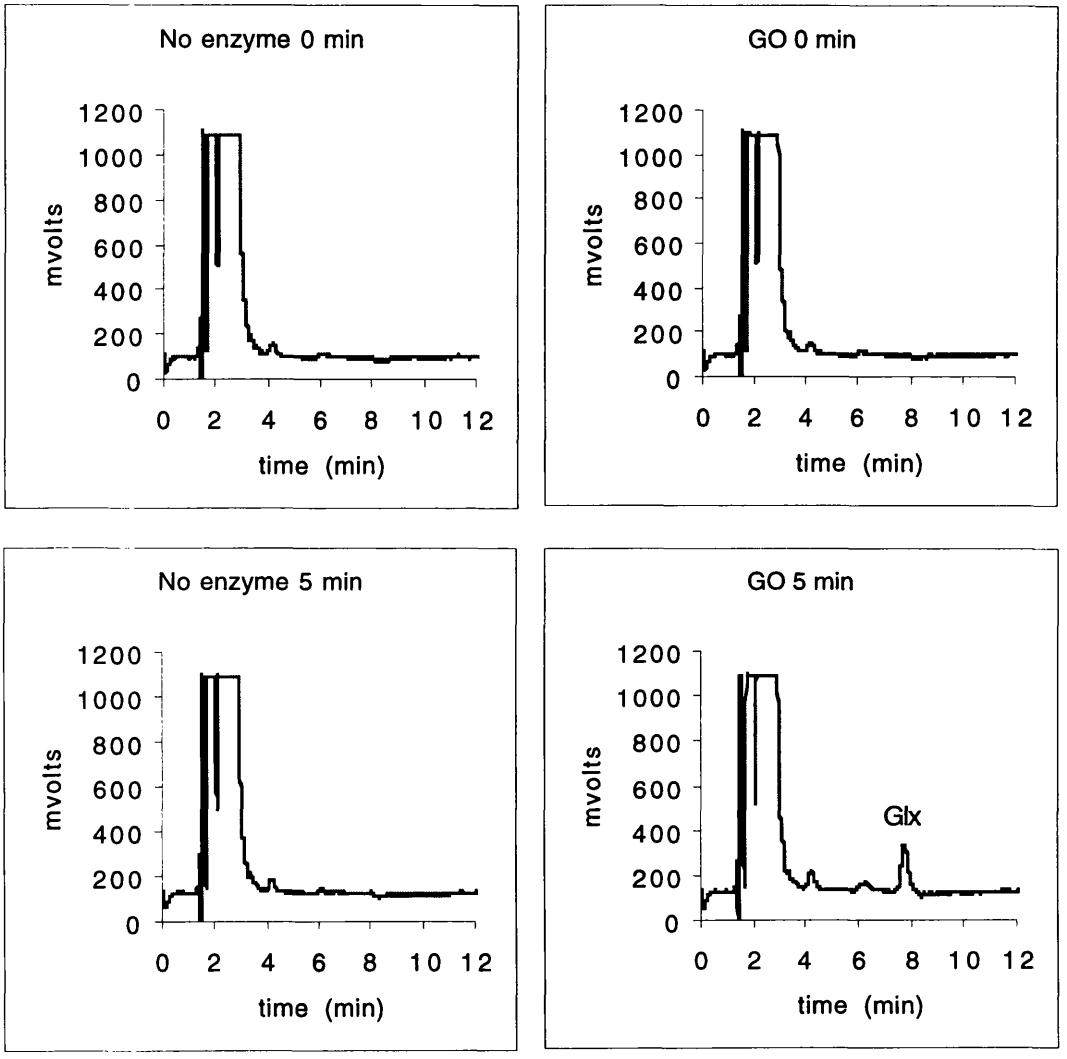

Figure 7.10 (a) HPLC chromatograms to show formation of glyoxylate in reactions containing GO, glycolate, alanine and serine. *Reactions were stopped at 0, 5, 10, 15 and 25 minutes and aliquots were derivatised by OPD and injected into the HPLC. Chromatograms on the left are from incubations without enzyme and on the right from incubations with GO. Glx indicates the glyoxylate peak.*

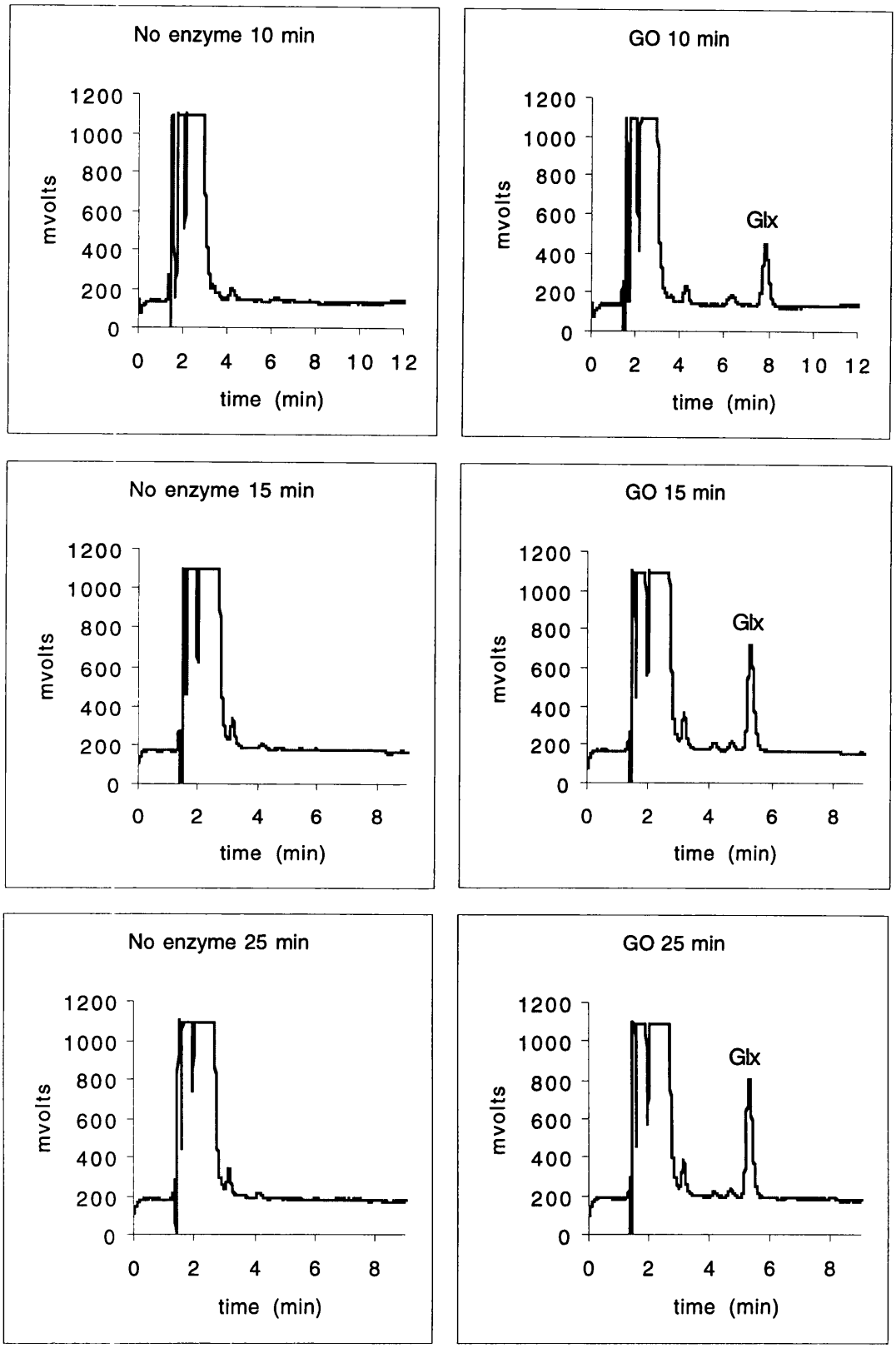

Figure 7.10 (a) Contd.

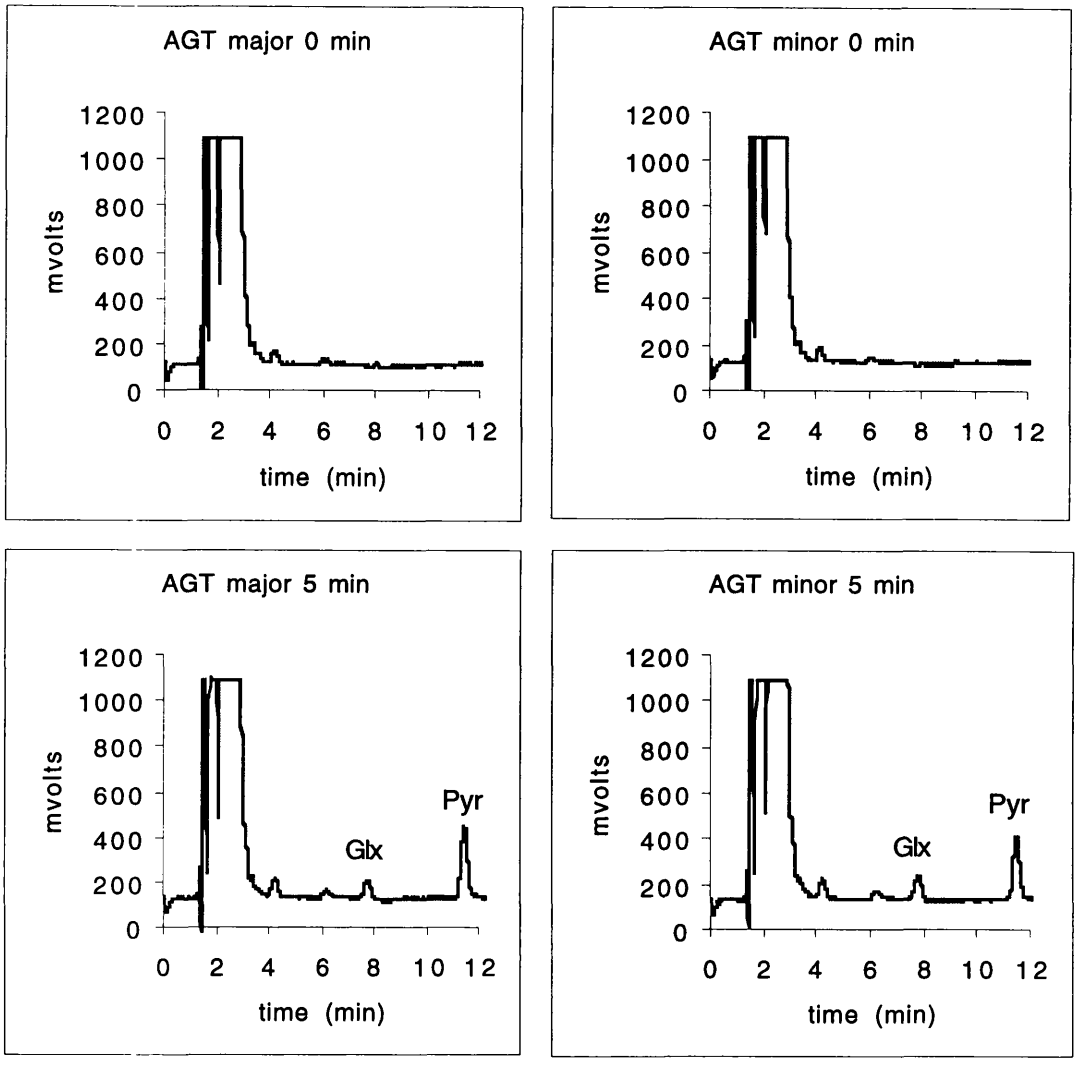

Figure 7.10(b) HPLC chromatograms to show formation of glyoxylate and pyruvate in reactions containing GO, AGT, glycolate, alanine and serine. *Reactions were stopped at 0, 5, 10, 15 and 25 minutes and aliquots were derivatised by OPD and injected into the HPLC. Chromatograms on the left are from incubations with GO and Pro11 AGT (major allele) and on the right from incubations with GO and Leu11 AGT (minor allele). Glx and Pyr represent the glyoxylate and pyruvate peaks respectively.*

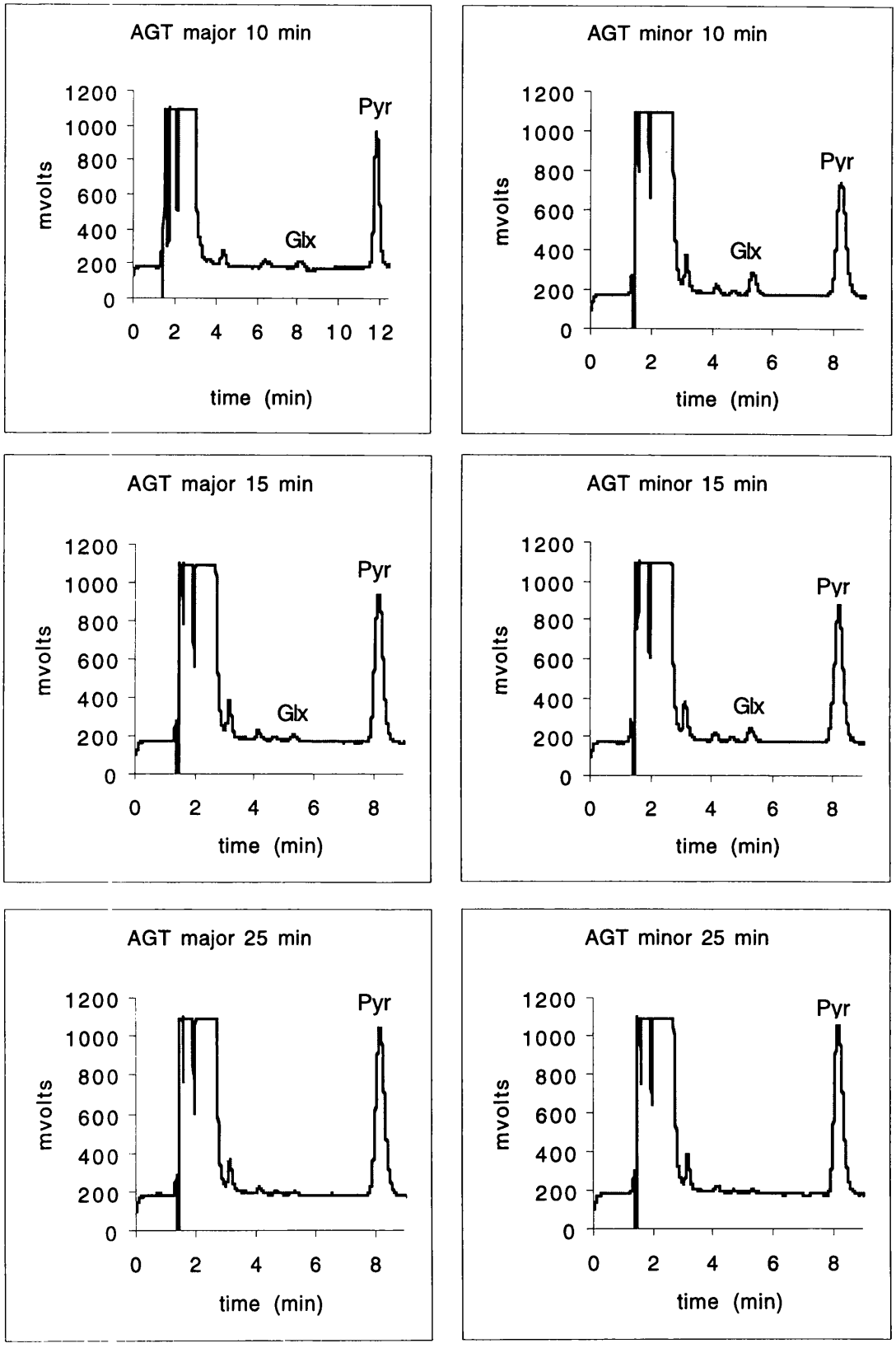

Figure 7.10 (b) Contd.

As can be seen from Figure 7.10 no glyoxylate or pyruvate were produced in the absence of GO and AGT. In the presence of GO alone, glyoxylate increased steadily over the course of the incubation, presumably due to the oxidation of glycolate by GO. This result is confirmed by the steady disappearance of glycolate during the time course of the incubation (Figure 7.11).

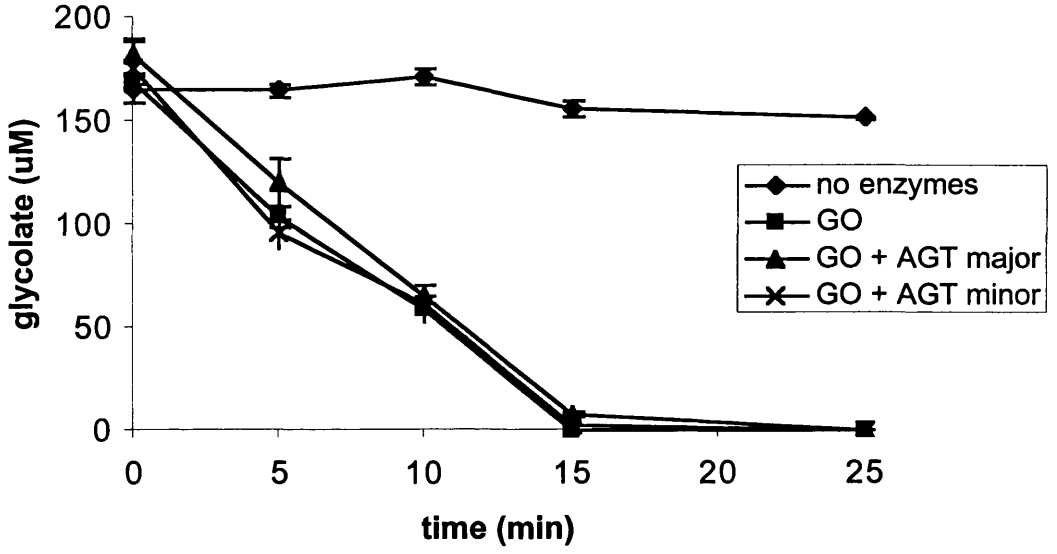

Figure 7.11 Time course of glycolate oxidation by GO incubated with glycolate, alanine and serine with and without AGT. *Results represent the mean ± S.D of duplicate measurements.*

In the presence of AGT, pyruvate steadily increased during the incubation, although at a slower rate with the Leu11 AGT (minor allele) in comparison to Pro11 AGT (major allele). This increase in pyruvate was only seen when AGT was present in the incubations, indicating that the reaction was not spontaneous but catalysed by AGT.

Pyruvate formation also mirrored the decrease in glyoxylate, indicating that pyruvate was formed as a result of glyoxylate transamination (Figure 7.12).

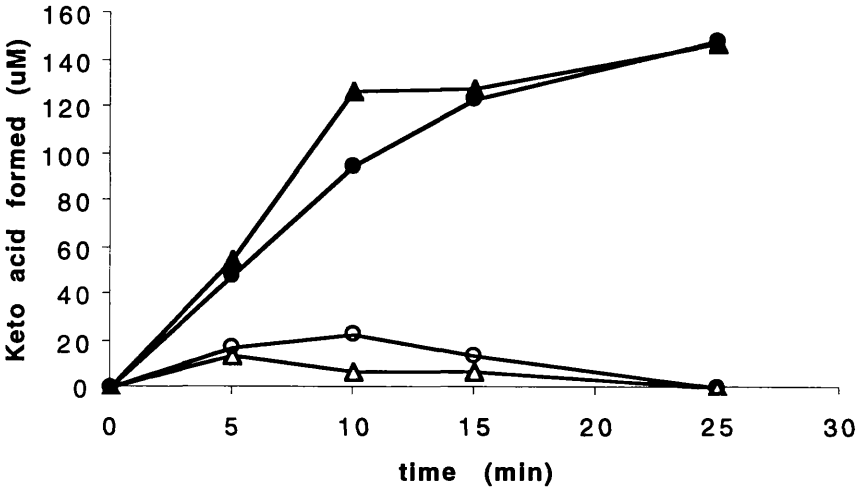

Figure 7.12 Time course of glyoxylate and pyruvate formation by GO and AGT incubated with glycolate, alanine and serine. *Triangles are the results of incubations with GO and Pro 11 AGT (major allele) and circles are the results of incubations with GO and Leu 11 AGT (minor allele), open symbols represent glyoxylate and closed symbols represent pyruvate.*

No increase in hydroxypyruvate was observed indicating that the SPT reaction of AGT was not functioning, despite the presence of serine in the reaction. Furthermore, no oxalate was detected in any samples tested and no decrease in glyoxylate was observed with GO alone suggesting that this enzyme was not oxidising glyoxylate to oxalate. To further investigate the potential of GO to produce oxalate, the incubations were repeated with equimolar concentrations of glycolate and glyoxylate. The results of HPLC analysis for the incubations with glycolate, glyoxylate, alanine and serine are shown in Figure 7.13.

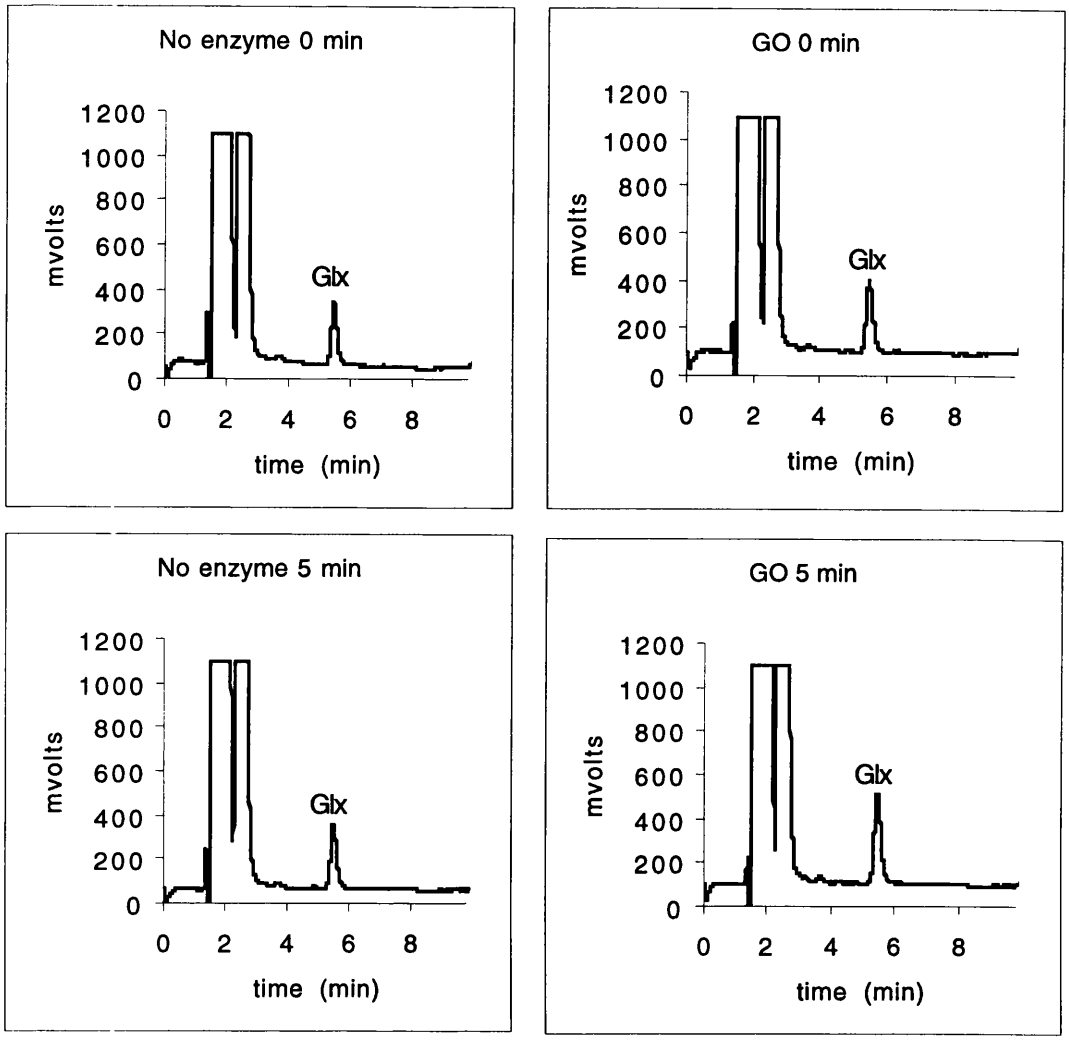

Figure 7.13 (a) HPLC chromatograms to show formation of glyoxylate in reactions containing GO, glycolate, glyoxylate, alanine and serine. *Reactions were stopped at 0, 5, 10, 15 and 25 minutes and aliquots were derivatised by OPD and injected into the HPLC. Chromatograms on the left are from incubations without enzyme and on the right from incubations with GO. Glx indicates the glyoxylate peak.*

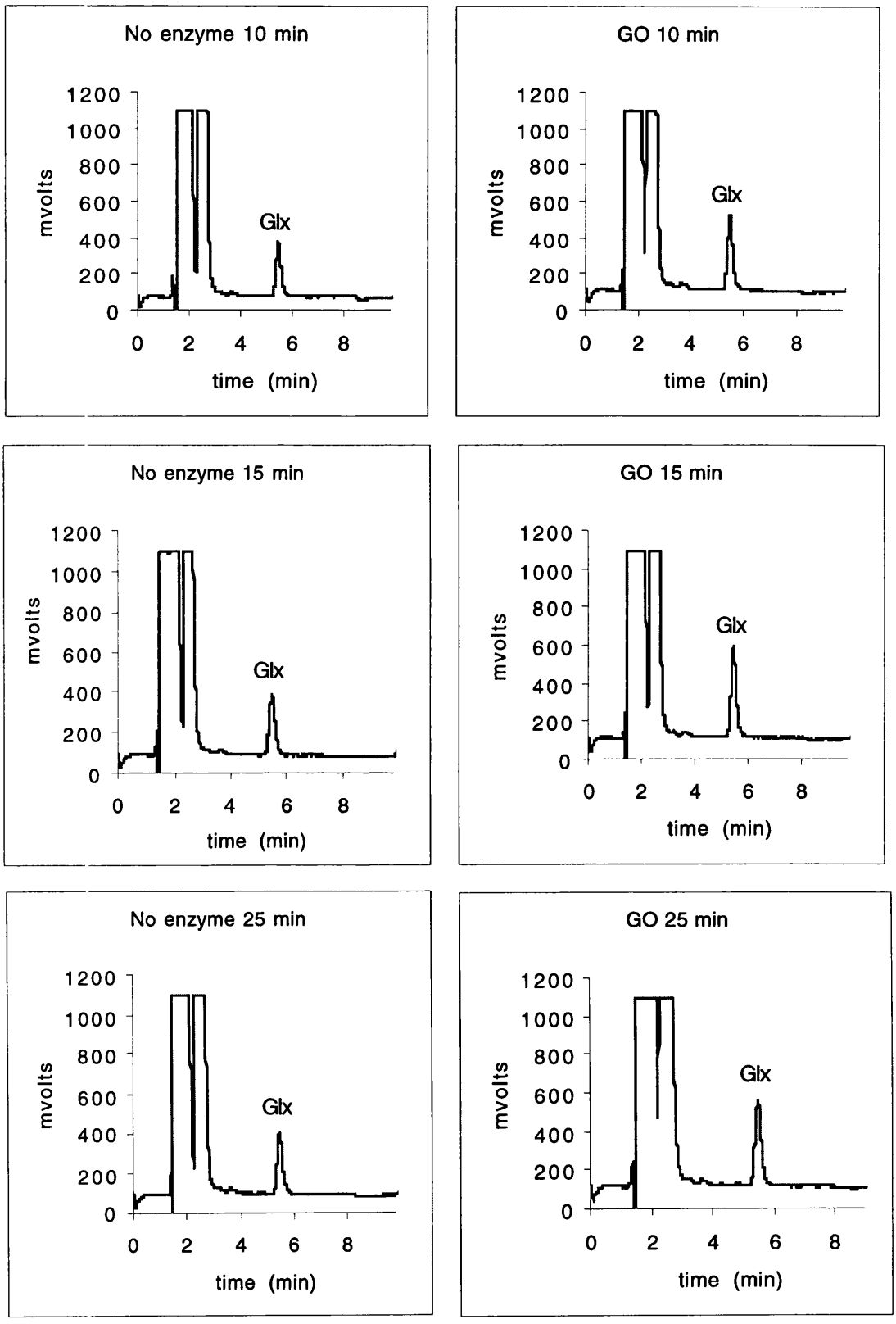

Figure 7.13 (a) Contd.

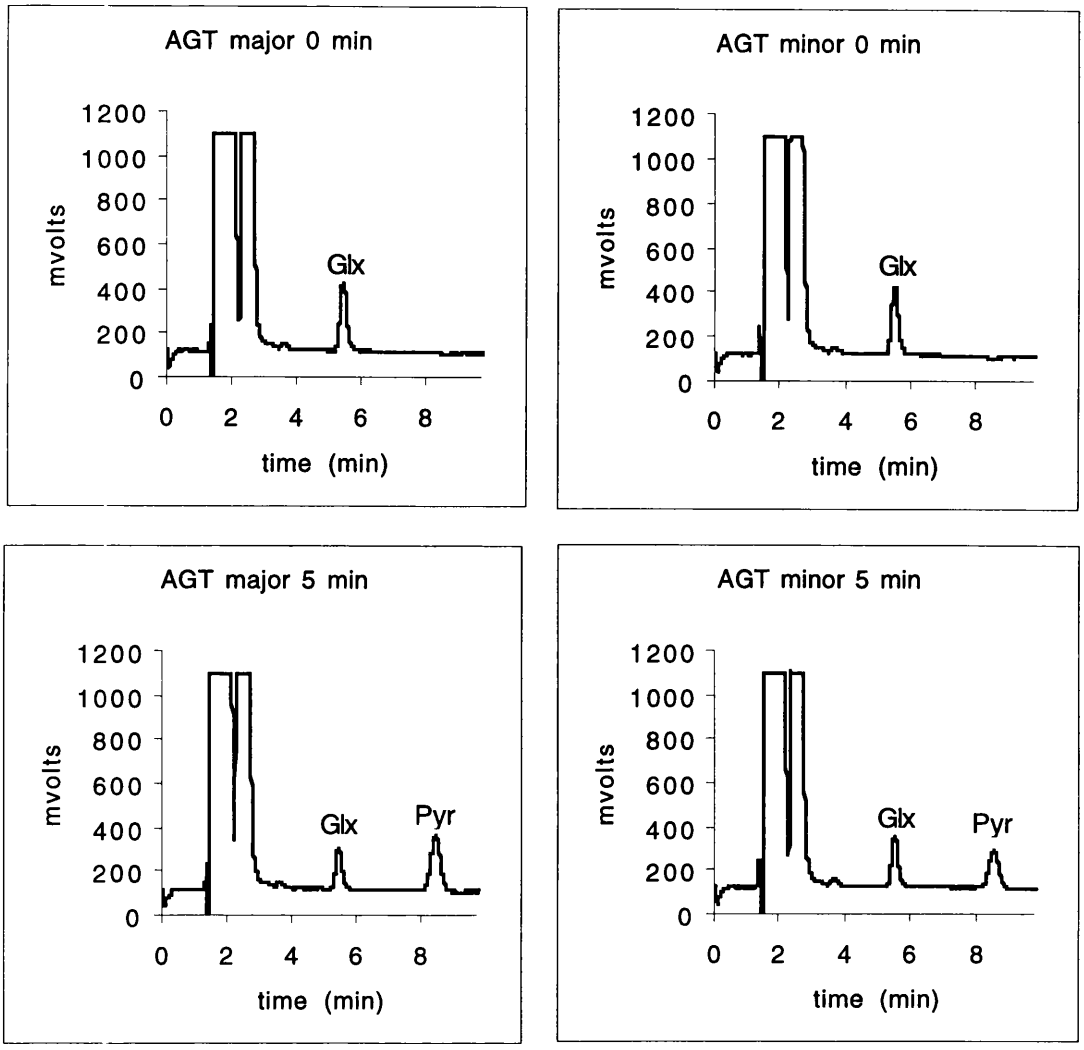

Figure 7.13(b) HPLC chromatograms to show formation of glyoxylate and pyruvate in reactions containing GO, AGT, glycolate, glyoxylate, alanine and serine. *Reactions were stopped at 0, 5, 10, 15 and 25 minutes and aliquots were derivatised by OPD and injected into the HPLC. Chromatograms on the left are from incubations with GO andPro11 AGT (major allele) and on the right from incubations with GO and Leu11 AGT (minor allele). Glx and Pyr indicate the glyoxylate and pyruvate peaks respectively.*

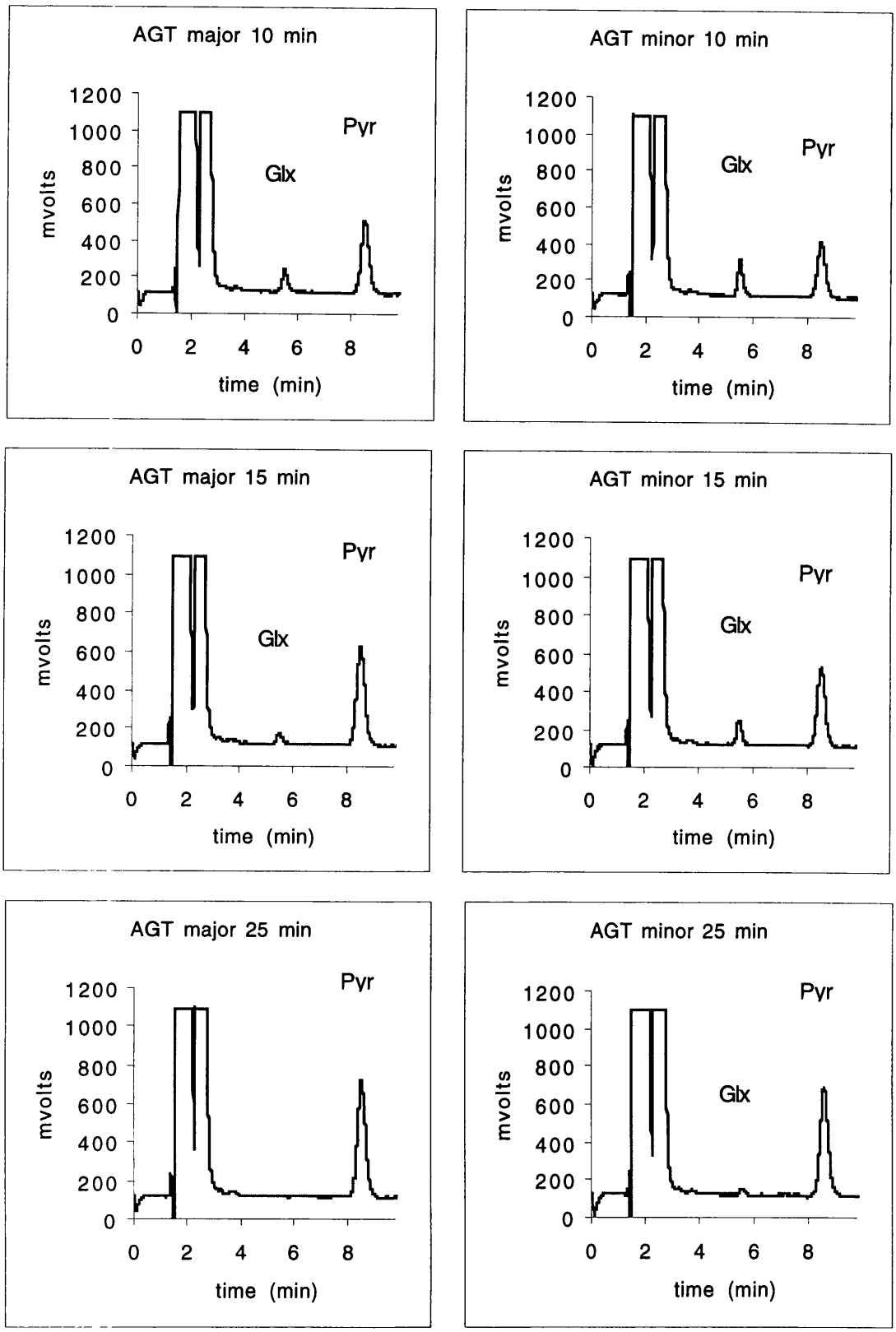

Figure 7.13 (b) Contd.

As can be seen from Figure 7.13 (a) GO continued to synthesise glyoxylate from glycolate in the presence of equimolar amounts of glycolate and glyoxylate. This indicates that GO is only utilising glycolate as substrate and that glyoxylate oxidation is not favourable. This was confirmed by the absence of oxalate in all samples tested. Glycolate oxidation by GO occurred at comparable rates both in the presence and absence of AGT as reflected by the glycolate disappearance (Figure 7.14). In the incubations containing AGT in addition to GO, glyoxylate did not increase but fell gradually over the time course of the incubation as shown in Figure 7.13 (b). This decrease in glyoxylate was mirrored by an increase in pyruvate and the reaction progressed at a faster rate with Pro 11 AGT (major allele) in comparison to Leu 11 AGT (minor allele) (Figure 7.15).

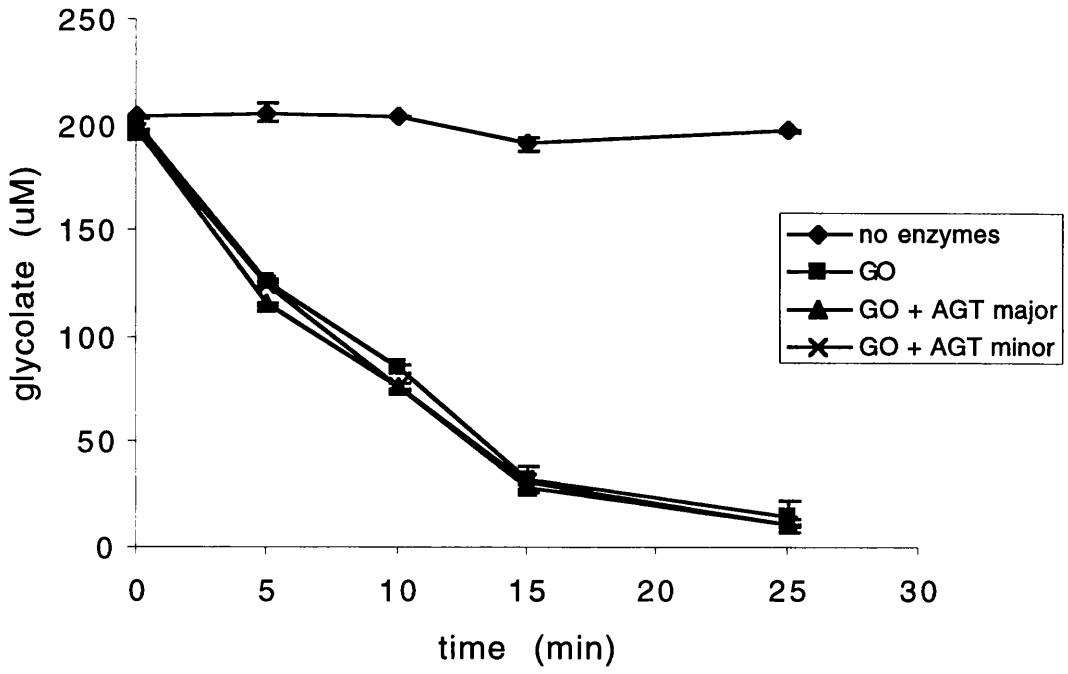

Figure 7.14 Time course of glycolate oxidation by GO incubated with glyoxylate, glycolate, alanine and serine with and without AGT. *Results represent the mean ± S.D of duplicate measurements.*

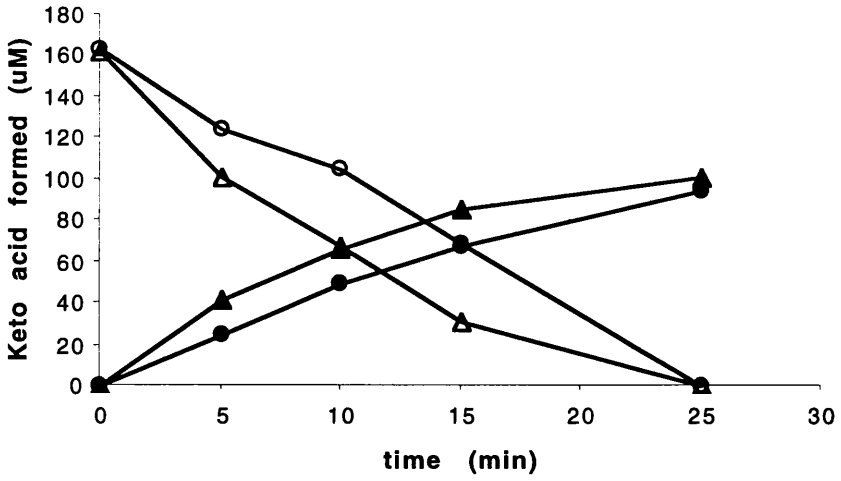

Figure 7.15 Time course of glyoxylate and pyruvate formation by GO and AGT incubated with glyoxylate, glycolate, alanine and serine. *Triangles are the results of incubations with GO and Pro 11 AGT (major allele) and circles are the results of incubations with GO and Leu 11 AGT (minor allele), open symbols represent glyoxylate and closed symbols represent pyruvate.*

To determine whether GO was capable of catalysing the production of oxalate from glyoxylate in the absence of glycolate, incubations were carried out in which GO was incubated with glyoxylate, alanine and serine in the absence of AGT. The production of oxalate was not detected in any samples tested and glyoxylate levels remained the same over the time course of the incubation. This finding indicates that GO does not catalyse the oxidation of glyoxylate to produce oxalate at the 200 μM glyoxylate concentration tested.

7.4 Discussion

An HPLC assay for the simultaneous detection of glyoxylate, pyruvate and hydroxypyruvate has been developed and successfully applied to the study of glycolate metabolism *in vitro*. The initial HPLC method investigated utilised derivatisation by PHZ. This procedure has a number of advocates and has been described for the analysis of glyoxylate in metabolic studies (Holmes, 1993; Poore *et al.*, 1997) and in body fluids (Petrarulo *et al.*, 1988; Lange and Malyusz, 1994). However, this method was found to be unsatisfactory for several reasons. Firstly, a huge excess of derivatisation reagent was required and this interfered with the detection of the peaks of interest in the chromatographs. Furthermore, the derivatives showed varying signal intensity and poor stability. This method was therefore rejected in favour of OPD derivatisation, which produced highly absorbing derivatives that were stable for 24 hours. The response of the HPLC instrument as assessed by peak height was linear over the range 0 to 1000 pmoles. The limits of detection, defined as a peak height giving a signal to noise ratio of less than three was 50 mvolts, which equates to 100 pmoles. The method developed can be applied to the measurement of α-keto acids in bodily fluids and tissues, although further validation of the assay will be required before being adopted for routine use. This evaluation would include an assessment of the accuracy, specificity and precision of the assay.

To evaluate the HPLC system for future use in *in vitro* investigations, the metabolic pathway from glycolate was studied by following the metabolism of the organic acid over time in the presence of GO and AGT, both major and minor allelic forms. The

experiments were designed as far as possible to include AGT and GO in amounts reflecting the situation in liver. Thus the concentration of both enzymes was estimated by comparison of pure enzymes with liver. The amount of AGT present in human liver sonicates was estimated to be 3% of soluble liver proteins; a value 10 fold higher than that observed for GO (Chapter 6). These differences are consistent with findings based upon the measurement of catalytic AGT and GO. AGT activity was found to be 10 fold higher than GO activity in guinea pig liver (Holmes *et al.*, 1995). The same study found the activity of catalase to be 7 fold higher than that of AGT. Therefore the levels of GO, AGT and catalase in the incubations carried out here were of these relative amounts.

For the *in vitro* incubations, in order to produce relevant results the concentrations of metabolites used were based upon previous estimates of these metabolites in liver tissue. The concentrations of alanine and serine in human liver have been estimated to be 5 mM and 2 mM respectively (Holmes and Assimos, 1998). The concentration of glycolate in guinea pig liver has been estimated to be 0.2 mM (Holmes *et al.*, 1995). Little is known about the concentration of glyoxylate in human liver and hence the concentration of glyoxylate chosen for the incubations was the same as that for glycolate. Clearly other metabolites would be present *in vivo*, which have not been considered in these studies. For example, the concentration of lactate in liver has been found to be 200 times higher than glycolate. Hence the lactate level would be expected to be in the region of the K_m of GO for lactate (K_m = 30.9) and this suggests that lactate oxidation, catalysed by GO, is physiologically favourable.

The results of the incubations indicated that GO was effective at catalysing the oxidation of glycolate to glyoxylate as evidenced by the disappearance of glycolate coupled with

the production of glyoxylate. AGT was very efficient at the removal of glyoxylate as reflected by its rapid disappearance coupled with the production of pyruvate. The minor allele AGT was slightly less efficient than the major allele AGT as evidenced by the slower rate of glyoxylate removal by the former (Figure 7.15). The rates of glycolate oxidation by GO were not influenced by the presence or absence of AGT. However, in the absence of AGT it was surprising that GO did not appear to metabolise the accumulated glyoxylate to oxalate. Further experiments using glyoxylate alone in the presence of GO also failed to elicit any oxalate production. There could be several reasons for these observations. Firstly, GO may have been oxidising the glyoxylate at a very slow rate and the levels of oxalate formed were below the limits of detection of the oxalate assay. Alternatively, the findings could simply reflect the fact that glyoxylate is not a satisfactory substrate for oxidation by GO.

The findings that GO did not produce oxalate from the accumulated glyoxylate in the absence of AGT are not consistent with similar studies of isolated peroxisomes. In a study with isolated guinea pig peroxisomes oxalate production occurred when the glycolate concentration fell below 50 μM. In total 25 μM oxalate was formed from 200 μM glycolate in the absence of an amino donor for AGT transamination (Holmes *et al.*, 1995). This observation was attributed to GO activity, however GO did not produce oxalate in the study described here. This discrepancy may be due to differences in the kinetics of glyoxylate oxidation between guinea pig and human GO or may indicate that another enzyme is present in guinea pig peroxisomes, which is capable of oxalate production from glyoxylate.

The findings obtained here suggest that oxalate production by GO is not favoured and that the enzyme would not contribute to the pathophysiology of PH1. This suggests that the investigation of the potential role for LDH in oxalate production should be pursued. Whether or not LDH would catalyse glyoxylate oxidation to oxalate will be influenced by the concentrations of the relevant metabolites. Lactate has been estimated to be 1 μmol / g wet weight (Yanagawa *et al.*, 1990) compared to 5 nmol glyoxylate / g wet weight in rat liver (Funai and Ichiyama, 1986). These differences would suggest that glyoxylate oxidation would be unfavourable in normal metabolism, due to the dominance of lactate oxidation. However, it is not known how high the level of glyoxylate becomes in the hyperoxaluric liver. Although it has been postulated that deficiency of AGT and GRHPR results in hepatic glyoxylate accumulation in PH1 and PH2, an increase in liver glyoxylate concentration in these inherited diseases has not been demonstrated (Holmes, 2000). With the HPLC methods developed, it will now be possible to establish the concentration of glyoxylate in liver samples from normal individuals and PH patients, and this will be attempted in the future.

8.0 Concluding remarks and future research

The main aims of this thesis have been achieved. The human HAO1 gene has been cloned and the resulting recombinant GO protein has been expressed *in vitro*. Kinetics studies of purified GO showed that the enzyme has highest activity with glycolate as substrate and has 10 fold less affinity for glyoxylate as substrate. HPLC methods have been developed to enable the analysis of the metabolic pathways *in vitro*. However, *in vitro* studies of glyoxylate metabolism showed no evidence of oxalate production from glyoxylate in the presence of GO. Thus the studies reported in this thesis do not provide evidence of a role for GO in oxalate production in PH. However, a role for GO in glyoxylate production from glycolate has been firmly established. Furthermore, the efficiency of AGT in removing the potentially toxic glyoxylate has been shown *in vitro*.

The feasibility of a glyoxylate pathway in liver metabolism, previously only inferred by the observation of hyperoxaluria resulting from AGT deficiency, has been demonstrated *in vitro*. The liver specificity of such a pathway has been reinforced by the observation that GO is a liver specific enzyme. Whether or not other pathways of glyoxylate metabolism, catalysed by alternative enzymes, occur in other tissues such as kidney is not known and awaits investigation. The deficiency of these enzymes, should they exist, would be potential causes of hyperoxaluria not due to AGT or GRHPR deficiency, so-called atypical hyperoxaluria (Monico and Milliner, 1999).

It has been estimated that dietary intake can provide 33 mg of glycolate per day and that 5% or more of urinary oxalate may be derived from dietary glycolate (Harris and

Richardson, 1980). Since GO is responsible for the conversion of glycolate to glyoxylate its inhibition may reduce the production of oxalate. The extent to which this would be effective at reducing oxalate production in hyperoxaluric patients depends upon how much endogenously derived glyoxylate is formed from glycolate as opposed to other precursors such as glycine. The relative contribution of these precursors to glyoxylate production is not yet established. Furthermore, the inhibition of GO may have metabolic consequences as a result of the subsequent accumulation of glycolate. This metabolite is not thought to be toxic, although patients with hyperglycolic aciduria and normal levels of oxalate with nephrocalcinosis have been documented (Kist-van Holthe *et al.*, 2000).

The genes for GO, GRHPR and AGT have now all been cloned and the kinetics of the enzyme reactions catalysed by these proteins has been established. However, metabolic studies of the intact pathway at the cellular and whole body level have tended to focus on rodent metabolism. As discussed in chapter 1, a number of differences exist between rodent and human glyoxylate metabolism. These differences would limit the usefulness of knock out mice as animal models of PH1 or PH2. Furthermore, human hepatocellular hepG2 cell lines show very different levels of expression of the crucial enzymes in the pathway including GO in comparison to human liver expression (Wanders *et al.*, 1991). Hence, studies have been initiated to form stable transformants expressing AGT, GRHPR and GO at levels equivalent to their human liver concentration. Figure 8.1 shows immunocytochemistry images of Chinese hamster ovary (CHO) cells transfected with AGT and GO, where GO has been visualised by means of the anti-GO antibody developed here (chapter 6). As can be seen from the figures, GO co-localises with AGT

confirming its peroxisomal location. The HPLC methods developed here are to be utilised in the study of glyoxylate metabolism in CHO cells expressing GO, AGT and GRHPR.

Further investigation of GO would include the kinetics of inhibition by metabolites such as oxalate. This metabolite would be expected to inhibit human GO since this effect has been documented with the spinach enzyme (Richardson and Tolbert, 1961). Studies are also underway within the laboratory to express and purify recombinant human liver LDH. Kinetic characterisation of purified LDH will assess the potential of the enzyme to catalyse oxalate production from glyoxylate and the effect of different redox states upon the reaction. Finally, cytosolic glyoxylate metabolism catalysed by purified GRHPR and LDH will be investigated *in vitro*, by means of HPLC as described in chapter 7. This analysis may establish a role for LDH in the pathophysiology of PH. However, the possibility remains of the existence of as yet undiscovered enzymes, which may be responsible for oxalate production in the primary hyperoxalurias.

(a)

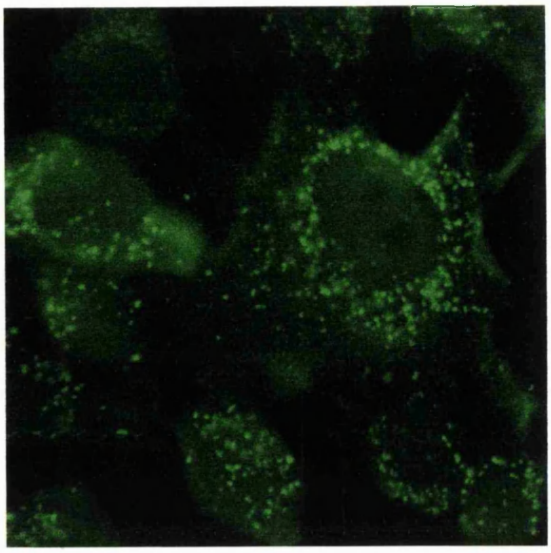

(b)

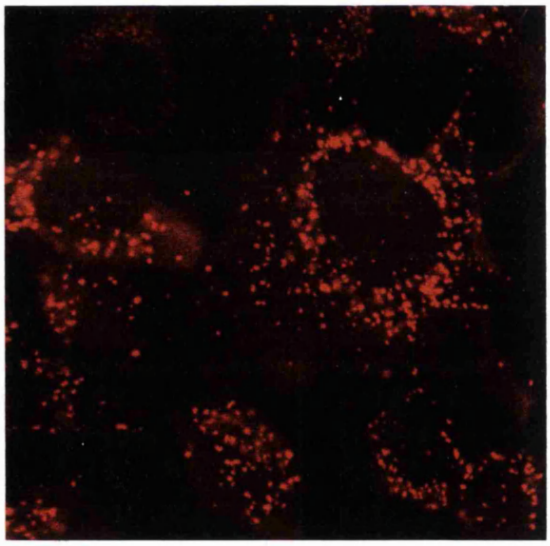

Figure 8.1 Immunocytochemistry images of GO and AGT expressed in CHO cells. *(a) GO shown in green, visualised by means of anti-GO antibody and (b) AGT shown in red, visualised by means of anti-AGT antibody.*

Bibliography

Adams, M., J. Kelley, J. Gocayne, M. Dubnick, M. Polymeropoulos, H. Xiao, C. Merril, A. Wu, B. Olde, R. Moreno, A. Kerlavage, W. McCombie and J. Venter (1991). "Complementary DNA sequencing: Expressed sequence tags and the human genome project." Science **252**: 1651-1656.

Allen, A., E. Thompson, G. Williams, R. Watts and C. Pusey (1996). "Selective renal transplantation in primary hyperoxaluria type 1." Am J Kidney Dis **27**: 891-895.

Allison, M., H. Cook, D. Milne, S. Gallagher and R. Clayman (1986). "Oxalate degradation by gastrointestinal bacteria from humans." J Nutr **116**: 455-460.

Allison, M., S. Daniel and N. Cornick (1995). "Oxalate-degrading bacteria." In: Khan, S. editor. Calcium oxalate in biological systems. Boca Raton, CRC Press Inc: 131-168.

Appleby, C. and R. Morton (1954). "Crystalline cytochrome b2 and lactic dehydrogenase of yeast." Nature **173**: 749-752.

Applewhite, J., M. Kennedy, D. Assimos and R. Holmes (2000). "Renal oxalate synthesis." Mol Urol **163**: S229.

Armstrong, J. (1964). "The molar extinction coefficient of 2,6-dichlorophenol indophenol." Biochim Biophys Acta **86**: 194-197.

Aronson, P. and G. Giebisch (1997). "Mechanisms of chloride transport in the proximal tubule." Am J Physiol **273**: F179-192.

Asker, H. and D. Davies (1983). "Purification of rat liver enzymes involved in the oxidation of glyoxylate." Biochim Biophys Acta **761**: 103-108.

Bairoch, A., P. Bucher and K. Hofmann (1997). "The PROSITE database, its status in 1997." Nucleic Acids Res **25**: 217-221.

Bais, R., A. M. Rofe and R. A. Conyers (1989). "Inhibition of endogenous oxalate production: biochemical considerations of the roles of glycollate oxidase and lactate dehydrogenase." Clin Sci **76**: 303-309.

Barham, D. and P. Trinder (1972). "An improved colour reagent for the determination of blood glucose by the oxidase system." Analyst **97**: 142-145.

Barnes, R. H. and A. Lerner (1943). "Metabolism of glycolic and glyoxylic acids." Proc Soc Exp Biol **52**: 216-219.

Barton, H., R. Eisenstein, A. Bomford and H. Munro (1990). "Determination of the interaction between the iron-response element-binding protein and its binding site in rat L-ferritin mRNA." J Biol Chem **265**: 7000-7008.

Binder, H. (1974). "Intestinal oxalate absorption." Gastroenterology **67**: 441-446.

Boguski, M. S. (1995). "The turning point in genome research." TIBS **20**: 295-296.

Bourke, E., G. Frindt, P. Flynn and G. Schreiner (1972). "Primary hyperoxaluria with normal alpha-ketoglutarate: glyoxylate carboligase activity." Ann Intern Med **76**: 279-284.

Bourke, E., G. Frindt, P. Flynn and G. Schreiner (1972). "Primary hyperoxaluria with normal alpha-ketoglutarate: glyoxylate carboligase activity." Ann Intern Med **76**: 279-284.

Brent, J., K. McMartin, S. Phillips, K. K. Burkhart, J. W. Donovan, M. Wells and K. Kulig (1999). "Fomepizole for the treatment of ethylene glycol poisoning." N Engl J Med **340**: 832-838.

Brinkley, L., J. McGuire and J. Gregory (1981). "Bioavailability of oxalate in foods." Urology **17**: 534-538.

Campbell, W. and W. Ogren (1990). "Glyoxylate inhibition of ribulosebisphosphate carboxylase/oxygenase activation in intact, lysed, and reconstituted chloroplasts." Photosynthesis Res **23**: 257-268.

Chalmers, R. A., B. M. Tracey, J. Mistry, K. D. Griffiths, A. Green and M. H. Winterborn (1984). "L-Glyceric aciduria (primary hyperoxaluria type 2) in siblings in two unrelated families." J Inherit Metab Dis **2**: 133-4.

Chlebeck, P. T., D. S. Milliner and L. H. Smith (1994). "Long-term prognosis in primary hyperoxaluria type II (L-glyceric aciduria)." Am J Kidney Dis **23**: 255-9.

Chomczynski, P. (1993). "A reagent for the single-step simultaneous isolation of RNA, DNA and protein from cell and tissue samples." Biotechniques **15**: 532-534, 536-537.

Cochat, P., J. M. Gaulier, P. C. Koch Hogueirrra, J. Feber, N. V. Jamieson, M.-O. Rolland, P. Divry, D. Bozon and L. Dubourg (1999). "Combined liver-kidney transplantation in primary hyperoxaluria type 1." Eur J Pediatr **158**: S75-S80.

Cochat, P. and O. Basmaison (2000). "Current approaches to the management of primary hyperoxaluria." Arch Dis Child **82**: 470-473.

Cochat, P., A. Deloraine, M. Rotily, I. Liponski and N. Deries (1995). "Epidemiology of primary hyperoxaluria type 1." Nephrol Dial Transplant **10**: S3-S7.

Cooper, P., C. Danpure, P. Wise and K. Guttridge (1988). "Immunocytochemical localisation of human hepatic alanine:glyoxylate aminotransferase in control subjects and patients with primary hyperoxaluria type 1." J Histochem Cytochem **36**: 1285-1294.

Cornish-Bowden, A. (1995). Analysis of enzyme kinetic data. New York, Oxford University Press.

Craigen, W. J. (1996). "Persistent glycolic aciduria in a healthy child with normal alanine-glyoxylate aminotransferase activity." J Inher Metab Dis **19**: 793-794.

Cramer, S. D., P. M. Ferree, K. Lin, D. S. Milliner and R. P. Holmes (1999). "The gene encoding hydroxypyruvate reductase (GRHPR) is mutated in patients with primary hyperoxaluria type II." Hum Mol Genet **8**: 2063-2069.

Cramer, S. D., K. Lin and R. P. Holmes (1998). "Towards identification of the gene responsible for primary hyperoxaluria type II. A cDNA encoding human D-glycerate dehydrogenase." J Urol **159**: S661.

Crawhall, J. and R. Watts (1962a). "The metabolism of glyoxylate by human- and rat-liver mitochondria." Biochem J **85**: 163-171.

Crawhall, J. C. and R. W. E. Watts (1962b). "The metabolism of [1-^{14}C] glyoxylate by the liver mitochondria of patients with primary hyperoxaluria and non-hyperoxaluric subjects." Clin Sci **23**: 163-168.

Cregeen, D. and G. Rumsby (1999). "Recent developments in our understanding of primary hyperoxaluria type 2." J Am Soc Nephrol **10**: S348-S350.

Cregeen, D. (2001). Molecular and kinetic analysis of human glyoxylate/ hydroxypyruvate reductase. Molecular Pathology. London, University College London.

Cromartie, T. H. and C. T. Walsh (1975). "Rat kidney L-α-hydroxy acid oxidase: isolation of enzyme with one flavine per two subunits." Biochemistry **14**: 2588-2596.

Daff, S., F. Manson, G. Reid and S. Chapman (1994). "Strategic manipulation of the substrate specificity of *Saccharomyces cerevisiae* flavocytochrome b_2." Biochem J **301**: 829-834.

Danpure, C., P. Jennings, P. Freyer, P. Purdue and J. Allsop (1994a). "Primary hyperoxaluria type 1: Genotypic and phenotypic heterogeneity." J Inherit Metab Dis **17**: 487-499.

Danpure, C. and P. Purdue (1995). "Primary Hyperoxaluria." In: Scriver, C., A. Beaudet, W. Sly and D. Valle editors. The Metabolic and Molecular Bases of Inherited Disease. New York, McGraw-Hill: 2385-2424.

Danpure, C. and G. Rumsby (1995). "Enzymology and Molecular Genetics of Primary Hyperoxaluria Type 1. Consequences for Clinical Management." In: Khan, S. editor Calcium Oxalate In Biological Systems. Boca Raton, CRC Press Inc: 189-205.

Danpure, C. J. (1989). "Recent advances in the understanding, diagnosis and treatment of primary hyperoxaluria type 1." J Inherit Metab Dis **12**: 210-24.

Danpure, C. J. (1991). "Molecular and clinical heterogeneity in primary hyperoxaluria type 1." Am J Kidney Dis **17**: 366-9.

Danpure, C. J., G. M. Birdsey, G. Rumsby, M. J. Lumb, P. E. Purdue and J. Allsop (1994b). "Molecular characterization and clinical use of a polymorphic tandem repeat in an intron of the human alanine:glyoxylate aminotransferase gene." Hum Genet **94**: 55-64.

Danpure, C. J., K. M. Guttridge, P. Fryer, P. R. Jennings, J. Allsop and P. E. Purdue (1990). "Subcellular distribution of hepatic alanine:glyoxylate aminotransferase in various mammalian species." J Cell Sci **97**: 669-678.

Danpure, C. J. and P. R. Jennings (1986). "Peroxisomal alanine:glyoxylate aminotransferase deficiency in primary hyperoxaluria type I." FEBS Lett **201**: 20-4.

Danpure, C. J. and P. R. Jennings (1988). "Further studies on the activity and sub-cellular distribution of alanine:glyoxylate aminotransferase in the livers of patients with primary hyperoxaluria type 1." Clin Sci **75**(3): 315-22.

Danpure, C. J., P. E. Purdue, P. Fryer, S. Griffiths, J. Allsop, M. J. Lumb, K. M. Guttridge, P. R. Jennings, J. I. Scheinman, S. M. Mauer and et al. (1993). "Enzymological and mutational analysis of a complex primary hyperoxaluria type 1 phenotype involving alanine:glyoxylate aminotransferase peroxisome-to-mitochondrion mistargeting and intraperoxisomal aggregation." Am J Hum Genet **53**: 417-32.

Danpure, C. J., P. Purkiss, P. R. Jennings and R. W. E. Watts (1986). "Mitochondrial damage and the subcellular distribution of 2-oxoglutarate:glyoxylate carboligase in normal human and rat liver and in the liver of a patient with primary hyperoxaluria type 1." Clin Sci **70**: 417-425.

Danpure, D. J. (2001). "Primary hyperoxaluria." In: Scriver, C., A. Beaudet, W. Sly and D. Valle editors. The Metabolic and Molecular Bases of Inherited Disease. New York, McGraw-Hill: 3323-3367.

Davis, W., D. Goodman, L. Crawford, O. Cooper and J. Matthews (1990). "Hibernation activates glyoxylate cycle and gluconeogenesis in black bear brown adipose tissue." Biochim Biophys Acta **1051**: 276-278.

Davis, W. L. and D. B. P. Goodman (1992). "Evidence for the glyoxylate cycle in human liver." Anat Rec **234**: 461-468.

Dawkins, P. and F. Dickens (1965). "The oxidation of D- and L-glycerate by rat liver." Biochem J **94**: 353.

De Duve, C. and P. Baudhuin (1966). "Peroxisomes (microbodies and related particles)." Physiol Rev **46**: 323-357.

Dobbins, J. W. and H. J. Binder (1976). "Effect of bile salts and fatty acids on the colonic absorption of oxalate." Gastroenterology **70**: 1096-1100.

Duley, J. A. and R. S. Holmes (1976). "L-alpha-hydroxyacid oxidase isozymes." Eur J Biochem **63**: 163-173.

Duncan, R. J. S. (1980). "The disproportionation of glyoxylate by lactate dehydrogenase." Arch Biochem Biophys **201**: 128-136.

Dupuis, L., J. Caro de, P. Brachet and A. Puigserver (1990). "Purification and some characteristics of chicken liver l-2-hydroxyacid oxidase A." FEBS Lett **266**: 183-186.

Ellis, S., S. Hulton, P. McKiernan, J. de Ville de Goyet and D. Kelly (2001). "Combined liver-kidney transplantation for primary hyperoxaluria type I in young children." Nephrol Dial Transplant **16**: 348-354.

Fell, D. (1997). Understanding the control of metabolism. London, Portland Press Ltd.

Finch, A., G. Kasidas and G. Roase (1981). "Urine composition in normal subjects after oral ingestion of oxalate-rich foods." Clin Sci **60**: 41418.

Fitzpatrick, J. M., G. P. Kasidas and G. A. Rose (1981). "Hyperoxaluria following glycine irrigation for transurethral prostatectomy." Br J Urol **53**: 250-252.

Fraaije, M. W. and A. Mattevi (2000). "Flavoenzymes: diverse catalysts with recurrent features." TIBS **25**: 126 - 132.

Franceschi, V. and H. J. Horner (1980). "Calcium oxalate crystals in plants." Bot Rev **46**: 361-427.

Fry, D. W. and K. E. Richardson (1979a). "Isolation and characterisation of glycolic acid oxidase from human liver." Biochim Biophys Acta **568**: 135-144.

Fry, D. W. and K. E. Richardson (1979b). "Isolation and characterization of glycolic acid dehydrogenase from human liver." Biochim Biophys Acta **567**: 482-491.

Funai, T. and A. Ichiyama (1986). "High-performance liquid chromatographic determination of glyoxylate in rat liver." J Biochem **99**: 579-589.

Gambardella, R. L. and K. E. Richardson (1977). "The pathways of oxalate formation from phenylalanine, tyrosine, tryptophan and ascorbic acid in the rat." Biochim Biophys Acta **499**: 156.

Giegal, D. A., C. H. Williams and V. Massey (1990). "L-lactate 2-monooxygenase from *Mycobacterium smegmatis* cloning, nucleotide sequence and primary structure homology within an enzyme family." J Biol Chem **265**: 6626-6632.

Ghisla, S. and V. Massey (1980). "Studies on the catalytic mechanism of lactate oxidase, formation of enantiomeric flavin-N(5)-glycolate adducts via carbanion intermediates." J Biol Chem **12**: 5688-5696.

Ghisla, S. and V. Massey (1991). "L-Lactate Oxidase." In: Muller, F. editor. Chemistry and biochemistry of the flavoenzymes. Boca Raton, Fl, CRC Press, Inc. **2:** 243-289.

Ghrir, R. and A.-M. Becam (1984). "Primary structure of flavocytochrome b_2 from baker's yeast." Eur J Biochem **139**: 59-74.

Giafi, C. F. and G. Rumsby (1998a). "Kinetic analysis and tissue distribution of human D-glycerate dehydrogenase/glyoxylate reductase and its relevance to the diagnosis of primary hyperoxaluria type 2." Ann Clin Biochem **35**: 104-109.

Giafi, C. F. and G. Rumsby (1998b). "Primary Hyperoxaluria type 2: enzymology." J Nephrol **11**: S29-S31.

Gibbs, A. G. and R. W. E. Watts (1967). "Oxalate formation from glyoxylate in primary hyperoxaluria: studies on liver tissue." Clin Sci **32**: 351-359.

Gibbs, D. and R. Watts (1970). "The action of pyridoxine in primary hyperoxaluria." Clin Sci **38**: 277-286.

Gibbs, D. and R. Watts (1973). "The identification of the enzymes that catalyse the oxidation of glyoxylate to oxalate in the 100,000g supernatant fraction of human hyperoxaluric and control liver and heart tissue." Clin Sci **44**: 227-241.

Gibbs, D. A. and R. W. E. Watts (1966). "An investigation of the possible role of xanthine oxidase in the oxidation of glyoxylate to oxalate." Clin Sci **31**: 285-297.

Giegal, D. A., C. H. Williams and V. Massey (1990). "L-lactate 2-monooxygenase from *Mycobacterium smegmatis*cloning, nucleotide sequence and primary structure homology within an enzyme family." J Biol Chem **265**: 6626-6632.

Gietl, C. (1990). "Glyoxysomal malate dehydrogenase from water melon is synthesised with an amino terminal transit peptide." Proc Natl Acad Sci **87**: 5773 - 5777.

Gondry, M., J. Dubois, M. Terrier and F. Lederer (2001). "The catalytic role of tyrosine 254 in flavocytochrome b_2 (L-lactate dehydrogenase from baker's yeast)." Eur J Biochem **268**: 4918-4927.

Gould, S. J., G. A. Keller, N. Hosken, J. Wilkinson and S. Subramani (1989). "A conserved tripeptide sorts proteins to peroxisomes." J Cell Biol **108**: 1657 - 1664.

Greenfield, N. and R. Pietruszko (1977). "Two aldehyde dehydrogenases from human liver. Isolation via affinify chromatography and characterisation of the isozymes." Biochim Biophys Acta **483**: 35-45.

Gruessner, R. W. (1998). "Pre-emptive liver transplantation from a living related donor for primary hyperoxaluria type 1." N Engl J Med **338**: 1924.

Hahn, R. G. and M. Sikk (1994). "Glycine loading and urinary oxalate excretion." Urol Int **52**: 14-16.

Halestrap, A. and N. Price (1999). "The proton-linked monocarboxylate transporter (MCT) family: structure, function and regulation." Biochem J **343**: 281-299.

Harris, K. S. and K. E. Richardson (1980). "Glycolate in the diet and its conversion to urinary oxalate in the rat." Invest Urol **18**: 106-109.

Hatch, M., R. Freel and N. Vaziri (1999). "Regulatory aspects of oxalate secretion in enteric oxalate elimination." J Am Soc Nephrol **10**: S324-S328.

Hatch, M. and R. W. Freel (1995). "Oxalate transport across intestinal and renal epithelia." In: Khan, S. editor. Calcium oxalate in biological systems. Boca Raton, CRC Press Inc: 217-238.

Hatch, M., R. W. Freel and N. Vaziri (1994). "Intestinal excretion of oxalate in chronic renal failure." J Am Soc Nephrol **5**: 1339-1343.

Hatch, M. and N. D. Vaziri (1994). "Do thiazides reduce intestinal oxalate absorption?: a study using rabbit colon." Clin Sci **86**: 353-357.

Hautman, R. E. (1993). "The stomach: a new and powerful oxalate absorption site in man." J Urol **149**: 1401-1404.

Hess, B., C. Jost, L. Zipperle, R. Takkinen and P. Jaeger (1998). "High-calcium intake abolishes hyperoxaluria and reduces urinary crystallization during a 20-fold normal oxalate load in humans." Nephrol Dial Transplant **13**: 2241-2247.

Hockaday, T. D. R., J. E. Clayton and L. H. J. Smith (1965). "The metabolic error in primary hyperoxaluria." Arch Dis Child **40**: 485-491.

Hodgkinson, A. (1977). Oxalic acid in biology and medicine. London, Academic Press.

Holmes, R. (1998). "Pharmacological approaches in the treatment of primary hyperoxaluria." J Nephrol **11**: S32-S35.

Holmes, R. (2000). "Oxalate synthesis in humans: Assumptions, problems and unresolved issues." Mol Urol **4**: 329-332.

Holmes, R. P. (1993). "The absence of glyoxylate cycle enzymes in rodent and embryonic chick liver." Biochim Biophys Acta **1158**: 47-51.

Holmes, R. P. and D. G. Assimos (1998). "Glyoxylate synthesis, and its modulation and influence on oxalate synthesis." J Urol **160**: 1617-1624.

Holmes, R. P., C. H. Hurst, D. G Assimos and H. O Goodman (1995). "Glucagon increases urinary oxalate excretion in the guinea pig." Am J Physiol **32**: E568-E574.

Holmes, R. P., W. J. Sexton, J. C. Applethwaite, M. Kennedy and D. Assimos (1999). "Glycolate metabolism by HepG2 cells." J Am Soc Nephrol **10**: S345-S347.

Hoppe, B., A. Hesse, S. Bromme, E. Rietschel and D. Michalk (1998). "Urinary excretion substances in patients with cystic fibrosis: risk of urolithiasis?" Pediatr Nephrol **12**: 275-279.

Hustad, S., M. McKinley, H. McNulty, J. Schneede, J. Strain, J. Scott and P. Ueland (2002). "Riboflavin, flavin mononucleotide and flavin dinucelotide in human plasma and erythrocytes at baseline and after low dose riboflavin supplementation." Clin Chem **48**: 1571-1577.

Hylander, E., S. Jarnum and J. Jensen (1978). "Enteric Hyperoxaluria: Dependence on small intestinal resection, colectomy and steatorrhoea in chronic inflammatory bowel disease." Scand J Gastroenterol **13**: 577-588.

Illais, R., R. Sinclair, D. Robertson, A. Neu, S. Chapman and G. Reid (1998). "L-mandelate dehydrogenase from *Rhodotorula graminis*: cloning, sequencing and kinetic characterisation of the recombinant enzyme and its independently expressed flavin domain." Biochem J **333**: 107-115.

Jacobsen, D. (1999). "New treatment for ethylene glycol poisoning." N Engl J Med **340**: 879-880.

James, H. M., R. Bais and J. B. Edwards (1982). "Models for the metabolic production of oxalate from xylitol in humans: A role for fructokinase and aldolase." Aust J Exp Biol Med Sci **60**: 117 - 122.

Jamieson, N. (1998). "The results of combined liver/kidney transplantation for primary hyperoxaluria (PH1) 1984-1997. The European PH1 transplant registry report." J Nephrol **11**: S36-S41.

Johnson, S. A., G. Rumsby, D. Cregeen and S. Hulton (2002). "Primary hyperoxaluria type 2 in children." Pediatr Nephrol **17**: 597-601.

Jones, J. M., J. C. Morrell and S. J. Gould (2000). "Identification and characterization of HAOX1, HAOX2 and HAOX3, three human peroxisomal 2-hydroxy acid oxidases." J Biol Chem **275**: 12590-12597.

Kamoda, N., Y. Minatogawa, M. Nakamura, J. Nakanishi, E. Okuno and R. Kido (1980). "The organ distribution of human alanine-2-oxoglutarate aminotransferase and alanine-glyoxylate aminotransferase." Biochem Med **23**: 25.

Karniski, L. P. and P. S. Aronson (1987). "Anion exchange pathways for Cl-transport in rabbit renal microvillus membranes." Am J Physiol **253**: F513.

Kasidas, G. P. and G. A. Rose (1979). "A new enzymatic method for the determination of glycolate in urine and plasma." Clin Chem Acta **96**: 25-36.

Kasidas, G. P., S. Nemat and G. A. Rose (1990). "Plasma oxalate and creatinine and oxalate/creatinine clearance ratios in normal subjects and in primary hyperoxaluria. Evidence for renal hyperoxaluria." Clin Chim Acta **191**: 67-78.

Kasidas, G. P. and G. A. Rose (1980). "Oxalate content of some common foods: determination by an enzymatic method." J Hum Nutr **34**: 255-266.

Kemper, M. J., S. Conrad and D. E. Muller Wiefel (1997). "Primary hyperoxaluria type 2." Eur J Pediatr **156**: 509-12.

Kemper, M. J. and D. E. Muller Wiefel (1996). "Nephrocalcinosis in a patient with primary hyperoxaluria type 2." Pediatr Nephrol **10**: 442-4.

Kenten, R. and P. Mann (1952). "Hydrogen peroxide formation in oxidations catalysed by plant α-hydroxyacid oxidase." Biochem J **52**: 130-134.

Kerr, M. and D. Groves (1975). "Purification and properties of glycolate oxidase from *Pisum Sativum* leaves." Phytochemistry **14**: 359-362.

Kirkby, E. A. and D. J. Pilbeam (1984). "Calcium as plant nutrient." Plant Cell Environ **7**: 397-405.

Kist-van Holthe, J. E., W. Onkenhout and A. J. van der Heijden (2000). "Pyridoxine-responsive nephrocalcinosis and glycolic aciduria in two siblings without hyperoxaluria and with normal alanine:glyoxylate aminotransferase." J Inher Metab Dis **23**: 91-92.

Koch, J. and L. R. Stockstad (1966). "Partial purification of a 2-oxo-glutarate:glyoxylate carboligase from rat liver mitochondria." Biochem Biophys Res Commun **23**: 585-591.

Kohler, S. A., E. Menotti and L. C. Kuhn (1999). "Molecular Cloning of Mouse Glycolate Oxidase." J Biol Chem **274**: 2401 - 2407.

Kopp, N. and E. Leumann (1995). "Changing pattern of primary hyperoxaluria in Switzerland." Nephrol Dial Transplant **10**: 2224-2227.

Kuo, S. and P. S. Aronson (1988). "Oxalate transport via the sulfate/HCO3 exchanger in rabbit renal basolateral membrane vesicles." J Biol Chem **263**: 9710-9717.

Kuo, S. and P. S. Aronson (1996). "Pathways for oxalate transport in rabbit renal microvillus mambrane vesicles." J Biol Chem **271**: 15491-15497.

Lange, M. and M. Malyusz (1994). "Fast method for the simultaneous determination of 2-oxo acids in biological fluids by high performance liquid chromatography." J Chromatogr **662**: 97 - 102.

Latta, K. and J. Brodehl (1990). "Primary hyperoxaluria I." Eur J Pediatr **149**: 518-522.

Le, K. H. Diep. and F. Lederer (1991). "Amino acid sequence of long chain alpha-hydroxy acid oxidase from rat kidney, a member of the family of FMN-dependent alpha-hydroxy acid-oxidising enzymes." J Biol Chem **266**: 20877-20881.

Lehoux, I. and B. Mitra (2000). "Role of arginine 277 in (S)-mandelate dehydrogenase from *Pseudomonas putida* in substrate binding and transition state stabilization." Biochemistry **39**: 10055-10065.

Leiper, J. M., P. B. Oatey and C. J. Danpure (1996). "Inhibition of alanine:glyoxylate aminotransferase 1 dimerization is a prerequisite for its peroxisome-to-mitochondrion mistargeting in primary hyperoxaluria type 1." J Cell Biol **135**: 939-951.

Lennon, G. G., C. Auffray, M. Polymeropoulos and M. B. Soares (1996). "The I.M.A.G.E. Consortium: An integrated molecular analysis of genomes and their expression." Genomics **33**: 151-152.

Leumann, E. (1985). "Primary hyperoxaluria: an important cause of renal failure in infancy." Int J Pediatr Nephrol **6**: 13-16.

Leumann, E. and B. Hoppe (1999). "What is new in primary hyperoxaluria?" Nephrol Dial Transplant **14**: 2556-2558.

Leumann, E. and B. Hoppe (2001). "The Primary Hyperoxalurias." J Am Soc Nephrol **12**: 1986-1993.

Leumann, E., B. Hoppe and T. Neuhaus (1993). "Management of primary hyperoxaluria:efficacy of oral citrate administration." Pediatr Nephrol **7**: 207-211.

Leumann, E., B. Hoppe, T. Neuhaus and N. Blau (1995). "Efficacy of oral citrate administration in primary hyperoxaluria." Nephrol Dial Transplant **10**: S14-S16.

Liao, L. L. and K. E. Richardson (1972). "The metabolism of oxalate precursors in isolated perfused rat liver." Arch Biochem Biophys **153**: 438 - 448.

Liao, L. L. and K. E. Richardson (1973). "The inhibition of oxalate biosynthesis in isolated perfused rat liver." Arch Biochem Biophys **154**: 68-75.

Liao, L. L. and K. E. Richardson (1978). "The synthesis of oxalate from hydroxypyruvate by isolated perfused rat liver. The mechanism of hyperoxaluria in L-glyceric aciduria." Biochim Biophys Acta **538**: 76-86.

Lindqvist, Y. (1989). "Refined structure of spinach glycolate oxidase at 2 A resolution." J Mol Biol **209**: 151-166.

Lindqvist, Y. and C. I. Branden (1989). "The active site of spinach glycolate oxidase." J Biol Chem **264**: 3624-3628.

Lindqvist, Y., C. I. Branden, F. Scott Mathews and F. Lederer (1991). "Spinach glycolate oxidase and yeast flavocytochrome b2 are structurally homologous and evolutionarily related enzymes with distinctly different function and flavin mononucleotide binding." J Biol Chem **266**: 3198-3207.

Lluis, C. and J. Bozal (1977). "Relationship between hydroxypyruvate and the production of oxalate *in vitro*." Biochim Biophys Acta **461**: 209-217.

Lowry, O., N. Rosebrough, A. Farr and R. Randall (1951). "Protein measurement with the Folin-Phenol reagents." J Biol Chem **193**: 265-275.

Ludt, C. and H. Kindl (1990). "Characterisation of a cDNA encoding *Lens culinaris* glycolate oxidase and developmental expression of glycolate oxidase mRNA in cotyledons and leaves." Plant physiol **94**: 1193-1198.

Ludwig, B., E. Schindler, J. Bohl, J. Pfeiffer and G. Kremer (1984). "Renocerebral oxalosis induced by xylitol." Neuroradiology **26**: 517-521.

Lumb, M. J. and C. J. Danpure (2000). "Functional synergism between the most common polymorphism in human alanine:glyoxylate aminotransferase and four of the most common disease causing mutations." J Biol Chem **275**: 36415-36422.

Macheroux, P., V. Massey, D. J. Thiele and M. Volokita (1991). "Expression of Spinach Glycolate Oxidase in *Saccharomyces cerevisiae*: Purification and Characterisation." Biochemistry **30**: 4612 - 4619.

Macheroux, P., V. Kieweg, V. Massey, E. Soderland, K. Stenberg and Y. Lindquist (1993). "Role of tyrosine 129 in the active site of spinach glycolate oxidase." Eur J Biochem **213**: 1047-1054.

Maitra, U. and E. E. Dekker (1964). "Purification and properties of rat liver 2-keto-4-hydroxyglutarate aldolase." J Biol Chem **239**: 1485.

Mansell, M. A. (1995). "Primary hyperoxaluria type 2." Nephrol Dial Transplant **10**: S58-S60.

Marangella, M. (1999). "Transplantation strategies in type 1 primary hyperoxaluria:the issue of pyridoxine responsiveness." Nephrol Dial Transplant **14**: 301-303.

Marangella, M., M. Petrarulo, D. Cosseddu, C. Vitale, A. Cadario, M. Portigliatti Barbos, L. Gurioli and F. Linari (1995). "Detection of primary hyperoxaluria type 2 (L-glyceric aciduria) in patients with end stage renal failure." Nephrol Dial Transplant **10**: 1381-1385.

Massey, V., S. Ghisla and K. Kieschke (1980). "Studies on the reaction mechanism of lactate oxidase, formation of two covalent flavin-substrate adducts on reaction with glycollate." J Biol Chem **255**: 2796-2806.

Massey, V. and P. Hemerich (1980). "Active-site probes of flavoproteins." Biochem Soc Trans **8**: 246-257.

Masters, C. (1997). "Gluconeogenesis and the peroxisome." Mol Cell Biochem **166**: 159-168.

Mazze, R. I., J. R. Trudell and M. J. Cousins (1971). "Methoxyflurane metabolism and renal dysfunction:clinical correlation in man." Anesthesiology **35**: 247-252.

McGroarty, E., B. Hsieh, D. M. Wied, R. Gee and N. E. Tolbert (1974). "Alpha hydroxy acid oxidation by peroxisomes." Arch Biochem Biophys **161**: 194-210.

Meyers, R. D. and M. Schuman Jorns (1981). "Identification of the factor responsible for autogenous bleaching of glycollate oxidase." Biochim Biophys Acta **657**: 438-447.

Milliner, D., D. Wilson and L. Smith (1998). "Clinical expression and long-term outcomes of primary hyperoxaluria types 1 and 2." J Nephrol **11**: S56-S59.

Milliner, D., D. Wilson and L. Smith (2001). "Phenotypic expression of primary hyperoxaluria: Comparative features of types I and II." Kidney Int **59**: 31-36.

Milliner, D. S., J. T. Eickholt, E. J. Bergstralh, D. M. Wilson and L. H. Smith (1994). "Results of long-term treatment with orthophosphate and pyridoxine in patients with primary hyperoxaluria." N Engl J Med **331**: 1553-8.

Mistry, J., C. J. Danpure and R. A. Chalmers (1988). "Hepatic D-glycerate dehydrogenase and glyoxylate reductase deficiency in primary hyperoxaluria type 2." Biochem Soc Trans **16**: 626-627.

Monico, C. G. and D. S. Milliner (1999). "Hyperoxaluria and urolithiasis in young children:an atypical presentation." J Endourol **13**: 633-636.

Monico, C. G., M. Persson, C. H. Ford, G. Rumsby and D. S. Milliner (2002). "Potential mechanisms of marked hyperoxaluria not due to primary hyperoxaluria I or II." Kidney Int **62**: 392-400.

Morris, M. and J. Garcia-Rivera (1955). "The destruction of oxalates by the rumen contents of cows." J Dairy Sci **38**: 1169.

Mowat, C., I. Beaudoin, R. Durley, J. Barton, A. Pike, Z. Chen, G. Reid, S. Chapman, F. Mathews and F. Lederer (2000). "Kinetic and crystallographic studies on the active site arg289lys mutant of flavocytochrome b_2 (yeast L-lactate dehydrogenase)." Biochemistry **39**: 3266-3275.

Muh, U., V. Massey and C. Williams (1994a). "Lactate monooxygenase I. Expression of the mycobacterial gene in *Escherichia coli* and site directed mutagenesis." J Biol Chem **269**: 7982-7988.

Muh, U., C. Williams and V. Massey (1994b). "Lactate Monooxygenase II. Site-directed mutagenesis of the postulated active site base histidine 290." J Biol Chem **269**: 7989-7993.

Muh, U., C. Williams and V. Massey (1994c). "Lactate Monooxygenase III. Additive contributions of active site residues to catalytic efficiency and stabilisation of an anionic transition state." J Biol Chem **269**: 7994-8000.

Nakano, M., Y. Tsutsumi and T. S. Danowski (1967). "Crystalline L-amino acid oxidase from the souble fraction of rat kidney cells." Biochem Biophys Acta **139**: 40-48.

Neims, A. H. and L. Hellerman (1962). "Specificity of the D-amino acid oxidase in relation to glycine oxidase activity." J Biol Chem **237**: 976-978.

Neuhaus, T. J., T. Belzer, N. Blau, B. Hoppe, H. Sidhu and E. Leumann (2000). "Urinary oxalate excretion in urolithiasis and nephrocalcinosis." Arch Dis Child **82**: 322-326.

Nishimura, M., Y. D. Akhmedov, K. Strzalka and T. Akazawa (1983). "Purification and characterisation of glycolate oxidase from pumpkin cotyledons." Arch Biochem Biophys **222**: 397 - 402.

Noguchi, T., E. Okuno, Y. Takada and e. al (1978). "Characteristics of hepatic alanine-glyoxylate aminotransferase in different mammalian species." Biochem J **169**: 113-122.

Noguchi, T. and Y. Takada (1978). "Peroxisomal localization of serine:pyruvate aminotransferase in human liver." J Biol Chem **253**: 7598-7600.

Noguchi, T. and Y. Takada (1979). "Peroxisomal localization of alanine:glyoxylate aminotransferase in human liver." Arch Biochem Biophys **196**: 645-647.

Noguchi, T., Y. Takada and Y. Oota (1979). "Intraperoxisomal and intramitochondrial localization, and assay of pyruvate (glyoxylate) aminotransferase from rat liver." Hoppe-Seyl Z **360**: 919-927.

Oda, T., M. Yanagisawa and A. Ichiyama (1982). "Induction of serum: pyruvate aminotransferase in rat liver organelles by glucagon and a high-protein diet." J Biochem Tokyo **91**: 219-32.

Okuno, E., Y. Minatogawa, J. Nakanishi, M. Namkamura, N. Kamoda, M. Makino and R. Kido (1979). "The subcellular distribution of alanine-glyoxylate aminotransferase and serine-pyruvate aminotransferase in dog liver." Biochem J **182**: 877-879.

Petrarulo, M., M. Marangella, D. Cosseddu and F. Linari (1992). "High-peformance liquid chromatogrphic assay for L-glyceric acid in body fluids. Application in primary hyperoxaluria type 2." Clin Chem Acta **211**: 143-153.

Petrarulo, M., M. Marangella and F. Linari (1991). "High performance liquid chromatographic determination of plasma glycolic acid in healthy subjects and in cases of hyperoxaluria syndromes." Clin Chem Acta **196**: 17-26.

Petrarulo, M., S. Pellegrino, O. Bianco, M. Marangella and F. Linari (1988). "High-performance liquid chromatographic determination of glyoxylic acid in urine." J Chromatogr **432**: 37-46.

Pfeiffer, J., E. Danner and P. F. Schmidt (1984). "Oxalate-induced encephalitic reactions to polyol-containing infusions during intensive care." Clin Neuropathol **3**: 76-87.

Poore, E. R., C. H. Hurst, D. G. Assimos and R. P. Holmes (1997). "Pathways of hepatic oxalate synthesis and their regulation." Am J Physiol **272**: C289.

Popov, V., S. Volvenkin, A. Eprintsev and A. Igambirdiev (1998). "Glyoxylate cycle enzymes are present in liver peroxisomes of alloxan-treated rats." FEBS Lett **440**: 55-58.

Popov, V. N., A. U. Igamberdiev, C. Schnarrenberger and S. V. Volvenkin (1996). "Induction of glyoxylate cycle enzymes in rat liver upon food starvation." FEBS lett **390**: 258-260.

Preisig-Muller, R. and H. Kindl (1993). "Thiolase mRNA translated *in vitro* yields a peptide with a putative N-terminal presequence." Plant Mol Biol **22**: 59 - 66.

Prenan, J. A. C., E. Boer, E. J. Dorhaut Mees and e. al. (1981). "Determination of oxalic acid clearance and plasma concentration by radioisotope infusion." Acta Med Scand **209**: 87-91.

Purdue, P. E., Y. Takada and C. J. Danpure (1990). "Identification of mutations associated with peroxisome-to-mitochondrion mistargeting of alanine/glyoxylate aminotransferase in primary hyperoxaluria type 1." J Cell Biol **111**: 2341-2351.

Raghavan, K. G., K. M. Lathika, N. M. Gandhi, S. J. D. Souza, U. Tarachand, V. Ramakrishnan and B. B. Singh (1997). "Biogenesis of l-glyceric aciduria, oxalosis and renal injury in rats simulating type 2 primary hyperoxaluria." Biochim Biophys Acta **1362**: 97 - 102.

Recalcati, S., E. Menoti and L. C. Kuhn (2000). "Peroxisomal targeting of mammalian hydroxyacid oxidase 1 requires the C-terminal tripeptide SKI." J Cell Sci **114**: 1625-1629.

Reid, G., S. White, M. Black, F. Lederer and F. S. Mathews (1988). "Probing the active site of flavocytochrome b_2 by site directed mutagenesis." Eur J Biochem **178**: 329-333.

Reumann, S., E. Maier, R. Benz and H. Heldt (1995). "The membrane of leaf peroxisomes contains a porin-like channel." J Biol Chem **270**: 17559-17565.

Reumann, S., E. Maier, H. Heldt and R. Benz (1998). "Permeability properties of the porin of spinach leaf peroxisomes." Eur J Biochem **251**: 359-366.

Richardson, K. E. (1964). "Effect of testosterone on the glycolic acid oxidase levels in male and female rat liver." Endocrinology **74**: 128.

Richardson, K. E. and N. E. Tolbert (1961). "Oxidation of glyoxylic acid to oxalic acid by glycolic acid oxidase." J Biol Chem **236**: 1280-1284.

Robertson, W. (1993). "Urinary tract calculi." In: Nordin, B., A. Need and H. Morris editors. Metabolic Bone and Stone Disease. Edinburgh, Churchill Livingstone: 249.

Robertson, W. G. (1990). "Epidemiology of urinary stone disease." Urol Res **18**: S3-S8.

Robertson, W. G., M. Peacock, P. J. Heyburn, F. A. Hanes, A. Rutherford, E. Clementson, R. Swaminathan and P. B. Clark (1979). "Should recurrent calcium oxalate stone formers become vegetarians?" Br J Urol **51**: 427-431.

Rofe, A., H. James, R. Bais and R. Conyers (1986). "Hepatic oxalate production: the role of hydroxypyruvate." Biochem Med Metab Biol **36**: 141-150.

Rouviere, N., M. Mayer, M. Tegoni, C. Capeillere-Blandin and F. Lederer (1997). "Molecular interpretation of inhibition by excess substrate in flavocytochrome b_2: A study with wild-type and Y143F mutant enzymes." Biochemistry **36**: 7126-7135.

Rumsby, G. and D. Cregeen (1999). "Identification and expression of a cDNA for human hydroxypyruvate/glyoxylate reductase." Biochim Biophys Acta **1446**: 383-388.

Rumsby, G., A. Sharma, D. Cregeen and L. Solomon (2001). "Primary hyperoxaluria type 2 without L-glyceric aciduria: is the disease under-diagnosed?" Nephrol Dial Transplant **16**: 1697-1699.

Rumsby, G., T. Weir and C. T. Samuell (1997). "A semiautomated alanine:glyoxylate aminotransferase assay for the tissue diagnosis of primary hyperoxaluria type 1." Ann Clin Biochem **34**: 400-404.

Sambrook, J., E. F. Fritsch and T. Maniatis (1989). Molecular cloning: A laboratory manual. NY, Cold Spring Harbour Laboratory Press, Cold Spring Harbour.

Samuell, C. T. and G. P. Kasidas (1995). "Biochemical investigations in renal stone formers." Ann Clin Biochem **32**: 112-122.

Sawaki, S., H. Hattori and K. Yamada (1967). "Glyoxylate dehydrogenase activity of lactate dehydrogenase." J Biochem **62**: 263-268.

Schuman, M. and V. Massey (1971a). "Purification and characterisation of glycolic acid oxidase from pig liver." Biochim Biophys Acta **227**: 500 - 520.

Schuman, M. and V. Massey (1971b). "Effect of anions on the catalytic activity of pig liver glycolic acid oxidase." Biochim Biophys Acta **227**: 521-537.

Schwam, H., S. Mitchelson, W. C. Randall, J. M. Sondey and R. Hirschmann (1979). "Purification and characterisation of human liver glycolate oxidase. Molecular weight, subunit, and kinetic properties." Biochemistry **18**: 2828-2833.

Seargeant, L. E., G. W. deGroot, L. A. Dilling, C. J. Mallory and J. C. Haworth (1991). "Primary oxaluria type 2 (L-glyceric aciduria): a rare cause of nephrolithiasis in children." J Pediatr **118**: 912-4.

Sharma, V. and P. O. Schwille (1997). "Clofibrate feeding to Sprague-Dawley rats increases endogenous biosynthesis of oxalate and causes hyperoxaluria." Metabolism **46**: 135-9.

Sidhu, H., B. Hoppe, A. Hesse, K. Tenbrock, S. Bromme, E. Rietschel and A. B. Peck (1998). "Absence of *Oxalobacter formigenes* in cystic fibrosis patients: a risk factor for hyperoxaluria." Lancet **352**: 1026-1029.

Sinclair, R., G. A. Reid and S. K. Chapman (1998). "Re-design of *Saccharomyces cerevisiae* flavocytochrome b2: introduction of L-mandelate dehydrogenase activity." Biochem J **333**: 117-120.

Snyder, L., J. Kirkland and J. Glajch (1997). Practical HPLC method development. New York, Wiley Interscience.

Stenberg, K., T. Clausen, Y. Lindqvist and P. Macheroux (1995). "Involvement of Tyr24 and Trp108 in substrate binding and substrate specificity of glycolate oxidase." Eur J Biochem **228**: 408-16.

Swinkels, B. W., S. J. Gould, A. G. Bodnar, R. A. Rachubinski and S. Subramani (1991). "A novel, cleavable peroxisomal targeting signal at the amino-terminus of the rat 3-ketoacyl-CoA thiolase." EMBO J **10**: 3255-3262.

Takada, Y., N. Kaneko, H. Esumi, P. E. Purdue and C. J. Danpure (1990). "Human peroxisomal L-alanine:glyoxylate aminotransferase:evolutionary loss of a mitochondrial targeting signal by point mutation of the initiation codon." Biochem J **268**: 517-520.

Tarn, A. C., C. von Schnakenburg and G. Rumsby (1997). "Primary hyperoxaluria type 1: diagnostic relevance of mutations and polymorphisms in the alanine:glyoxylate aminotransferase gene (AGXT)." J Inherit Metab Dis **20**: 689-96.

Thomas, D. W., J. B. Edwards, J. R. Gilligan, J. R. Lawrence and R. G. Edwards (1972). "Complications following intravenous administration of solutions containing xylitol." Med J Aus **1**: 1238-1246.

Thompson, J. and K. Richardson (1967). "Isolation and characterisation of an L-alanine:glyoxylate aminotransferase from human liver." J Biol Chem **242**: 3614-3619.

Thompson, J. S. and K. E. Richardson (1966). "Isolation and characterization of a glutamate-glycine transaminase from human liver." Arch Biochem Biophys **117**: 599-603.

Tokushige, M. and I. W. Sizer (1967). "Glycolate oxidase of hog kidney." J Biochem **62**: 719-725.

Tolbert, N. E. (1981). "Metabolic pathways in peroxisomes and glyoxysomes." Ann Rev Biochem **50**: 133-157.

Tsou, A., S. Ransom, J. Gerlt, D. Buechter, P. Babbitt and G. Kenyon (1990). "Mandelate pathway of *pseudomonas putida*: Sequence relationships involving mandelate racemase, (S)-mandelate dehydrogenase, and benzoylformate decarboxylase and expression of benzoylformate decarboxylase in *Escherichia coli.*" Biochemistry **29**: 9856-9862.

Urban, P. and F. Lederer (1985). "Intermolecular hydrogen transfer catalysed by a flavodehydrogenase, baker's yeast flavocytochrome b2." J Biol Chem **260**: 11115-11122.

Ushijima, Y. (1973). "Identity of aliphatic L-α-hydroxyacid oxidase and glycolate oxidase." Arch Biochem Biophys **155**: 361-7.

Vamecq, J. and J.-P. Draye (1989). "Pathophysiology of peroxisomal beta-oxidation." Essays in Biochem **24**: 115.

Van Acker, K. J., F. J. Eyskens, M. F. Espeel, R. J. A. Wanders, C. Dekker, I. O. Kerckaert and F. Roels (1996). "Hyperoxaluria with hyperglycoluria not due to alanine:glyoxylate aminotransferase defect: A novel type of primary hyperoxaluria." Kidney Int **50**: 1747-1752.

Van Schaftingen, E. (1989). "D-glycerate kinase deficiency as a cause of D-glyceric aciduria." FEBS Lett **243**: 127.

Van Schaftingen, E., J.-P. Draye and F. V. Van Hoof (1989). "Coenzyme specificity of mammalian liver D-glycerate dehydrogenase." Eur J Biochem **186**: 355-359.

Vandor, S. L. and N. E. Tolbert (1970). "Glyoxylate metabolism by isolated rat liver peroxisomes." Biochim Biophys Acta **215**: 449-55.

Verkoelen, C. F. and J. C. Romijn (1996). "Oxalate transport and calcium oxalate renal stone disease [editorial]." Urol Res **24**: 183-91.

Vilarinho, L., R. Araujo, A. Vilarinho, E. Pereira, K. Abdo, J. Bardet, P. Parvy and D. Rabier (1993). "A new case of hyperoxaluria type II." J Inherit Metab Dis **16**: 896-7.

Volokita, M. and C. R. Somerville (1987). "The primary structure of spinach glycolate oxidase deduced from the DNA sequence of a cDNA clone." J Biol Chem **262**: 15825-15828.

Wanders, R. J., C. W. van Roermund, M. Griffioen and L. Cohen (1991). "Peroxisomal enzyme activities in the human hepatoblastoma cell line HepG2 as compared to human liver." Biochim Biophys Acta **1115**: 54-9.

Wandzilak, T. and H. Williams (1990). "The Hyperoxaluria Syndromes." In: Smith, L. editor. Endocrinology and Metabolism Clinics of North America. Philadelphia, WB Saunders. **19:** 851-867.

Warren, W. A. (1970). "Catalysis of both oxidation and reduction of glyoxylate by pig heart lactate dehydrogenase isoenzyme 1." J Biol Chem **245**: 1675-1681.

Watts, R. (1994a). "Primary hyperoxaluria type 1." Q J Med **87**: 593-600.

Watts, R. (1998). "The clinical spectrum of the primary hyperoxalurias and their treatment." J Nephrol **11**: S4-S7.

Watts, R. W., R. Y. Calne, K. Rolles, C. J. Danpure, S. H. Morgan, M. A. Mansell, R. Williams and P. Purkiss (1987). "Successful treatment of primary hyperoxaluria type I by combined hepatic and renal transplantation." Lancet **2**: 474-5.

Watts, R. W. E. (1994b). "Treatment of primary hyperoxaluria type 1." J Nephrol **7**: 208-214.

Webster, K., P. Ferree, R. Holmes and S. Cramer (2000). "Identification of missense, nonsense and deletion mutations in the GRHPR gene in patients with primary hyperoxaluria type II (PH2)." Hum Genet **107**: 176-185.

Whitby, L. (1953). "A new method for preparing flavin-adenine dinucleotide." Biochem J **54**: 437-442.

Williams, A. W. and D. M. Wilson (1990). "Dietary intake, absorption, metabolism and excretion of oxalate." Seminars in Nephrol **10**: 2-8.

Williams, H. and L. J. Smith (1968a). "L-glyceric aciduria. A new genetic variant of primary hyperoxaluria." N Engl J Med **278**: 233-239.

Williams, H. and T. Wandzilak (1989). "Oxalate synthesis, transport and the hyperoxaluric syndromes." J Urol **141**: 742-749.

Williams, H. E., G. A. Johnson and L. H. Smith (1971). "The renal clearance of oxalate in normal subjects and patients with primary hyperoxaluria." Clin Sci **41**: 213-218.

Williams, H. and L. J. Smith (1983). "Primary hyperoxaluria." In: Stanbury, J., J.

Wyngaarden, D. Fredrickson, J. Goldstein and M. Brown Editors. The Metabolic Basis of Inherited Disease. New York, McGraw-Hill**:** 204.

Williams, H. E. and J. R. Smith (1968b). "The identification and determination of glyceric acid in human urine." J Lab Clin Med **71**: 495-500.

Williams, H. E. and L. H. Smith (1971). "Hyperoxaluria in L-glyceric aciduria: Possible pathogenic mechanism." Science **171**: 390-391.

Williamson, D. and J. Brosnan (1974). "Concentrations of metabolites in animal tissues." In: Bergmeyer, H. editor. Methods of Enzymatic Analysis. New York, London, Academic Press. **4:** 2266-2302.

Willis, J. E. and H. J. Sallach (1962). "Evidence for a mammalian D-glyceric acid dehydrogenase." J Biol Chem **237**: 910-915.

Wise, P. J., C. J. Danpure and P. R. Jennings (1987). "Immunological heterogeneity of hepatic alanine:glyoxylate aminotransferase in primary hyperoxaluria type 1." FEBS Lett **222**: 17-20.

Wulkan, R., R. Verwers, M. Neele and M. Mantel (2001). "Measurement of pyruvate in blood by high-performance liquid chromatography with flourescence detection." Ann Clin Biochem **38**: 554-558.

Wyngaarden, J. and T. Elder (1966). "Primary Hyperoxaluria and oxalosis." In: Stanbury, J., J. Wyngaarden and D. Fredrickson editors. The Metabolic Basis of Inherited Disease. New York, McGraw-Hill**:** 189-212.

Xia, Z.-x. and F. Mathews (1990). "Molecular structure of flavocytochrome b2 at 2.4 angstrom resolution." J Mol Biol **212**: 837-863.

Xu, Y. and B. Mitra (1999). "A highly active, soluble mutant of the membrane associated (S)-mandelate dehydrogenase from *Pseudomonas putida*." Biochemistry **38**: 12367-12376.

Xue, H., T. Sakaguchi, M. Fujie, H. Ogawa and A. Ichiyama (1999). "Flux of the L-serine metabolism in rabbit, human and dog livers. Substantial contributions of both mitochondrial and peroxisomal serine:pyruvate/alanine:glyoxylate aminotransferase." J Biol Chem **274**: 16028-16033.

Yanagawa, M., E. Maeda-Nakai, K. Yamakawa, I. Yamamoto, J. Kawamura, S. Tada and A. Ichiyama (1990). "The formation of oxalate from glycolate in rat and human liver." Biochim Biophys Acta **1036**: 24-33.

Yoshihara, H., S. Yamaguchi and S. Yachiku (1999). "Effect of sex hormones on oxalate-synthesizing enzymes in male and female rat livers." J Urol **161**: 668 - 673.

Zelitch, I. and S. Ochoa (1953). "Oxidation and reduction of glycolic acids in plants. I Glycolic acid oxidase." J Biol Chem **201**: 707-718.

Zhang, X., S. M. Roe, L. H. Pearl and C. J. Danpure (2001). "Crystallization and preliminary crystallographic analysis of human alanine:glyoxylate aminotransferase and its polymorphic variants." Acta Cryst **D57**: 1936-1937.

Appendices

Appendix 1 – Oligonucleotide primer sequences and PCR conditions

Primers were synthesised to order by Sigma Genosys Biotechnologies (Pampisford, UK).

Primer	Primer sequence	Extension time (secs)	Annealing temp. (°C)
RT-PCR to produce HAO1 cDNA			
GO1	5'AACTGCAGTGAAAATGCTCCCCC	90	66
GO2	5' TCAAGCTTTGTGCACTGTCAGAT		
3' RACE to produce 3'UTR			
GSP1A	5' CTGAGTGGGTGCCAGAATGTG	45	58
AUAP	5' GGCCACGCGTCGACTAGTAC		
GSP2A	5' AAAGTCATCGACAAGACATTG	45	55
AUAP	5' GGCCACGCGTCGACTAGTAC		
5'RACE to produce 5'UTR			
AAP	5' GGCCACGCGTCGACTAGTACG IIGGGIIGGGIIG	30	58
GSP2B	5' GCAACATTCCGGAGCATCCT		
AUAP	5' GGCCACGCGTCGACTAGTAC	30	58
GSP3B	5' CATCATTTGCCCCAGACCTGTA		

PCR reactions were carried out in an OmniGene thermal cycler (Hybaid, Ashford, UK)

The PCR conditions were as follows:

3 minutes denaturation at 94°C

30 cycles of:

10 seconds denaturation at 94°C

10 seconds annealing at temperature listed above

30-90 seconds extension at 72°C

7 minutes extension at 72°C

Appendix 2 – Calibration curves

a) Standard curve for determination of protein concentration (mg/ml) by the Lowry assay

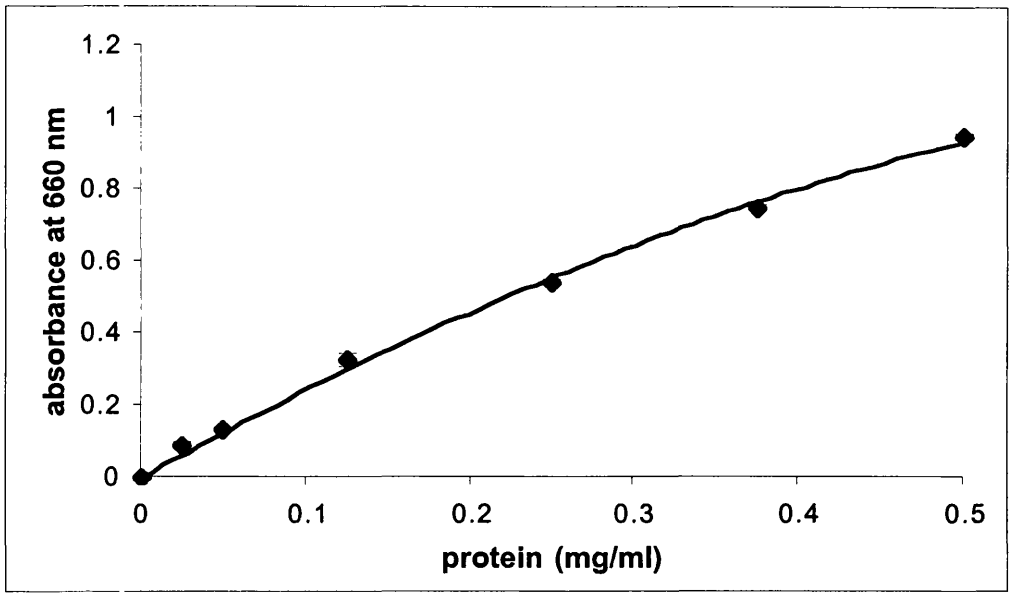

b) Calibration curve for determining the size of transcript observed in northern blot

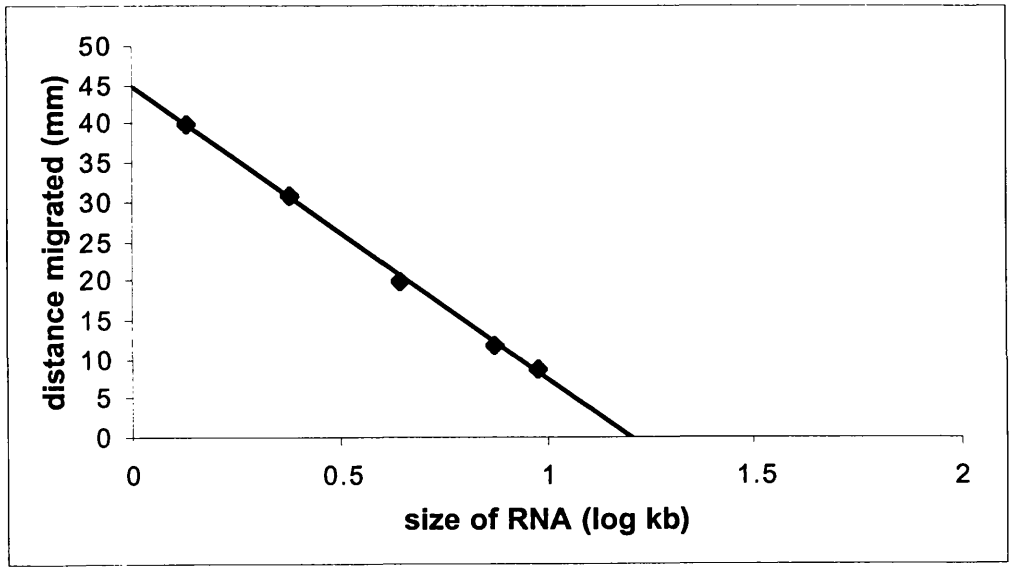

c) Calibration curve for determining size of protein bands seen in SDS-PAGE gels

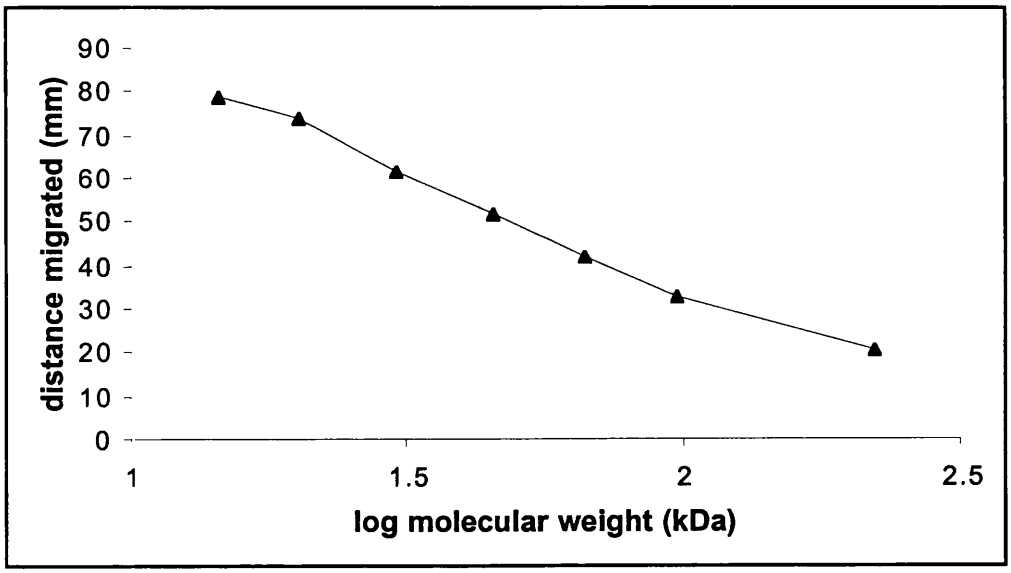

Appendix 3 – cDNA, EST and protein sequences

a) Human cDNA with peptide sequence similarity to *Arabidopsis thaliana*
Accession number T64673

Insert size 1176, high quality sequence stops at base 333

```
1    ataaccttgt gaaaatgctc ccccggctaa tttgtatcaa tgattatgaa
51   caacatgcta aatcagtact tccaaagtct atatatgact attacaggtc
101  tggggcaaat gatgaagaaa ctttggctga taatattgca gcattttcca
151  gatggaagct gtatccaagg atgctccgga atgttgctga aacagatctg
201  tcgacttctg ttttaggaca gagggtcagc atgccaatat gtgtgggggc
251  tacggcattg cagcgcngcc taatngtggg acggcgagct tgccactgtg
301  aggagcctgt cagtccctgg ggaacgggca tgatgttgag ttcctggggc
351  cacctcctcc aatttgaagg aagttngccg g
```

b) Longer length human cDNA identified by screening of EST database
Accession number T74667

Insert size 1195, high quality sequence stops at base 264

```
1    tgggatagca ataaccttgt gaaaatgctc ccccggctaa tttgtatcaa
51   tgattatgaa caacatgcta aatcagtact tccaaagtct atatatgact
101  attacaggtc tggggcaaat gatgaagaaa ctttggctga taatattgca
151  gcattttcca gatggaagct gtatccaagg atgctccgga atgttgctga
201  aacagatctg tcgacttctg ttttaggaca gagggtcagc atgccaatat
251  gtgtgggggc tacggcatgc agcgngttcn aattgttggg acggcgagct
301  ttccnggggn caactnctca attgaaggag ttgccggaa
```

c) Full length cDNA sequence of longer length clone T74667

```
1    tgggatagca ataaccttgt gaaaatgctc ccccggctaa tttgtatcaa
51   tgattatgaa caacatgcta aatcagtact tccaaagtct atatatgact
101  attacaggtc tggggcaaat gatgaagaaa ctttggctga taatattgca
151  gcattttcca gatggaagct gtatccaagg atgctccgga atgttgctga
201  aacagatctg tcgacttctg ttttaggaca gagggtcagc atgccaatat
251  gtgtgggggc tacggccatg cagcgcatgg ctcatgtgga cggcgagctt
301  gccactgtga gagcctgtca gtccctggga acgggcatga tgttgagttc
351  ctgggccacc tcctcaattg aagaagtggc ggaagctggt cctgaggcac
401  ttcgttggct gcaactgtat atctacaagg accgagaagt caccaagaag
451  ctagtgcggc aggcagagaa gatgggctac aaggccatat ttgtgacagt
501  ggacacacct tacctgggca accgtctgga tgatgtgcgt aacagattca
551  aactgccgcc acaactcagg atgaaaaatt ttgaaaccag tactttatca
601  ttttctcctg aggaaaattt tggagacgac agtggacttg ctgcatatgt
651  ggctaaagca atagacccat ctatcagctg ggaagatatc aaatggctga
701  gaagactgac atcattgcca attgttgcaa agggcatttt gagagggtga
751  tgatgccagg gaggctgtta aacatggctt gaatgggatc ttggtgtcga
801  atcatggggc tcgacaactc gatggggtgc cagccactat tgatgttctg
851  ccagaaattg tggaggctgt ggaagggaag gtggaagtct ttcctggacg
901  ggggtgtgcg gaaaggcact gatgttctga aagctctggc tcttggcgcc
1001 aaggctgtgt ttgtggggag accaatcgtt tggggctta
```

d) tblast of full length T74667 to show similarity to spinach GO

```
Query: T74667
Sbjct: P05414 GOX_SPIOL (S)-2-hydroxy-acid oxidase, peroxisomal (GOX)
Identity 54%

Query: 45  INDYEQHAKSVLPKSIYDYYRSGANDEETLADNIAAFSRWKLYPRMLRNVAETDLSTSVL
           +N+YE  AK  LPK +YDYY SGA D+ TLA+N  AFSR    PR+L +V   D++T++L
Sbjct: 6   VNEYEAIAKQKLPKMVYDYYASGAEDQWTLAENRNAFSRILFRPRILIDVTNIDMTTTIL

Query: 225 GQRVSMPICVGATAMQRMAHVDGELATVRACQSLGTGMMLSSWATSSIEEVAEAGPEALR
           G ++SMPI +  TAMQ+MAH +GE AT RA  + GT M LSSWATSS+EEVA  GP  +R
Sbjct: 66  GFKISMPIMIAPTAMQKMAHPEGEYATARAASAAGTIMTLSSWATSSVEEVASTGP-GIR

Query: 405 WLQLYIYKDREVTKKLVRQAEKMGYKAIFVTVDTPYLGNRLDDVRNRFKLPPQLRMKNFE
           + QLY+YKDR V  +LVR+AE+ G+KAI +TVDTP LG R  D++NRF LPP L +KNFE
Sbjct: 125 FFQLYVYKDRNVVAQLVRRAERAGFKAIALTVDTPRLGRREADIKNRFVLPPFLTLKNFE

Query: 585 TSTLSFSPEENFGDDSGLAAYVAKAIDPSISWEDIKWLRRLTSLPIVAKGILRGDDAREA
              L    + N   DSGL++YVA  ID S+SW+D+ WL+ +TSLPI+ KG++  +DAR A
Sbjct: 185 GIDLGKMDKAN---DSGLSSYVAGQIDRSLSWKDVAWLQTITSLPILVKGVITAEDARLA

Query: 765 VKHGLNGILVSNHGARQLDGVPATIDVLPEIVEAVEGKVEVFLDGGVRKGTDXXXXXXXX
           V+HG  GI+VSNHGARQLD VPATI  L E+V+A +G++ VFLDGGVR+GTD
Sbjct: 242 VQHGAAGIIVSNHGARQLDYVPATIMALEEVVKAAQGRIPVFLDGGVRRGTDVFKALALG

Query: 945 XXXXXXXRPIVWGL
                 RP+V+ L
Sbjct: 302 AAGVFIGRPVVFSL
```

e) Full length cDNA sequence of clone AB024079 identified by BLAST search

```
   1 atgctccccc ggctaatttg tatcaatgat tatgaacaac atgctaaatc agtacttcca
  61 aagtctatat atgactatta caggtctggg gcaaatgatg aagaaacttt ggctgataat
 121 attgcagcat tttccagatg gaagctgtat ccaaggatgc tccggaatgt tgctgaaaca
 181 gatctgtcga cttctgtttt aggacagagg gtcagcatgc caatatgtgt gggggctacg
 241 gccatgcagc gcatggctca tgtggacggc gagcttgcca ctgtgagagc ctgtcagtcc
 301 ctgggaacgg gcatgatgtt gagttcctgg gccacctcct caattgaaga agtggcggaa
 361 gctggtcctg aggcacttcg ttggctgcaa ctgtatatct acaaggaccg agaagtcacc
 421 aagaagctag tgcggcaggc agagaagatg ggctacaagg ccatatttgt gacagtggac
 481 acaccttacc tgggcaaccg tctggatgat gtgcgtaaca gattcaaact gccgccacaa
 541 ctcaggatga aaaattttga aaccagtact ttatcatttt ctcctgagga aaattttgga
 601 gacgacagtg gacttgctgc atatgtggct aaagcaatag acccatctat cagctgggaa
 661 gatatcaaat ggctgagaag actgacatca ttgccaattg ttgcaaaggg cattttgaga
 721 ggtgatgatg ccagggaggc tgttaaacat ggcttgaatg ggatcttggt gtcgaatcat
 781 ggggctcgac aactcgatgg ggtgccagcc actattgatg ttctgccaga aattgtggag
 841 gctgtggaag ggaaggtgga agtcttcctg gacgggggtg tgcggaaagg cactgatgtt
 901 ctgaaagctc tggctcttgg cgccaaggct gtgtttgtgg ggagaccaat cgtttggggc
 961 ttagctttcc agggggagaa aggtgttcaa gatgtcctcn agatactaaa ggaagaattc
1021 cggttggcca tggctctgag tgggtgccag aatgtgaaag tcatcgacaa gacattggtg
1081 aggaaaaatc ctttggccgt ttccaagatc tga
```

f) Genomic structure of GO derived from clone accession number AL021879. Exons are shown in capital letters with partial flanking intronic sequences, both upstream and downstream, in small font. Bases are numbered as in clone AL021879.

```
17281  aaatttcaaa ggctaagcat ataatgtttg ctcacttgat gtaagcaaca gagaactaaa
17341  tctgaacttt ggcaaaagtc tattaataat tgacaaataa cagaacagtg aggatgtaga
17401  aagcaataca ttaaaaaaaa aaaaacaacg aactccatct gggatagcaa taacctgtga
17461  aaATGCTCCC CCGGCTAATT TGTATCAATG ATTATGAACA ACATGCTAAA TCAGTACTTC exon1
17521  CAAAGTCTAT ATATGACTAT TACAGGTCTG GGGCAAATGA TGAAGAAACT TTGGCTGATA
17581  ATATTGCAGC ATTTTCCAGg taagaaaatt tatttttaa aatcatgttt taaaattaca
17641  caaagaccgt accaaaataa gatctcctag ttttacgttg gtggtgtgta attatttgtt
17701  cagatttgtg cttagtagag agggaaaagt tcttggggct gtaagaaatc ttgggccttt
17761  aaattgttaa aaaatattcc aagcctgtga atcttgagga actgactgca aaagccaaac

23041  tgcttgggaa attcattatc ctctaattgt taactttcta accaaacaaa cagtaaaatt
23101  gcctcttttc cattagcttt atgaagtcat ttgcttgttt ggaaaaaatc caattatatt
23161  ttttctttta actaaaatgt aatgtcaaag ttttggttat gattctgaaa ctctaaagcc
23221  ttttatttta ttttatttttt taattctagA TGGAAGCTGT ATCCAAGGAT GCTCCGGAAT exon2
23281  GTTGCTGAAA CAGATCTGTC GACTTCTGTT TTAGGACAGA GGGTCAGCAT GCCAATATGT
23341  GTGGGGGCTA CGGCCATGCA GCGCATGGCT CATGTGGACG GCGAGCTTGC CACTGTGAGA
23401  Ggtaggagga agattgtcac cacagggaca gaaggaggct aacgtttatc gacctccttc
23461  tctgaatgca ccaagcaaat atgttccttg atgtttttac actcagaaac attaagctca
23521  tggactctat catcaaaata cttgttcttg catgtcctgc tcctcttctt tccagctgtg
23581  tgactgggca agatatcctc tctctgcatt ggtttccttg gctgtaaaat agggacaaaa

43261  gaaataactc cagtagccat ttgtatcaga ggaggtagaa tcaggaaata gatggtatgg
43321  gccagacttt cttctctctt taagagattt gacttcatat tgccaaattg cccttctaga
43381  tgtctttact catccaacta caattcaaag gtttgggagg gtaagcaatg ccaggcccat
43441  cttgatcatc ccctttcttt ctcagCCTGT CAGTCCCTGG GAACGGGCAT GATGTTGAGT exon3
43501  TCCTGGGCCA CCTCCTCAAT TGAAGAAGTG GCGGAAGCTG GTCCTGAGGC ACTTCGTTGG
43561  CTGCAACTGT ATATCTACAA GGACCGAGAA GTCACCAAGA AGCTAGTGCG GCAGGCAGAG
43621  AAGATGGGCT ACAAGGCCAT ATTTGTGACA GTGGACACAC CTTACCTGGG CAACCGTCTG
43681  GATGATGTGC GTAACAGATT CAAACTGCCG CCACAACTCA Ggtaaccatg atcatgtggg
43741  ccccgagctg aggcgaaagg gatcttgact gggaatgtta gggtctgggt tctactgata
43801  gcaacgttgc taaacatcta gttaatcttc agctaatcac atccctttg tagacatcac
```

```
43861  ttttttgag atacacaata gaaacagaaa tggcctctat aaaagtccaa taaattttca

51361  taagaccact agagtatcac atttagtcta gagtcctaca tcaaaatatg gaaaatatgt
51421  gtgcaattga cttatagata aatgagcagt gaacagccaa ttgatttgaa aagggtaaca
51481  tttttcattg aatgaatcat tggaaacgta tttctaattt ggcaaatttc tcattttatg
51541 catttcttat tttagGATGA AAAATTTTGA AACCAGTACT TTATCATTTT CTCCTGAGGA exon4
51601  AAATTTTGGA GACGACAGTG GACTTGCTGC ATATGTGGCT AAAGCAATAG ACCCATCTAT
51661  CAGCTGGGAA GATATCAAAT GGCTGAGAAG ACTGACATCA TTGCCAATTG TTGCAAAGGG
51721  CATTTTGAGA Ggttcgttta tttctctact tgaattcata ctgactttgt gatcctttgt
51781  ggatacgttc ataatattct taaaggaaaa taacaaggaa aaattaacat ggaaattgag
51841  agagacattc caactctcaa ttctctgttt tcatgttagt gagtaaatat ttcttcattc
51901  ttaggtaata ttctgaagca gagctaaact ctcatgaagc acaaagtgag ctttttcaaa

62461  acatttttt gttgtttttg gccaagaaaa ctaccactaa tattctagcg ctaaccctag
62521  ggtatacttt tatgctaaga ttattgaccc aggtatgcag atgggagtca gcctccattt
62581  gactggaatg tggaggcctc taaacccaag ctgcctgtta agttacagtt tccctaaggt
62641  gcttgtttta ctctctccag GTGATGATGC CAGGGAGGCT GTTAAACATG GCTTGAATGG exon5
62701  GATCTTGGTG TCGAATCATG GGGCTCGACA ACTCGATGGG GTGCCAGCCA CTgtgagttt
62761  tggcagacgc taagatttcc ttttggagtt cccatttcca tcactgtgtt actatctcta
62821  tgtcttcctc ctctctgtgt gtactttgtg taatcactca aggtgaaata cgtgcaaata
62881  tgtgagatct tggattttaa gtttagtggc acataactac ccaagttaaa aatttattta

71821  ttccaaattt agttggtgtt ttagttacta gcatttgtac ctctcttctt tgagaaggaa
71881  ataattttac catttacccc aaacctactt ggcttctttc actctaagcc ctagctggat
71941  gtgtcagtgg tttttggagg tggagttgaa taacaattca gtgttaatag agtcacatta
72001  ttgaactttt ctttccccag ATTGATGTTC TGCCAGAAAT TGTGGAGGCT GTGGAAGGGA exon6
72061  AGGTGGAAGT CTTCCTGGAC GGGGGTGTGC GGAAAGGCAC TGATGTTCTG AAAGCTCTGG
72121  CTCTTGGCGC CAAGGCTGTG TTTGTGGGGA GACCAATCGT TTGGGGCTTA GCTTTCCAGg
72181  taactggaca aagaaatgaa tatataaaat agacaacttg acagtaaaac aaatgaataa
72241  aacaagtcag actgatttag ttctgaatca ctctgtatct tttcacttgg ttaggggggag
72301  AAAGGTGTTC AAGATGTCCT CGAGATACTA AAGGAAGAAT TCCGGTTGGC CATGGCTCTG exon7
72361  AGTGgtaaga ctcattcttg tttacaactt tcttttcttt tatgatcttt aagtcaaggt
72421  ccttggtgga gagaagtgaa tttgaaaggg aagagtgtgg gatcatttga gtacattaaa
72481  tttgacgttg actccatatt tacagctttg aggaactctg catgtgcagt ctctagtaat
72541  tacttaacct ctgtttttca cagctttatt aggaatattt tggtgagtac gagtacttgg


74041  tcattttgtg ttaaggactg tttaggtaat aaaaaatggt ctcatgccac ataagatttg
74101  gcaagcctac cttgaatcat aaaccttaca tttgtcaaat tttacattcc ttgggaaaac
74161  gattacctgc ctgattatta ttgcattcag ttcatattaa atgtatgcat tatttttca
74221  gGGTGCCAGA ATGTGAAAGT CATCGACAAG ACATTGGTGA GGAAAAATCC TTTGGCCGTT exon8
74281  TCCAAGATCT GAcagtgcac aatattttcc catctgtatt attttttttc agcatgtatt
74341  acttgacaaa gagacactgt gcagagggtg accacagtct gtaattcccc acttcaatac
74401  aaagggtgtc gttcttttcc aacaaaatag caatcccttt tatttcattg cttttgactt
74461  ttcaatgggt gtcctaggaa ccttttagaa agaaatggac tttcatcctg gaaatatatt
```

Publications

Williams, E., D. Cregeen and G. Rumsby (2000). "Identification and expression of a cDNA for human glycolate oxidase." Biochim Biophys Acta 1493: 246-248.

Williams, E. and G. Rumsby (2002). "Identification and characterisation of human liver glycolate oxidase." In: Chapman, S., R. Perham and N. Scrutton. Flavins and Flavoproteins 2002. Berlin, Rudolf Weber: 923-926.

Conference abstract:

"The identification and characterisation of human liver glycolate oxidase."

6th European Workshop on Hyperoxaluria (Hannover, 2002)

The identification and characterisation of human liver glycolate oxidase (GO)

Authors:
Emma Williams and Gill Rumsby

Institution:
Department of Immunology & Molecular Pathology
University College London

GO is a peroxisomal flavoenzyme which catalyses the oxidation of short chain hydroxy acids. The enzyme utilises glycolate as substrate in a reaction which produces glyoxylate, a major precursor of endogenous oxalate. The pivotal role of the enzyme in glyoxylate production makes it of relevance to the field of hyperoxaluria.

We have recently cloned and expressed the gene for human liver GO, which has enabled characterisation of the protein. Comparison of the peptide sequence to GO from other species reveals 89% similarity to mouse and 53% to the enzyme from spinach. The protein shows hydroxy acid oxidase activity *in vitro*, and has been purified to homogeneity. The pure enzyme displays an absorption spectrum characteristic of the flavoproteins, with absorption peaks at 370 and 450 nm. Crosslinking studies indicate the protein has a tetrameric sub-unit structure. Kinetic analysis of the pure enzyme with several hydroxy acids shows it has highest affinity for glycolate (Km = 0.54 mM) as substrate, but has 10 fold less affinity for glyoxylate (Km = 5.1 mM).

Multiple tissue northern blot analysis detects a 1.8 kb mRNA with expression restricted to liver. Western blot analysis with polyclonal anti-GO antibody raised in rabbits detects a 43 kDa liver protein. Work is ongoing to assess the potential of GO to contribute to oxalate production in the primary hyperoxalurias.